



University
of Glasgow

Tho, Lye Mun (2011) *Investigating the Role of Chk1 in Mouse Skin Homeostasis and Tumourigenesis*. PhD thesis, University of Glasgow.

<http://theses.gla.ac.uk/2504/>

Copyright and moral rights for this thesis are retained by the author

A copy can be downloaded for personal non-commercial research or study, without prior permission or charge

This thesis cannot be reproduced or quoted extensively from without first obtaining permission in writing from the Author

The content must not be changed in any way or sold commercially in any format or medium without the formal permission of the Author

When referring to this work, full bibliographic details including the author, title, awarding institution and date of the thesis must be given.

Investigating the Role of *Chk1* in Mouse Skin Homeostasis and Tumourigenesis

Lye Mun Tho
MBBS, MRCP, FRCR

This thesis is submitted in fulfilment of the requirements for the Degree of
Doctor of Philosophy

Beatson Institute for Cancer Research
Garscube Estate
Switchback Road
Bearsden
Glasgow G61 1BD, United Kingdom

and

Faculty of Medicine
University of Glasgow
Glasgow G12 8QQ, United Kingdom

Abstract

Chk1 is a key regulator of DNA damage response and genome stability in eukaryotes. To better understand how checkpoint proficiency affects cancer development particularly tumours induced by chemical carcinogens in murine skin, I investigated the effect of conditional genetic ablation of *chk1*. I found that complete deletion of *chk1* immediately prior to carcinogen exposure strongly suppressed papilloma formation, and the few, small lesions that did form always retained Chk1 expression. Remarkably, *chk1* deletion was accompanied by spontaneous cell proliferation followed by DNA damage and cell death within the hair follicle. This also affected and led to proliferation and ultimately depletion of label-retaining stem cells (LRCs) within the bulge region of hair follicles, the principal source for carcinogen-induced tumours. At later times, ablated skin became progressively repopulated by Chk1-expressing cells and normal sensitivity to tumour induction was restored if carcinogen treatment was delayed. In marked contrast, papillomas formed normally in *chk1* hemizygous skin but showed an increased propensity to progress to carcinomas. I conclude that Chk1 is essential for the survival of incipient cancer cells but that partial loss of function (haploinsufficiency) fosters tumour progression.

Table of Contents

Abstract	ii
Table of Contents	iii
List of Figures	vi
Acknowledgement	viii
Author's Declaration	ix
Abbreviations	x
Chapter 1. Introduction	12
1.1. Cell Cycle Control.....	13
1.1.1. The Cell Cycle.....	15
1.1.1.1. G0 & G1-phase	15
1.1.1.2. S-phase	16
1.1.1.3. G2-phase	17
1.1.1.4. Phosphatases	18
1.1.1.5. Negative Regulation of the Cell Cycle.....	18
1.2. DNA Damage Repair Mechanisms	20
1.3. Cell Cycle Checkpoints.....	26
1.3.1. ATM/Chk2.....	27
1.3.2. ATR/Chk1	28
1.4. The Role of Chk1 and Other DNA Damage Checkpoints in Either Preventing or Treating Cancer - Opposing Paradigms.....	31
1.4.1. Checkpoints as a Barrier to Tumorigenesis.....	31
1.4.2. Therapeutic Potential of Chk1 Inhibition.....	34
1.4.2.1. Synthetic Lethality	35
1.5. <i>Chk1</i> Mouse Models	37
1.6. Murine Skin as an Experimental Model	40
1.6.1. The Two Stage DMBA/TPA Skin Carcinogenesis Protocol.....	40
1.7. Stem Cells And Cancer	44
1.7.1. Identification of Stem Cells and Markers	44
1.7.2. Important Pathways in Stem Cells.....	47
1.7.3. Role of the Host Environment in Transplantation Assays	49
1.7.4. Quiescence versus Proliferation - the LGR5 Positive Stem Cell.....	50
1.7.5. Tissue Specific Stem Cells are Targets for Chemical Carcinogenesis	54
1.8. Objectives of the thesis.....	56
Chapter 2. Materials and Methods.....	57
2.1. Generation of <i>Chk1</i> Null mice	58
2.2. Generation of <i>Chk1</i> Flox Mice.....	58
2.3. Generation of Rosa26-LacZ Mice	58
2.4. Breeding Strategy and Colony Maintenance	59
2.5. B-Galactosidase Assay.....	59
2.6. DNA Preparation and PCR Genotyping.....	59
2.7. Tamoxifen (4-OHT) Preparation and Administration.....	61

2.8.	DMBA/TPA Chemical Carcinogenesis.....	61
2.9.	Antibodies.....	62
2.10.	Labelling Mice with BrdU to Assay for Label Retaining Cell (LRC) Properties	62
2.11.	Preparation of Tail Epidermal Wholemounts.....	63
2.12.	Confocal Microscopy of Tail sections	63
2.13.	Tissue Fixation	64
2.14.	Immunohistochemistry	64
2.15.	Antigen retrieval	65
2.16.	Deriving Carcinoma Cell Lines from Mice	65
2.17.	Mouse Tail Keratinocyte Culture	66
2.18.	Passaging Adherent Cells	66
2.19.	DT40 Cell Culture	67
2.20.	Cryogenic Preservation of Cell lines	67
2.21.	Making Protein Extracts From Mouse Tissue	68
2.22.	SDS-PAGE.....	68
2.23.	Western Blotting	69
2.24.	Irradiating Cells and Mice	70
Chapter 3.	Characterization of the <i>Chk1</i> Knockout Mouse	71
3.1.	Results	72
3.1.1.	Genetically Engineered Mice - <i>Chk1</i> Flox and Null Alleles.....	72
3.1.2.	Breeding Strategy	72
3.1.3.	Cre-LoxP // ROSA26 LacZ Reporter System and B-Gal Assay.....	72
3.1.4.	Genotyping of Mice.....	75
3.1.5.	Phenotype of <i>Chk1</i> Null, Heterozygous and Flox Mice	75
3.1.6.	Achieving Conditional Knockout of <i>Chk1</i> in the Skin.....	76
3.1.7.	Phenotype of Conditional <i>Chk1</i> Knockout in the Skin	87
3.1.8.	<i>Chk1</i> Expression in Different Organs	88
3.2.	Discussion	89
Chapter 4.	<i>Chk1</i> Ablation and Tumour Formation	91
4.1.	Results	92
4.1.1.	<i>Chk1</i> Ablation in the Skin Delayed Papilloma Formation and Reduced Papilloma Numbers and Sizes	92
4.1.2.	Papilloma Formation Requires <i>Chk1</i>	99
4.1.3.	<i>Chk1</i> Expression in Carcinomas Varies in Intensity.....	100
4.2.	Discussion	101
Chapter 5.	<i>Chk1</i> Ablation Affects Skin and Label Retaining Cell Homeostasis	104
5.1.	Results	105
5.1.1.	BrdU Label Retention Can be Imaged in Bulge Stem Cells.....	105
5.1.2.	<i>Chk1</i> Ablation Induces Label Retaining Cell (LRC) Proliferation ..	107
5.1.3.	<i>Chk1</i> Ablation Results in an Accumulation of DNA Damage in the Skin	117
5.1.4.	<i>Chk1</i> Ablation Results in Increased Apoptosis in the Skin.....	127
5.1.5.	The Frequency of Staining Events Suggest LRC Proliferation Precedes DNA Damage and Apoptosis	128
5.1.6.	<i>Chk1</i> Loss Results in p53 Induction	128

5.1.7.	<i>Chk1</i> Ablated Skin is Repopulated by Unrecombined Cells (Unfloxed “Wild Type”)	129
5.1.8.	Hair Follicle Stem Cells May be Responsible for Repopulation of the Interfollicular Epidermis	130
5.2.	Discussion	131
Chapter 6.	Mechanisms for Explaining <i>Chk1</i> Ablation and Resultant Tumour Suppression	137
6.1.	Results	138
6.1.1.	<i>Chk1</i> Ablation Caused a Depletion of Label Retaining Cells and Reduced Tumour Formation but Homeostasis is Maintained	138
6.1.2.	<i>Chk1</i> Ablation Reduces Hyperplasia Normally Caused by TPA.....	144
6.1.3.	<i>Chk1</i> Ablation May be Selectively Targeting <i>H-Ras</i> Mutant Stem Cells for Apoptosis	144
6.1.4.	<i>Chk1</i> Ablation Delays Hair Regrowth	148
6.2.	Discussion	152
6.2.1.	Models for Label Retaining Cell / Stem Cell Fate Following <i>Chk1</i> Ablation	152
6.2.2.	<i>Chk1</i> Ablation May be Causing Bulge Niche Exhaustion	156
6.2.3.	<i>H-Ras</i> and Non- <i>H-Ras</i> Transformed Stem Cells do not Repopulate the Bulge Niche Symetrically	156
Chapter 7.	Additional Results	160
7.1.	Results	161
7.1.1.	Hemizygous <i>Chk1</i> Ablation did not Affect Papilloma Incidence but Increased the Rate of Conversion to Carcinomas	161
7.1.2.	<i>Chk1</i> Ablation in Formed Papillomas Resulted in Regression in Smaller Papillomas but did not Lead to an Overall Reduction in Tumour Burden	164
7.1.3.	Generation of Murine Carcinoma Cell Lines from DMBA/TPA Induced Carcinomas	165
7.1.4.	<i>Chk1</i> Loss Sensitizes Tumour Cells to the Cytotoxic Effects of Anti-Cancer Therapy in DT40 Lymphoma Cells	168
7.2.	Discussion	169
Chapter 8.	Summary Conclusion and Future Perspectives.....	173
8.1.	Summary Conclusion.....	174
8.1.1.	Summary of Chapter 3.....	174
8.1.2.	Summary of Chapter 4.....	175
8.1.3.	Summary of Chapter 5.....	175
8.1.4.	Summary of Chapter 6.....	176
8.1.5.	Summary of Chapter 7.....	177
8.2.	Future Perspectives	179
	List of References	185

List of Figures

Figure 1 - Cell Cycle Checkpoint - ATR/Chk1 and ATM/Chk2	25
Figure 2 - The Role of Chk1 and Other DNA Damage Checkpoints in Either Preventing or Treating Cancer - Opposing Paradigms	32
Figure 3 - DMBA/TPA Chemical Carcinogenesis Protocol	41
Figure 4 - Epidermal Stem Cell Populations	53
Figure 5 - The <i>LacZ</i> Reporter Allele.....	73
Figure 6 - Diagnostic PCR for <i>Chk1</i> , <i>Cre</i> and <i>LacZ</i> Alleles	74
Figure 7 - Phenotype of Constitutive and Conditional <i>Chk1</i> Knockout Mice.....	77
Figure 8 - Conditional Floxed <i>Chk1</i> Allele and K14- <i>CreER</i> ^{T2} Allele.....	78
Figure 9 - <i>Chk1</i> Knockout in Adult Mouse Skin	79
Figure 10 - PCR for Recombined <i>Chk1</i> Allele	83
Figure 11 - Early Deaths Associated with <i>Chk1</i> Knockout	84
Figure 12 - Chk1 Expression in Different Mouse Tissues	85
Figure 13 - <i>Chk1</i> ablation Prior to DMBA/TPA Carcinogenesis	93
Figure 14 - Rate of Conversion of Papillomas to Carcinomas	95
Figure 15 - Chk1 Expression in Papillomas	96
Figure 16 - Chk1 Expression in Carcinomas	97
Figure 17 - BrdU Label Retaining Cell (LRC) Assay in Mouse Epithelium	106
Figure 18 - Chk1 Expression in Wholmount Epidermis.....	108
Figure 19 - Label Retaining Cell Quantification Following <i>Chk1</i> Abaltion	109
Figure 20 - Dilution of Long Term BrdU Label and Cell Proliferation Following <i>Chk1</i> Abaltion.....	112
Figure 21 - Label Retaining Cells and the Hair Follicle Cycle.....	115
Figure 22 - Activated Caspase 3 and γ -H2AX Expression in Skin After Irradiation	116
Figure 23 - γ -H2AX Expression in Skin Following <i>Chk1</i> Abaltion	118
Figure 24 - Activated Caspase 3 Expression in Skin Following <i>Chk1</i> Abaltion ...	120
Figure 25 - Timelines for Tissue Changes Following <i>Chk1</i> Abaltion.....	122
Figure 26 - p53 Expression in Skin Following <i>Chk1</i> Abaltion	123
Figure 27 - Repopulation of Skin by Unrecombined Cells Following <i>Chk1</i> Abaltion	124
Figure 28 - The Interfollicular Epidermis Maybe Repopulated by Cells from the Follicle Following <i>Chk1</i> Abaltion	126
Figure 29 - Models of Stem Cell Fate Following <i>Chk1</i> Ablation.....	139
Figure 30 - Keratin 15 Expression Following <i>Chk1</i> Ablation	140
Figure 31 - Delaying DMBA Application Following <i>Chk1</i> Ablation	142
Figure 32 - TPA Induced Skin Hyperplasia and <i>Chk1</i> Ablation	145
Figure 33 - TPA Induced Skin Hyperplasia and <i>Chk1</i> Ablation	146
Figure 34 - Effect of <i>Chk1</i> Ablation on Hair Growth	149
Figure 35 - The Effect of <i>Chk1</i> Ablation on the Stem Cell Niche and Tumour Formation	157

Figure 36 - The Effect of <i>Chk1</i> Hemizyosity on Tumour Formation	162
Figure 37 - The Effect of <i>Chk1</i> Ablation on Pre-Formed Papillomas.....	163
Figure 38 - Generation of Murine Cancer Cell Lines from DMBA/TPA Induced Carcinomas.....	166
Figure 39 - Genotoxic Treatment and <i>Chk1</i> Knockout DT40 Lymphoma Cells ..	167
Figure 40 - <i>In vivo</i> RFP Reporter System	180
Figure 41 - LGR5 Stem Cells.....	181

Acknowledgement

I would like to express my gratitude to my laboratory supervisor, Prof. David Gillespie and my clinical supervisor Prof. Roy Rampling, for their support throughout my entire research project. I would like to thank my advisor, Prof. Owen Sansom, for his guidance and collaboration.

I would also like to thank all the members of the R11 group both past and present (Elizabeth Black, Mark Walker, Mary Scott, Naihan Xu, Conor Larkin, Helen Robinson, George Zachos, Verena Oehler, Joanne Smith and Silvana Libertini) for their help. I am especially grateful to Conor Larkin for his help and guidance with laboratory methods. I would like to acknowledge the assistance provided by various technology services within the Beatson Institute including Biological Services, Histopathological Services, Molecular Technology Services, Imaging Services, Information Technology, Administration, Finance, Reagent Support Services and Central Services.

I am grateful to Cancer Research UK and the Royal College of Radiologists for providing funding for this work.

Author's Declaration

I declare that I am the sole author of this thesis. The work presented here is my own, unless otherwise acknowledged. This thesis has not been submitted for consideration for another degree in this or any other university.

Abbreviations

4-OHT	4 Hydroxy Tamoxifen
ATM	Ataxia telangiectasia mutated
ATR	Ataxia telangiectasia and Rad3 related
BrdU	5-bromo-2-deoxyuridine
BSA	Bovine Serum Albumin
Chk1	Checkpoint Kinase 1
Chk2	Checkpoint Kinase 2
cm	Centimetres
DAB	3,3-diaminobenzidine
DAPI	4',6-diamidino-2-phenylindole
DMBA	7,12-dimethyl-benz[a]anthracene
DMF	Dimethylformamide
DMSO	Dimethyl sulfoxide
DNA	Deoxyribonucleic Acid
DSB	Double Strand Break
dsDNA	double stranded DNA
DTT	Dithiothreitol
EDTA	Ethylene-diamine-tetra-acetic acid
ES Cells	Embryonic Stem Cells
FACS	Fluorescence Activated Cell Sorting
H&E	Hematoxylin and Eosin Stain
HCl	Hydrchloric Acid
HR	Homologous Recombination
HU	Hydroxyurea
ICC	Immunocytochemistry
IF	Immunofluorescence
IHC	Immunohistochemistry
IP	Intraperitoneal
LRC	Label Retaining Cells
MGMT	O-6-methylguanine-DNA methyltransferase
min	Minute
mm	Milimetre
mM	Milimolar

ms	Miliseconds
mTOR	Mammalian target of Rapamycin
NaCl	Sodium Chloride
NHEJ	Non-homologous End Joining
PAGE	Polyacrylamide Gel Electrophoresis
PBS	Phosphate Buffered Saline
PCR	Polymerase Chain Reaction
RNA	Ribonucleic Acid
RT-PCR	Reverse Transcriptase - Polymerase Chain Reaction
s	Seconds
SDS	Sodium Dodecyl Sulfate
ssDNA	Single stranded DNA
TEMED	Tetra-methyl-ethylene-diamine
TPA	12- <i>O</i> -tetra-decanoyl-phorbol-13-acetate
TRIS	Tris(hydroxymethyl)amino-methane
μL	Microlitre
μm	Micrometre
μM	Micromolar
X-gal	5-bromo-4-chloro--3-indolyl-βD-galactopyranoside
γ-IR	Gamma Ionising Irradiation

Chapter 1. Introduction

1.1. Cell Cycle Control

Progression through the cell cycle is a highly ordered process consisting of distinct phases which are regulated by a network of proteins, kinases and phosphatases [reviewed by (Pollard TD, 2004)]. The serine-threonine family of kinases known as cyclin dependent kinases (Cdks) are mainly responsible for cell cycle progression and are activated by binding to cyclins, the name alluding to their cyclical accumulation and destruction throughout different phases of the cell cycle. CDK-cyclins are negatively regulated by an equally complex network of proteins including phosphatases, the INK4 and CIP/KIP family of proteins and through proteolysis. When the cell acquires DNA mutations or damage either through external stressors or errors in replication, it has in reserve a variety of different repair mechanisms equipped to deal with specific lesions for example non homologous end joining and homologous recombination to deal with double stranded breaks and base excision repair that deals with single or short patches of nucleotide damage. However in order for DNA repair to occur, normal progression through the cell cycle needs to be temporarily suspended to allow the appropriate recognition of the lesion and the recruitment of various repair proteins and the actual repair process to proceed without error. Checkpoint proteins are central to this process and defects in these pathways have a significant effect of tumour formation and progression [reviewed by (Smith et al, 2010)].

Chk1 is a key DNA damage and replication stress-response kinase that controls a variety of cell cycle checkpoints function and is activated in primarily in the S and G2/M phases. *Chk1* triggers cell cycle delay by down-regulating key cell-cycle regulatory components such as Cdc25, Cdk2-cyclinE (A) and Cdk1-cyclinB complexes, and acts to stabilize stalled replication forks and suppress replication origin firing when DNA replication is blocked [reviewed by (Smith et al, 2010)]. As mentioned above, collectively, these responses are thought to facilitate DNA repair, prevent aberrant replication, and minimise potentially lethal genetic damage under conditions of genotoxic stress (Zachos et al, 2003a). Increasing evidence suggest tumours are particularly reliant on Chk1 as they often have functional defects within other cell cycle components eg. p53, p21,

Chk2/ATM (Bartkova et al, 2005) and reviewed by (Zhou & Bartek, 2004). Chk1 is now emerging as a potential anti-cancer target and selective kinase inhibitors are currently being developed [reviewed by (Dai & Grant, 2010; Garber, 2005)]. It is still unclear how best to combine Chk1 inhibition with current anti-cancer strategies. However the successful introduction of novel DNA damage modulators (Fong et al, 2009) do serve as a template for the use of agents that interfere with DNA repair within cancer cells.

In cancer development, malignant cells can often acquire somatic mutations of various components of the cell cycle leading ultimately to dysregulated progression [reviewed by (Malumbres & Barbacid, 2009; Pines, 1995; Sherr, 1996; Smith et al, 2010)]. This can include an overexpression of cyclins for example amplification and aberrant nuclear accumulation of cyclin D1 [reviewed by (Kim & Diehl, 2009)]. High total cyclin E levels or high levels of the low molecular weight forms of cyclin E have significantly correlated with poorer outcomes in breast cancer patients (Keyomarsi et al, 2002). Negative regulation of cell cycle is frequently affected leading to carcinogenesis. The *INK4-ARF* locus has been frequently found to be deleted or inactivated in a variety of cancers including melanoma [reviewed by (Sharpless & Chin, 2003)], glioma (Tachibana et al, 2000) and pancreatic cancer (Gerdes et al, 2001). Mutations or direct alteration in Cdk function is less well documented. In murine models Cdk4 has been shown to be important in cyclin D1 mediated breast tumorigenesis driven by the ErbB-2 oncogene (Yu et al, 2006) but there is emerging evidence that the chromosomal region responsible is amplified in human cancer (Mejia-Guerrero et al, 2010). Phosphatases which promote Cdk-cyclin binding have been found to be overexpressed, for instance CDC25A has been found to be overexpressed in human breast cancer (Cangi et al, 2000; Ray & Kiyokawa, 2008) and more examples have been reviewed by (Boutros et al, 2007). Emerging evidence suggest checkpoint proteins are also important in preventing tumorigenesis, particularly by acting as a counterpoint or barrier against incipient cancer formation and by facilitating oncogene induced senescence (Bartkova et al, 2005; Gorgoulis et al, 2005). They may also play a central role in modulating response to cancer therapies (Bao et al, 2006) and reviewed by (Zhou & Bartek, 2004).

1.1.1. The Cell Cycle

1.1.1.1. G0 & G1-phase

Post mitotic cells are in G0, which is term also applied to cells in quiescence or senescence. G0 is usually a relative state of metabolic inactivity and can be triggered by starvation (Pardee, 1974). It is a period where Cdk and cyclin expression is low or absent. To begin replication, quiescent cells in G0 have to pass through a restriction point (Zetterberg & Larsson, 1985) before they can become committed to completing cell division. This is usually associated with the availability and the production/synthesis of growth factors and nutrients in the environment.

The E2F family of genes plays a key role in the G1 phase of cell cycle [reviewed (Harbour & Dean, 2000)] which is in turn primarily regulated by retinoblastoma (Rb) [reviewed by (Dyson, 1998)]. In early studies involving serum stimulation of quiescent fibroblasts it has been shown that c-Fos, c-Jun (Kovary & Bravo, 1991) are required for cell cycle progression. Additionally a variety of Cdks and cyclin D are expressed to sustain progression through G1 (explained subsequently). The E2F family of transcription factors functions [reviewed by (Muller & Helin, 2000; Neuman et al, 1996)] by stimulating transcription of proteins involved in the next step of progression to late G1 (such as Cdk2, cyclin E) and S-phase (such as Cdk2, cyclin A). E2F is normally inhibited by binding to Rb (Helin et al, 1993; Lees et al, 1993). As cyclin D levels increase, Cdk4-cyclin D and Cdk6-cyclin D complexes are activated during G1 and phosphorylate Rb thus releasing E2F [reviewed by (Polager & Ginsberg, 2009)]. Cdk2-cyclin E has also been shown to cooperate with Cdk4/6 and cyclinD to inactivate Rb (Khleif et al, 1996). This allows self-propagation of the cell cycle once the restriction point is passed despite the eventual decline of Cdk4-cyclinD and Cdk6-cyclinD levels in late G1. This maintains the cell's course into S-phase [reviewed by (Hochegger et al, 2008; Pollard TD, 2004)].

1.1.1.2. S-phase

In S phase, DNA is replicated by a complex process involving proteins that unwind the double stranded DNA in order to synthesize a new complementary strand using either single stranded DNA or chromatid as the template. This aims to duplicate the DNA with high fidelity and avoid mutational errors as much as possible.

Eukaryotic DNA synthesis is initiated at multiple origins of replication (in the order of tens of thousands) throughout the chromosomes in S phase. Due to the relatively huge length of DNA needing to be completely duplicated, multiple origins facilitate timely replication within the constraints of the cell cycle. Pre-replication complexes (pre-RC) [reviewed by (Mechali, 2010; Takisawa et al, 2000)] are crucial to initiation and are assembled in G1 when Cdk levels are low (Nguyen et al, 2001). In late M phase or G1 phase, protein complexes ORC (origin recognition complex) act as landing pads for the replication factors Cdc6 (Liang et al, 1995) and chromatin licensing and DNA replication factor 1 (Cdt1) (Maiorano et al, 2000), which in turn recruits the mini chromosome maintenance proteins (MCM) 2-7 to chromatin (Chong et al, 1995; Forsburg, 2008). MCMs possess a ring structure with a central pore that accommodates double-stranded DNA and functions as helicases that unwind DNA when activated. The assembled structure, or pre-replication complex (pre-RC), allows the initiation of DNA synthesis at that site.

As Cdk and cyclin levels increase in S-phase, pre-RC competence is destroyed. Cdc6 and Cdt1 are removed from the complex and this ensures the pre-RC is able to initiate only one round of replication till the following G1, thereby preventing so called relicensing of replication origins. Cdc6 is phosphorylated by Cdk2-cyclin A and released from pre-RCs and relocalised to the cytoplasm (Petersen et al, 1999) and Cdt1 undergoes proteolysis (Liu et al, 2004). An additional mechanism involves geminin which binds Cdt1 to block the loading of the MCM complex onto DNA (McGarry & Kirschner, 1998). Geminin is subsequently degraded by anaphase promoting complex/cyclosome (APC/C) at the metaphase-anaphase transition allowing reformation of pre-RCs at a later stage (McGarry & Kirschner, 1998).

As cells enter S phase two serine threonine protein kinases are activated the S-phase Cdk (SCdk) (Masumoto et al, 2002) and Dbf4-dependent Cdc7 kinase (DDK). Their activity triggers replication at pre-RCs by recruiting a number of proteins onto the pre-RC and activating MCM helicase activity. Stillman and colleagues (Sheu & Stillman, 2006) report that DDK promotes assembly of a stable cell division control protein 45 (Cdc45)-MCM complex exclusively on chromatin in S phase. Cdc45-MCM recruits the single stranded binding protein replication protein A (RPA) which stabilizes single stranded DNA and prevents reannealing (Tanaka & Nasmyth, 1998).

Cdc45 and RPA recruit the DNA polymerase and primase complex Pol α /Primase (Walter & Newport, 2000). The primase synthesizes short segments of RNA primer to initiate strand elongation. Replication factor C (RFC) binds the 3' end DNA and recruits proliferating cell nuclear antigen (PCNA) that surrounds DNA and forms a clamp (Podust et al, 1998; Stoimenov & Helleday, 2009). The RFC-PCNA complex displaces the initial Pol α /Primase and loads DNA polymerase δ and ϵ which continue strand elongation. DNA polymerase adds deoxy-NTPs onto to the growing strand in a 5'→3' direction. DNA polymerase δ and ϵ can also proofread and repair the DNA via their exonuclease capability. On the leading strand 5'→3' elongation is continuous but on the 3'→5' lagging strand Okazaki fragment synthesis is discontinuous; these are eventually joined by DNA ligases [reviewed by (Kao & Bambara, 2003)].

DNA replication in S-phase can be assayed using a thymidine analogue, Br-dUTP (BrdU) (Gratzner, 1982), which incorporates into synthesizing strands and can be detected using appropriate antibodies. In S-phase euchromatic regions typically replicate first followed by heterochromatic regions. Replication origins generally cluster in groups of approximately 5 to form replication foci. In terms of spatial distribution of replicating events, early replicating-foci are said to be found throughout the nucleus and later-replicating foci at the nuclear periphery /perinucleolar regions (Dimitrova & Gilbert, 1999).

1.1.1.3. G2-phase

The Cdk1-cyclin B complex is the main effector for entry into mitosis (Santamaria et al, 2007). Cyclin B transcription starts in S phase and peaks in G2

and falls dramatically once the cell enters mitosis (Pines & Hunter, 1989; Solomon et al, 1990). After Cdk1 binds to cyclin B (Pines & Hunter, 1989), Cdk1 is then activated by Cdk-activating kinase or CAK (Kaldis et al, 1996) by phosphorylation of Thr161. In addition to this Cdk1 activity is normally inhibited by phosphorylation at Thr14 and Tyr15 which is then dephosphorylated by Cdc25 (Archambault & Glover, 2009; Boutros et al, 2007; Timofeev et al). Negative regulators of the Cdk1-cyclinB1 complex include Wee1 (Lundgren et al, 1991) which phosphorylate Cdk1 on Tyr15 (Gould & Nurse, 1989). Myelin transcription factor 1 (Myt1) also function to phosphorylate Cdk1 at Thr14 and Tyr15 (Mueller et al, 1995). Degradation of cyclin B is regulated by APC/C [reviewed by (Peters, 2002)]. A peak or rise in Cdk2-cyclin A (Pagano et al, 1992) levels at the end of S-phase is also likely to contribute to mitotic entry. Cells with abnormal levels of activated Cdk2-cyclin A were demonstrated to enter into mitosis prematurely.

1.1.1.4. Phosphatases

Phosphatases (Cdc25A in G1 and Cdc25B/Cdc25C in G2/M) regulate Cdk-cyclin complexes by de-phosphorylating and activating Cdk-cyclin complexes [reviewed by (Aressy & Ducommun, 2008; Boutros et al, 2007)]. In the G1→S transition, Cdc25A (transcriptionally regulated by E2F) (Vigo et al, 1999) is activated causing Cdk2 de-phosphorylation and allowing its activation together with cyclin E and A. Cdc25B and cdc25C are active at the G2-M transition causing Cdk1 de-phosphorylation. Checkpoint activation in response to DNA insult targets phosphatases for degradation thus stalling cycle progression [reviewed by (Aressy & Ducommun, 2008; Boutros et al, 2007)].

1.1.1.5. Negative Regulation of the Cell Cycle

There are 3 other negative regulatory networks to controlling Cdk activity and thus cell cycle progression in addition to positive and negative phosphorylation; these are CIP/KIP family of Cdk inhibitors (CdkIs), inhibitors of kinase 4 (INK4) and protein degradation.

The 3 known Cdk Inhibitors (CdkIs) are p21(CIP 1/WAF 1), p27 (KIP 1) and p57 (KIP 2) (Malumbres & Barbacid, 2009), all of which can bind Cdk-cyclin to exert negative regulation. p21 inhibits Cdk2-cyclin E causing G1 arrest. p27 inactivates Cdk4-cyclin D, Cdk2-cyclin A and Cdk2-cyclin E (Polyak et al, 1994). This targets

Cdk-cyclin complexed for degradation via polyubiquitination by SCF (Tsvetkov et al, 1999). p27 protein levels are highest during G0 and early G1 phases, then rapidly declines in late G1 and S phases (Reynisdottir et al, 1995). P57 is particularly associated with Cdk-cyclin complexes in G1 phase (Matsuoka et al, 1995).

Inhibitors of kinase 4 (INK4) (Gil & Peters, 2006) family consisting of p15, p16, p18 and p19 whose overexpression can induce G1 arrest. Whereas CIP/KIP protein have a broader spectrum of inhibition, the INK4 family more specifically inhibit Cdk4 and Cdk6. They do so by binding and distorting its N- and C-terminal lobes preventing their binding to cyclin D, thus preventing phosphorylation of Rb and therefore activation of E2F.

Many proteins involved in cell cycle regulation are degraded via ubiquitination. E1 (ubiquitin activating enzyme) activates ubiquitin by binding via a thioester bond (Hoeller & Dikic, 2009). E2 (ubiquitin conjugating enzyme) and E3 (ubiquitin ligase) functions to transfer ubiquitin to the targeted protein and to elongate its lengthening polyubiquitin tail. Polyubiquitinated proteins are targeted for destruction by 26s proteasomes and the ubiquitin molecules released are recycled. Two E3 ligases are prominent for cyclin degradation - anaphase promoting complex/cyclosome (APC/C) (Matyskiela et al, 2009) and SCF (Skp1, Cullin, F-Box). APC/C bound to specificity factor Cdc20 ie. APC/C^{Cdc20} is inactive during S and G2 phases but is activated by Cdk1-cyclinB during mitosis and targets licensing factor, geminin. SCF is synthesized as cells approach G1 → S transition targets Cdk2-cyclinE for degradation.

1.2. DNA Damage Repair Mechanisms

Cellular DNA is constantly subjected to exogenous (eg. chemical agents, ultraviolet light, tobacco smoke, alcohol) and endogenous stressors (eg. replication errors, products of metabolism, oxidation) that may result in damage. To that end, cells have evolved complex mechanisms to ensure that damaged DNA is recognised and repaired in a timely fashion [reviewed by (Ciccia & Elledge, 2010; Lindahl & Barnes, 2000)]. However, in order for these processes to occur effectively, cell cycle progression needs to be temporarily halted and cell cycle checkpoints play a key role in this step [reviewed by (Smith et al, 2010; Zhou & Bartek, 2004)]. If unrepaired, damage lesions can result in mutations that can then lead to a variety of human diseases, including cancer [reviewed by (Jackson & Bartek, 2009)]. Conversely, inhibition of DNA repair mechanisms either alone or in conjunction with chemotherapy agents or radiotherapy may offer exciting new opportunities in cancer treatment [reviewed by (Chalmers et al, 2010; Pallis & Karamouzis, 2010)].

Environmental mutagens can transfer methyl or ethyl alkylating groups onto guanine at the O⁶ position to form O⁶-methylguanine (other bases can also be alkylated, however O⁶-methylguanine is generally considered to be the most cytotoxic lesion) thereby modifying base structure and interfering with base pairing [reviewed by (Beranek, 1990)]. O⁶-methylguanine-DNA methyltransferase (MGMT) is one of the principal cellular defences against methyl/alkyl damage. Utilising a single step, direct repair mechanism, MGMT transfers the methyl/alkyl group from the O⁶ position of guanine onto a cysteine residue found in its catalytic pocket (Pegg, 2000). This process occurs at a one to one ratio (enzyme to DNA lesion) and irreversibly inactivates MGMT leading to its ubiquitination (Srivenugopal et al, 1996) and subsequent proteosomal degradation (Xu-Welliver & Pegg, 2002). Epigenetic silencing of MGMT has been shown to be an important predictor of tumour response to temozolomide and radiotherapy in glioblastoma multiforme (Hegi et al, 2005), and has been adopted as a stratification factor in new therapeutic trials in this disease (Prof. Roy Rampling, *personal communication*). A large number of chemotherapeutic alkylating agents used in clinical practice have been shown to be able to cause cellular kill via this mechanism and the recently uncovered role of MGMT in

modulating chemosensitivity may be a useful tool in predicting their effectiveness (Kaina et al, 2007).

The base excision repair (BER) pathway is engaged to repair either single or short sections of DNA bases that have been altered by oxidation, alkylation, deamination or through inappropriate incorporation of uracil [reviewed by (Pallis & Karamouzis, 2010)]. Short patch repair deals with single base repairs and long patch repair processes stretches of 2-10 nucleotides [reviewed by (Pallis & Karamouzis, 2010)]. Damaged, mismatched, or abnormal bases are recognised by DNA glycolases which initiate repair by removing the damaged base(s) via hydrolyzation of the *N*-glycosidic bond (Chakravarti et al, 1991). This forms an abasic site (AP) which is recognised by apurinic or apyrimidinic endonuclease (APE1). APE1 cleaves the abasic site to form a single strand break (Izumi et al, 2005). In short patch BER, DNA polymerase β then incorporates the single correct nucleotide at the AP site. It also excises the deoxyribose phosphate moiety via lyase activity and releases the 5'-dRP residues from the incised AP site (Sobol et al, 2000). The final ligation step is carried out by DNA ligase III in partnership with the XRCC1 (Cappelli et al, 1997). In long patch repair, DNA polymerases ϵ or δ (Stucki et al, 1998) in association with proliferating cell nuclear antigen (PCNA) carry out nucleotide resynthesis. DNA ligase III and DNA ligase I are then responsible for ligation (Tomkinson et al, 2001). Poly (ADP-ribose) polymerase (PARP) is an important enzyme involved in BER. It binds to single strand breaks and catalyzes polymerisation and formation of poly (ADP-ribose) complexes on itself and other protein substrates at the site of damage. This serves to recruit proteins involved in BER including DNA polymerase β (Dantzer et al, 2000), DNA ligase III and X-ray repair cross-complementing protein-1 (XRCC1) (Caldecott et al, 1996). PARP inhibition therefore results in inhibition of BER. In the clinic the use of PARP inhibitors are being trialled with promising results (Audeh et al, 2010; Fong et al, 2009), therefore serving as a prototypical DNA repair inhibitor therapy.

Nucleotide excision repair (NER) removes bulky DNA adducts (eg. formed by chemicals such as nitrosamines, benzo[a]pyrenes and aromatic amines that bind DNA to form bulky adducts), intra-strand crosslinks and is particularly important for removing UV induced dimers [reviewed by (Nouspikel, 2009; Pallis & Karamouzis, 2010)]. A common crosslinking agent used in oncological practice is

cisplatin. There are two type of NER, global genome NER (GG-NER) and transcription coupled NER (TC-NER), which is specifically involved in recognition of lesions affecting transcribed regions. They differ in the types of proteins involved in recognising the lesions causing DNA distortion. In GG-NER the xeroderma pigmentosum C (XPC)-HR23B dimer (Sugasawa et al, 1998; Sugawara et al, 1997) is primarily responsible for lesion recognition whereas in TC-NER cockayne syndrome A and B (CSA) and (CSB) perform this role. The following steps between both are similar. Helicases such as xeroderma pigmentosum B (XPB) (Coin et al, 2007) and XPD (Winkler et al, 2000) open up the helix around the damaged site. Proteins such as transcription factor II H (TFIIH), XPA and replication protein A (RPA) (Ito et al, 2007) are recruited and help stabilise the opening. Two NER endonucleases then perform strand incision; XPG endonuclease cuts DNA on the 3' side of the lesion (O'Donovan et al, 1994) and the excision repair cross-complementing 1 (ERCC1)/XPF heterodimer cleaves DNA on the 5' side (Mu et al, 1996), releasing an oligonucleotide segment containing the damaged bases. DNA polymerase δ and/or ϵ then resynthesize the excised sequence using the complementary DNA as a template. It has been shown that ERCC1 expression in lung cancer may be a marker of chemotherapy response, particularly for cisplatin containing regimes (Olaussen et al, 2006), and is currently being used as a biomarker/stratification marker for a national trial in the UK (see ET Trial, National Cancer Research Network United Kingdom, Trials Number 02370070).

Double strand breaks (DSB) are potentially lethal DNA lesions that are repaired primarily by the non-homologous end joining (NHEJ) and homologous recombination (HR) pathways. NHEJ repairs DSBs by direct ligation of damaged ends and is active throughout the cell cycle [reviewed by (Pallis & Karamouzis, 2010)]. The Ku70-Ku80 heterodimer binds the damaged ends and recruits DNA dependent protein kinase catalytic subunit (DNA-PKcs) (Gottlieb & Jackson, 1993; West et al, 1998) which is then activated and undergoes autophosphorylation. The DNA-PKcs-Artemis complex can then act as an endonuclease (Ma et al, 2002) to process and remove any single-stranded overhangs in order to prepare the ends for ligation. Alternatively, DNA Polymerase μ and λ are also attracted by the Ku70-80 heterodimer and can fill in gaps in the overhang regions (Daley et al, 2005; Ma et al, 2004). The two

adjoining ends then undergo the ligation step of reformation of the phosphodiester bond mediated by XRCC4 like factor (XLF), XRCC4 and DNA ligase IV (Critchlow et al, 1997; Grawunder et al, 1997). NHEJ is an effective repair system but one that is necessarily imprecise and can result in the loss or insertion of nucleotides at the site of repair. This is however preferable to the much greater loss of genetic information that would result from failure to repair DSBs [reviewed by (Kotnis et al, 2009)]. A Ku70-80-independent NHEJ pathway known as microhomology mediated end joining (MMEJ) has also been described. The molecular mechanism of MMEJ is less well understood however it is also error-prone and frequently results in sequence deletions (Liang et al, 1996; Roth & Wilson, 1986).

Homologous recombination repairs DSBs with much greater fidelity than NHEJ (Richardson & Jasin, 2000; Richardson et al, 1998). Due to the requirement for the use of the sister chromatid as a template, this process is restricted to certain phases of the cell cycle namely late S or G2 (Rothkamm et al, 2003; Saleh-Gohari & Helleday, 2004) and various cell cycle regulatory mechanisms interact with HR processes to ensure this temporal specificity. HR is a more complicated and time consuming affair compared to NHEJ due to the requirement for DNA processing in order to generate tracts of single stranded DNA (ssDNA). Therefore it is not surprising that cell cycle regulation plays an integral role within HR. I will discuss basic mechanism of HR and its relationship to the ATM/Chk2 and ATR/Chk1 pathways below (see also 1.3).

The MRN complex, meiotic-recombination protein-11 (MRE11), RAD50 and Nijmegen-breakage-syndrome (NBS1) (MRE11/Rad50/NBS1) plays an important role in the early response to DSBs by binding DNA ends. NBS1 interacts with ataxia telengectasia mutant (ATM) (see 1.3.1) which promotes recruitment of ATM to DSBs (Gatei et al, 2003). Carboxy-terminal-interacting protein (CtIP) together with breast cancer 1 (BRCA1) (Sartori et al, 2007; Yun & Hiom, 2009) and ATM (Ciccica & Elledge, 2010), function to activate the MRE11 endo- and exonuclease activity to resect DNA at damaged sites to generate 3' single-stranded tails [reviewed by (Pallis & Karamouzis, 2010)]. Exonuclease 1 (EXO1), bloom (BLM) and Artemis are also thought to play roles in promoting efficient DNA resection [reviewed by (Ciccica & Elledge, 2010)], whereas p53-binding protein 1 (53BP1) may exert a negative effect (Bunting et al, 2010). The ssDNA formed by

resection then becomes coated with RPA which promotes strand stabilization. BRCA2 subsequently promotes recruitment and displacement of RPA by RAD51 to form the nucleofilament that initiates strand invasion into the homologous sequences of the sister chromatid. A displacement loop (D loop) is formed during strand invasion between the invading 3' ssDNA and the homologous chromosome after which DNA polymerase catalyses the formation of newly synthesized DNA to achieve repair. Because ATM and Rad3 related protein (ATR) (see 1.3 and 1.3.2) is activated through recruitment onto RPA coated ssDNA in association with ATR interacting protein (ATRIP), ATR activation in response to DSBs is also intimately linked to DNA strand resection and thus dependent on ATM and the MRN complex. In contrast, activation of ATR by replication arrest does not depend on strand resection or ATM-MRN, since in this situation ssDNA is created directly by uncoupling of the replicative DNA polymerase and MCM helicase activities (Byun et al, 2005).

In summary, the ATM/ Chk2 pathway is activated directly by DSBs whereas ATR/Chk1 is activated by ssDNA. Not all DNA damage lesions therefore activate ATR/ Chk1 signalling directly. In the context of DSBs, ssDNA generated via ATM and MRN-dependent strand resection is the key intermediate in initiating both ATR/Chk1 activation and HR.

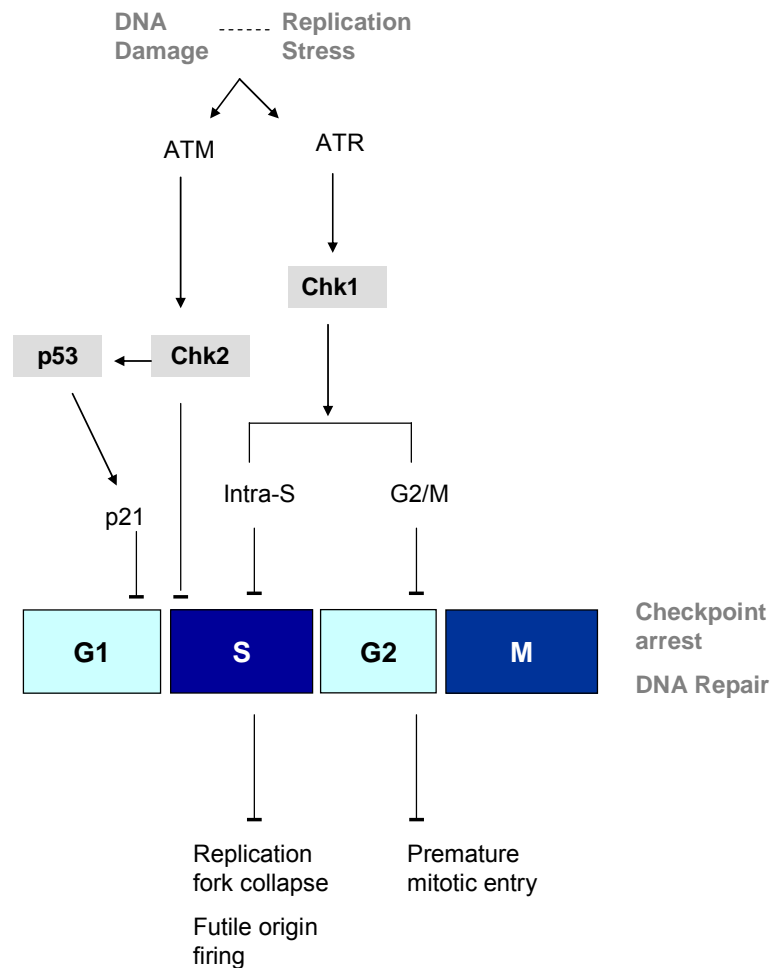


Figure 1 - Cell Cycle Checkpoint – ATR/Chk1 and ATM/Chk2

In the presence of DNA damage and/or replication stress, highly conserved protein kinases mediate signals between checkpoint sensor proteins and their effectors. The earliest intermediary signals involve ATM (ataxia telangiectasia mutant) and ATR (ATM and Rad3 related) which activate the downstream serine/threonine kinases respectively Chk1 and Chk2 respectively. Subsequent activation of cell cycle checkpoints delay progression at the S-M and G2-M phases which allow DNA repair processes to occur.

1.3. Cell Cycle Checkpoints

An orderly progression through each cell cycle phase allows time for completion of DNA synthesis in S phase and alignment and segregation of chromosomes prior to division into daughter cells in mitosis. When replication errors occur or mutations are caused by exogenous sources, then time is required for repair to be completed (see 1.2). Premature exit from S-phase or mitosis is highly likely to lead to DNA damage and mutations being propagated in the daughter cells [reviewed by (Carr, 2002)] and this is not considered a desirable outcome. Cell cycle checkpoints therefore play a crucial function in dividing cells as they detect such errors and via downstream signalling cascades slow and halt replication in order for repair to occur [reviewed by (Ciccio & Elledge, 2010; Jackson & Bartek, 2009; Smith et al, 2010)]. There are checkpoints active at various cell cycle stages including at the G1/S boundary, G2/M checkpoint (Zachos et al, 2003b) and at the spindle checkpoint in early mitosis (regulating attachment and tension at tubules at kinetochores prior to anaphase) (Zachos et al, 2007) - see Figure 1.

Highly conserved protein kinases mediate signals between checkpoint sensor proteins and their effectors when DNA aberrations are present. The crucial intermediary signals involve ATM (ataxia telangiectasia mutant) and ATR (ATR and Rad3 related protein) which activate the downstream serine/threonine kinases respectively checkpoint kinase 1 (Chk1) and Chk2 respectively. ATR and ATM are large kinases homologous to the phosphatidylinositol 3-kinases family of kinases (PI3K) without lipid kinase activity but instead phosphorylate proteins (Kastan & Bartek, 2004). ATM/Chk2 seem to be primarily activated following double strand DNA damage whereas ATR/Chk1 is activated by ssDNA [reviewed by (Bartek et al, 2004; Kastan & Bartek, 2004; Smith et al, 2010)]. There is emerging data to suggest a degree of crosstalk between both pathways (Wakabayashi et al, 2008; Zaugg et al, 2007). Under physiological conditions, the ATM/Chk2 pathway is not essential for cellular division as humans and mice lacking either ATM or Chk2 are viable (Shiloh & Kastan, 2001; Takai et al, 2002). This contrasts with ATR/Chk1 pathway where embryonic lethality is observed in

ATR and *chk1* null mice (Brown & Baltimore, 2000; Lam et al, 2004; Zhou & Bartek, 2004).

1.3.1. ATM/Chk2

ATM is thought to exist as homodimers in its inactive state. In response to DNA damage, ATM undergoes a conformational change which stimulates its kinase domain to auto-phosphorylate Serine 1981 which leads to dissociation of the ATM homodimer producing the active monomer (Bakkenist & Kastan, 2003). The initial signal for ATM activation is still unclear but may be linked to changes in higher order chromatin structure (Kim et al, 2009) in addition to signals originating from the DSB itself. This was also noted by earlier studies that showed global ATM activation in cells almost immediately in response to DSBs and not just focally at damage sites (Bakkenist & Kastan, 2003). Although Serine1981 was the first autophosphorylation site to be described but subsequent studies showed that it was non-essential in knockout mice (Pellegrini et al, 2006) and other autophosphorylation sites have been shown to be important in ATM activation (Kozlov et al, 2006).

As previously discussed (see 1.2) although not entirely understood, a key player in sensing DSB is the MRN complex (Ljungman, 2005; Usui et al, 1998). ATM monomers are then recruited to DSB via interactions with the MRN complex (Lee & Paull, 2005). ATM kinase targets downstream activators such as p53 (Lee & Paull, 2005), H2AX (Burma et al, 2001), 53BP1 (DiTullio et al, 2002), BRCA1 (Cortez et al, 1999) and Chk2 (Matsuoka et al, 1998) to promote key components of DNA damage response to localize at DSBs and mediate checkpoint activation. ATM phosphorylates Chk2 on Thr68 (Ahn et al, 2000) and this leads to homodimerisation involving binding with the fork head associated (FHA) domain (Li et al, 2002). Dimerisation is required for the activation of the kinase domain through loop autophosphorylation (Cai et al, 2009; Schwarz et al, 2003; Xu et al, 2002). Known Chk2 substrates include p53 (Chehab et al, 2000; Hirao et al, 2000), BRCA1 (Lee et al, 2000) and CDC25 (Falck et al, 2001).

Activation at G1 and S-phase is achieved by ATM/Chk2 (and ATR/Chk1) via phosphorylation of Cdc25A at Serine 123 which targets it for degradation (Falck et al, 2001) prevents dephosphorylation of Cdk2. Chk2 is known to stabilise p53 (Chehab et al, 2000) and [reviewed by (Riley et al, 2008)] and promote transcription of p21 in response to DNA damage (Hirao et al, 2000). Cdk2 activity is required for progression at the G1/S boundary (Tsai et al, 1993). p21 has been shown to inhibit Cdk2-cyclin E activity and thus restrain progression into S-phase (Stewart et al, 1999) and reviewed by (Abbas & Dutta, 2009). In addition, Chk2 appears critical in inducing apoptosis following ionizing radiation as Chk2^{-/-} thymocytes are resistant to apoptosis and do not activate p53 (Hirao et al, 2000). Chk2 is also shown to phosphorylate CDC25C (Ahn & Prives, 2002) which leads to inactivation of Cdk1 which is key at the G2/M boundary. However, the evidence for Chk2 playing a major role in the G2/M checkpoint is not extensive [reviewed by (Naim & Rosselli, 2009)] at least compared to the central role played by Chk1 here.

1.3.2. ATR/Chk1

The ATR/Chk1 pathway is activated most strongly when encountering DNA replication stress and ssDNA generation [reviewed by (Cimprich & Cortez, 2008; Smith et al, 2010)] and as previously discussed (see 1.2), has a central role in responding to external DNA damage particularly in cooperation with HR DNA repair. Replication stress maybe encountered due to misincorporation/mismatch pairing of nucleotides or direct damage caused by exogenous agents on newly synthesized strands [reviewed by (Cox et al, 2000)].

The ATR/Chk1 checkpoint response is important in :

- 1) Preventing replication fork collapse and maintain replication fork viability in S-phase to allow resumption of DNA synthesis when conditions permit
- 2) Preventing futile origin firing in S-phase (eg. when newly formed forks cannot elongate)

3) Preventing premature entry into mitosis because incompletely replicated DNA and premature chromosome condensation or segregation lead to the propagation of mutations and/or cell death.

Single-stranded DNA (ssDNA) becomes coated by replication protein A (RPA) to create a platform for the recruitment of the ATR-interacting-protein ATRIP-ATR complex (Zou & Elledge, 2003). The concomitant loading of other factors – such as DNA topoisomerase binding protein-1 (TopBP1) (Delacroix et al, 2007; Kumagai et al, 2006), the 9-1-1 complex (Delacroix et al, 2007) and claspin (Kumagai & Dunphy, 2000; Kumagai & Dunphy, 2003) cooperate with ATR to achieve efficient phosphorylation of Chk1 by ATR. It is important to note that DSB can activate the ATR/Chk1 pathway but this requires prior processing of the breaks to generate ssDNA for example during NER or HR [reviewed by (Smith et al, 2010)]. ATR phosphorylates Chk1 at multiple sites within its C-terminal regulatory domain but most notably at serine 317 and serine 345 which are often used as surrogate indicators for Chk1 activity. However, only serine 345 phosphorylation seems to be critical for actual Chk1 biological activity (Niida et al, 2007; Walker et al, 2009) and it is still unclear how Chk1 phosphorylation events influence catalytic activity. There is some evidence that Chk1 release from chromatin following phosphorylation at Ser 317 and/or Ser 345 is required for its activity (Smits et al, 2006).

Chk1 phosphorylation inhibitory targets include CDC25A (Sorensen et al, 2003) and CDC25C (Blasina et al, 1999). CDC25A is targeted for ubiquitin mediated degradation (Falck et al, 2001) and phosphorylation of CDC25C at Serine 123 promotes binding with 14-3-3 leading to cytoplasmic sequestration (Peng et al, 1997). The CDC25 family of proteins are of course important in progressing the cell cycle by targeting Cdk1 for dephosphorylation/activation (see 1.1.1.4). Chk1 activating phosphorylation of Wee1 results in inhibition of Cdk1 activity and delayed progression at the G2/M checkpoint (Rowley et al, 1992). Other positive Chk1 phosphorylation targets include BRCA2 (Bahassi et al, 2008) and RAD51 (Bahassi et al, 2008; Sorensen et al, 2005) which promote HR DNA repair. More recently Nakanishki and colleagues have shown a novel role for Chk1 in Histone H3 Threonine 11 phosphorylation which represses transcription of pro-cell cycle factors such as cyclin B/A/E and Cdk1 in response to DNA damage (Shimada et al, 2008).

When DT40 cells are treated with the DNA polymerase inhibitor aphidicolin, Chk1 phosphorylation (at Serine 345) results in cells being able to delay entry into mitosis for prolonged periods (Lopez-Girona et al, 2001; Zachos et al, 2005). However, when aphidicolin is added to Chk1 knockout mutants, an initial delay is observed for up to 9 hours but the cells eventually progress into mitosis. A large proportion of these cells exhibit 2N and sub-4N DNA content indicating mitotic entry prior to completion of DNA replication (Zachos et al, 2005). Thus Chk1 appears important for sustained but not initial S-M checkpoint activation. When Chk1^{-/-} cells are arrested for >4 hrs in aphidicolin and then released, they demonstrate a loss of viability of replication forks and cannot resume synthesis when released (Zachos et al, 2003b). Also new (futile) origin firing occurs in these Chk1 deficient cells. When blocked for >8hrs, a significant decrease in clonogenic survival and increased cell fragmentation is observed. Inhibition of the ATR/Chk1 pathway has been shown to result in DSBs (Syljuasen et al, 2005) and activation of p38 mediated S-phase checkpoint and apoptosis (Jirmanova et al, 2005). Consistent with these results, Chk1^{-/-} cells were viable but proliferated more slowly and exhibited higher levels of spontaneous apoptosis by Annexin V staining (Zachos et al, 2003b). In response to ionizing radiation (IR) DT40 cells activate Chk1 and accumulate in G2. However, Chk1 deficient DT40 cells (Zachos et al, 2003b), as well as conditional knockout mouse cells (Liu et al, 2000b), demonstrated premature mitotic entry (phospho-Ser10 histone H-3 staining) and continued cell cycling. Consequently Chk1 deficient cells were hypersensitive to killing by IR via with evidence of premature mitotic entry in the presence of incompletely replicated or repaired DNA (Zachos et al, 2003b).

1.4. The Role of Chk1 and Other DNA Damage Checkpoints in Either Preventing or Treating Cancer – Opposing Paradigms

1.4.1. Checkpoints as a Barrier to Tumorigenesis

During the transformation of normal cells into cancer cells, incipient tumours often need to acquire multiple oncogenic mutations (see Figure 2). These can evoke counter-responses by tumour suppressor mechanisms to engage senescence or apoptosis in order to halt carcinogenesis. Cell cycle checkpoint and DNA damage response proteins are thought to play a major role in this process (Bartkova et al, 2005; Bartkova et al, 2006; Gorgoulis et al, 2005). In a study by Bartkova et al (Bartkova et al, 2005), early tumours (carcinoma in situ or early T1 lesions) were found to high constitutive expression and activation of DNA damage response proteins including ATM/Chk2, H2AX, p53. In contrast, more advanced tumours (T2-4) appear to have lower levels of staining. Functional loss of these pathways was then shown to precede the presence of increased genomic instability as assayed by genome-wide SNP array analysis. *In vitro* overexpression of cyclin E, Cdc25A and E2F1 induced DNA damage responses in U2OS cells. The authors postulate that mutations affecting checkpoint function, particularly those affecting the ATM–Chk2–p53 pathway, confer inordinate survival advantage and promote genomic instability and tumour progression. In another study by Gorgoulis et al (Gorgoulis et al, 2005) they observed activation of DNA damage response proteins and checkpoint pathways in a panel of human non-small cell cancer and preneoplastic and neoplastic melanoma lesions. In hyperplastic tissue, 53BP1 was present in a discrete nuclear localization, histone H2AX and Chk2 were phosphorylated, and apoptosis observed, all signs of ongoing/active DNA damage response. However, in more advanced disease, there were several tumours that displayed a suppression of apoptosis accompanied by lack of 53BP1 localization, presence of p53 mutation, lack of Chk2 phosphorylation but a persistence of histone H2AX phosphorylation. Finally Bartkova et al (Bartkova et al, 2006) reported that

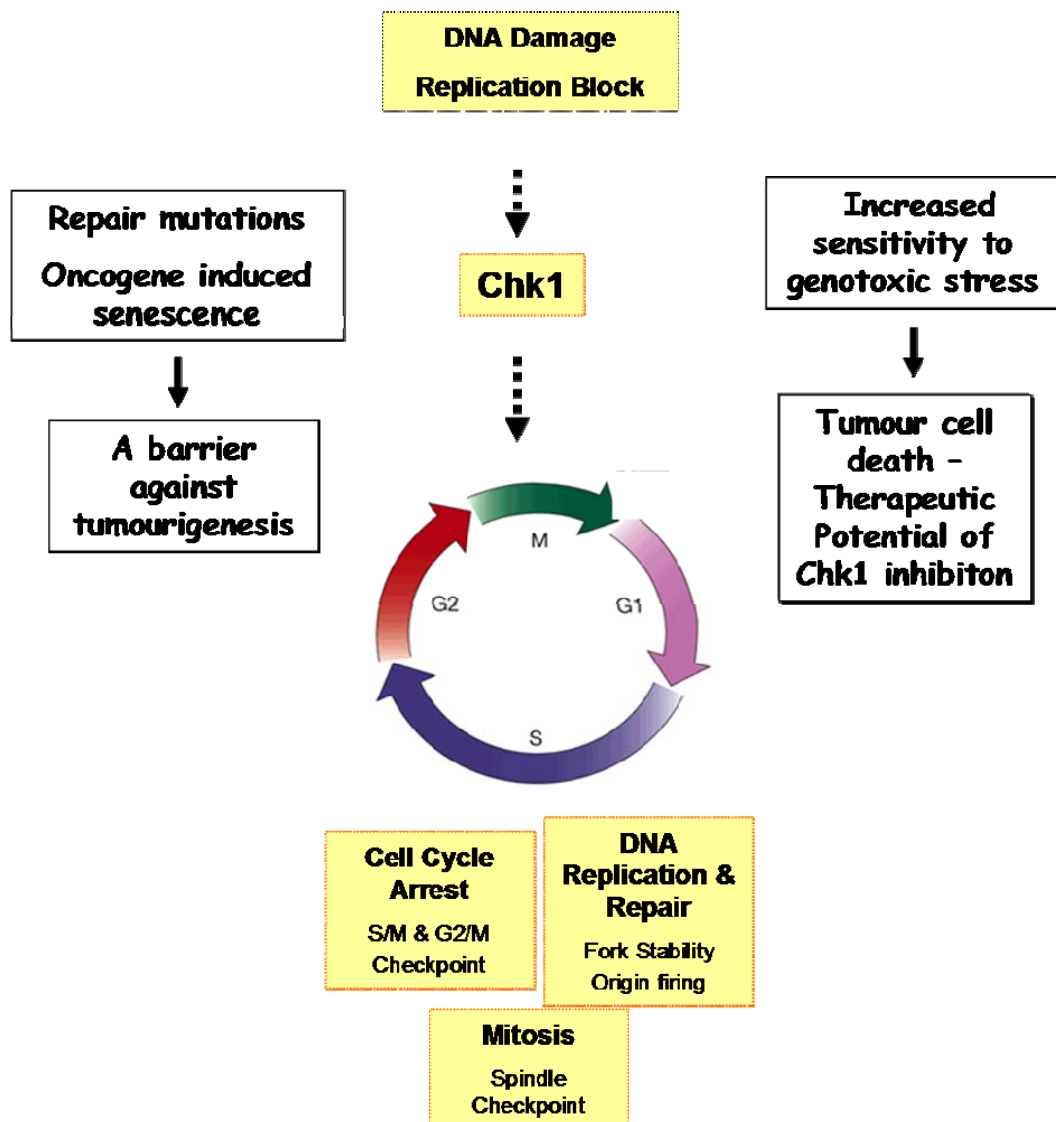


Figure 2 - The Role of Chk1 and Other DNA Damage Checkpoints in Either Preventing or Treating Cancer – Opposing Paradigms

During the transformation of normal cells into cancer cells, incipient tumours acquire multiple oncogenic mutations. These can evoke counter-responses by tumour suppressor mechanisms to engage senescence or apoptosis in order to halt carcinogenesis and DNA damage response proteins are thought to play a major role in this process. On the other hand it has been shown that loss of cell cycle checkpoints can enhance tumour cell death and thus, has been proposed as a novel anti-cancer strategy. Whereas most studies have focussed on the ATM/Chk2 pathway, relatively less is known about the potential role of the ATR/Chk1 pathway.

oncogene induced senescence may represent a tumorigenesis barrier mechanism initiated by DNA damage checkpoints. They show that oncogene induced senescence is commonly associated with precancerous lesions and in cancer cells, *mos*, *cdc6* and cyclin E over expression led to activation of the DNA damage checkpoints and the presence of senescence associated β -galactosidase activity. U2OS cells expressing cyclin E were assayed with IdU and CldU to distinguish ongoing and newly fired replication forks and this demonstrated an increase in DNA DSBs and prematurely terminated replication forks. In tumour cells injected into SCID mice, inhibition of ATM resulted in suppressed activation of cell cycle checkpoints and led to larger and more invasive tumours. When human cancer paraffin-embedded tissue was studied, progression from preneoplastic lesions to more aggressive tumours was associated with decreased expression of markers for senescence and cell cycle checkpoint activation and these two factors demonstrated close co-segregation.

Whereas most studies have focussed on the ATM/Chk2 pathway, relatively little is known about the potential role of the ATR/Chk1 pathway as a barrier to carcinogenesis [reviewed by (Smith et al, 2010)]. In contrast to ATM/Chk2/p53, complete loss of Chk1 appears to be a very rare event in tumorigenesis. Instead Chk1 appears to be upregulated in various tumour types (Sriuranpong et al, 2004; Stawinska et al, 2008; Tort et al, 2005; Verlinden et al, 2007) and has only shown to be downregulated in only one study within a small group of highly aggressive lymphomas (transcriptionally and post-transcriptionally) (Tort et al, 2005). *Chk1* mutation has rarely been reported (Bertoni et al, 1999; Kim et al, 2007). This suggests that Chk1 function might be particularly important for tumours, even into the latter stages of cancer development. Extrapolating from what we already understand about Chk1 function, presumably Chk1 is playing a role in maintaining DNA repair/orderly cell cycle progression competence in the face of genotoxic stress. It has been suggested that reliance on the ATR/Chk1 pathway may be (Zhou & Bartek, 2004) marked in cancer cells since p53 function is commonly lost in advanced cancers and as recent evidence suggests, so is ATM/Chk2 function (Bartkova et al, 2005; Gorgoulis et al, 2005). According to our current understanding, it is not clear if the loss of Chk1 will promote the development of more aggressive tumours or instead, cause tumour cell death due to loss of competence for genomic replication (see Figure 2).

1.4.2. Therapeutic Potential of Chk1 Inhibition

Whilst checkpoints may have an important role as a barrier against cancer progression, it has also been shown that Chk1 inhibition can be an effective means to enhance tumour cell death and thus, has been proposed as a novel anti-cancer strategy (Dai & Grant, 2010; Zhou & Bartek, 2004) (see Figure 2). Whilst a cell is undergoing DNA replication, this is particularly sensitive period when replication errors or DNA damage if not repaired, may lead to genomic instability and cell death. To overcome this, checkpoint responses are engaged to allow replication forks to stall, undergo repair and restart synthesis (Jackson & Bartek, 2009). Chk1 is central in mediating the S-phase and G2/M checkpoint delay (Zachos et al, 2003b; Zachos et al, 2005) in response to a wide variety of genotoxic anti-cancer therapies (Zhou & Bartek, 2004). Taking this forward therapeutically it suggests that Chk1 inhibition in combination with the delivery of chemotherapy and radiotherapy has the potential to overcome the natural defences of tumour cells thus causing lethality.

As approximately 50% of cancers are thought to have an inactivated p53 pathway (Zhou & Bartek, 2004) and that a significant proportion have defects in the ATM/Chk2 pathway (Bartkova et al, 2005; Bartkova et al, 2006; Gorgoulis et al, 2005), this creates a situation where cancer cells are deficient G1 checkpoint which hampers the tumour cell's ability to arrest in response to genotoxic stress. As discussed previously (see 1.4.1) studies have also shown a role for intact checkpoint pathways in mediating oncogene induced senescence thereby preventing early and incipient tumours (Bartkova et al, 2005). Thus it has been postulated that when other defects in checkpoint pathways already exist, these cancer cells become extremely reliant on Chk1 in order to respond to DNA damage (Dai & Grant, 2010; Zhou & Bartek, 2004). Therefore the strategy of Chk1 inhibition may have the advantage of preferentially sensitizing tumour cells, as opposed to normal tissue which does not have p53 inactivation, to DNA damage thus achieving a desirable therapeutic ration between tumour cell death and acceptable side effects on normal tissue.

This idea is beginning to be tested in the clinic. UCN-01 originally a well-known laboratory checkpoint inhibitor and protein kinase C inhibitor (PKC) was tested as a single agent in early phase clinical trials (Sausville et al, 2001) and in combination with various chemotherapy drugs (Edelman et al, 2007; Jimeno et al, 2008; Welch et al, 2007). There was some early indication of anti-tumour activity but disappointingly the toxicity profile was unacceptable with dose-limiting toxicities of pulmonary dysfunction, nausea and vomiting, and metabolic acidosis observed. It has been shown subsequently that an unusual pharmacokinetic profile with a prolonged elimination time due to increased plasma protein binding and also the fact it was not a “clean” kinase inhibitor (it targeted PKC as well) might have explained the results (Mackay & Twelves, 2003). More recently, a new generation Chk1 inhibitors with an improved pharmacokinetic profile and enhanced Chk1 selectivity are being developed and several are on the cusp of entering Phase I clinical trials (Dai & Grant, 2010; Garber, 2005; Tao & Lin, 2006). The results of these agents are eagerly awaited.

1.4.2.1. Synthetic Lethality

Synthetic lethality is where mutations in two genes individually have no deleterious effect on the organism, but combining the mutations leads to death (Dobzhansky, 1946). In the context of the delivery of DNA damaging agents to destroy cancer cells, the concept of synthetic lethality relies on the knowledge of particular genetic profiles in the tumour and delivering appropriate therapy to take advantage of an inability to respond to and repair DNA damage [reviewed by (Kaelin, 2005) and (Chalmers et al, 2010)]. This concept can be illustrated in human gliomas where O⁶-methylguanine-DNA methyltransferase (MGMT) protects tumours against methyl/alkyl damage. Utilising a one step, direct repair mechanism, MGMT transfers the methyl/alkyl group from the O⁶ position of guanine onto the cysteine residue found in its catalytic pocket (Pegg, 2000). This process occurs at a one to one ratio (enzyme to DNA lesion) and will irreversibly inactivate MGMT. In recent clinical trials the addition of temozolomide to radiation has been shown to significantly improve outcomes in glioblastoma multiforme a disease in which outcomes have remained poor for many decades (Stupp et al, 2005). Indeed in the trial at 5 years, there were up to 10% of patients alive and this has never been seen before. Temozolomide is a classical alkylating agent that alkylates DNA with particular affinity to the O⁶ position of

guanine. On closer analysis of the trial data, it appears that the patients who had epigenetic silencing of MGMT derived significant benefit from the addition of temozolomide in contrast to the non-silenced group (Hegi et al, 2005). Therefore, we are now able to identify glioma patients who are susceptible to alkylating agent damage and by adding temozolomide to radiotherapy achieve even more effective killing of cancers leading to a dramatic improvement in outcomes. Another recent example is PARP inhibition in BRCA1 patients (Chalmers et al, 2010; Fong et al, 2009). PARP is a key component of base excision repair (discussed in 1.2) and BRCA1 is essential in HR (discussed in 1.2). Here in tumours already known to be defective in responding to DNA damage such as platinum intra-strand crosslinking (Taniguchi et al, 2003) and HR repair (Bunting et al, 2010), targeting these cells by inhibiting a separate DNA repair pathway (ie. base excision repair) achieves enhanced cell killing (Farmer et al, 2005; Loser et al, 2010; Rottenberg et al, 2008) and dramatic clinical results in research trials (Audeh et al, 2010; Fong et al, 2009).

As it pertains to Chk1 inhibitor, the concept of synthetic lethality applies because the majority of cancer cells are already deficient in some components of checkpoint pathway activation (discussed in 01.4.2) and by removing the ATR/Chk1 axis this would potentially sensitize these cells to lethality using a number of conventional anti-cancer drugs. Furthermore due to the apparent reliance of cancer cells on the ATR/Chk1 pathway compared to the normal cells, the latter could potentially be spared cytotoxicity thus achieving a favourable therapeutic ratio (discussed in 01.4.2).

1.5. *Chk1* Mouse Models

Chk1 knockout mice (Lam et al, 2004; Liu et al, 2000b) have been generated by ES cell gene targeting, where homologous recombination with the targeting vector replaced 3kb of *chk1* containing exons 2 to 5 which encodes the initiator methionine, the “GxGxxG” ATP-bonding motif and half of the kinase domain. Chimeras were bred to produce germ-line transmission. When *chk1*^{+/-} heterozygotes were intercrossed, complete *chk1*^{-/-} knockout offspring were never observed due to embryonic lethality around E3.5 to E7.5 (Lam et al, 2004; Liu et al, 2000b). *In utero* examination revealed empty deciduas and remains of resorbed embryos were often observed at E6.5 to E7.5. Analysis of early blastocysts at E3.5 showed grossly abnormal morphology and increased apoptosis which appears independent of p53 (evidence obtained when *chk1* knockout mice were crossed with *p53*^{-/-} mice). This suggests that *chk1* is required for the survival of cells during embryonic development.

Conditional knockouts were therefore necessary to study the effect of complete absence of *chk1*. *Chk1*^{+/-} ES cells were targeted with a construct containing *loxP* sites flanking exon 2 where the translational initiation sequence and ATP-binding site of the kinase are found (Liu et al, 2000b). No viable clones were obtained from *chk1*^{flox/-} ES cells after undergoing Cre-*loxP* mediated excision. Analysis of DNA content by FACS revealed a significant sub-G1 population at 72 hours post recombination. In the interim, these cells exhibited defective G2/M DNA damage checkpoint in response to ionising radiation and entered mitosis prematurely. In *chk1*^{flox/+} ES cells, Cre-*loxP* mediated excision resulted in viable *chk1*^{Δ/+} cell lines. *Chk1*^{+/-} heterozygous mice were healthy, fertile and tumour free up to 1.5 years (Liu et al, 2000b). To determine if allelic loss of *chk1* could enhance tumour formation, *chk1*^{+/-} mice were crossed to *WNT-1* transgenic mice, driven by a mammary specific promoter, MMTV. Heterozygous mice showed a modest and only marginally statistically significant increase in tumourigenesis compared to the wild type (WT). Southern blot assays noted that none of the tumours were found to have loss of heterozygosity (LOH) of *chk1*, and the authors postulate that the possible explanation being homozygous lethality when *chk1* is completely absent.

Due to embryonic lethality as a result of constitutive *chk1* loss, as is the case in cell lines, conditional knockouts have been employed to investigate the biological consequences of gene deletion in adult mice. This has been modelled in 3 different physiological systems - the mammary gland (Lam et al, 2004), gut (Greenow et al, 2009) and thymus (Zaugg et al, 2007). As described above (Liu et al, 2000b), the same *loxP* system flanking exon 2 of *chk1* was used- these mice being termed *chk1flox* mice. Cre-mediated recombination was possible in different tissue types by using tissue specific promoters to drive Cre expression.

Lam et al (Lam et al, 2004) used a system where Cre is expressed under the control of a mammary specific WAP (whey acid protein) promoter which allows conditional *chk1* deletion in somatic lobuloalveolar precursor cells in the mammary gland. This achieved 50-60% recombination during day 10 of pregnancy and a further 10-15% at the beginning of lactation. Complete *chk1* loss resulted in impaired development of mammary cells, increased apoptosis and non-viability by day 11. Hemizygous loss only marginally impaired mammary cell development and survival. However, hemizygous cells displayed marked cell cycle dysregulation with premature entry into mitosis (with incompletely replicated DNA) and greater levels of endogenous DNA damage. From these results, the authors inferred that *chk1* hemizygosity revealed a haploinsufficient tumour suppressor role by virtue of the presence of multiple defects relating to cell cycle regulation potentially increasing the propensity for propagating carcinogenic mutations. However they did not go on to demonstrate the presence of genomic instability in *chk1* deficient tissues *in vivo* nor if the cell cycle aberrations they observed *in vitro* translated into a phenotype in mice or increase in tumour development. Therefore although a haploinsufficient tumour suppressor effects is inferred from their *in vitro* data it has not been clarified whether *chk1* loss complete or hemizygous, promotes carcinogenesis (Liu et al, 2000a) or alternatively causes death of incipient cancer cells and acts as a barrier for cancer formation (Bartkova et al, 2005; Bartkova et al, 2006; Gorgoulis et al, 2005) (see 1.4).

Greenow et al (Greenow et al, 2009) investigated the effect of *chk1* loss in gut epithelium. The mice they used were gifted by our laboratory (Prof David Gillespie, Beatson Institute for Cancer Research - see 2.1 and 2.2) and were crossed with mice expressing Cre under the control of a CYP1A1 (*AhCre*)

promoter. Genetic recombination was achieved after treatment with β -naphthoflavone intraperitoneally. The investigators noted efficient *chk1* deletion in the gut as evidenced by a marked reduction in Chk1 mRNA expression and western blot analysis. An increase in the presence of the recombined allele was also demonstrated by semi-quantitative PCR of genomic DNA. Recombination resulted in intestinal crypt death, DNA damage and p53 induction. However, after an initial peak of recombination detected at around day 2 (D2), Chk1 expression returned in the tissue and was restored by D5 and D21. The authors concluded that unrecombined cells repopulate the tissue after death of the *chk1* recombined cells. Overall the mice remained viable, without any apparent gross pathological changes suggesting that repopulation was able to maintain intestinal homeostasis. In contrast, the authors observed that *chk1* excision in the liver was not accompanied by a similar repopulation phenomenon and that recombination persisted even up to 35 weeks. It was suggested that *chk1* loss is tolerated better in post mitotic organs such as the liver and this might be explained because *chk1* is essential only in actively cycling cells which is predominant in the intestine.

Finally Zaugg et al (Zaugg et al, 2007) bred the conditional *chk1* mice to Lck-Cre mice which causes T-cell lineage specific recombination in the thymus gland. Their findings were in agreement with the other studies described. The investigators observed that *chk1* was essential for thymocyte development and that its absence resulted in apoptosis. When crossed to a *bcl2*-tg background they did not observe an increase in tumourigenesis associated in *chk1*^{flox/flox} animals but the authors did not go on to establish the *chk1* status of the tumours nor did they report the observation of a repopulation phenomena (Greenow et al, 2009).

1.6. Murine Skin as an Experimental Model

The skin is the largest organs found in mammals with both neuroectodermal and mesodermal lineages contributing to its structure. The epithelium consists of keratinocytes, merkel cells, melanocytes and Langerhans cells (Schmidt-Ullrich & Paus, 2005). Mitosis in the basal layer of the epidermis produces skin cells which move up the strata changing shape and composition and eventually die due to isolation from their blood source. Various cytoskeletal proteins or keratins are expressed in these cells which can be used as markers for identifying the various layers of the epidermis; for example keratin-14 or K14 (Arin et al, 2001) is expressed in keratinocytes in the basal layer of the epidermis, the outer root sheath of the hair follicle and the sebaceous gland and also in epidermal stem cells and multipotent stem cells that reside in the bulge region of the hair follicle (Tumbar et al, 2004). I will describe genetic manipulation using a K14 promoter [(Li et al, 2000; McLean et al, 2004) see 3.1.3] to drive expression of certain genes within specific layers of the skin in this thesis. The skin is amenable for experimentation as it presents an externally accesible organ which can be visualised directly in living mice and a variety of procedures can be performed without the need for invasive surgery.

1.6.1. The Two Stage DMBA/TPA Skin Carcinogenesis Protocol

In this thesis I utilise the two-stage DMBA/TPA tumour initiation and promotion protocol (see Figure 3). This is a well described and proven model for studying the evolution of tumours in mouse skin (Kemp, 2005; Perez-Losada & Balmain, 2003; Quintanilla et al, 1986). It involves treating the dorsal skin with an initiating dose of DMBA (7,12-dimethyl-benz[a]anthracene) (Berenblum & Shubik, 1949) as a single application typically, followed by multiple applications of tumor promoter TPA (12-O-tetra-decanoyl-phorbol-13-acetate) (Roe et al, 1972) over several months. This gives rise to benign, pre-malignant papillomas, which

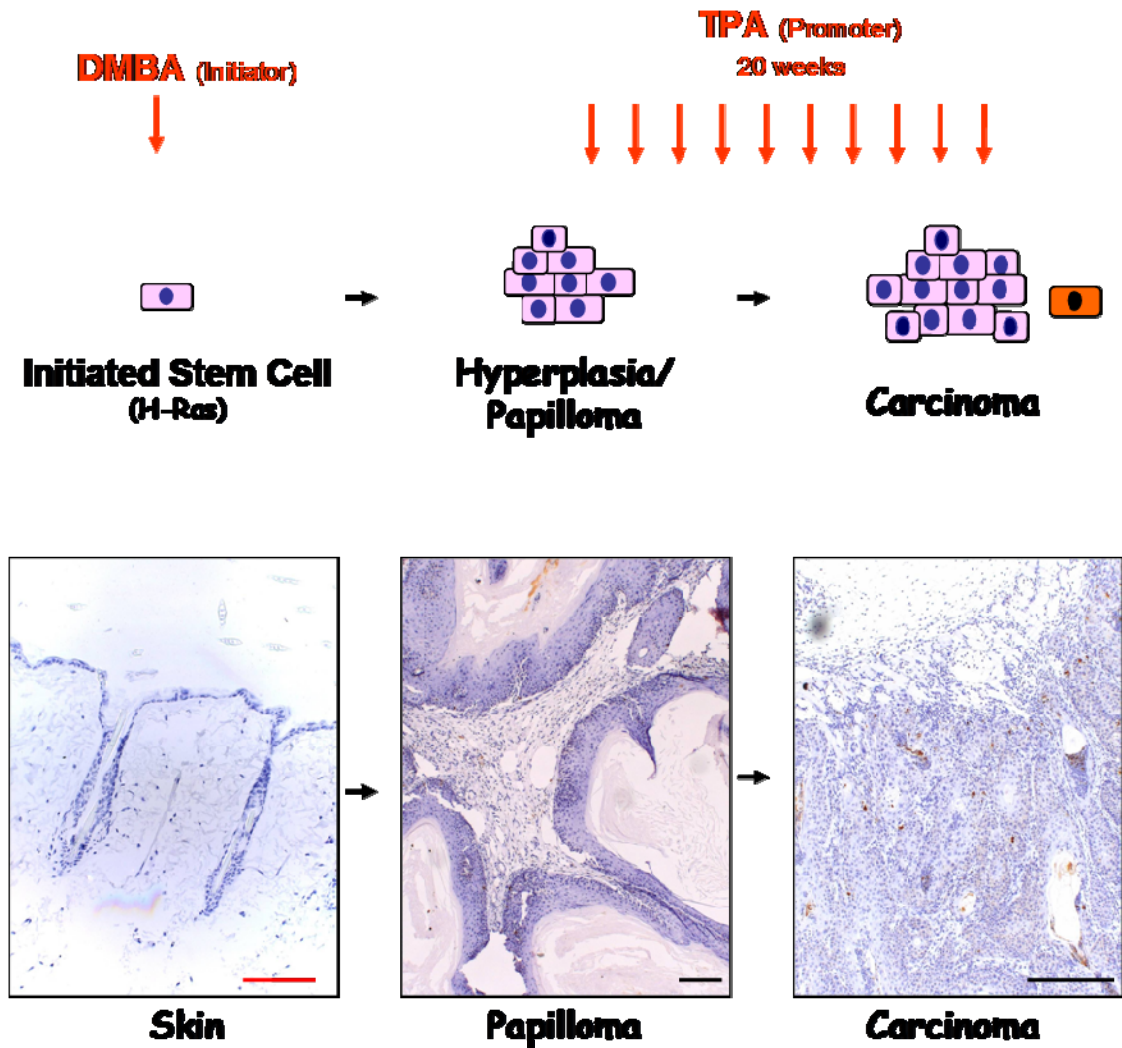


Figure 3 - DMBA/TPA Chemical Carcinogenesis Protocol

The two stage DMBA/TPA tumour initiation and promotion protocol is a well described and proven model for studying the evolution of tumours in mouse skin (Kemp, 2005; Perez-Losada & Balmain, 2003). It involves treating the dorsal skin with an initiating dose of DMBA (7,12-dimethyl-benz[a]anthracene) as a single application typically, followed by multiple applications of tumor promoter, TPA (12-O-tetra-decanoyl-phorbol-13-acetate) over several months. This gives rise to hyperplastic epidermis and stroma and outgrowths of pre-malignant papillomas. With continued TPA promotion, these lesions enlarge and a small percentage of papillomas transform into malignant, invasive squamous cell carcinomas. [Scale bars represent (black) 200 μ m and (red) 100 μ m]

comprise hyperplastic epidermis and stroma. With continued TPA promotion, these lesions enlarge and a small percentage of papillomas develop into malignant, invasive squamous cell carcinomas. The number, size, and growth rate of these tumors is readily quantified and the tumours harvested for further laboratory analysis. Various pharmacological treatments or genetic manipulations can be built into the protocol to test their effect on the different stages of carcinogenesis - namely to test the effects of experimental manipulation on papilloma initiation and outgrowth or papilloma to carcinoma transition respectively [reviewed by (Kemp, 2005)].

In this protocol the vast majority of tumours produced following DMBA initiation possess a *h-ras* mutation with amino acid change CAA to CTA in codon 61, over 90% (Balmain et al, 1984; Quintanilla et al, 1986). Even though DMBA can induce different types of mutations, eg. *k-ras* (it's mutagenic action is random) it appears that promotion specifically by TPA selects for outgrowth of *h-ras* bearing papillomas. For instance, when the DMBA treated skin is subject to a different method of tumour promotion such as a constitutive overexpression of ornithine decarboxylase (Megosh et al, 1998), less than 50% showed typical codon 61 *h-ras* mutation, instead a variety of *k-ras* mutations were observed in the majority (Megosh et al, 1998). It has been found that in tumours promoted by TPA, there is an associated overexpression of adhesion molecules, keratins, growth factors, cyclins and cyclin-dependent kinases (Owens et al, 1999). The prolonged duration of promotion is conducive for the acquisition of additional genetic mutations, commonly found hits include, *p53* mutation (Burns et al, 1991) and trisomy of chromosome 7 (*h-ras* is found on chromosome 7) (Bianchi et al, 1990). These additional hits appears to be crucial in promoting transformation from benign papilloma into malignant carcinoma (Perez-Losada & Balmain, 2003).

Mice treated with DMBA without subsequent promotion by TPA do not develop tumours or where TPA is discontinued, tumours regressed (Kemp, 2005). Mice only treated with TPA without DMBA likewise do not develop tumours (Boutwell et al, 1982; Perez-Losada & Balmain, 2003). Age of initiation of carcinogenesis appears crucial, the younger the age of commencement, the more papillomas that develop. Mice that commenced DMBA/TPA at ages 6, 44, and 56 weeks, showed a decreasing average number of papillomas per mouse (Van Duuren et

al, 1975). The effect of DMBA initiation can have a long latency period. Even when promotion with TPA is started 1 year after exposure to DMBA, papilloma burden was considerable albeit less than when TPA was started 1 week after initiation (Van Duuren et al, 1975). Taken together, this indicates that increasing age of the mouse at commencement of TPA reduces tumour burden. However, the initiating effect of DMBA persists over a long duration, even if promotion is delayed.

1.7. Stem Cells And Cancer

According to a workshop convened by the American Association for Cancer Research (AACR), the consensus definition of a cancer stem cell is a “cell within a tumor that possesses the capacity to self-renew and to cause the heterogeneous lineages of cancer cells that comprise the tumor” (Clarke et al, 2006). This is essentially a functional definition which has come to rely on *in vivo* growth assays to test the ability of cells to seed tumours in animal hosts. Phenotypic features of cancer stem cells have been well described [reviewed by (Alison et al, 2010; Bomken et al, 2010; Clarke et al, 2006; Lathia et al, 2010; Rosen & Jordan, 2009; Visvader & Lindeman, 2008)]. Cancer stem cells are thought to possess the capacity for self-renewal and longevity. In addition they are thought to possess multipotency and the capability to produce differentiated progeny. Cancer stem cells are said to be able to undergo either asymmetric or symmetrical cell division. The former term refers to a type of cell division that results in a daughter stem cell and another possessing a more differentiated phenotype, lacking tissue regeneration ability. Indeed after transplantation of a suspension of cells enriched for stem cells into an animal host, the resultant tumour often shows loss of this enrichment leading to cellular heterogeneity resembling the original tumour from which the putative stem cells were derived.

1.7.1. Identification of Stem Cells and Markers

Pioneering studies performed by Dick and colleagues (Lapidot et al, 1994) in the 1990s showed that using an *in vivo* assay involving transplantation of acute myeloid leukaemic cells into severe combined immune-deficient (SCID) mice, they were able to isolate a small sub-population of cells (1 in 250,000 cells) that displayed pluripotency and the ability to reconstitute the phenotype of the human disease. The leukaemia-initiating cells were identifiable by surface markers CD34+ve and CD38-ve. However, historically as far back as Furth and Kahn in 1937 (Furth & Kahn, 1937) it had been observed that a single cancer cell was able to cause leukaemia in inoculated mice from the same strain but that only around 5% of inoculations were successful. These and other early studies

along the same lines [(Hewitt, 1953; Ishibashi, 1950; Makino, 1956), reviewed by (Bomken et al, 2010)] established the conceptual paradigm that a hierarchical organisation may exist within tumours whereby only a small but distinct sub-population of cancer cells possess the properties of self-renewal, longevity and the ability to differentiate into multiple cell types and reconstitute the heterogeneity found in tumours.

Extrapolation of these ideas into solid tumour oncology has led to extensive efforts to identify and characterise “cancer stem cells” functionally and molecularly in numerous tumour types. One of the first pieces of *in vivo* experimental evidence in solid tumours was provided by Clarke and colleagues (Al-Hajj et al, 2003) who used a system to grow human breast cancers in the mouse mammary fat pad of non-obese diabetic/severe combined immunodeficient (NOD/SCID) mice. Using limited dilution and flow cytometry techniques they were able to identify a CD44+ve/ CD24-ve/ lo/ lineage-ve (lineage markers: CD2, CD3, CD10, CD16, CD18, CD31, CD64 and CD140b) sub-population of putative stem cells with high engraftment potential. The tumours which arose from these were observed to reflect the phenotypic heterogeneity of the original tumours. In this study, samples were primarily obtained from pleural effusions from patients and in doing so avoided what has become a controversial area in solid tumour work as compared to haematological malignancies - ie. the necessity to dissociate an intact tumour in order to obtain single cells for experimentation. It is unclear and some propose potentially confounding how the process of dissociating the intact tumour to isolate single cells affects cell behaviour or indeed compromises viability [reviewed by (Rosen & Jordan, 2009)]. Another objection to studying solid tumours after disaggregation is the uncertainty about the origin of the cells being investigated and the role within the context of the tissue and host microenvironment (Gupta et al, 2009). Following the delineation of cancer stem cells in breast tumours, this was followed by work in brain cancers where Dirks and colleagues (Singh et al, 2004) using a xenograft NOD/SCID mice implantation assay found that only brain tumour cells positive for CD133 surface markers were able to initiate tumour formation. As few as 100 injected cells could reproduce tumours which could then be serially transplanted, in contrast injecting as many as 10^5 CD133-ve tumour cells did not result in tumour formation.

What both these seminal studies showed was that it was possible to separate a heterogeneous population of cancer cells based on cell surface markers ie. in breast cancer cell CD44+ve/ CD24-ve/ lo/ lineage-ve (Al-Hajj et al, 2003), and in brain cancer cells CD133+ve (Singh et al, 2004), thereby obtaining a small but distinct sub-population with “stem cell” like properties. Following on from this a substantial amount of work was directed at analysing a variety of different tumour types in order to define unique features which mark out cancer stem cells. A summary of markers has been reviewed by (Alison et al, 2010; Lathia et al, 2010; Visvader & Lindeman, 2008). These include, for example, for colon cancer CD133+ve (O'Brien et al, 2007; Ricci-Vitiani et al, 2007), for lung cancer CD133+ve (Eramo et al, 2008), and for head and neck cancer CD44+ve (Prince et al, 2007). In addition to markers found on the cell surface other biological characteristics have also been suggested to identify stem cells. One is the ability of to exclude Hoechst dye (Hoechst₃₃₃₄₂ binds AT rich regions of DNA), enabling living dye-negative cells to be isolated using fluorescence activated cell sorting [(Goodell et al, 1996), reviewed by (Wu & Alman, 2008)]. The Hoechst negative cells are known as a “side” population as they were initially discovered as a small but distinct group on FACS plots. The efflux pumps ATP-binding cassette subfamily G (ABCG) in particular ABCG2 (Scharenberg et al, 2002) and ABCG5 are largely thought to be responsible for this phenomenon (Jonker et al, 2005). ABCG pumps also seem to be involved in conferring chemotherapy resistance via drug efflux capacity (Doyle & Ross, 2003; Kusuhara & Sugiyama, 2007), thus raising the possibility of being able to direct therapy specifically at cancer stem cells. Another marker found to be distinct in both haemopoietic (Pearce et al, 2005) and solid tumours (Ginestier et al, 2007) cancer stem cells is high aldehyde dehydrogenase expression or activity, an enzyme originally studied for its role in detoxifying metabolic waste products particularly in the liver.

Another method of detecting stem cells involves BrdU pulse-labelling neonatal mice followed by extended chase periods (Bickenbach, 1981; Cotsarelis et al, 1990). This reveals the existence of so-called label retaining cells (LRCs) that incorporate BrdU during neonatal tissue development but which subsequently enter quiescence, thus retaining the incorporated label for months or even years. This technique has been widely used to visualise normal stem cells in mouse skin (Bickenbach, 1981; Cotsarelis et al, 1990). I describe the use of this

technique in this thesis (see 2.10 and 5.1.1). Although a well characterised tool for stem cell work in a non malignant context, its use for detecting the cancer stem cells remains unproven. Furthermore, the use of both Hoechst dye staining and BrdU labelling has been criticised due to potential toxicity as a result of incorporation and interference with DNA structure and integrity [reviewed by (Wu & Alman, 2008)]. Another drawback seems to be the inability of isolate BrdU labelled cells for further experimentation [reviewed by (Li & Clevers, 2010)]. Fuchs and colleagues seem to have overcome this limitation by using a doxycycline induced H2B-GFP system and further *in vivo* work was able to be performed (Tumbar et al, 2004). I do not utilise the H2B-GFP system in this thesis.

It is becoming increasingly evident that there is uncertainty over the application of markers to define cancer stem cells as the field continues to evolve. Furthermore although we currently utilise various markers to pursue stem cell research, little is understood about their role in cellular physiology, and even less is known about their role in cancer formation and progression.

1.7.2. Important Pathways in Stem Cells

The field of cancer stem cell research has illuminated several pathways, some of which overlap with the fields of developmental biology and cellular renewal and whose significance was previously unrecognised in cancer development. WNT signalling is involved in embryonic development and tissue homeostasis [reviewed by (Espada et al, 2009; Grigoryan et al, 2008; Wend et al, 2010)]. High WNT activity was noted originally in cancers of familial adenomatous polyposis patients (Kinzler et al, 1991) caused by APC mutations. In skin it has been shown that WNT signalling is crucial for hair development and stem cell differentiation (Castilho et al, 2009; DasGupta & Fuchs, 1999; Gat et al, 1998; Greco et al, 2009; Huelsken et al, 2001; Nguyen et al, 2006). In skin tumours induced by DMBA/TPA carcinogenesis, isolated putative cancer stem cells with high engraftment potential displayed high nuclear localization of β -catenin, and ablation of β -catenin resulted in loss of cancer stem cells and tumour regression (Malanchi et al, 2008). In the intestine, WNT signalling appears to be essential

for maintaining crypt stem cells. In colon cancer, it has been shown that high WNT activity functionally defines the cancer stem cell population (Vermeulen et al, 2010).

The DNA damage and checkpoint pathways have been shown to be preferentially activated in glioma stem cells following radiotherapy and appear to play an important role in mediating radioresistance (Bao et al, 2006). Rich and colleagues showed that CD133+ve glioma cells growing in xenografts were more radioresistant than their CD133-ve counterparts with lower rates of apoptosis seen. Further analysis showed an upregulation of phosphorylated Rad17, Chk1 and Chk2. If treated with debromohymenialdisine (a Chk1 and Chk2 inhibitor) prior to irradiation, the radioresistance of CD133+ve cells was able to be reversed.

This raises the clinically relevant question to whether cancer stem cells can be targeted for therapy. It has long been considered that cancer stem cells might represent the “Holy Grail” of cancer treatment [reviewed by (Alison et al, 2010; Baumann et al, 2008)]. Certainly this has been proposed as a potentially important mechanism of resistance to anti-cancer therapy ie. although the vast majority of cancer cells might be destroyed by the treatment initially, unique characteristics of the stem cell confers resistance and due to multipotency and longevity they proliferate to reconstitute the recurrent tumour. One problem is that directing therapy towards pathways or processes crucial to the cancer stem cell may also do the same in normal stem cells. This could potentially limit normal tissue tolerability due to an unacceptable side effect profile. If we consider the case of checkpoint pathways in glioma stem cell resistance, normal brain stem cells are likely to utilise the same checkpoint pathways to deal with replication errors and/or DNA damage incurred by the anti-cancer treatment/radiotherapy given concurrently. In the case of checkpoint pathways however, there is substantial evidence to suggest cancer cells compared to normal tissue may be overly reliant on particular components of these pathways ie. ATR/Chk1 axis and anti-cancer agents being designed should take advantage of this [reviewed by (Dai & Grant, 2010; Smith et al, 2010; Zhou & Bartek, 2004)] and see 1.4.2. Other studies have similarly investigated differences in pathway activation between normal versus cancer stem cells and have offered potential opportunities which might be exploited for therapeutic purposes (Wei et al,

2008; Yilmaz et al, 2006). Morrison and colleagues (Yilmaz et al, 2006) showed that conditional mutation and functional deletion of PTEN in haemopoetic cells led to excessive proliferation of haemopoetic stem cells and their depletion from bone marrow. But these mice also developed myeloproliferative type disorder and eventually leukaemia. They showed that treatment with rapamycin (mTOR inhibition) was able to prevent leukaemia formation but on the other hand restore normal haemopoetic stem cell function.

1.7.3. Role of the Host Environment in Transplantation Assays

As the field expands, it is becoming more apparent that there are many areas of debate and controversy which have yet to be resolved in the cancer stem cell field. There is evidence to suggest that the prevalence of cancer stem cells may be higher than thought and frequency of detection may be determined by experimental methodology. The fraction of cancer cells possessing stem cell-like properties compared to non stem cells, obtained from the conventional limited dilution and *in vivo* implantation assays (Quintana et al, 2008; Shackleton et al, 2006), have typically been found in the order of 1 to 10^{3-6} [reviewed by (Quintana et al, 2008)]. However several studies have challenged these findings. In a study by Morrison and colleagues (Quintana et al, 2008) they show altering the host environment of the transplanted cancer cells radically increased the tumourigenic potential. Instead of using NOD/SCID mice, which retain some natural killer cell activity (Shultz et al, 2005), they used a more highly immunocompromised variant lacking the interleukin-2 receptor gamma chain (NOD/SCID IL2R γ^{null}). They showed that the tumourigenic frequency was markedly increased, around one in 4 cells were able to produce tumours from unselected melanoma samples from human patients. To see if growth in NOD/SCID IL2R γ^{null} mice selected out aggressive clones, subsequent tumours were re-implanted in NOD/SCID mice and the frequency of tumourigenic cells decreased suggesting host factors were solely responsible. In fact using xenografted tumors obtained from 4 different patients, flow cytometry sorted single cells were mixed with Matrigel and injected into NOD/SCID IL2R γ^{null} , and a stunning 27% of cells developed into tumours. In contrast, studies of melanoma

stem cells using NOD/SCID mice have only typically demonstrated a 1 in 10^6 tumourigenic capacity (Schatton et al, 2008). Similar studies using other types of more highly immunocompromised host mice have also shown an increased tumourigenic proclivity (Agliano et al, 2008; Feuring-Buske et al, 2003; Taussig et al, 2008) but even then antibody mediated clearance has been observed to reduce engraftment (Archambault & Glover, 2009). Therefore it is now becoming recognised that experimental assay conditions or host microenvironment plays a crucial role in identifying stem cells and the gold standard *in vivo* engraftment assay for cancer stem cell detection is unlikely to be NOD/SCID mice (Bomken et al, 2010). It is also unclear how emerging data obtained from these newer, more immunocompromised models will alter our existing criteria for defining cancer stem cells based on previous studies that have identified various marker using NOD/SCID mice.

1.7.4. Quiescence versus Proliferation – the LGR5 Positive Stem Cell

It has been a long held belief that adult stem cells are relatively quiescent compared to the rest of the surrounding tissue [reviewed by (Moore & Lyle, 2010) and (Li & Clevers, 2010) and (Cotsarelis et al, 1990)]. Experimental evidence from BrdU assays for label retaining cells suggest that label-retention in the skin bulge region can be detected even after 1 year in murine models (Cotsarelis et al, 1990; Lyle et al, 1999). Work from intestinal murine models also suggests a slow-cycling stem cell population occupying the crypts (Potten et al, 2002). This is in contrast to germ stem cells which have been shown to be actively dividing [reviewed by (Kimble & White, 1981; Spradling et al, 2001) and (Crittenden et al, 2006)] and are thought to go into a quiescent only under certain specific circumstances such as a starvation (Narbonne & Roy, 2006). As maintenance of homeostasis in adult tissue, particularly in rapidly dividing tissue such as skin and gut, requires constant cell renewal (Lajtha, 1979) this has posed a conundrum - to explain the mechanism by which a pluripotent but crucially quiescent sub-population of cells is able to be responsible for the generation of a continual supply of replacement cells. Most researchers up till now have used the transit amplifying population (TA cells) model to explain the “bridge”

between these two populations (Potten, 1981) and reviewed by (Jones et al, 2007). TA cells are thought originate from asymmetric stem cell division to produce a quiescent stem cell and an actively dividing TA cell which obviously enters into cell cycle. TA cells are thought to be committed to a number of finite symmetric cell divisions but they lack any significant degree of pluripotency or more specifically, the capacity to return into a state of “stemness” [reviewed by (Jones et al, 2007)]. The evidence to support this hypothesis however has not been satisfactory [reviewed by (Jones et al, 2007)]. The TA cell model suggests the existence of two distinct cell types each with different cell kinetic properties. However, data from cell labelling experiments in the adult interfollicular epidermis have shown otherwise, and thus questions the existence of an intermediary TA population (Clayton et al, 2007). The investigators observed that genetically inducible labelled stem cells were responsible for repopulating a distinct tissue area. The cells were able to undergo both symmetric and asymmetric division and in a subset of cells doing so demonstrated cell kinetics of an actively cycling population (Clayton et al, 2007; Klein et al, 2007).

Because of the likelihood that cancer stem cells arise from normal stem cells, or at least this the pre-eminent hypothesis (Clarke et al, 2006), it follows that cancer stem cells are also likely to be quiescent. Again there remains limited evidence for this. Krauss and colleagues using [Vybrant-Dil™] cell-labelling, a slowly-cycling population of pancreatic cancer cells (Dil+/SCC) showed the necessary propensity for engraftment in xenograft models as well as *in vitro* colony forming assays. (Moore & Lyle, 2010)]. CD24+ve ovarian cancer cells (Gao et al, 2010), which express *nestin*, *Bim-1*, *β-catenin*, *oct* and *notch*, were found to proliferate more slowly compared to other tumour cells as well as displaying relative chemoresistance.

In a series of paradigm changing discoveries in intestinal (Barker et al, 2007) and skin (Jaks et al, 2008) models, our conventional understanding of the stem cell is now being challenged. These studies have described a previously unrecognised sub-population of cells expressing LGR5 (leucine-rich G protein-coupled receptor 5), a downstream target of WNT signalling, possessing all the classical properties of stem cells including pluripotency, longevity, self-renewal potential and

enhanced engraftment potential, yet are continually cycling. They do not retain BrdU, are located in separate tissue sites from the quiescent population and demonstrate minimal co-expression of conventional markers.

In the skin, it has been previously shown that stem cells represent a quiescent sub-population, particularly through label retaining cell (LRC) experiments (Braun et al, 2003; Cotsarelis et al, 1990; Fuchs, 2007; Tumber et al, 2004). There are only a few situations where LRC proliferation has been documented. In the anagen phase of the hair cycle LRCs have been shown to enter into cell cycle and proliferate (Blanpain et al, 2004) in a limited manner. When there is direct tissue damage to the skin, and when wound healing is required (Ito et al, 2005), LRCs appear to proliferate to a much greater degree in response to this stimuli. Hence, it has been postulated that LRCs represent a quiescent population that acts as a “reserve” in cases of tissue perturbation. However Toftgard and colleagues (Jaks et al, 2008) have described a sub-population of LGR5 expressing cells located between the dermal papilla and lower bulge (or hair germ) see Figure 4, which are continually cycling. They display all the accepted hallmarks of stem cells including pluripotency as confirmed by *in vivo* lineage tracing and transplantation experiments. In contrast to LRCs, LGR5 cells continue to proliferate throughout the hair cycle and actively contribute to tissue renewal. They are also long lived and are able to self-renew.

Therefore a new model is being proposed that suggests that there exists two distinct stem cell populations within the skin, a quiescent LRC population and an actively dividing LGR5 population (Li & Clevers, 2010). Each has a defined niche and interestingly apparently different roles in homeostasis, which has also been referred to as the “zoned” model previously (Scoville et al, 2008). The LGR5 expressing population actively divides to renew constant cell turnover whereas the quiescent population appears to function as a “reserve” in case of tissue perturbation (Ito et al, 2005). It is less clear however how these two cell populations are maintained in their different states or whether they signal between each other in a dynamic interplay. It is also unknown if one population may revert to the other and under what circumstances this may occur. In Chapter 5 (see 5.2) and Chapter 8 (see 8.2) I go on to discuss the role of WNT signalling and the different microenvironments of the bulge and dermal papillae

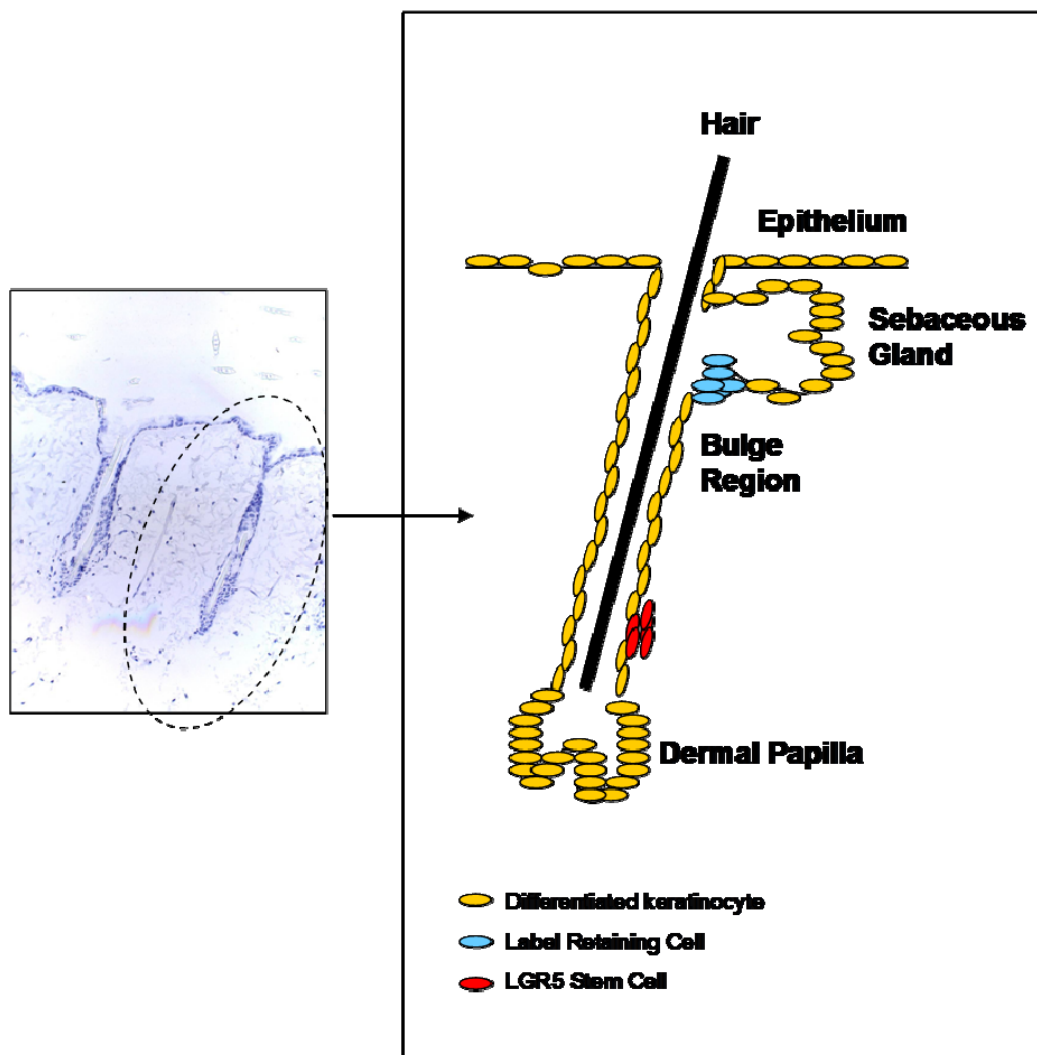


Figure 4 - Epidermal Stem Cell Populations

Stem cells have previously been identified in both the bulge region of the hair follicle and interfollicular epidermis and it appears both populations may be responsible for giving rise to DMBA/TPA induced papillomas.

which is beginning to offer clues as to how these two distinct populations are regulated. Finally, this new model appears to offer a more credible alternative to the transit amplifying cell model (Jones et al, 2007) which as mentioned, has limited supportive data and has failed to explain important aspects of stem cell kinetics (Clayton et al, 2007).

1.7.5. Tissue Specific Stem Cells are Targets for Chemical Carcinogenesis

Despite controversy, substantial data exists to suggest that skin tumours arising due to chemical carcinogenesis derive from stem cells within the skin [reviewed by (Frame & Balmain, 1999; Fuchs et al, 2004; Morris, 2004; Perez-Losada & Balmain, 2003)]. There are three main reasons as to why stem cells are thought to be the cell of origin for tumours, reviewed by (Perez-Losada & Balmain, 2003). The first is that these cells are long lived. This feature is advantageous for the accumulation of multiple genetic alterations required for transformation and undergoing tissue promotion over time. As described, the initiating effect of DMBA within the skin can persist for prolonged periods even when TPA promotion was delayed for a year. This supports the view that stem cells are targets because they are the only cell population which could potentially retain these changes over this period (Van Duuren et al, 1975). The second reason is that stem cells generally possess intrinsic genetic advantages, for example bulge stem cells are adept at invading the surrounding dermis as a prerequisite for normal hair follicle formation, which is conferred onto the newly transformed cancer cell and this sets them apart from non-stem cells. Third, it has been well documented that tumours consist of heterogenous cell types. Tumours are generally enriched with a subpopulation of cells possessing stem cell like properties including increased clonogenic potential for example, CD133 cells in glioma brain tumours which confer regenerative ability and resistance to treatment (Bao et al, 2006; Singh et al, 2004).

In this thesis, my experimental work was largely performed prior to the LGR5 population being described (Jaks et al, 2008) and hence, my investigations pertain to the LRC stem cells only. LRC stem cells have previously been

identified in both the bulge region of the hair follicle and interfollicular epidermis (see Figure 4) and it appears both populations may give rise to papillomas. Epidermal abrasion experiments have been shown to reduce papilloma formation which suggests interfollicular stem cells may be targets for transformation (Argyris & Slaga, 1981). However, more detailed experiments have been performed to investigate the relative contribution of the two populations of stem cells - the hair bulge versus the interfollicular region. Using Keratin-10 to direct mutant *h-ras* expression in the interfollicular epidermis (Bailleul et al, 1990) and Keratin-5 in the bulge region (Brown et al, 1998), with the advantage of lineage traceability, it was shown that malignant conversion in the interfollicular epidermis is much less frequent than in the bulge. Additionally in experiments performed by Morris et al (Morris et al, 1997) in which treatment with 5-fluorouracil (5FU) induced epidermal sloughing and cell loss, prior to carcinogen exposure, caused a significant reduction in papilloma formation from DMBA/TPA carcinogenesis. Taken together although there appears to be a role for interfollicular stem cells in the genesis of tumours, the majority of malignant tumours seem to originate from bulge stem cells in the hair follicle.

At this stage it is also entirely unknown if these LGR5+ve stem cell develop into cancer stem cells if subjected to appropriate pro-carcinogenic stimulus. It is also unknown whether these cells constitute human cancers nor in what way they may contribute to tumourigenesis (Li & Clevers, 2010).

1.8. Objectives of the thesis

This thesis had 3 broad aims which were to :

1. Establish and characterise the effects of conditional *chk1* deletion in mouse skin.
2. Study the effect of conditional *chk1* loss on tumour formation and carcinoma progression using DMBA/TPA skin chemical carcinogenesis
3. Study the effect of *chk1* loss on epithelial biology and skin homeostasis - with a specific focus on the putative LRC stem cell population, in the bulge region of the skin.

Chapter 2. Materials and Methods

2.1. Generation of *Chk1* Null mice

These mice were made by Stephen Elledges's group, Harvard Medical School, Boston (Liu et al, 2000b). Briefly, *chk1* was disrupted in ES cells by homologous recombination using a targeting vector containing a neo positive selection marker, TK negative selection marker, flanked by 1.9kb and 4.5kb homologous sequences. Targeting replaced 3kb of genomic sequence, exons 2, 3, 4 and 5 that encode the putative first methionine, the "GxGxxG" ATP-binding motif and half of the kinase domain. Cell lines generated were injected into females to generate chimeric offspring and these were bred on to produce germ-line transmission. Heterozygote *chk1* +/- were healthy, fertile and tumour free up to 1.5 years. When heterozygote mice were intercrossed, no *chk1* -/- progeny were obtained. Analysis of pregnant females revealed constitutive *chk1* -/- knockout resulted in embryonic lethality between day E4.5 to E7.5 (Liu et al, 2000b; Takai et al, 2000). Attempts at sequential gene targeting of *chk1* +/- ES with a second targeting vector, using an hprt marker was also unsuccessful underlying the lethality of a complete knockout.

2.2. Generation of *Chk1* Flox Mice

These mice were made by Stephen Elledges's group at the Harvard Medical School, Boston (Liu et al, 2000b). A *chk1* flox targeting vector was used to replace exon 2 of *chk1* which contains the translational initiation sequence and ATP-binding site of the kinase. No viable clones were obtained from *chk1*flox/- ES cells after undergoing Cre-loxP mediated excision. Cre-loxP mediated excision of *chk1*flox/+ ES cells resulted in viable *chk1*Δ/+ cell lines.

2.3. Generation of Rosa26-LacZ Mice

These mice were made by Philippe Soriano, Fred Hutchinson Cancer Research Centre, Seattle (Soriano, 1999; Tsien et al, 1996). To generate mice that express LacZ, the ROSA26 locus was targeted with a 5kb genomic fragment containing LacZ and a triple polyadenylation 3' sequence to prevent transcriptional read

through flanked by loxP sites (referred to as a “stop” sequence). Only after Cre-loxP mediated recombination is LacZ expressed under control of the endogenous locus promoter and this was assayed using a B-galactosidase reaction.

2.4. Breeding Strategy and Colony Maintenance

Mice bearing the *chk1* null and flox alleles and the Rosa-LacZ allele were kindly provided by Jeffrey Rosen, Baylor College of Medicine, Houston (Lam et al, 2004) in Sept 2003. Our colony was maintained on an FVB genetic background and all mice undergoing experiments were on this background unless stated otherwise. Mice were bred and maintained in the animal facility, Beatson Institute for Cancer Research, Glasgow as stipulated by Home Office project licence conditions, rules and regulations. Animals were humanely culled using Schedule 1 techniques as stipulated in our project licence.

2.5. B-Galactosidase Assay

Lac Z activity and expression was assayed using a B-galactosidase reaction. Mouse tissue, for example dorsal skin (shaved), tail skin (with bone removed) or oesophageal tissue, was dissected and secured on wax plates with pins. Wax plates were made by heating 100ml ralwax beads, adding 10ml paraffin oil and cooling solution in a 15cm plate. 50-100mls of a 0.1g magnesium chloride, 0.48g potassium ferricyanide and 0.64g potassium ferrocyanide in 500mls PBS solution and 200 μ L of 5% X-Gal in DMF or DMSO was added. The plate was allowed to incubate in the dark for 24-48 hours, room temperature.

2.6. DNA Preparation and PCR Genotyping

Mice were genotyped by PCR analysis. Ear or tail tips were prepared in lysis buffer (100mM Tris HCl pH8.5, 5mM EDTA, 0.2% SDS, 200mM NaCl, 100 μ g/mL proteinase K) at 55°C overnight. The following day samples were heated to 96°C

for 5 minutes, cooled then stored at 4°C. The following were primers and conditions used (Lam et al, 2004; Liu et al, 2000b; Rijnkels & Rosen, 2001).

chk1 - F^{chk1} 5'acc tgc ccg caa ctc cct ttc 3', R^{chk1} 5'cca tga ctc caa gca cag cga 3', 94°C /3min (1 cycle), 94°C /30s then 54°C /40s then 65°C/70s (40 cycles), 4°C hold. Product is 380bp (flox allele) and 318bp (wild type allele).

LacZ - F^{LacZ} 5'aaa gtcgct ctg agt tgt tat 3', R^{LacZ1} 5'gcg aag agt ttg tcc tca acc 3', R^{LacZ2} 5' gga gcg gga gaa atg gat atg 3', 94°C /30s then 54°C /40s then 65°C/70s (40 cycles), 4°C hold. Product is 500bp (wild type untargeted locus) and 250bp (lacZ allele).

Neo (this PCR will detect both chk1 null or LacZ and cannot differentiate between the two) - F^{Neo} 5'gat cgg cca ttg aac aag atgg 3', R^{Neo} 5'cct gat gct ctt cgt cca gatc 3', 94°C /3min (1 cycle), 94°C /30s then 57°C /40s then 65°C/70s (40 cycles), 4°C hold. Product is 500bp.

K14CreER^{T2} - F^{Cre} 5'att tgc ctg cat tac cgg tc 3', R^{Cre} 5'atc aacggtt ttc ttt tcgg 3', 94°C/60s then 55°C/30s then 72°C/30s (x30 cycles), 4°C hold. Product is 350bp (Indra et al, 1999)

PCR primers were designed to assay for *chk1* recombination. The exact sequence for the targeting insert was not obtainable from the original publication nor from the authors. Primers were therefore targeted at endogenous DNA, forward primer F^{chk1 Δ} 5'acc tgc ccg caa ctc cct ttc 3' was 5' upstream to exon 2 and first loxP sequence. Reverse primer R^{chk1 Δ} was 3' to the second loxP sequence and exon 3, 5'ggg aag tca tgt aca att tca ctac3'. Following 4OHT mediated recombination, DNA was prepared from dorsal skin of *chk1* flox/- // K14CreER^{T2} and *chk1* +/- // K14CreER^{T2} animals. PCR analysis using primers F^{rec} and R^{rec} using conditions as follows, 94°C /3min (1 cycle), 94°C /30s then 56-60°C /40s then 65°C/90s (40 cycles) then 4°C hold. This showed presence of recombined allele only in 4OHT treated *chk1* flox/- // K14CreER^{T2} animals and not in control animals. The product was cloned and sequenced which confirmed a 1216bp product. Sequence was compared with mouse *chk1* sequence (NC_000075) and aligned 5' to 3417 to 3925 and 3' to 5525 to 6233.

2.7. Tamoxifen (4-OHT) Preparation and Administration

Intraperitoneal 4-OHT was prepared by dissolving 5mg of 4-OHT (Sigma H7904, active Z-isomer >98%) in 500 μ L 100% ethanol. This was diluted further in 4500 μ L of autoclaved sunflower oil (Sigma S5007). Mice received 100 μ L of this solution of 4-OHT IP, daily over 5 days.

Topical 4-OHT was prepared by dissolving 50mg 4-OHT (Sigma H6278, active Z-isomer ~70%) in 7mL DMSO. 300 μ L was applied to shaved back skin or 150 μ L to tail, the solution was delivered in two separate applications, 30 minutes apart. At each application, the solution was rubbed onto skin using the back of plastic pipette.

2.8. DMBA/TPA Chemical Carcinogenesis

The DMBA/TPA protocol for chemical carcinogenesis is well characterised. DMBA (7,12-dimethylbenz[a]anthracene), D3254 SIGMA 100mg, was dissolved in 15mls acetone to make up a x40 stock solution. TPA (12-O-tetradecanoylphorbol-13-acetate), P8139 SIGMA 25mg, was dissolved in 15mls acetone to make up a x40 stock solution. Further dilution to x1 working solution was done in acetone.

Cohorts were matched for age and comprised only of females FVB mice. The mice had undergone backcrossing onto an FVB background for 7 generations. All were housed and cared for under identical conditions throughout the whole period of the experiment. Prior to topical application, dorsal hair was shaved and animals left for at least 2 days. DMBA (x1) 150 μ L or 25 μ g was applied once. This was followed by 20 weeks of twice weekly TPA (x1) 150 μ L or 6.25 μ g applications (McLean et al, 2004).

Papilloma and carcinoma appearance was directly visible and palpable on mouse skin. Tumour numbers was quantified weekly and dimensions measure as

necessary. Mice were culled if papilloma diameter exceeded 1.2cm or if carcinoma diameter exceeded 2cm. All animals were culled by 60 weeks of starting the experiment. All procedures were conducted according to the UKCCCR Guidelines for the Welfare of Animals in Experimental Neoplasia.

2.9. Antibodies

For western blotting, antibodies used include mouse monoclonal total Chk1 (Santa Cruz sc-8408, 1:1000), actin (Sigma AC-40, 1:1000).

For immunohistochemistry antibodies used include rabbit monoclonal total Chk1 (Epitomics Clone ID:EPR3952, 1:200), rabbit polyclonal total Chk1 (ProteinTech 65016-1-Ig, 1:200) - discontinued from production in 2008 (reason unknown), p53 (Labvision, MS104, 1:50), Ki67 (Vector Labs, VP-K452, 1:100).

For immunofluorescence and confocal microscopy, antibodies used include rabbit monoclonal total Chk1 (Epitomics Clone ID:EPR3952, 1:200), γ -h2ax (Upstate JBW 301, 1:200), Active (cleaved) caspase-3 Asp175 (Cell Signalling Technology Antibody 9661, 1:200), rat anti-brdu (Serotec OBT0030, 1:100). Secondary antibodies include Cy3 donkey anti-rat to detect BrdU (Jackson ImmunoResearch 712-165-153, 1:200), Alexa Fluoro 488, 568 (Invitrogen, 1:200).

2.10. Labelling Mice with BrdU to Assay for Label Retaining Cell (LRC) Properties

4 day old pups were injected with 50 μ L BrdU (Amersham RPN 201) intraperitoneally once a day, per mouse, over 3 days consecutive days.

2.11. Preparation of Tail Epidermal Wholemounts

The protocols were adapted from methods published by Braun (Braun et al, 2003).

Mouse tail skin was slit length wise with scalpel and peeled off bone. It was immersed into 20mls of 0.005M EDTA in PBS. It was heated in a water bath at 37°C for 4-5 hours.

The epidermis was peeled off the dermis with careful separation to ensure hair follicles remain intact. If not, then it was soaked in water bath for 30min longer. It was then fixed in 4% formaldehyde in PBS for 2 hours at room temperature. It was washed in PBS x3. The tail can be stored in 0.2% sodium azide at 4°C for up to 8 weeks.

2.12. Confocal Microscopy of Tail sections

The protocols were adapted from methods published by Braun (Braun et al, 2003).

The tail was cut into pieces according to size requirements, typically 1.0cm x 0.5cm. They were put into a 24 well plate. The pieces were blocked and permeabilized in PB Buffer (0.5% BSA + 0.5% Triton-X in PBS, make up fresh everytime) at 30 min minimum at room temperature. Tail pieces were then immersed in 2N HCl at 20 minutes at 37°C (if staining for BrdU, if not then this step was not necessary). It was important to adhere to an immersion time of 30 min, not more as it would adversely affect staining. Pieces were washed in PBS x3.

The primary antibodies were diluted in PB Buffer and incubated with the pieces overnight with gentle agitation at room temperature. The following day they were washed with 0.2% tween in PBS, 4-5 washes over at least 4 hours at room temperature. Secondary antibodies were diluted in PB Buffer and incubated with pieces overnight with gentle agitation at room temperature. The following day the pieces were washed in 0.2% tween in PBS, 4-5 washes over at least 4

hours at room temperature. They were then mounted on a glass slide using Cover Well chamber gasket to secure tail onto glass slide (Invitrogen C18161). The nuclei were counterstained with DAPI in Vectashield mounting medium. The slides could be stored in dark for up to 6 months.

2.13. Tissue Fixation

Tissue samples were harvested and fixed in 10% formaldehyde in PBS for 24 hours. They were paraffin embedded and tissue section cut and fixed onto slides.

2.14. Immunohistochemistry

For staining, the Dako EnVision™ System (Dako) was used for both primary mouse and rabbit antibodies. Slides were deparaffinized and rehydrated by x3 washes in Xylene, x2 washes in 100% ethanol (10min each), x1 wash in 95% ethanol (10min) and x1 wash in 70% ethanol (10min). This was followed by x2 washes in dH₂O (5min) and x1 wash in PBS (5 min). Antigen retrieval was then performed (see below). Slides were washed x3 in dH₂O (5min), peroxidase block performed (5 min) and primary antibody or negative control incubation performed (30 min). x3 in PBS wash (5min each). Slides were incubated with labeled peroxidase polymer (30 min). x3 in PBS wash (5min each). Liquid DAB+ substrate chromogen was applied to cover specimen (5-10 min). Slides were counterstained with Mayer's Haematoxylin for 45 seconds. They were then dehydrated with 70% ethanol (10min), 95% ethanol (10 min) and then 100% ethanol (10 min). Xylene washes were performed (at least 10min). Finally slides were mounted using HistoClear™ solution with coverslips.

2.15. Antigen retrieval

The following solutions were prepared, Solution A - 10.5g of citric acid in 500 mls dH₂O and Solution B - 29.4g sodium citrate in 1 litre dH₂O.

A 1.5L solution of 27mls of solution A + 123mls of solution B and made up to 1.5L with dH₂O with pH adjusted to 6.0. This solution was added to a pressure cooker to generously bathe the slides in solution contained in a slide holder. It was microwaved for 8 minutes or until solution is boiling (yellow top pops up) and microwave was continued for another 1 minutes or so. It was allowed to cool in pressure cooker uncovered for at least 20 min before removal.

2.16. Deriving Carcinoma Cell Lines from Mice

About a $\frac{1}{4}$ of the tumour was harvested. It was placed immediately into sterile PBS (universal bottle). Subsequent work was performed in a fume hood which had been thoroughly cleaned with ethanol wipes. Two scalpels were put into a beaker of ethanol for sterilization and allowed to air dry. On a sterile petri dish, the tumour was cut into small pieces of less than 0.5cm. They were then positioned on the bottom surface of T25 flasks (use 4 flasks) with 6 pieces evenly spread out. They left for 2-5 minutes in order for them to become adherent to the plastic surface. Medium was then slowly trickled in to the flask, roughly 5mls. Medium consists of MEM 500mls (INVITROGEN 21090-022 +Earle's, -ve L-Glut), NEAA 10mls, Glutamine 5mls (2mM), 10% fetal bovine serum 50mls, Sodium Pyruvate 5mls, Vitamins 5mls, Penicillin 2.5mls (30 μ g/ml), Streptomycin 2.5ml (50 μ g/mls), Amphotericin B 5mls. The flask was left in an incubator at 37°C, 5%CO₂, no O₂ for 5-7 days initially. The purpose is not to disturb the tissue pieces so as not to detach them from the bottom of T25 flasks. After 5-7 days, the tumour cells were observed to be growing out from bottom of tumour adherent to plastic base.

Being careful not to dislodge tumour, the medium was either changed or add further 5 mls of medium was added and the medium changed after another 2-3

days. Once the cells had established growth the tumour pieces were discarded and the culture was passaged as per the adherent cell protocol.

2.17. Mouse Tail Keratinocyte Culture

Mouse tail skin was slit length wise with scalpel and peeled off bone and immersed in PBS. They were then transferred into 8mg/ml Dispase II in PBS (eg. 1 tail = 10mls) and incubated overnight at 4°C. The following day, the epidermis was separated from the dermis with forceps & scalpel (epidermis being the thinner, white upper layer). The epidermis was cut into small pieces and put into a trypsin solution for 10 min at 37°C water bath or incubator. The mix was vortexed to help dissociation of cells. The trypsin was neutralised with DMEM (+20% FCS) - equal volumes of each used. The vortexed sample was then strained through a cell strainer and the solution spun down at 1min 1000rpm. This was resuspended with PBS and spun down again for 1min at 1000rpm. The supernatant was removed and resuspended in Keratinocyte Growth Medium (KGM) and plated out.

Keratinocyte Growth Medium (KGM) :

Supplements supplied as a 5 pack from manufacturer, Clonetics KGM Single Aliquots (Catalog No. CC-4131) - Gentamicin/Amphotericin-1000 0.5ml (CC 4081E), BPE 2.0ml (CC 4002E), Insulin 0.5ml (CC 4021E), hEGF 0.5ml (CC 4015E), Hydrocortisone 0.5ml (CC 4031E). Additionally 83µL calcium (CaCl₂ tissue culture grade, stored at room temp) was added.

The cells were grown in a humidified incubator at 37°C, 5% CO₂ and 3% humidity.

2.18. Passaging Adherent Cells

All work was performed in a sterile fume hood. The media was aspirated away leaving the cells which were then washed x3 with 10mls of pre-warmed PBS. The cells were then washed with 10mls of pre-warmed PE. 1ml of pre-warmed

0.25% trypsin in PE was added to the flask (the volume of trypsin depended on the size of the flask/dish eg. 1ml is sufficient for a T25 flask). The flask was tipped to allow the trypsin solution to become evenly distributed over the cells on the surface of the flask/dish. The flask was then returned to the incubator for 2-3 minutes until the cells had detached from the plate, this was checked under a microscope. Once detached, 10mls of fresh pre-warmed media was added to the cells to inactivate the trypsin. An aliquot of this cell suspension was then added to a flask containing fresh media. The cells were then returned to the incubator to allow re-attachment of the cells to the bottom surface of the flask.

2.19. DT40 Cell Culture

DT40 cells were cultured in high glucose DMEM containing pyruvate supplemented with 10% FBS, 1% heat inactivated chicken serum, 2mM Glutamine, 10 μ M β -mercaptoethanol, 50U/ml penicillin G and 50 μ g/ml Streptomycin. The cells were grown in a humidified incubator at 39°C. Cells were passaged by diluting 1:10-1:20 into fresh media every 2-3 days to maintain the cells in exponential growth phase.

2.20. Cryogenic Preservation of Cell lines

In order to store cells for future use, cells were cryogenically frozen and preserved in liquid nitrogen tanks. Cells growing exponentially (trypsinised if needed to overcome adherence to the flask) were resuspended in 90% FBS/10% DMSO and divided into 500 μ l aliquots in 1.5ml cryovials. Initial freezing was carried out in a container containing isopropanol at -70°C to give a cooling rate of 1°C/minute. Once a temperature of -70°C was reached the cells were transferred to storage in liquid nitrogen vapour phase tanks at -180°C. To recover the cells the vials were immersed into a 37°C water bath. Once thawed the cells were added to pre-warmed media. The following day the cells were passaged or the media was changed depending on the confluency of the cells.

2.21. Making Protein Extracts From Mouse Tissue

The mice were sacrificed. The tissue of interest was harvested and cut into small <0.5cm sections. They were then put into an extract buffer without delay (x5 pieces into approximately 1 to 1.5mls of buffer). Ten millilitres (10mL) of buffer consisted of 4.2mls dH₂O, 100µL 0.5M Ethylenediamine tetraacetic acid, 4mls 1M Potassium Chloride, 40µL Triton X-100, 1mL Glycerol, 100µL 0.5M Sodium Fluoride, 100µL 100mM Benzamidine, 100µL 100mM Sodium Vanadate, 20µL 0.5M DTT, 25µL 25µg/mL Okadaic Acid, 25µL 2mg/mL Leupeptin, 57µL 50mM Phenylmethylsulphonyl fluoride, 200µL 1M Hepes, 28µL 1.8mg/mL Aprotinin. Tissue in buffer was collected and stored on ice. Tissue was mashed using a tissue grinder, microfuged x3min 3000rpm, the supernatant removed for use.

2.22. SDS-PAGE

Sodium dodecyl sulfate polyacrylamide gel electrophoresis (SDS-PAGE) was carried out in order to separate proteins so they could be analysed further by Western Blotting. To cast the resolving gel a solution containing 6-15% acrylamide (acrylamide:bisacrylamide 37.5:1), 375mM Tris-HCl pH 8.8 and 0.1% SDS was made. To polymerise the gel ammonium persulphate and TEMED was added to a final concentration of 0.1% and 0.08% respectively. The gel mix was placed in the gel casting apparatus and over-laid with water-saturated butanol. Once set the stacking buffer (5% acrylamide (acrylamide:bisacrylamide 37.5:1), 125mM Tris-HCl pH6.8, 0.1% SDS, 0.1% ammonium persulphate and 0.1% TEMED) was layered on top and the combs were inserted to allow the loading of samples. Once set the gel apparatus was correctly assembled and 1 × Running Buffer was added to the upper and lower chambers of the tank.

Samples to be analysed were added to an equal volume of 2 × SDS-PAGE loading buffer (120mM Tris-HCl pH6.8, 20% Glycerol, 5% SDS, Bromophenol blue supplemented with 100mM DTT before use) and were boiled for 5 minutes to

denature the proteins. The samples were centrifuged briefly to remove debris and the samples were then loaded into the wells. Molecular weight markers were also run to estimate the size of the proteins to be analysed. The gels were then run at 180V at constant voltage until the dye front had just entered the running buffer.

To examine Chk1 phosphorylation by an electrophoretic mobility shift a 10% acrylamide gel but used and the acrylamide to bisacrylamide ratio was changed to 125:1.

2.23. Western Blotting

Western Blotting was carried out using the semi dry blotting technique. Once the SDS-PAGE was run it was placed on top of 6 sheets of 3MM paper pre-soaked in dry blot buffer and cut to the size of the gel. On top of this was placed the nitrocellulose membrane and 6 more sheets of soaked 3MM paper. Air bubbles were removed by gently rolling with a marker pen. The 'sandwich' was placed on the transfer apparatus such that the gel was closest to the negative electrode. The proteins were transferred as standard at 20V, 200mA, 8W for 1 hour 20 minutes. In order to transfer high molecular weight proteins onto the membrane they were transferred at 12V, 200mA, 8W for 2 hours and 30 minutes. Then the membrane was blocked in blocking buffer 5% Marvel (non-fat dried milk powder) solution in 1 × TBS-T for 1 hour at room temperature with gentle agitation. The membrane was then incubated with the appropriate primary antibody. Membrane was washed x3 10 minutes with 1 × TBS-T with gentle agitation. Membrane was incubated with the secondary antibody coupled to horseradish peroxidase for 1 hour at room temperature. The appropriate secondary antibodies were diluted 1:5000 in blocking buffer. After this incubation the membrane was washed as before and the bound secondary antibody was detected using enhanced chemiluminescence and autoradiography film. The film was developed in a Kodak X-Omat 3000RA automatic film processor.

2.24. Irradiating Cells and Mice

As a method of inducing DNA damage cells and mice were treated with γ -IR. Cells were irradiated with γ -IR using an Alcyon II Cobalt-60 Teletherapy Unit. Dose rates varied from 1-2.5 Gymin-1. Cells were irradiated directly in the media in the culture flask. Mice were treated in a specialized mouse holding chamber which allowed a large degree of immobilization whilst keeping the mice safe and in minimal distress.

Chapter 3. Characterization of the *Chk1* Knockout Mouse

3.1. Results

3.1.1. Genetically Engineered Mice - *Chk1* Flox and Null Alleles

The generation of the conditional and constitutive *chk1* knockout alleles have been previously described (see 2.1 and 2.2) (Liu et al, 2000b). The mice bearing these alleles were donated to us by our collaborator Prof Stephen Elledge, Harvard Medical School, and maintained in our animal facility (see 2.4).

3.1.2. Breeding Strategy

In Sept 2003, a *chk1flox/-* female and *chk1flox/flox // Rosa26-LacZ* male were donated to our group by Jeffrey Rosen (Lam et al, 2004), Baylor College, Houston, a collaborator of Stephen Elledge. The male mouse was bigenic, possessing both the *chk1flox* allele and *LacZ* allele (*Rosa26* locus). The *chk1* floxed, *chk1* null and *LacZ* alleles were non sex-linked. Both donated mice were on a mixed C57/BL6 and FVB background. I then bred them with FVB wild type mice and the colony was subsequently maintained on an FVB background.

3.1.3. Cre-LoxP // ROSA26 LacZ Reporter System and B-Gal Assay

Cre recombinase catalyzes recombination between 34 bp *loxP* recognition sequences. The DNA sequence between two directly repeated *loxP* sequences is excised as a circular molecule upon Cre activation. In our model, it was necessary to monitor that Cre activity had occurred under the required temporal [ie. Cre-ER^{T2} (Indra et al, 1999) activation only after treating with tamoxifen] and spatial (ie. activation only in hair follicles and epidermal skin where Cre expression is under control of the keratin-14 promoter) control, and not for example, spontaneously during embryogenesis or in aberrant tissue sites.

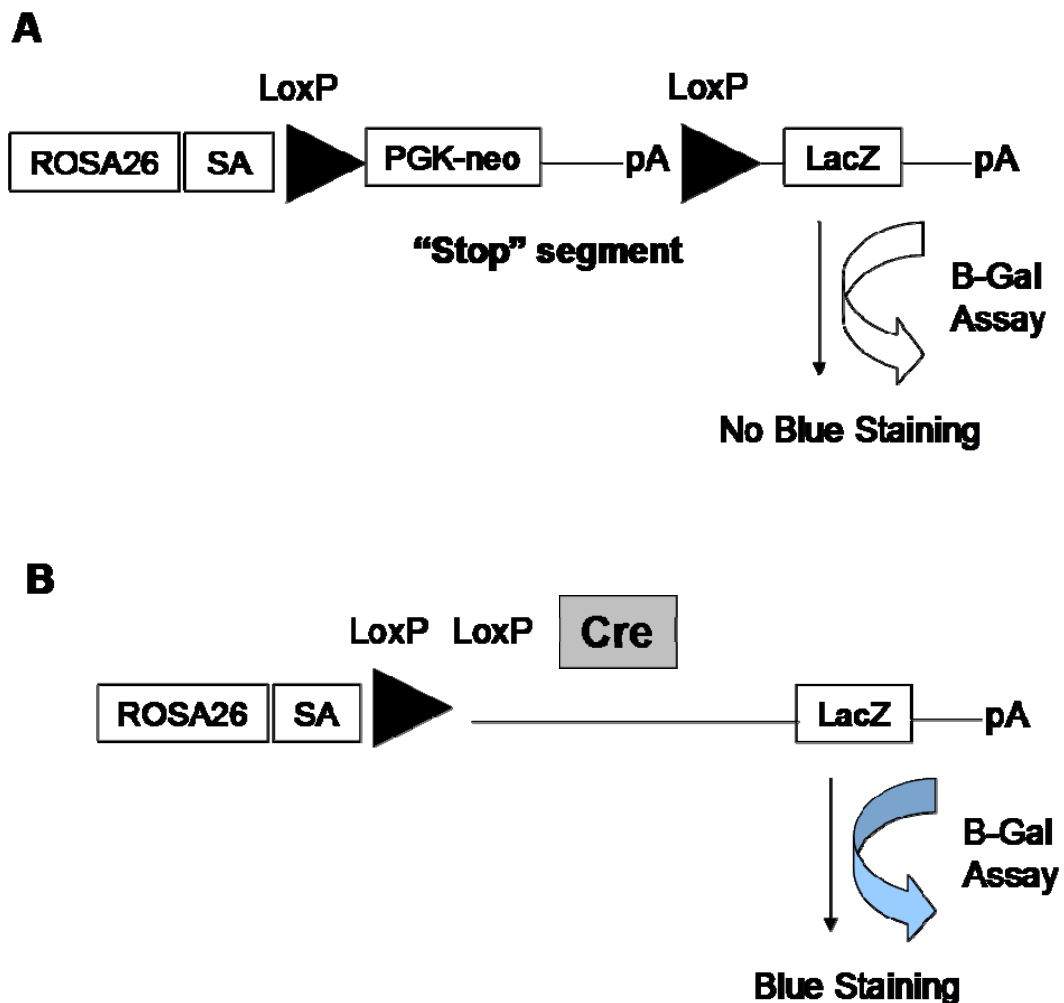


Figure 5 - The *LacZ* Reporter Allele

A The *LacZ* transgene is inserted into the ROSA26 locus under control of the endogenous promoter (Soriano, 1999). Inserted 5' upstream to *LacZ* is a *PGK-neo* expression cassette and polyadenylation sequence flanked by *loxP* sites also known as the "stop" segment. (SA) splice acceptor sequence. **B** *LacZ* expression is conditional on Cre-recombinase mediated recombination and removal of this intervening "stop" segment. Using a B-gal assay (see Methods) performed either on fixed or fresh wholemount tissue we were able to assay for *LacZ* activity and *chk1* recombination by the detection of blue staining.

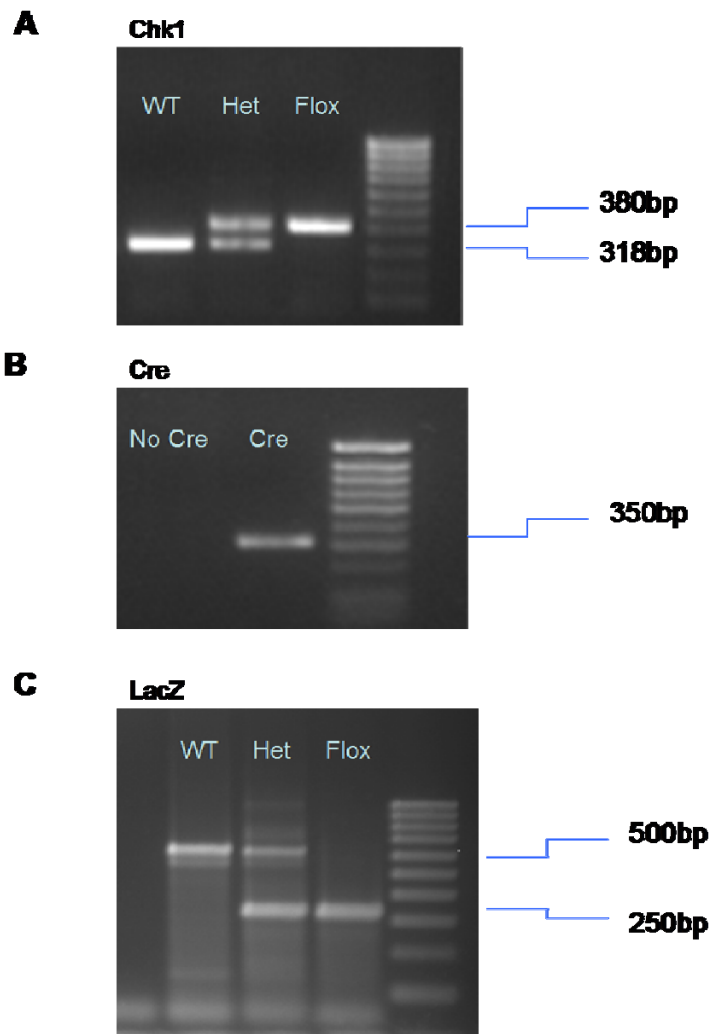


Figure 6 - Diagnostic PCR for *Chk1*, *Cre* and *LacZ* Alleles

Animals were genotyped using PCR analysis, full details can be found in Methods. Diagnostic PCR products are shown for A *chk1* wild type (318bp) and *chk1* floxed (unrecombined) alleles (380bp) B *cre* allele (350bp) C *LacZ* (250bp) and wild type (500bp) allele.

The *LacZ* gene encodes β -galactosidase, an enzyme which ordinarily cleaves the disaccharide lactose into glucose and galactose. *LacZ* can also cleave a colourless substrate X-gal (4-chloro-5-bromo-3-indolyl- β -galactosidase) into galactose and a blue insoluble product which forms the basis for a chemical assay referred to as the β -Gal Assay.

We acquired transgenic mice expressing *LacZ*, under the control of the ROSA26 promoter (see Figure 5A). ROSA26 is active in embryonic development and throughout adulthood (Soriano, 1999) and the locus has been proven to be a reliable integration site allowing strong and predictable transgene expression (Soriano, 1999; Tsien et al, 1996). Inserted 5' upstream to *LacZ* was a *PGK-neo* expression cassette and polyadenylation sequence flanked by *loxP* sites. Therefore *LacZ* expression was conditional on Cre mediated recombination and removal of this intervening “stop” segment, (see Figure 5B). Using a β -Gal assay performed using either fixed paraffin embedded sections or fresh wholemounted tissue I was able to detect *LacZ* activity and hence, assay for recombination.

3.1.4. Genotyping of Mice

Mice were genotyped by PCR analysis. Ear or tail tips were harvested into lysis buffer and DNA extracts prepared. Primers and PCR conditions are described fully in Methods and Materials (see 2.6) (Lam et al, 2004; Liu et al, 2000b; Rijnkels & Rosen, 2001). Typical genotyping results are shown in Figure 6A (*chk1*), Figure 6B (Cre) and Figure 6C (*LacZ*).

3.1.5. Phenotype of *Chk1* Null, Heterozygous and Flox Mice

When interbreeding *chk1*^{+/-} or *chk1*^{flox/-} mice, it was observed that no homozygous *chk1* knockouts were born. For example when a *chk1*^{+/-} male is crossed with a *chk1*^{+/-} female, offspring ratios were approximately $\frac{1}{3}$ (+/+), $\frac{2}{3}$ (+/-), $\frac{0}{3}$ (-/-) instead of the expected $\frac{1}{4}$ (+/+), $\frac{2}{4}$ (+/-), $\frac{1}{4}$ (-/-) (see Figure 7A). This is consistent with previous observations that complete *chk1* loss is

embryonically lethal. Liu (Liu et al, 2000b) observed empty decidua and remains of resorbed embryos at E6.5 to E7.5. Takai (Takai et al, 2000) observed lethality between E3.5 to E7.5 with embryonic nuclei demonstrating aberrant nuclear morphology, defective growth and defective cell cycle regulation.

Heterozygote *chk1*^{+/-} mice (see Figure 7B) were viable and demonstrated no gross pathology. They had normal lifespan, were fertile, displayed no premature ageing and no increased incidence of tumourigenesis. This is also consistent with previous observations (Lam et al, 2004; Liu et al, 2000b; Takai et al, 2000). In the paper by Lam (Lam et al, 2004), they noted that mammary gland tissue in *chk1*^{+/-} mice was viable and the mice were able to lactate normally.

Chk1^{flox/flox} (Cre uninduced) mice (see Figure 7B) had a normal lifespan, were fertile, displayed no premature ageing and no increased incidence of tumourigenesis. No previous phenotype was reported for *chk1* ^{flox/flox} mice (Cre uninduced) (Lam et al, 2004; Liu et al, 2000b; Takai et al, 2000).

3.1.6. Achieving Conditional Knockout of *Chk1* in the Skin

Bigenic *chk1* ^{flox} mice bearing the loxP-*stop*-loxP *LacZ* marker were crossed with mice expressing Cre-recombinase-ER^{T2} (CreER^{T2}) under the control of a Keratin-14 (K14) promoter (see Figure 8), the latter being donated by Prof Margaret Frame from the Beatson Institute in Glasgow (Indra et al, 1999; McLean et al, 2004). The result of these crosses produced *chk1*^{flox/flox} // *K14CreER*^{T2} // *LacZ* trigenic animals. The fusion protein CreER^{T2} allows Cre-recombinase to activate only when 4-hydroxytamoxifen (4OHT) is bound to the modified oestrogen receptor ER^{T2} (Indra et al, 1999). The keratin14 promoter is expressed in the squamous epithelia of the skin including the basal layer of the epidermis interfollicular epidermis, outer root sheath and bulge region of the hair follicle (McLean et al, 2004; Serrels et al, 2009; Vassar et al, 1989). The bulge region is part of the outer root sheath and is located below the sebaceous glands,

A *chk1^{+/-}* X *chk1^{+/-}* → (1/3) *+/+*, (2/3) *+/-*, (0) *-/-*
chk1^{+/-} → died in-utero, E3.5 – E7.5

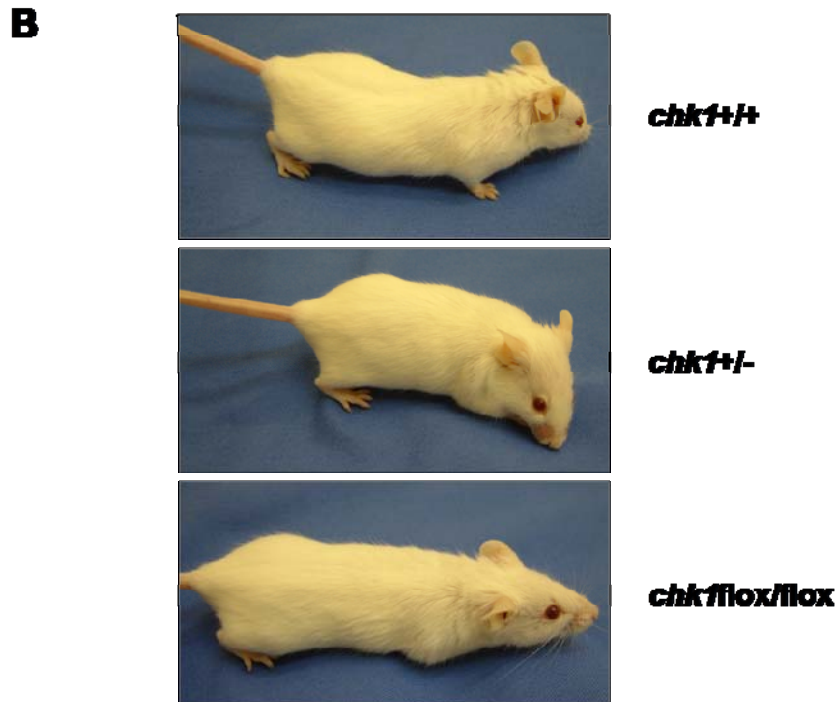


Figure 7 - Phenotype of Constitutive and Conditional *Chk1* Knockout Mice

A Schematic representation of a *chk1^{+/-}* male with a *chk1^{+/-}* female cross, the offspring ratios were approximately $\frac{1}{3}$ (*+/+*), $\frac{2}{3}$ (*+/-*), 0 (*-/-*) instead of the expected $\frac{1}{4}$ (*+/+*), $\frac{2}{4}$ (*+/-*), $\frac{1}{4}$ (*-/-*) ratios. This is due to *chk1* loss being embryonically lethal at around E3.5 to E7.5 (Liu et al, 2000b). **B** Photographs of a *chk1^{+/+}* (wild type), *chk1^{+/-}* and *chk1^{flox/flox}* and mouse at 1 year. There were no distinguishable differences in phenotype between mice from these genotypes. They had a normal lifespan, were fertile, displayed no premature ageing and no increased incidence of spontaneous tumourigenesis.

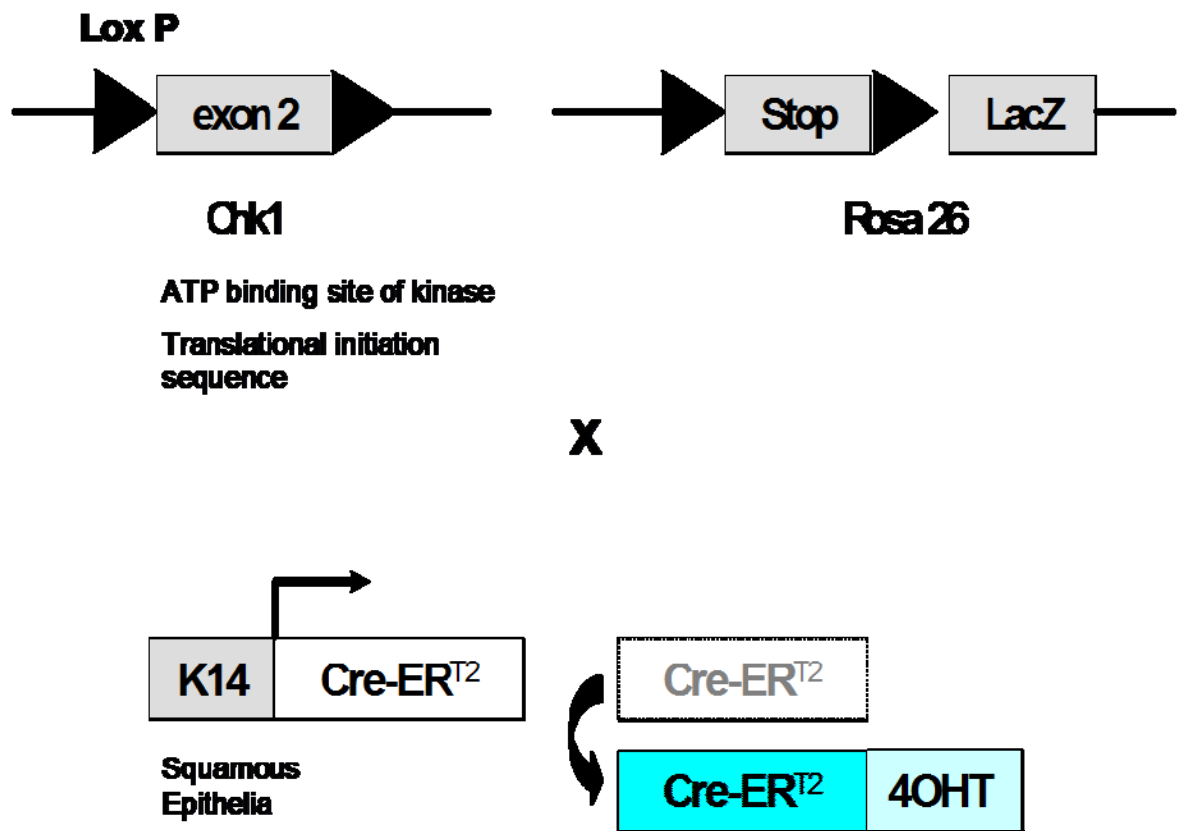


Figure 8 - Conditional Floxed *Chk1* Allele and K14-*CreER^{T2}* Allele

Chk1 flox mice bearing the loxP-*stop*-loxP *LacZ* transgene were crossed with mice expressing Cre-recombinase-ER^{T2} (CreER^{T2}) under the control of a Keratin-14 (K14) promoter. The CreER^{T2} fusion protein allows an inducible Cre system that is activated only in the presence of the synthetic oestrogen tamoxifen (4OHT). The result of these crosses produced trigenic *chk1*flox/flox // *K14CreER^{T2}* // *LacZ* animals which were used to conditionally delete *chk1* in the skin.

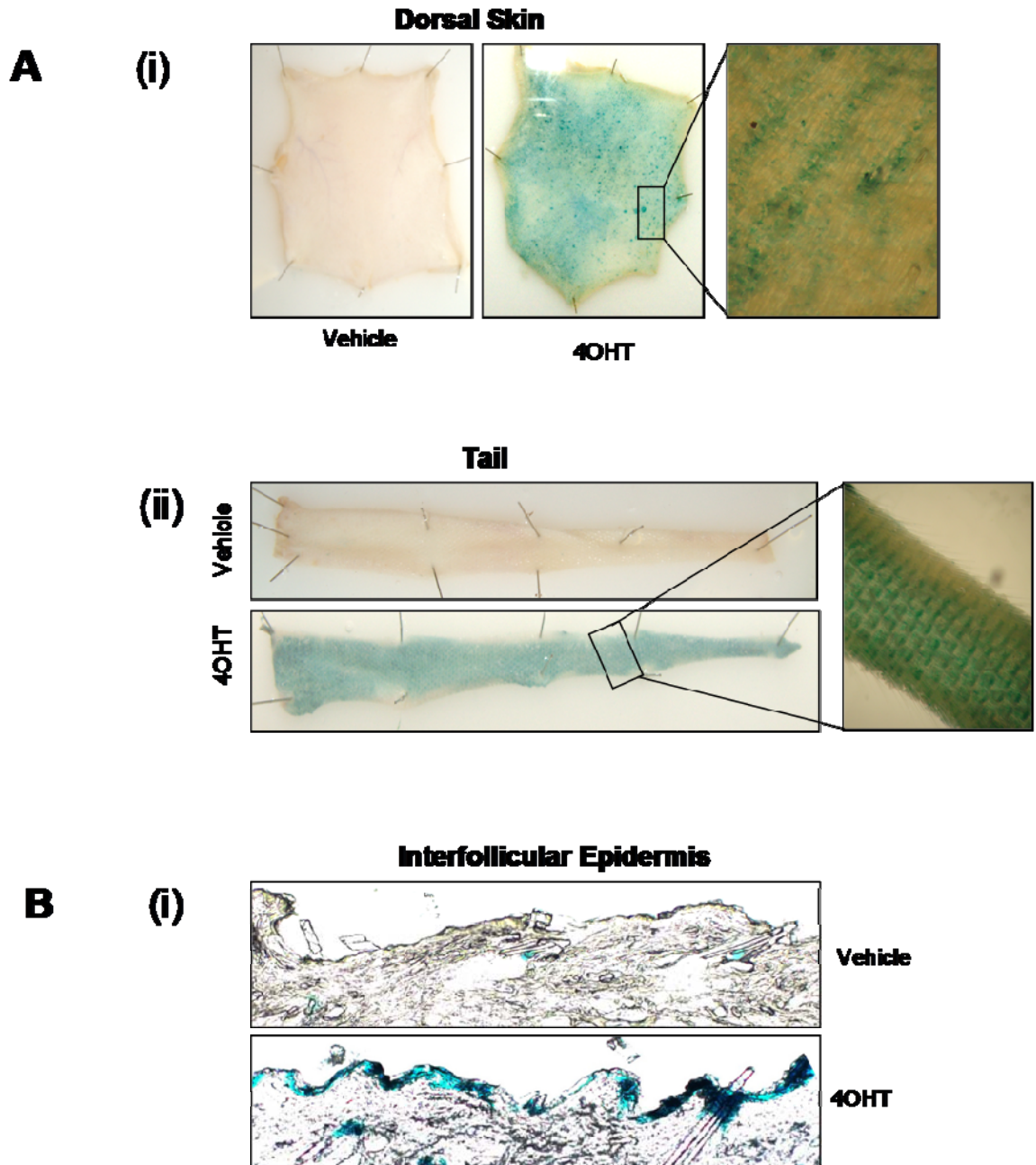
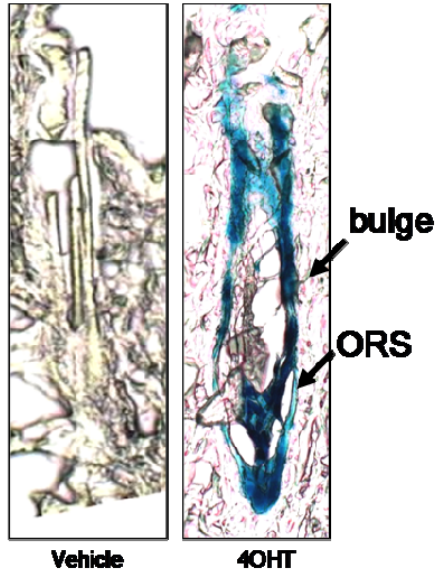


Figure 9 - *Chk1* Knockout in Adult Mouse Skin

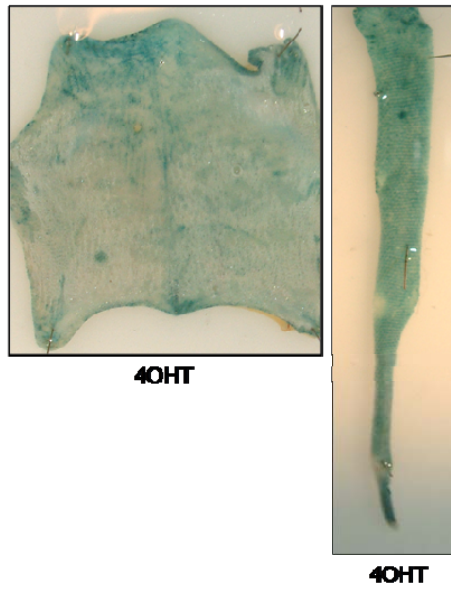
Chk1^{flox/flox} // *K14CreERT2* // *LacZ* mice were treated with either vehicle or 4OHT (both intraperitoneally and topically). **A** β -Gal assay showed strong positivity in whole mounted (i) skin and (ii) tail in animals treated with 4OHT. Vehicle treated animals displayed no positive reaction. **B** Microscopy of sectioned skin wholemounts showed strong β -Gal assay positivity in animals treated with 4OHT but not vehicle. β -Gal staining was confined to keratin 14 (K14) expressing regions in keeping with anticipated tissue distribution i.e. the (i) epidermis and (ii) hair follicles including the outer root sheath (ORS) and bulge region. **C** *Chk1*^{+/+} // *K14CreERT2* // *LacZ* animals treated with 4OHT demonstrated strong β -Gal positivity and served as the positive control. **D** Immunohistochemistry of formalin-fixed tissue showed substantial reduction in Chk1 protein expression in the epidermis and hair follicles using two separate antibodies. **E** Western blot of protein extracts from epidermal tissue (as shown in D) showed gradual knockdown of Chk1 detected over the course of a 5 day (Day -5 to -1) intraperitoneal injection protocol. Scale bar represents 200 μ m.

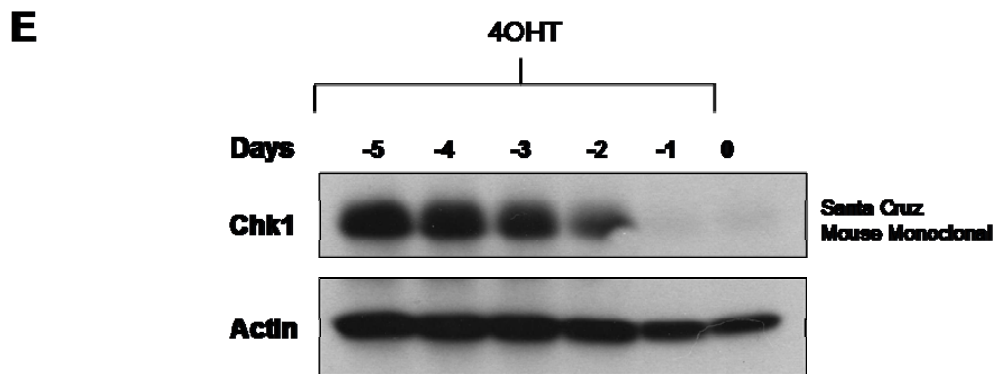
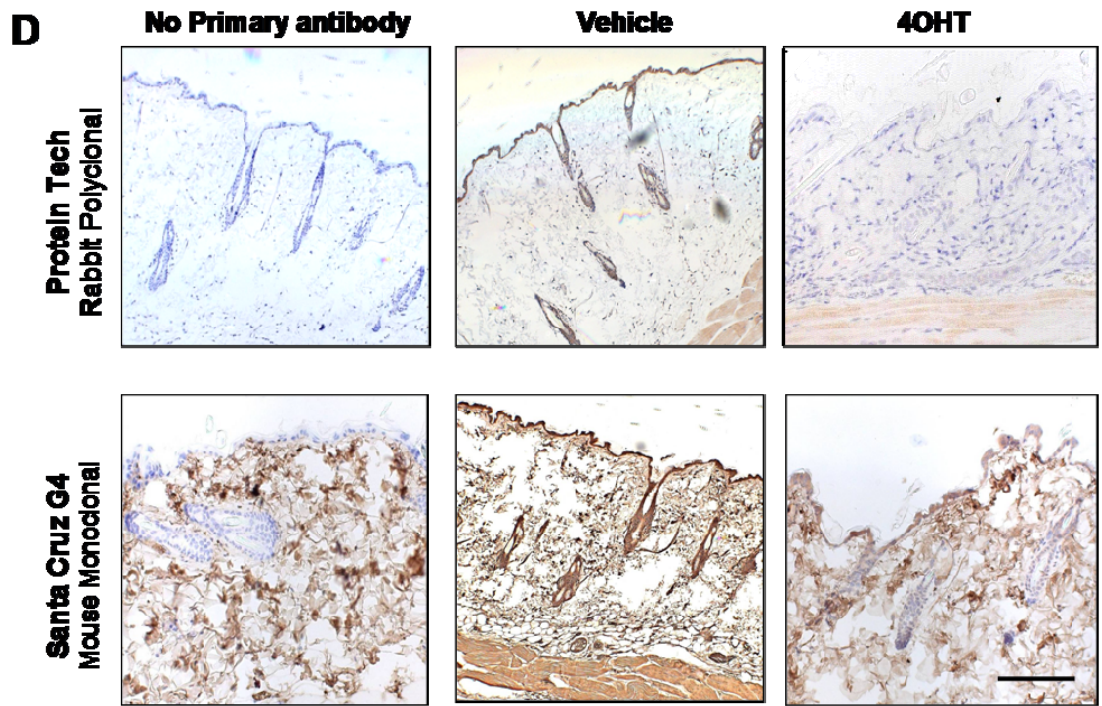
Hair Follicle

(ii)



C





adjacent to the insertion site of the erector pili muscle and is considered to be the niche for tissue specific stem cells in the hair follicle (Perez-Losada & Balmain, 2003). K14 is also expressed in the interfollicular epidermis and other squamous epithelia including tail and aerodigestive mucosa.

Following tamoxifen treatment in *chk1flox/flox // K14CreER^{T2} // LacZ* trigenic animals, either injected intraperitoneally or applied topically onto skin, β -Gal assay performed on wholemounted tissue showed strong staining, approximately 70-90% of tissue in skin and tail (see Figure 9A (i) skin and (ii) tail). Microscopy of these sections showed staining confined to K14 expressing regions (Coulombe et al, 1989) which are primarily the basal epidermis and hair follicles excluding the inner root sheath, cuticle and hair shaft. As shown in Figure 9B both the interfollicular epidermis (i) and hair follicles (ii) particularly the outer root sheath (ORS) and bulge region stained strongly. No β -Gal activity was seen in *chk1flox/flox // K14CreER^{T2} // LacZ* mice that had not been exposed to 4OHT or treated with vehicle alone. Positive control *chk1+/+ // K14CreER^{T2} // LacZ* animals treated with 4OHT showed a similar pattern for β -Gal staining to *chk1flox/flox // K14CreER^{T2} // LacZ* animals treated with 4OHT (see Figure 9C).

Immunohistochemistry of formalin fixed skin from *chk1flox/flox // K14CreER^{T2} // LacZ* mice treated with IP 4OHT (D -5 to -1), showed markedly reduced Chk1 expression in the interfollicular epidermis and hair follicles using 2 separate antibodies (see Figure 9D). Protein extracts were made from dorsal skin of *chk1flox/flox // K14CreER^{T2} // LacZ* mice treated with IP 4OHT (D -5 to -1). Care was taken to separate out as much subcutaneous fat and dermis as possible from samples. Western blot analysis showed strong diminution of Chk1 protein expression after 5 days of 4-OHT (see Figure 9E).

PCR primers were designed to assay for *chk1* recombination (see Methods, 2.6). Following 4OHT mediated recombination, DNA was prepared from dorsal skin of *chk1F/- // K14CreER^{T2}* and *chk1+/- // K14CreER^{T2}* animals. PCR analysis using primers F^{rec} and R^{rec} showed presence of recombined allele only in 4OHT treated *chk1 F/- // K14CreER^{T2}* animals (see Figure 10) and not in control animals. The product was cloned and sequenced which confirmed a 1216bp product which aligned to mouse *chk1* sequence (NC_000075).

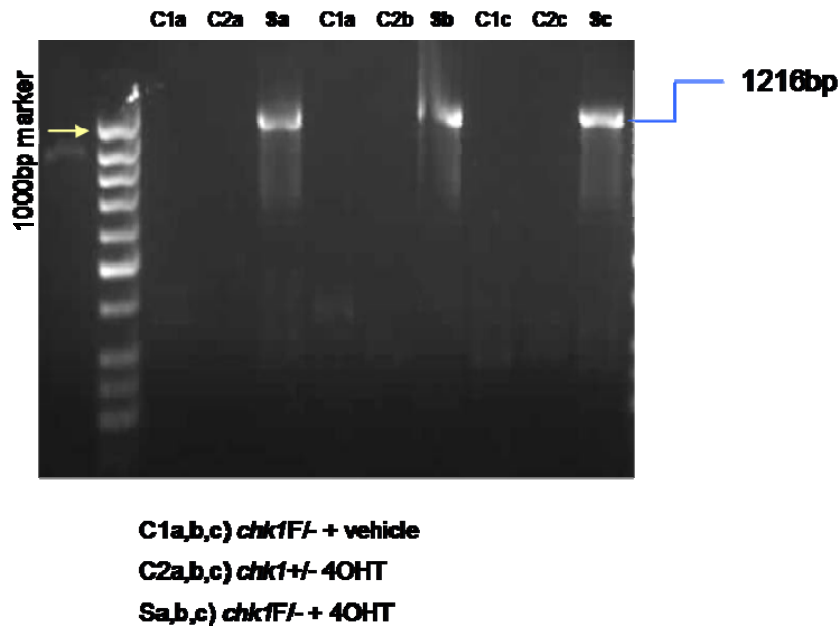
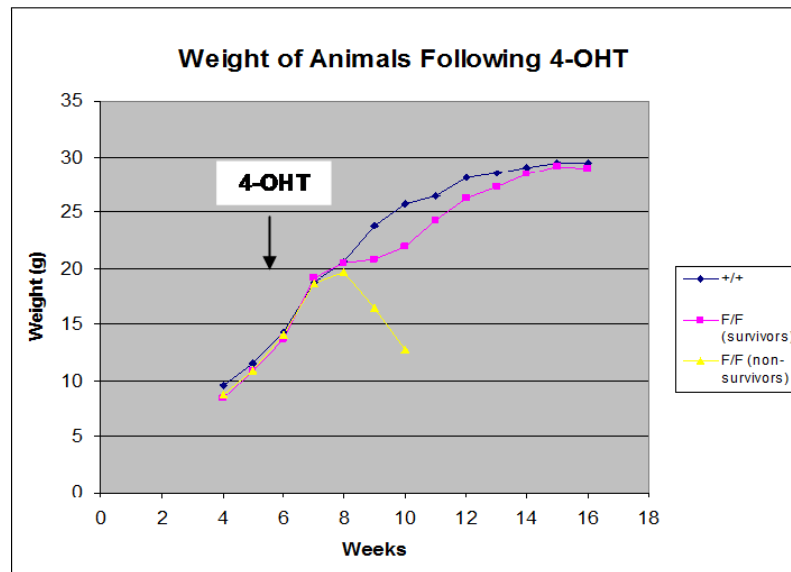
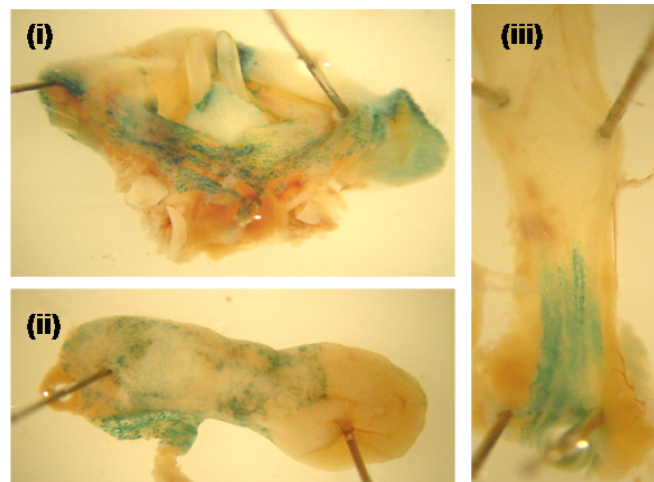


Figure 10 - PCR for Recombined *Chk1* Allele

PCR analysis of skin DNA preparations are shown on a 100bp ladder gel. A 1216bp product from the recombinated allele is seen from 3 different mice, *chk1*^{flox/null} // *K14CreER*^{T2} // *LacZ* treated with 4OHT. No recombinated product is seen from *chk1*^{+/+} // *K14CreER*^{T2} // *LacZ* animals treated with 4OHT or *chk1*^{flox/null} // *K14CreER*^{T2} // *LacZ* treated with vehicle. The PCR product was cloned and sequenced. This aligned to bp positions 3417 to 3925 and 5525 to 6233 of the mouse *chk1* gene accession number CHEK1 NC_000075.

A**B****B-Galactosidase Assay****(i) Buccal Mucosa (ii) Tongue (iii) Oesophagus****Figure 11 - Early Deaths Associated with *Chk1* Knockout**

A Weight charts were plotted for *chk1*^{+/+} // *K14CreER*^{T2} // *LacZ* mice (control group) and *chk1*^{flox/flox} // *K14CreER*^{T2} // *LacZ* mice treated with 4OHT at 5 week of age. In the control (blue line), weight increased steadily till plateau adult weight was achieved. However in *chk1*^{flox/flox} & 4OHT (pink line) the rate of weight gain temporarily decreased for approximately 3-4 weeks following Cre induction. Following that the majority of the mice were able to revert back to normal weight gain patterns and eventually achieve similar adult plateau weights as controls. However, a small proportion of *chk1*^{flox/flox} & 4OHT animals (yellow line) continued to lose weight and this was associated with feeding difficulties. They eventually died within 2-3 weeks. **B** Pathological examination of the *chk1*^{flox/flox} // *K14CreER*^{T2} // *LacZ* animals which died revealed positive β-Gal staining in the aerodigestive mucosa including the (i) buccal mucosa (ii) tongue (iii) oesophagus. It is postulated that *chk1* loss, which is associated with epithelial cell death (see Chapter 3 for further details), was responsible for causing feeding difficulties and subsequent death due to compromised aerodigestive tract epithelial function.

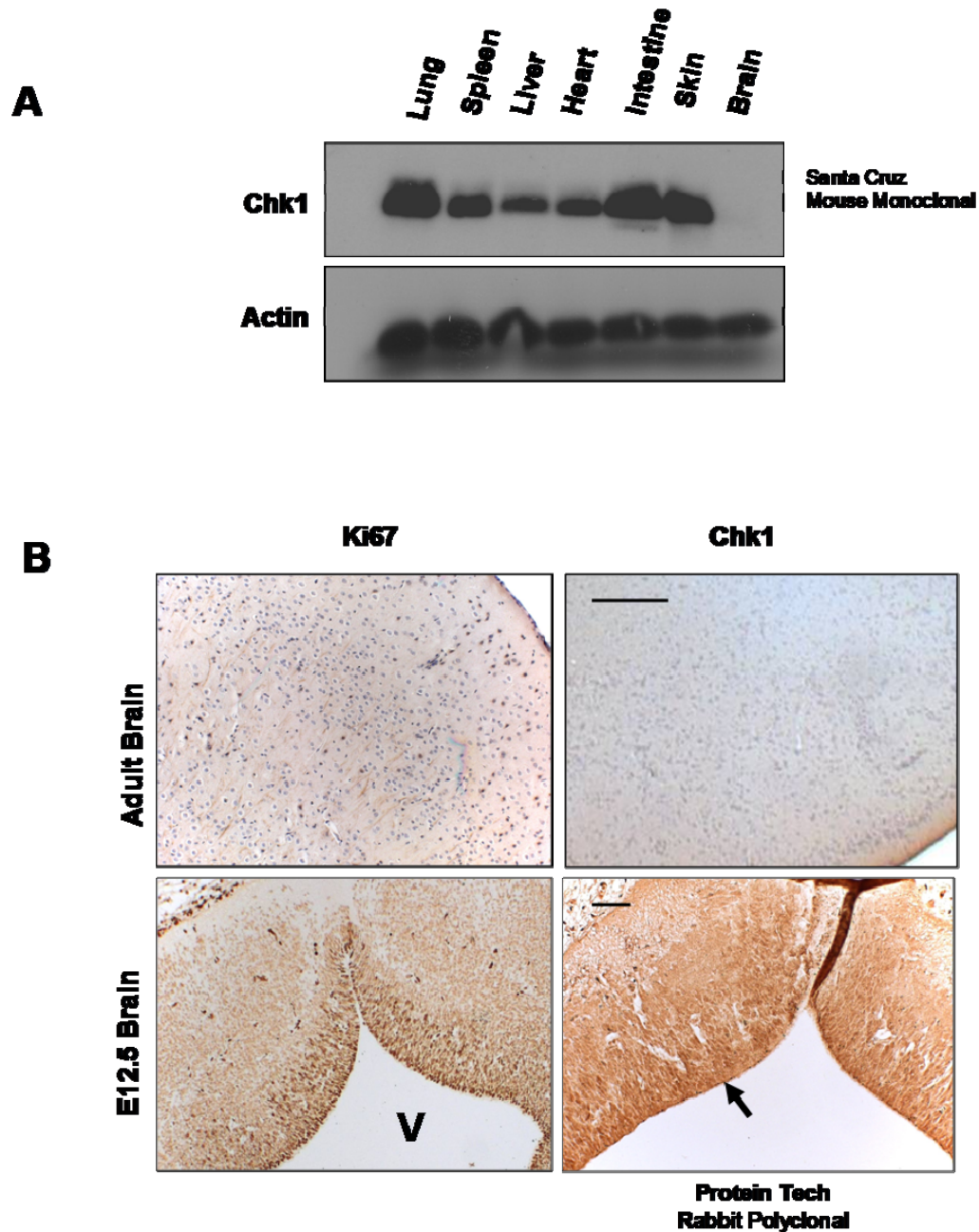


Figure 12 - Chk1 Expression in Different Mouse Tissues

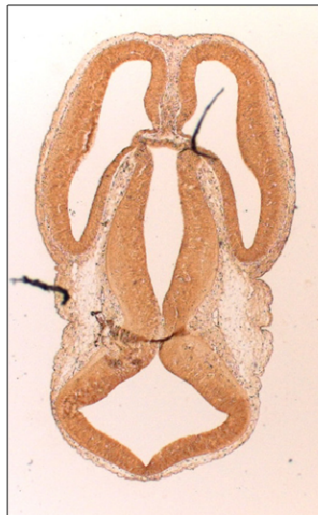
A Differential expression of Chk1 protein in different mouse tissues. Tissue from various organs were harvested and protein extracts made. Total Chk1 was measured by western blot which showed varying expression levels from very low expression in the brain to relatively high expression in skin and intestine. Higher expression roughly correlated with higher proliferative potential and activity of the organ. **B** Comparing adult brain to embryonic brain. Adult cerebral cortex showed low proliferative activity (Ki67) and low Chk1 expression. Developing embryonic brain, E12.5, however showed high proliferative activity and Chk1 expression, in particular the periventricular regions (black arrows) which is the region of brain known to have high proportion of S-phase and G2/M phase cells. V:ventricle **C** Cranial-caudal cross section of embryonic brains E12.5 show high expression of Ki67 with corresponding strong total Chk1 and the active phosphorylated serine-345 form of Chk1 staining. Again highest expression concentrated in the periventricular regions. Scale bar represents 100 μ m.

C

E12.5 Mouse Brain



Ki67



Total Chk1
Santa Cruz



P345
Cell Signalling

Given that *chk1*^{-/-} embryos are non-viable, the survival and normal litter numbers of *chk1* flox/flox // *K14CreER*^{T2} mice suggests *CreER*^{T2} was not spontaneously activated at any significant level during embryogenic development.

3.1.7. Phenotype of Conditional *Chk1* Knockout in the Skin

*Chk1*flox/flox // *K14CreER*^{T2} // *LacZ* mice were treated with 4OHT over age ranges 5 weeks to 1 year. The majority of animals survived 4OHT treatment without incident except when 4OHT was applied to 5 week old *chk1*flox/flox // *K14CreER*^{T2} // *LacZ* animals. In this cohort mortality was observed in 7/24 animals (29.2%) which was associated with feeding difficulties, weight loss and death occurring within 2 weeks (see Figure 11A). In the remaining 17/24 animals, the rate of weight gain temporarily decreased following *Cre* induction, for approximately 3-4 weeks but the mice were then able to recover and achieve similar adult plateau weights. *K14* is known to be expressed in squamous epithelia in organs other than the skin, namely the upper aerodigestive tract which is involved in feeding (Hosoya et al, 2008; Mulherkar et al, 2003). Pathological examination of the *chk1*flox/flox // *K14CreER*^{T2} // *LacZ* and 4OHT animals which died revealed positive B-Gal staining in the (i) buccal mucosa (ii) tongue (iii) oesophagus (see Figure 11B). It is possible that *chk1* loss is associated with epithelial cell death in the upper aerodigestive tract leading to feeding difficulties and subsequent death due to compromised epithelial function (see Chapter 5 for further details on the effects of *chk1* loss on epithelial homeostasis). The surviving animals were aged up to one and a half years, displayed no premature ageing or deaths compared to control, were fertile and displayed no increased incidence of tumourigenesis. There were no overt phenotypic differences between control animals, *chk1*flox/flox // *K14CreER*^{T2} // *LacZ* treated with vehicle and *chk1*^{+/+} // *K14CreER*^{T2} // *LacZ* treated with 4OHT and experimental animals *chk1*flox/flox // *K14CreER*^{T2} // *LacZ* treated with 4OHT.

3.1.8. Chk1 Expression in Different Organs

Little is known about the level of Chk1 protein expression in different organs. In general Chk1 is important in maintaining genomic integrity during cell replication and it is expected that higher Chk1 expression will correlate with a higher degree of proliferation (Tort et al, 2005; Zhou & Bartek, 2004).

Tissue from various organs were harvested from wild type animals and protein extracts made. Total Chk1 was measured by western blot and showed varying expression levels from very low levels in the brain to high levels in skin and intestine (see Figure 12A). Higher expression roughly correlated with known relative proliferative activity of the organ.

More detailed analysis of brain tissue was performed (see Figure 12B). Adult cerebral cortex showed very low proliferative activity, as shown by very weak Ki67 staining and correspondingly low Chk1 expression. Developing embryonic brain, E12.5, however showed high proliferative activity (Ki67 staining) and abundant Chk1 expression, in particular the peri-ventricular regions, which is known to have high number of S-phase and G2/M phase cells (Frade, 2002; Takahashi et al, 1995). Cranial-caudal cross section of the brain shows corresponding high expression of Ki67 with total Chk1 and the active phosphorylated serine-345 form of Chk1. Again highest expression of phosphorylated serine-345 Chk1 concentrated in the periventricular regions.

3.2. Discussion

Due to the embryonic lethality in constitutive *chk1* knockout mice (Liu et al, 2000b; Takai et al, 2000), it was necessary to employ a conditional knockout model to study the effect of *chk1* loss in an adult somatic system. Both the constitutive and conditional *chk1* alleles were kindly provided by our collaborator Prof. Stephen Elledge, in 2003 (Liu et al, 2000b). Using a 4-hydroxy tamoxifen (4OHT) activated CreT2-LoxP system (Indra et al, 1999) driven by a Keratin 14 (K14) promoter (Li et al, 2000; McLean et al, 2004) I was able to effect *chk1* genetic recombination and inactivation under appropriate spatial and temporal control within the skin. When *chk1*^{flox/flox} // K14CreERT2 // LacZ trigenic animals were treated with 4OHT, β -Gal assay showed strong staining in K14 expressing regions. Immunohistochemistry and western blotting of skin protein extracts showed markedly reduced Chk1 expression. PCR confirmed presence of *chk1* recombined allele. Control wild type animals treated with 4OHT and floxed animals treated with vehicle controls served as reliable controls.

I observed no overt pathology with *chk1* loss in *chk1*^{flox/flox} animals apart from early mortality in very young (5 weeks old) mice. This was not due to skin abnormalities but rather associated with feeding difficulties and weight loss which was attributed to K14 activation and *chk1* loss in the aerodigestive mucosa. As will be shown and discussed later in Chapter 5, *chk1* loss resulted in apoptosis in epithelial cells and replacement by unrecombined cells. Therefore, disruption of epithelial function in juvenile mice is a likely explanation for the observations. This phenomenon was not observed in older mice. Hemizygous *chk1* loss was again not associated with pathology.

I also found a differential level of Chk1 protein expression in various tissues which correlates with the proliferative activity within that organ. In skin, expression was moderate to high. Interestingly Chk1 expression was also found to be substantial in embryonic brain but virtually absent in adult brain. As Chk1 function is crucial in preventing genomic instability during cellular division, the highly proliferative developing brain may be particularly reliant on its activity.

From an cancer treatment perspective perhaps targeting Chk1 in proliferating tumours in the brain, set amongst an environment of non-proliferating lowly expressing Chk1 brain tissue, may be a way to maximize tumour kill whilst reducing side effects to normal tissue. It has already been shown that pharmacological inhibition of checkpoint mechanisms in glioma stem cells is a novel and effective method to reverse radioresistance; radiotherapy being the mainstay of brain tumour therapy (Bao et al, 2006).

**Chapter 4. *Chk1* Ablation and Tumour
Formation**

4.1. Results

4.1.1. *Chk1* Ablation in the Skin Delayed Papilloma Formation and Reduced Papilloma Numbers and Sizes

The DMBA/TPA protocol is a well characterised tool used for the study of papilloma and carcinoma development in mouse skin (see Figure 3). Tumours can be easily visualised, quantified and then harvested for further analysis. Additionally the genetic mutations caused by DMBA and TPA promotion are well known (Kemp, 2005). Details of the protocol are provided in Methods (see 2.8). The primary targets for carcinogen transformation are thought to be the bulge or hair follicle stem cells (Perez-Losada & Balmain, 2003) (see Figure 4).

Cohorts of 7-8 week old female mice were used. They underwent dorsal shaving prior to topical carcinogen application. *Chk1*^{flox/flox} // *K14CreER*^{T2} // *LacZ* mice (n=18) animals were treated with 5 days of 4OHT to induce Cre-recombinase and effect *chk1* conditional knockout in epidermis and hair follicles. A single topical dose of DMBA was applied 3 days later (D3) and this was followed by 20 weeks of twice weekly topical TPA application. Control *chk1*^{flox/flox} // *K14CreER*^{T2} // *LacZ* mice were treated with vehicle prior to DMBA (n=19) and control female *chk1*^{+/+} // *K14CreER*^{T2} // *LacZ* mice were treated with 4OHT prior to DMBA (n=20). Papilloma numbers were counted weekly till 30 weeks after the start date of TPA. Animals were culled if they developed either a papilloma or carcinoma burden exceeding the limit set in the project license (see Methods 2.4) or by 60 weeks whichever was earlier.

In the *chk1*^{flox/flox} // *K14CreER*^{T2} // *LacZ* + 4OHT group, the rate of papilloma formation was significantly delayed compared to the *chk1*^{flox/flox} // *K14CreER*^{T2} // *LacZ* + vehicle group (log rank, p<0.0001) and the *chk1*^{+/+} // *K14CreER*^{T2} // *LacZ* + 4OHT group (log rank, p<0.0001) (see Figure 13A). By 77 days, all control animals had developed papillomas. In contrast, 16.7% of

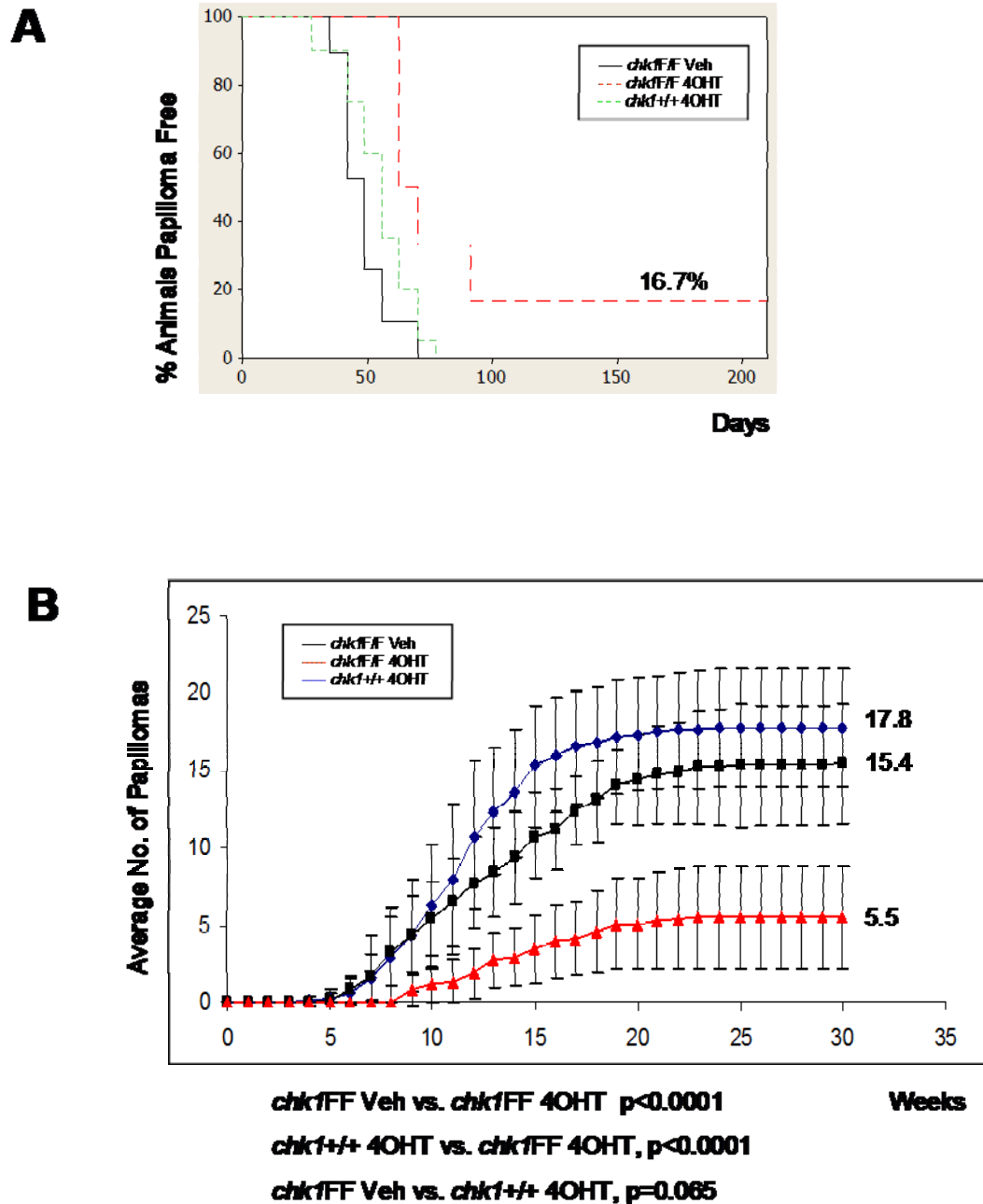
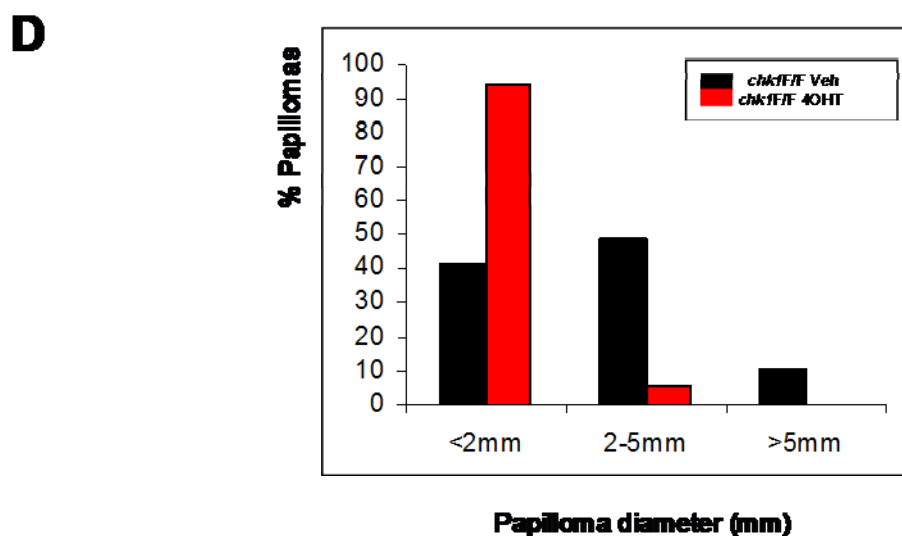
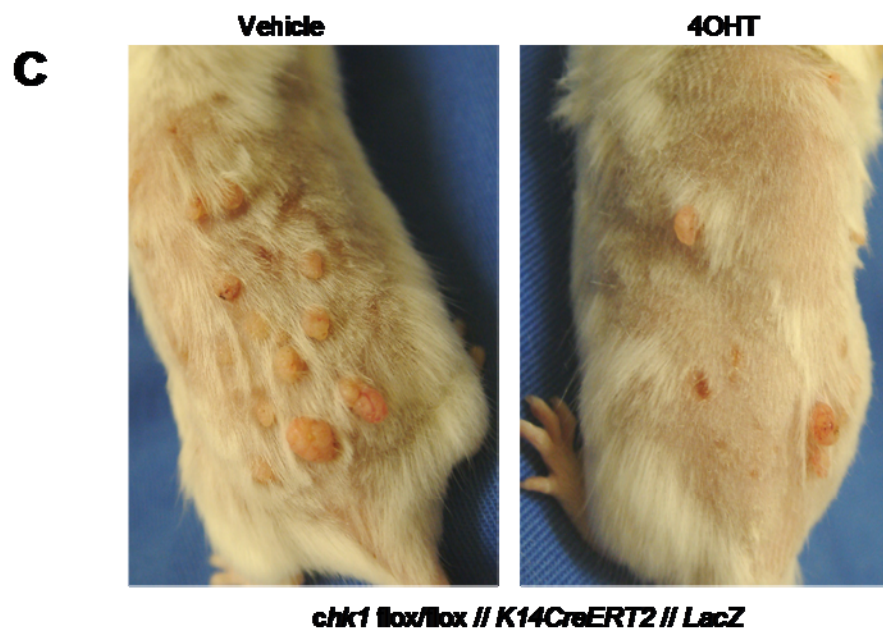


Figure 13 - *Chk1* ablation Prior to DMBA/TPA Carcinogenesis

Cohorts of 7-8 weeks old female mice underwent dorsal skin shaving and were treated with 5 days of intraperitoneal 4OHT to induce Cre-recombinase activity and effect *chk1* conditional knockout in epidermis and hair follicles or 5 days of vehicle. Three days later, a single dose of topical DMBA was applied (D3) and this was followed by 20 weeks of twice weekly TPA tumour promotion. Control mice were *chk1flox/flox // K14CreER^{T2} // LacZ* + vehicle (n=19) and *chk1+/+ // K14CreER^{T2} // LacZ* mice + 4OHT (n=20). Experimental group was *chk1flox/flox // K14CreER^{T2} // LacZ* + 4OHT (n=18). **A** In the experimental group (*chk1flox/flox* + 4OHT), the rate of papilloma formation was delayed compared to controls *chk1flox/flox* + vehicle (log rank, $p < 0.0001$) and *chk1+/+* + 4OHT (log rank, $p < 0.0001$). There was no statistical difference between the two control groups (log rank, $p = 0.075$). By 70 days, all control animals had developed papillomas. In contrast, 16.7% (3/18) of



experimental animals remained tumour free and never developed papillomas up to 30 weeks. The remaining 15/18 that developed papillomas, did so within 100 days. **B** The average number of papillomas per mouse in each cohort increased in an exponential fashion upon commencement of TPA and reached a plateau between 15-25 weeks. No new papillomas were observed after this maximum burden was reached. At 30 weeks, a significantly lower average number of papillomas per mouse was observed in the experimental *chk1flox/flox* + 4OHT cohort versus control *chk1flox/flox* + vehicle, 5.5 versus 15.4 (Mann Whitney $p < 0.0001$). A significantly lower average number of papillomas per mouse developed in the experimental *chk1flox/flox* + 4OHT cohort versus control *chk1+/+* + 4OHT, 5.5 versus 17.8 (Mann Whitney $p < 0.0001$). No statistically significant difference was seen between the two control groups, Mann Whitney, $p = 0.065$. **C** Photographs of a representative animals from the control *chk1flox/flox* + vehicle versus *chk1flox/flox* + 4OHT experimental groups. **D** The majority of papillomas that formed in *chk1flox/flox // K14CreERT2 // LacZ* + 4OHT animals were <2mm (94.6%) and none exceeded 5mm. This contrast with control *chk1flox/flox // K14CreERT2 // LacZ* + vehicle animals where papilloma diameters were larger <2mm (41.2%), 2-5mm (48.5%) and >5mm (10.3%).

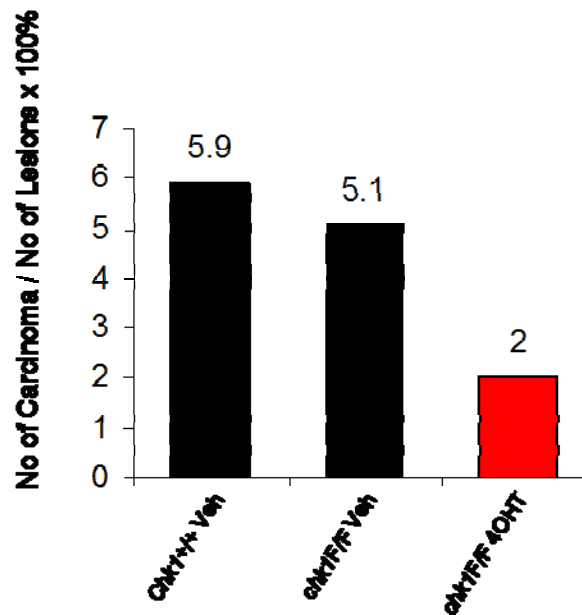


Figure 14 - Rate of Conversion of Papillomas to Carcinomas

The rate of conversion from papillomas to carcinomas in each cohort was calculated as the total number of carcinomas formed/total number of lesions (papillomas formed, including those that transformed into carcinomas) x100% **Figure 4**. Rates of conversion were as follows, *chk1*^{+/+} // *K14CreER*^{T2} // *LacZ* + 4OHT (5.9%, 21/355), *chk1* flox/flox // *K14CreER*^{T2} // *LacZ* + vehicle (5.1%, 15/293) and *chk1* flox/flox // *K14CreER*^{T2} // *LacZ* + 4OHT (2%, 2/99). There was no statistical difference between *chk1*^{+/+} + 4OHT and experimental group (chi squared p=0.191), *chk1* flox/flox + vehicle and experimental group (chi squared p=0.259) and no difference between control groups (chi squared p>0.25).

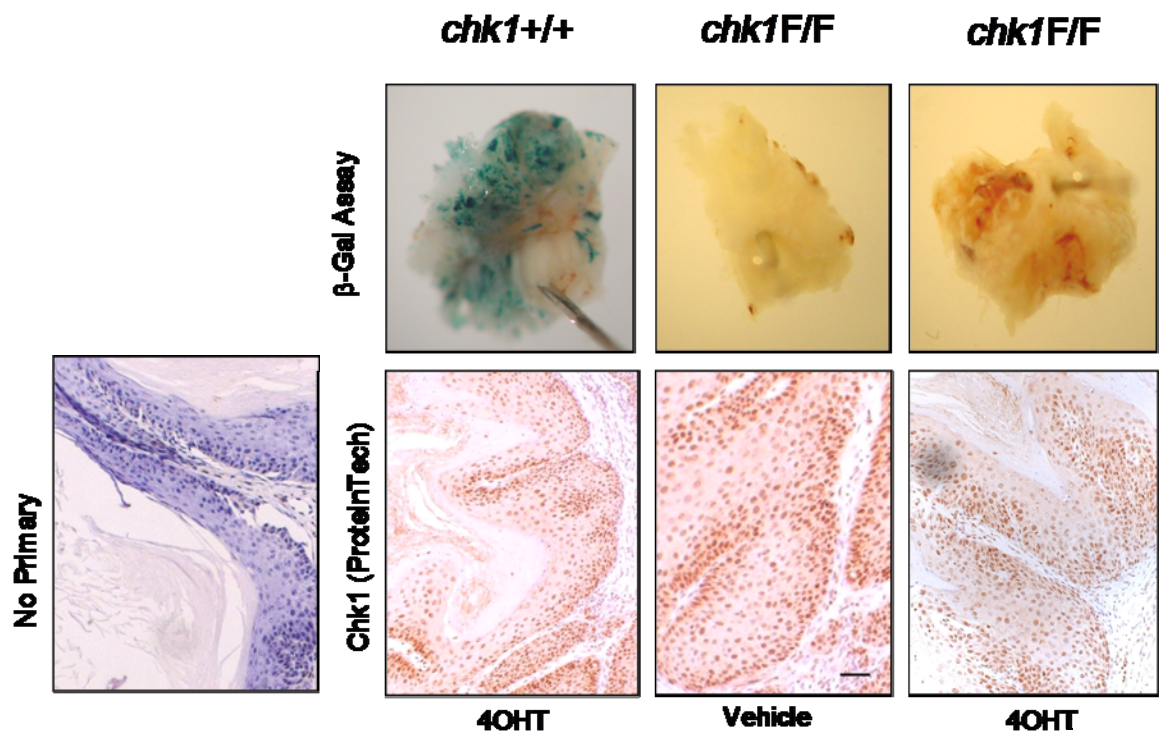


Figure 15 - Chk1 Expression in Papillomas

Papillomas from the experimental and control cohorts were analysed for recombination, using β -Gal assay, and for Chk1 expression, using Chk1 immunohistochemistry. All papillomas from the *chk1*^{+/+} // *K14CreER*^{T2} // *LacZ* + 4OHT cohort stained positive for β -Gal. In the other control group *chk1*^{flox/flox} // *K14CreER*^{T2} // *LacZ* + vehicle, none of the papillomas stained positive for β -Gal. In both control groups, all papillomas stained positive for Chk1 as determined by immunohistochemical staining of paraffin embedded sections, with the majority staining strongly positive. In the experimental *chk1*^{flox/flox} // *K14CreER*^{T2} // *LacZ* + 4OHT group, none of the papillomas stained positive for β -Gal. However, all papillomas stained positive for Chk1, with the majority staining strongly positive. Scale bar represents 50 μ m.

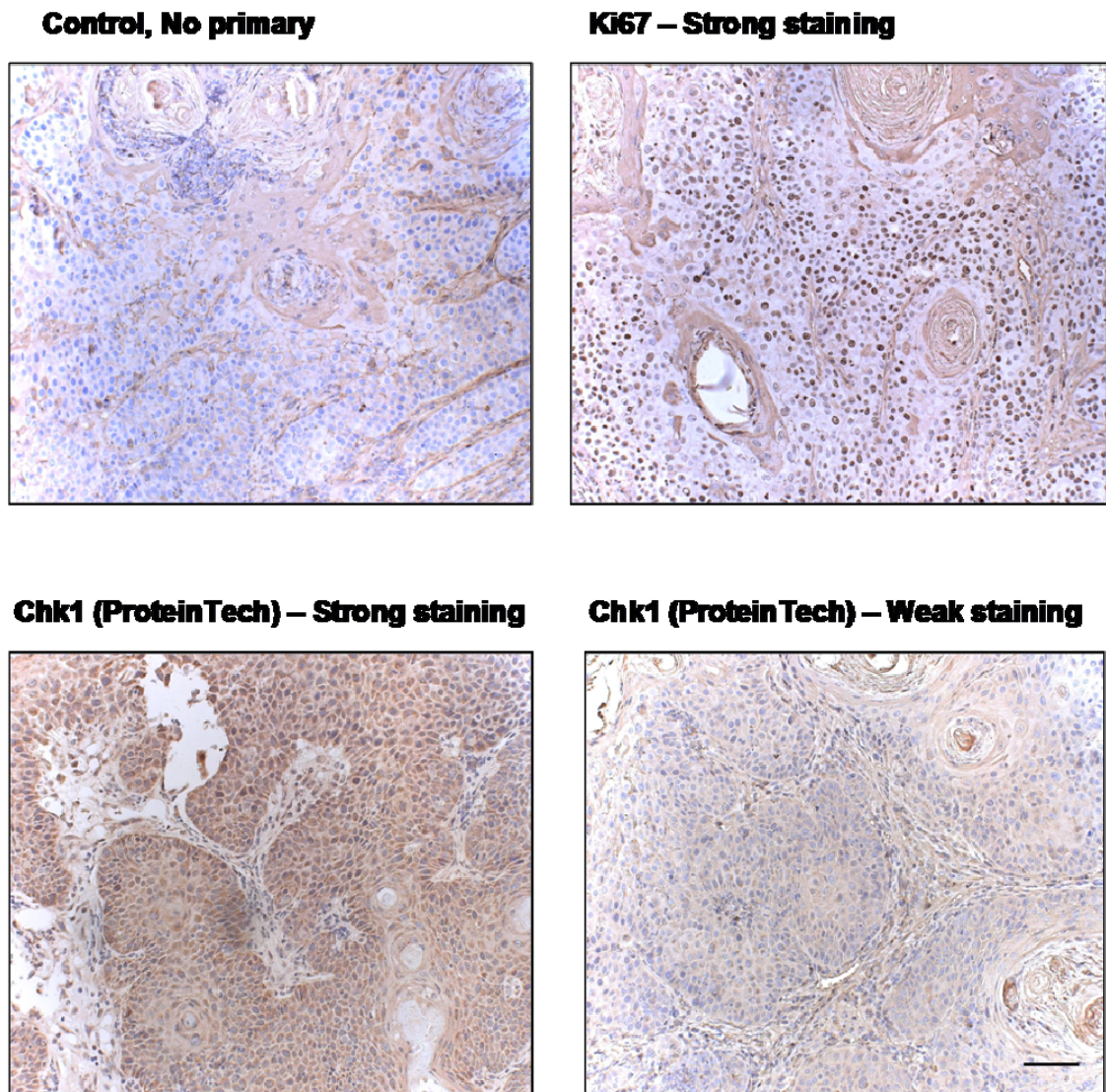


Figure 16 - Chk1 Expression in Carcinomas

Carcinomas that formed from papillomas were analysed for Chk1 expression by immunohistochemistry. All of the carcinomas from the *chk1*^{+/+} // *K14CreER*^{T2} // *LacZ* + 4OHT group displayed a degree of Chk1 staining however, approximately half displayed strong positivity but the other half low levels of staining only. Therefore, there was a greater variability of Chk1 staining amongst the carcinomas compared to papillomas. Scale bar represents 100 μ m.

*chk1*flox/flox // *K14CreER^{T2}* // *LacZ* + 4OHT animals remained tumour free and never developed papillomas up to 30 weeks. The average number of papillomas in each cohort increased in an exponential fashion upon commencement of TPA and plateaued between 20-25 weeks later (see Figure 13B). At 30 weeks the average number of papillomas that developed in *chk1*flox/flox // *K14CreER^{T2}* // *LacZ* + 4OHT group was significantly less than *chk1*flox/flox // *K14CreER^{T2}* // *LacZ* + vehicle mice were 5.5 versus 15.4 (Mann Whitney, $p < 0.0001$). A significantly smaller average number of papillomas per mouse developed in *chk1*flox/flox // *K14CreER^{T2}* // *LacZ* + 4OHT group versus *chk1*+/+ // *K14CreER^{T2}* // *LacZ* + 4OHT + 4OHT, 5.5 versus 17.8 (Mann Whitney, $p < 0.0001$). There was no statistically significance difference in the average number of papillomas between the control groups (Mann Whitney, $P = 0.065$). Maximum tumour diameter of each papilloma on each mouse was measured at 18 weeks post TPA commencement (see Figure 13D). The majority of papillomas that formed in *chk1*flox/flox // *K14CreER^{T2}* // *LacZ* + 4OHT animals were small <2mm (94.6%) and none exceeded 5mm. This contrasted with control *chk1* flox/flox // *K14CreER^{T2}* // *LacZ* + vehicle animals where papilloma diameters were larger <2mm (41.2%), 2-5mm (48.5%) and >5mm (10.3%).

The rate of conversion from papillomas to carcinomas in each cohort was calculated as the total number of carcinomas formed/total papillomas formed x100% (see Figure 14). Rates of conversion were as follows, *chk1*+/+ // *K14CreER^{T2}* // *LacZ* + 4OHT (5.9%, 21/355), *chk1*flox/flox // *K14CreER^{T2}* // *LacZ* + vehicle (5.1%, 15/293) and *chk1*flox/flox // *K14CreER^{T2}* // *LacZ* + 4OHT (2%, 2/99). There was no statistical difference between *chk1*+/+ + 4OHT and experimental group (chi squared $p = 0.191$), *chk1*flox/flox + vehicle and experimental group (chi squared $p = 0.259$) and no difference between control groups (chi squared $p > 0.25$).

Although not statistically significant, the results suggest a trend towards a reduction in conversion rate from papilloma to carcinoma when *chk1* was ablated. Indeed the only 2 carcinomas in the *chk1* ablated group developed and results were not able to be analysed using chi squared but required Fisher's testing due to the small number of events. In order to definitively test this effect, I propose that it is necessary to repeat the experiment with a larger *chk1*flox/flox // *K14CreER^{T2}* // *LacZ* + 4OHT cohort (approximately 60 animals).

It was not anticipated prior to the experiment that *chk1* ablation would result in markedly reduced papilloma (approximately 1/3 compared to control) and carcinoma numbers which subsequently presented limitations in terms of statistical analyses.

4.1.2. Papilloma Formation Requires Chk1

Papillomas from the experimental and control cohorts were analysed for recombination, using β -Gal assay, and for Chk1 expression, using Chk1 immunohistochemistry (see Figure 15). Analysis of papillomas from every animal was not always possible due to technical or collection difficulties (eg. discontinuation of the production of ProteinTech Chk1 antibody in 2008, animals that died on the weekend and tissue therefore not amenable for late harvesting). Papillomas from the *chk1+/+ // K14CreER^{T2} // LacZ + 4OHT* cohort (papillomas from 18/20 animals examined) stained positive for β -Gal. In the other control group *chk1flox/flox // K14CreER^{T2} // LacZ + vehicle* (papillomas from 18/19 animals examined), none of the papillomas stained positive for β -Gal. In the experimental *chk1flox/flox // K14CreER^{T2} // LacZ + 4OHT* group (papillomas from 16/18 animals examined), none of the papillomas stained positive for β -Gal.

In the *chk1+/+ // K14CreER^{T2} // LacZ + 4OHT* (papillomas from 15/20 animals examined) and *chk1flox/flox // K14CreER^{T2} // LacZ + 4OHT* (papillomas from 15/19 animals) control groups, papillomas stained positive for Chk1 by immunohistochemistry. In the experimental *chk1flox/flox // K14CreER^{T2} // LacZ + 4OHT* group (papillomas from 14/18 animals examined), papillomas also stained positive for Chk1 by immunohistochemistry. All papillomas examined demonstrated strong positivity for Chk1.

Given that 4OHT induced recombination in the skin is not complete, approximately 70-90% efficient (Ruzankina et al, 2007), it is expected that *chk1* unrecombined (or “wild type”) stem cells will persist in tissue. Papillomas that did arise in the *chk1flox/flox // K14CreER^{T2} // LacZ + 4OHT* group expressed Chk1 which implies they derived initially from cells which had escaped

recombination. This suggests that *chk1* is essential for papilloma formation. No papillomas that formed lacked Chk1 expression. Furthermore, the vast majority of papillomas stained strongly for Chk1 suggesting that this gene function plays an important role in continued tumour survival.

4.1.3. Chk1 Expression in Carcinomas Varies in Intensity

Carcinomas that formed from papillomas were also analysed for Chk1 expression by immunohistochemistry (see Figure 16). Not all carcinomas were evaluated for the same reasons as that described in 4.1.2. 11 of the 15 carcinomas were examined for Chk1 staining by immunohistochemistry in the *chk1^{flox/flox} // K14CreER^{T2} // LacZ* + vehicle group, all displayed positive Chk1 staining. 6 displayed strong positivity and the other 5 displayed a lower level of positivity. 8 of the 21 carcinomas examined for Chk1 staining by immunohistochemistry in the *chk1^{+/+} // K14CreER^{T2} // LacZ* + 4OHT group displayed positive Chk1 staining. 2 displayed strong positivity and the other 6 displayed a lower level of positivity. Therefore, there was a greater variability in the strength of Chk1 staining amongst the carcinomas compared to papillomas. Only 2 carcinomas developed in the *chk1^{flox/flox} // K14CreER^{T2} // LacZ* + 4OHT group, both of which stained strongly for Chk1.

4.2. Discussion

The two stage DMBA/TPA tumour initiation and promotion protocol (see Figure 3) is a well described and proven model for studying the evolution of tumours in mouse skin (Kemp, 2005; Perez-Losada & Balmain, 2003). This model was chosen for reasons outlined in the Introduction (for a full description and discussion see Introduction 1.6) as well as longstanding local expertise related to the development and utilization of this protocol for cancer research within the Beatson Institute (McLean et al, 2004; Quintanilla et al, 1986). It involves treating the dorsal skin with an initiating dose of DMBA (7, 12-dimethylbenz[a]anthracene) as a single application typically, followed by multiple applications of tumor promoter, TPA (12-*O*-tetradecanoylphorbol-13-acetate) over several months (Methods 2.8). The age of commencement of chemical carcinogens was standardized as age variations can alter the yield of tumours (Van Duuren et al, 1975). The primary targets for transformation are thought to be the bulge or hair follicle stem cell population (Brown et al, 1998; Owens & Watt, 2003; Perez-Losada & Balmain, 2003) (see Figure 4).

The original *chk1* mice we obtained in 2003 from our collaborators (Liu et al, 2000b) were genetically of a mixed FVB and C57BL6/J background. They were further backcrossed onto FVB for at least 6 generations in order to minimize genetic heterogeneity (see Methods, 3.1.2). The albino FVB is considered optimal for conducting skin carcinogenesis experiments as opposed to other strains such as C57BL6/J, which are less susceptible to tumour formation (Kemp, 2005; Naito & DiGiovanni, 1989). Papilloma numbers in the control cohort in my experiments were similar to those reported in the literature using the same DMBA/TPA protocol (Kemp, 2005; McLean et al, 2004). This indicated an acceptable level of genetic homogeneity within my mouse cohorts on the FVB strain which allows reliable comparisons to be made between the different experimental groups. In our experiments, the final yield of papillomas from the two different control cohorts *chk1*^{+/+} // *K14CreER*^{T2} // *LacZ* + 4OHT and *chk1*^{flox/flox} // *K14CreER*^{T2} // *LacZ* mice + vehicle were not statistically different (see Figure 13B). This indicated that, at least on gross observation, there was no evidence for the floxed *chk1* allele affecting tumour yield without

recombination (a hypomorphic effect for example). Similarly, previous studies published using this allele did not report any evidence for the floxed allele exerting a hypomorphic effect in embryogenesis, development and carcinogenesis (Greenow et al, 2009; Lam et al, 2004; Liu et al, 2000b; Zaugg et al, 2007). In my observations, treatment with 4OHT did not interfere with phenotype nor tumour yield which agrees with previous studies (Indra et al, 1999; McLean et al, 2004).

DMBA/TPA treatment gave rise to benign, pre-malignant papillomas, which comprise hyperplastic epidermis and stroma. The number, size and rate of development of these tumours were readily quantified (see Figure 13). I show that *chk1* ablation prior to DMBA significantly reduced the total yield of papillomas (1/3 the average number compared to control. Papilloma formation was delayed and the size of papillomas that formed were smaller. In fact in 16.7% of mice undergoing *chk1* ablation, this prevented completely the development of any papillomas. Furthermore, papillomas that did arise in the *chk1* ablated mice arose from cells that had escaped recombination (we know that recombination is only 70-90% effective) and they stained positive for *chk1* on immunohistochemistry and /or displayed absence of β -Gal positivity (see Figure 15). Taken together, this indicated that *chk1* ablation inhibited the formation of papillomas and the tumours that did form arose from cells that had escaped initial 4OHT mediated recombination. This suggests that papilloma formation required *chk1*.

After papilloma appearance, continued TPA promotion caused a small percentage of papillomas to develop into malignant, invasive squamous cell carcinomas. Although not statistically significant, the results suggest a trend towards a reduction in the rate of papilloma to carcinoma conversion following *chk1* ablation (see Figure 14). However, as only 2 carcinomas in the *chk1* ablated group developed, results were not able to be analysed using chi squared test but required the use of fisher's test due to small numbers. In order to verify this effect, I propose that it is of scientific interest and warranted to repeat the experiment with an expanded *chk1*flox/flox // *K14CreER*^{T2} // *LacZ* mice + 4OHT cohort (approximately 60 animals). It was not anticipated initially that such a significant reduction in papilloma and hence carcinoma numbers would be

observed and that this would present limitations in our ability to statistically analyse the true nature of this effect. Furthermore, I observed that carcinomas almost always originated from larger papillomas which were >5mm in diameter. As similar effect of papilloma size affecting propensity to carcinoma conversion, has previously been noted in Familial Adenomatous Polyposis (FAP) syndromes in human subjects (Lynch et al, 2008a; Lynch et al, 2008b; Rozen & Macrae, 2006) although the explanation for this phenomenon is unknown. Since *chk1* ablation significantly reduced that size of papillomas, this could be a potential explanation for the reduced rate of carcinoma conversion. Alternatively it is also possible that *chk1* ablation selectively removes a sub-population of stem cells which would ordinarily be at higher risk for carcinoma development.

**Chapter 5. *Chk1* Ablation Affects Skin and
Label Retaining Cell Homeostasis**

5.1. Results

5.1.1. BrdU Label Retention Can be Imaged in Bulge Stem Cells

The properties of bulge stem cells in the hair follicle have been discussed in the Introduction (see Introduction, 1.7.5). In addition to being pluripotent, they are long-lived and are thought to divide infrequently in the unperturbed epidermis (Braun et al, 2003; Cotsarelis et al, 1990). In order to label and identify these cells in tissue sections, neonatal mice undergoing a time of rapid tissue expansion, can be injected *in vivo* with BrdU (Bickenbach, 1981; Bickenbach & Chism, 1998; Braun et al, 2003; Cotsarelis et al, 1990; Morris & Potten, 1999). The thymidine analogue is incorporated into the DNA of cells undergoing replication and cell division. By adulthood, due to subsequent rounds of homeostatic cellular division the vast majority of cells will have diluted their BrdU DNA concentrations down to undetectable levels. However, bulge stem cells divide relative infrequently and are for the most part quiescent therefore they manage to retain a high BrdU concentration which can be readily detectable. When isolated, these cells have been shown to possess enhanced clonogenic potential and are capable of giving rise to progeny that differentiate into separate lineages (eg. keratinocytes, sebocytes etc) (Braun & Watt, 2004). These bulge label-retaining cells or LRCs are considered to represent one pool of stem cells within the skin. In order to investigate the effects of DMBA/TPA carcinogenesis on the skin, we have focused on LRCs in subsequent experiments as they are thought to be a primary source of tumours in this system (Bailleul et al, 1990; Brown et al, 1998; Owens & Watt, 2003; Perez-Losada & Balmain, 2003).

In our protocol, we injected 3-4 day old mice with 3 doses of BrdU on 3 consecutive days and allowed them to age to 8-10 weeks before sacrifice (see Figure 17A). Wholemout sections of tail epidermis were prepared, stained with an anti-BrdU antibody and visualised using confocal microscopy (Figure 17B, i, ii). Bulge LRCs (b) were generally observed just below the sebaceous glands (sg).

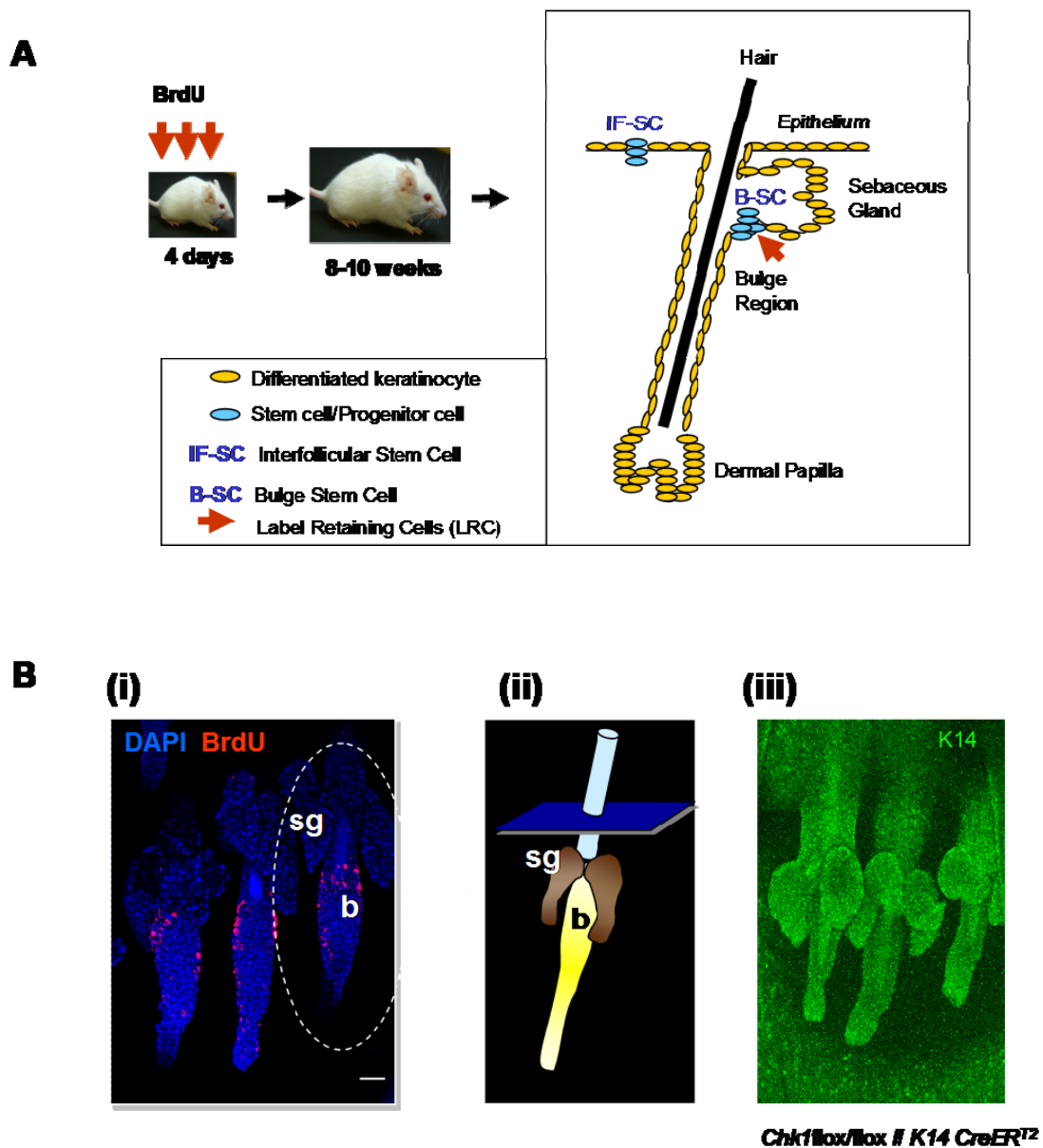


Figure 17 – BrdU Label Retaining Cell (LRC) Assay in Mouse Epithelium

A Neonatal mice aged 3-4 days old, which are undergoing a time of rapid tissue expansion, are injected with three consecutive daily doses of BrdU. The thymidine analogue is incorporated into the DNA of cells undergoing replication and cell division. By adulthood, due to subsequent rounds of homeostatic cellular division the vast majority of cells will have diluted their BrdU DNA concentrations down to undetectable levels. However, as bulge stem cells divide relative infrequently and are for the most part quiescent they manage to retain high BrdU concentrations which can be readily detectable. These BrdU-labelled cells are known as Label Retaining Cells (or LRCs). We have focused on bulge LRCs in subsequent experiments as they are thought to be the cells of origin of tumours derived from DMBA/TPA carcinogenesis. **B** (i) When mice reach adulthood at around 8 weeks, tail epidermal wholemounts are prepared, stained using anti-BrdU antibody and imaged using Z-stacked confocal microscopy. The presence of LRCs can be visualised in the bulge region (b) just below the sebaceous glands (sg). (ii) A schematic representation of the hair follicle is depicted. (iii) In the experimental *chk1^{flox/flox} // K14^{CreER^{T2}} // LacZ* trigenic animals, the fusion protein CreER^{T2} recombinase is transcribed only in keratin 14 expressing regions. In this image, confocal microscopy confirms widespread K14 expression in tail epidermis, including the bulge region. Scale bar represents 40µm.

In our experiments *chk1flox/flox // K14CreER^{T2} // LacZ* trigenic animals produced the fusion protein CreER^{T2} recombinase under the control of the K14 gene promoter and should therefore be transcribed only in keratin 14 expressing regions. We confirmed widespread K14 expression in tail epidermis, including the stem cell bulge region by staining with an anti-K14 antibody (Figure 17B, iii).

5.1.2. *Chk1* Ablation Induces Label Retaining Cell (LRC) Proliferation

To determine if 4OHT induced Chk1 protein knockdown can be imaged using confocal microscopy in mouse cells, adult *chk1flox/flox // K14CreER^{T2} // LacZ* mice treated with either vehicle or 4OHT. Two samples were used to assay Chk1 staining which were tail wholemount preparations (see Figure 18A) and keratinocyte cell suspensions prepared from the tail epidermis (Figure 18B). Both showed reduced level of Chk1 staining, albeit not all the cells became negative.

It is not known what the effect of *chk1* ablation on the normally quiescent LRC population would be. To investigate this, we performed neonatal BrdU labelling in *chk1flox/flox // K14CreER^{T2} // LacZ* pups. The mice were allowed to age to 8 weeks and then treated with either topical 4OHT or vehicle. At 8 weeks the skin is said to be undergoing a second phase of prolonged telogen lasting several weeks, thereby providing a synchronous hair follicle regeneration phase for standardised analysis (Muller-Rover et al, 2001). Wholemount tail epidermal preparations were taken over a time course, staining for BrdU and LRC numbers quantified using confocal imaging (see Figure 19A, B, C). The number of LRCs per follicle were counted for 3 triplet follicles (9 follicles) per animal in 3 separate animal for each data set at each time point. The difference in median number of LRCs was compared between control and experimental group using Mann Whitney Test. No significant difference was noted in the first 3 hours. Although statistically significant, only a small magnitude of difference appeared in the subsequent 24 hour period. In the following period from day 1-5 however, a

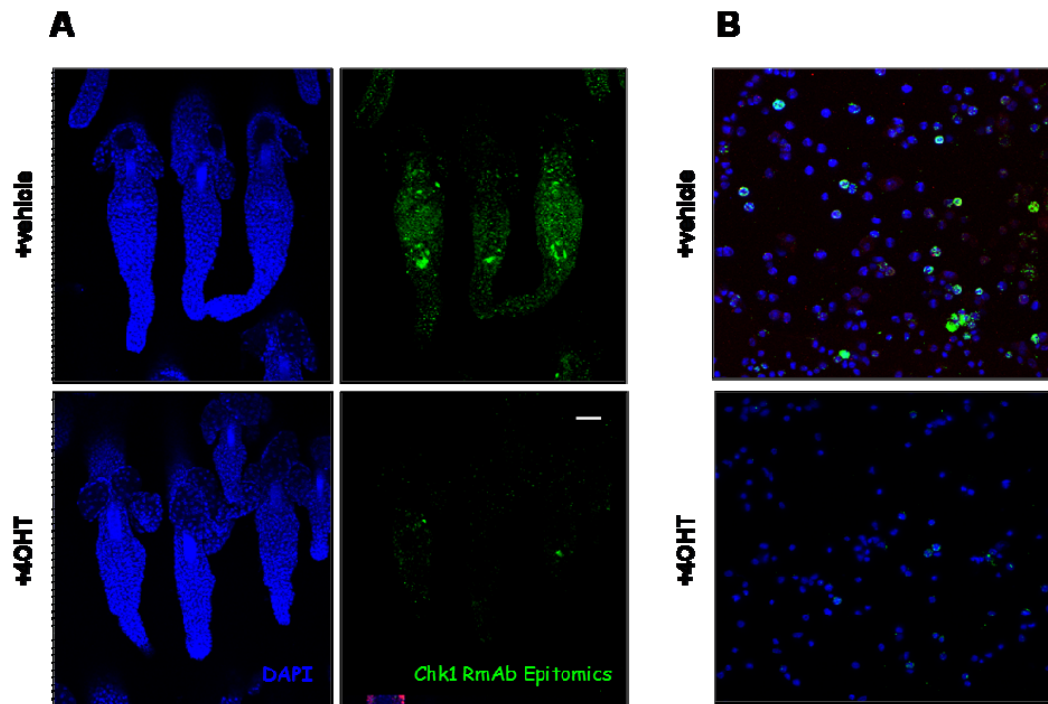


Figure 18 - Chk1 Expression in Wholmount Epidermis

A Wholmount tail epidermal preparations were made from *chk1^{flox/flox} // K14^{CreER}^{T2} // LacZ* mice treated either with vehicle or 4OHT (5 days of intraperitoneal 4OHT and sacrifice the day after the final injection) and stained for Chk1. **B** Cell suspensions were made from epidermal preparations taken from dorsal skin. Cells were adhered onto poly-L-lysine cover slips and stained for Chk1. Both were imaged using confocal microscopy. Mice treated with 4OHT showed a substantial reduction in Chk1 staining. Scale bar represents 20 μ m.

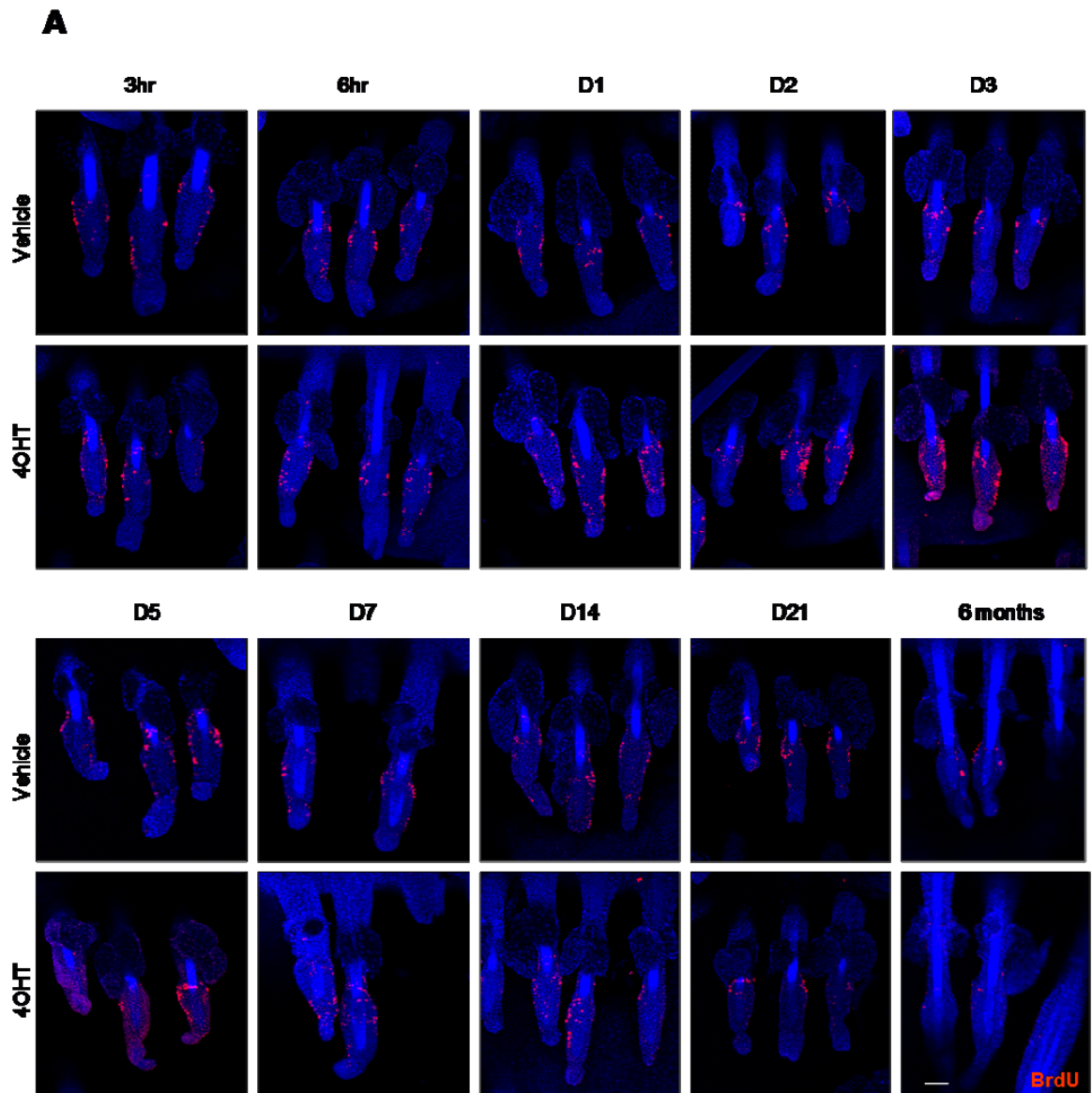
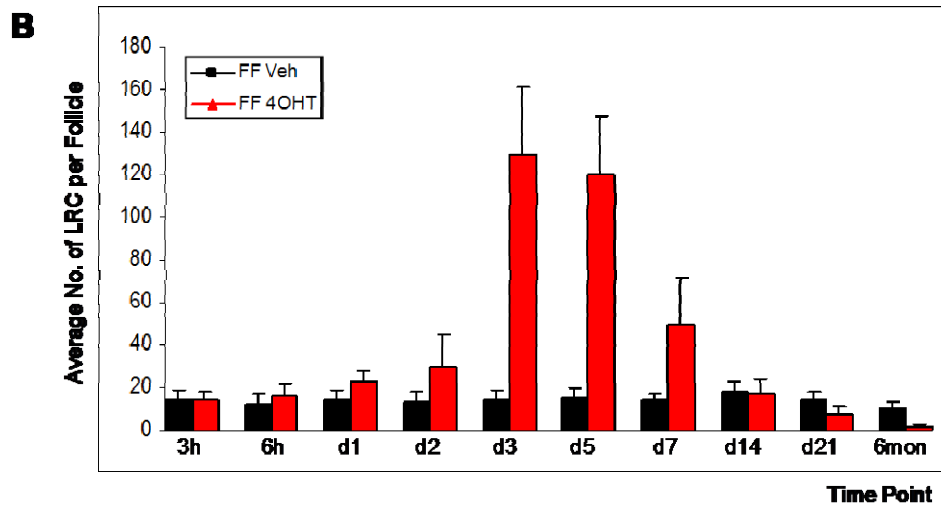


Figure 19 - Label Retaining Cell Quantification Following *Chk1* Ablation

A time course experiment was performed to follow LRC fate after *chk1* ablation in skin. Neonatal BrdU labelling was performed in *chk1*flox/flox // *K14CreER*^{T2} // *LacZ* mice treated with either vehicle or topical 4OHT and animals sacrificed at various time points. **A** Wholemount tail preparations made from tail skin, stained for BrdU and imaged using confocal microscopy. **B** LRC numbers were quantified per follicle, for 3 triplet follicles (9 follicles) per animal in 3 separate animals for each data set at each time point. This is shown as the mean \pm SD. **C** The difference in median LRC number was compared between control and experimental group using Mann Whitney Test. A marked increase in LRC numbers were seen at the D3 and D5 timepoints. Scale bar represents 40 μ m.



C

Time Point	Difference between median no. of LRC per follicle Mann Whitney Test (p value)
3hr	P=0.55
6hr	P=0.03
D1	P<0.0001
D2	P<0.0001
D3	P<0.0001
D5	P<0.0001
D7	P<0.0001
D14	P=0.76
D21	P<0.0001
6 months	P<0.0001

significant increase in LRC numbers was observed, with a peak recorded at D3 and D5, around x9 fold more than control. This gradually decreased by D14 with significantly fewer LRCs observed compared to control at D21 and at 6 months. My interpretation of this data is that following *chk1* loss, LRCs which normally exist in a quiescent state, are stimulated to proliferate. The long term loss of LRC numbers can also be explained by the premature recruitment of the LRCs into active proliferation following *chk1* loss thus depleting the original number of labelled cells.

In order refine this analysis, in the same wholmount tail preparations as used in the experiment above, strong (red arrow) versus weakly (yellow arrow) staining LRCs were quantified separately (see Figure 20A). Strong staining was taken to indicate cells that have not undergone division and weak staining to indicate cells that are actively undergoing division and thus diluting their label. The numerical results were plotted (Figure 20B) - in the *chk1flox/flox // K14CreER^{T2} // LacZ* + vehicle group, strong staining LRCs are represented as black bars versus weak staining LRCs in grey bars, and in the *chk1flox/flox // K14CreER^{T2} // LacZ* + 4OHT group, strong staining LRCs are represented in red bars versus weak staining LRCs in pink bars. In the control group, the proportion of strong staining LRCs remained fairly constant at around 85 to 95% throughout the time course. In the 4OHT treated group, the proportion of strong staining LRC at the beginning of the time course was similar to control but decreased after the first 24 hours. It continued to reduce to nadir around D5. At D5 only 26% of the LRCs were scored as strongly BrdU positive, the majority of cells were weakly stained implying active cell division. Following that, the proportion of strong staining LRCs increased and returned to control levels by D21.

Further confirmation of proliferation was sought by performing a short term BrdU labelling time course experiment (Figure 20C, D), which assayed active incorporation of BrdU during DNA synthesis. *Chk1 flox/flox // K14CreER^{T2} // LacZ* mice were treated with topical 4OHT and at various time points prior to sacrifice, BrdU was injected intraperitoneally 3 hours beforehand. Wholmount preparations were made, staining performed for BrdU, imaged using confocal microscopy and BrdU positive cells quantified. At D1, there was no significant difference in median number of BrdU positive cells in 4OHT treated mice

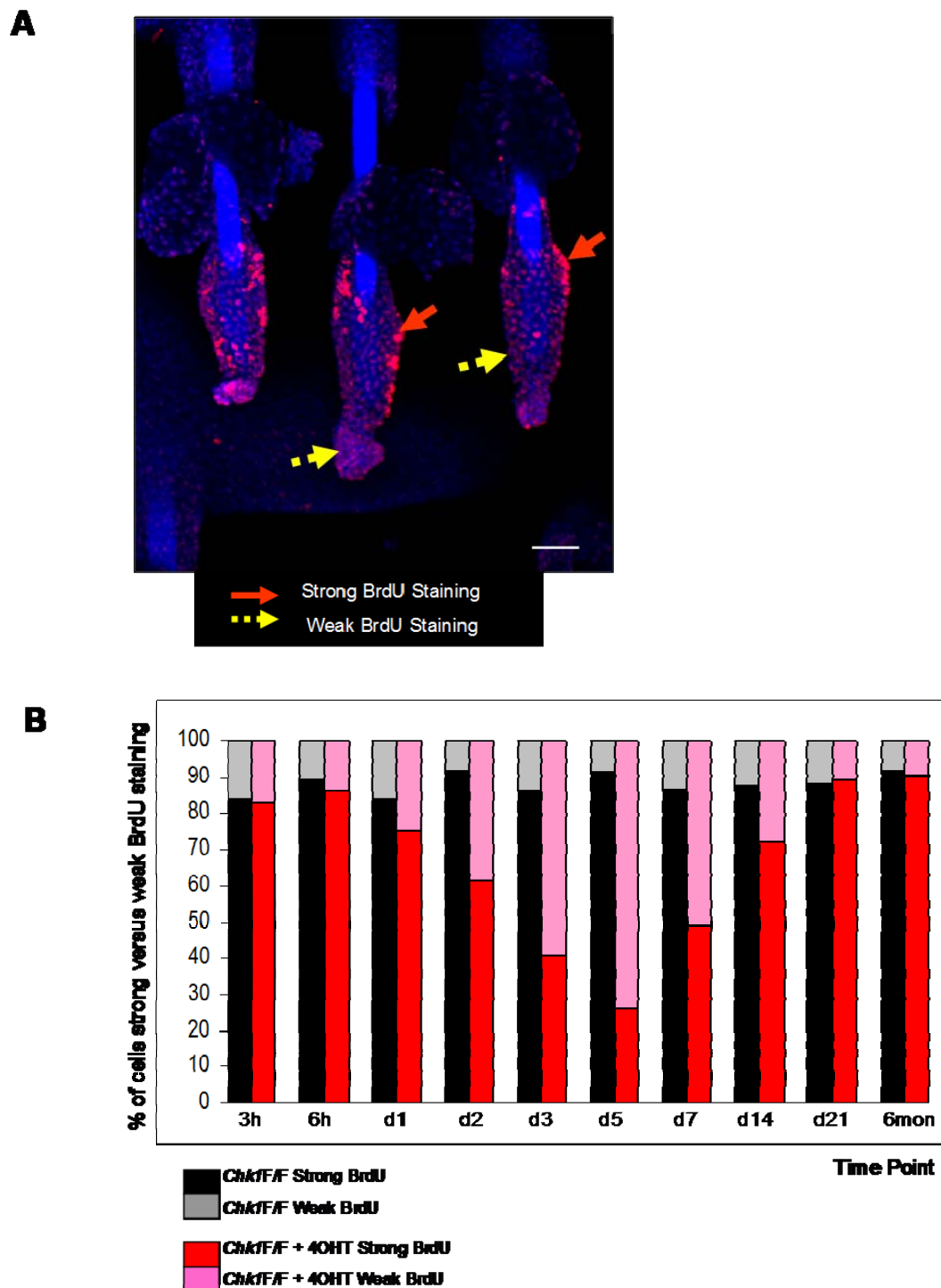
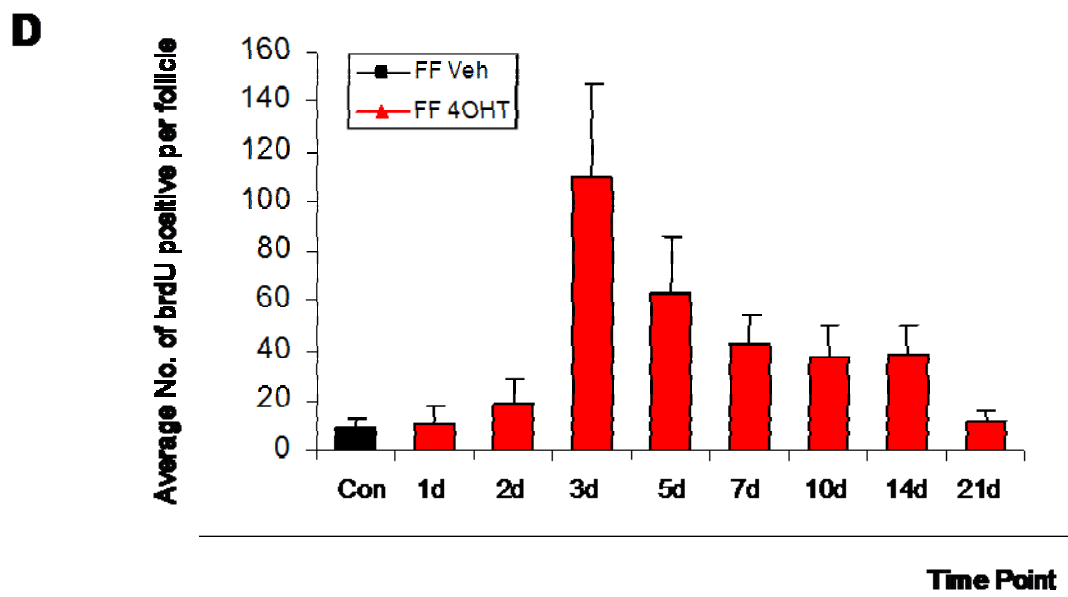
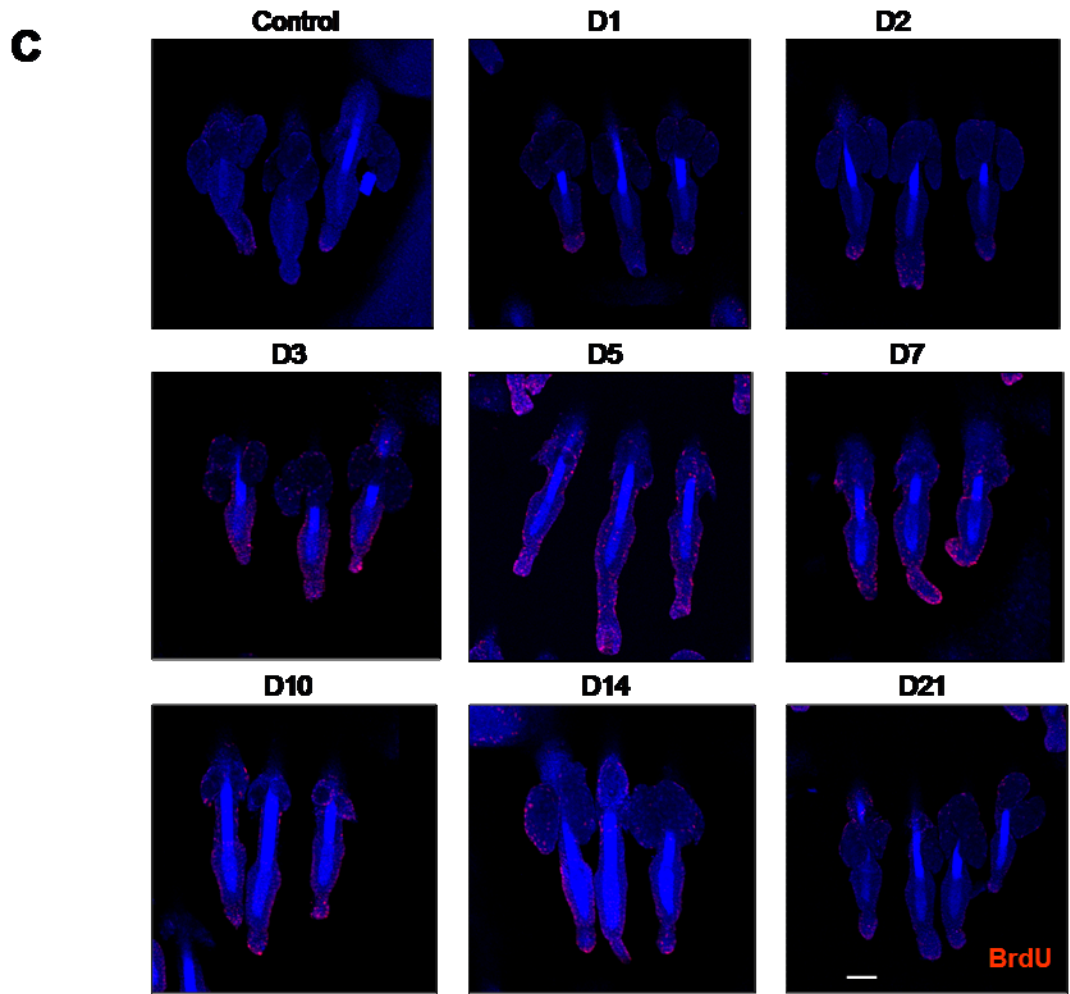


Figure 20 - Dilution of Long Term BrdU Label and Cell Proliferation Following *Chk1* Ablation

A In the same wholemount tail preparations as used in **Figure 3** the number of strong (red arrow) versus weak (yellow arrow) staining LRCs were quantified. Strongly stained LRC indicate cells that have not undergone division and weak staining indicates cells that are actively undergoing division. **B** The graph depicts in the control group, the proportion of strong staining LRCs (black) versus weak staining LRCs (grey), and in the experimental group, the proportion of strong staining LRCs (red) versus weak staining LRCs (pink). **C,D** A short term BrdU labelling time course experiment was performed to confirm active cell division. *Chk1*^{flox/flox} // *K14CreER*^{T2} // *LacZ* mice were treated with topical 4OHT and BrdU injected intraperitoneally 3 hours prior to sacrifice at various time points. Epidermal preparations were made and imaged using confocal microscopy and BrdU cells quantified. These results indicate that following *chk1* loss, LRCs in the bulge region are stimulated to undergo proliferation. Scale bar represents 40 μ m.



E

Time Point	Difference between median no. of BrdU +ve cells per follicle Mann Whitney Test (p-value)
D1	0.162
D2	0.0002
D3	<0.0001
D5	<0.0001
D7	<0.0001
D10	<0.0001
D14	<0.0001
D21	0.031

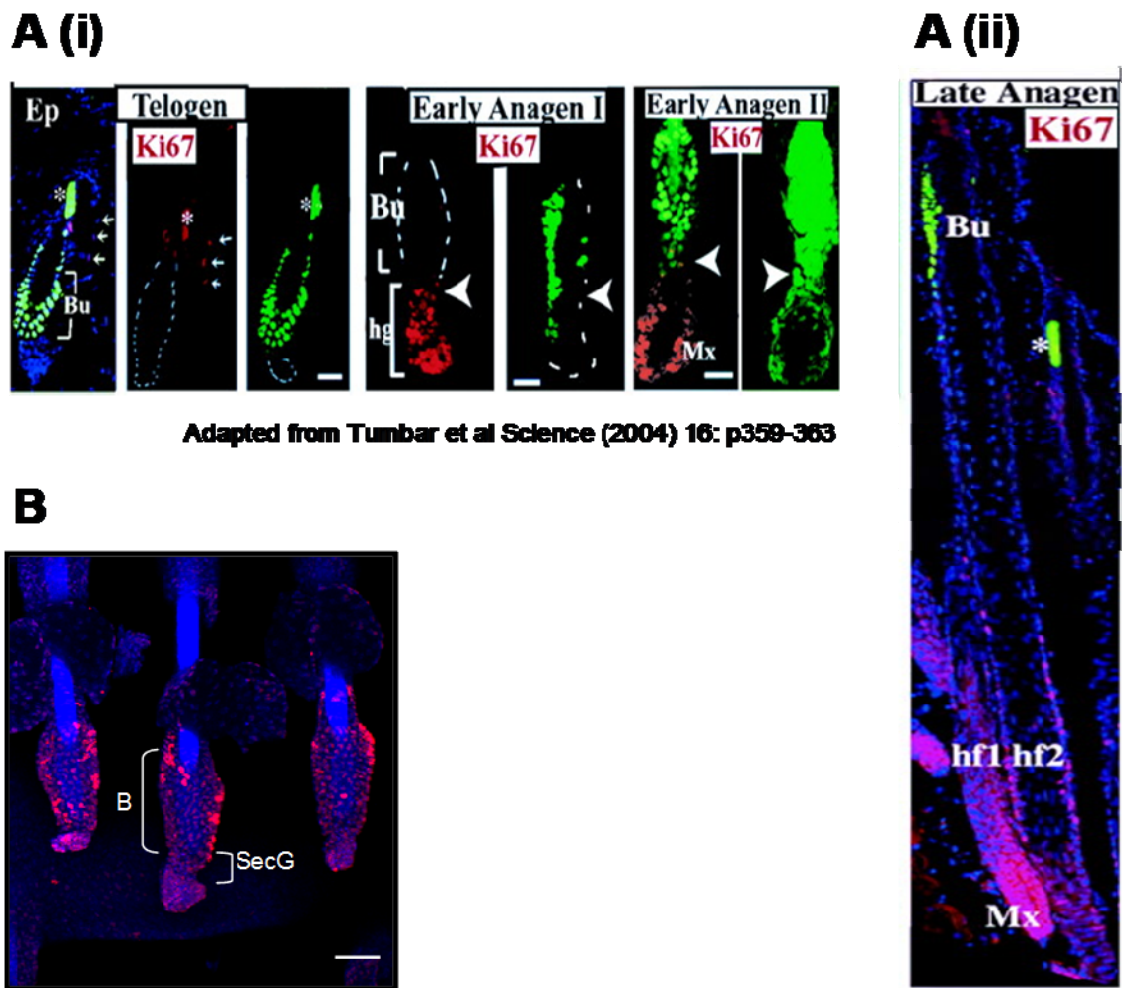


Figure 21 - Label Retaining Cells and the Hair Follicle Cycle

A Adapted from Tumbar et al Science (2004) 16: p359-363 (Tumbar et al, 2004). This shows confocal images of murine hair follicles at different stages of the hair cycle – **(i)** telogen, early anagen I, early anagen II and **(ii)** late anagen. Bulge label retaining cells (LRCs) which here are H2B-GFP expressing rather than BrdU labelled, only modestly contributes to hair follicle regrowth in early anagen but not in telogen or late anagen. Abbreviations: Bu, bulge; DP, dermal papilla; Mx, matrix; hg, hair germ; Ep, epidermis; asterisk, hair shaft (autofluorescent); hf, hair follicle; Cx, cortex; ORS/IRS, outer/inner root sheaths; BM, basement membrane; In, infundibulum; W, wound. Scale bars, 50 μ m. Arrowheads denote transition zone between bulge and newly generated follicle downgrowth. H2B-GFP (green), 4',6'-diamidino-2-phenylindole (DAPI) (blue), Ki67 (red). **B** This shows a confocal image of hair follicles 3 days following *chk1* ablation. In contrast to normal homeostasis, there is marked LRC proliferation with positive cells found in the entire bulge region (B) and secondary germ regions (SecG). Scale bar represents 40 μ m.

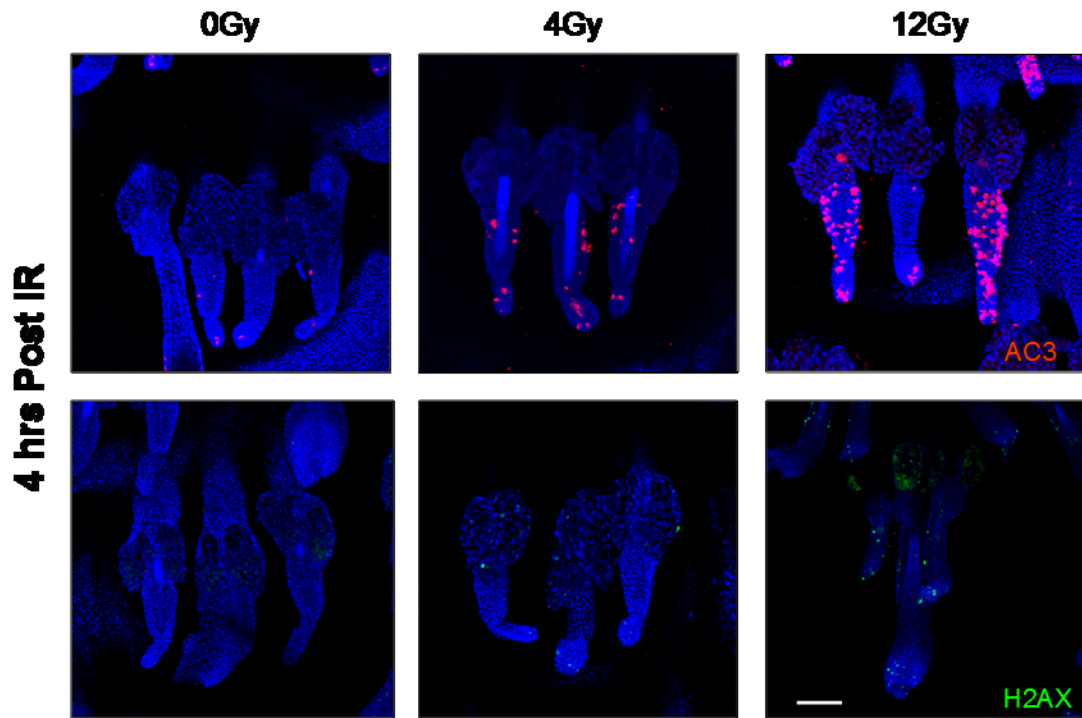


Figure 22 - Activated Caspase 3 and γ -H2AX Expression in Skin After Irradiation

Animals were irradiated with either 4Gy or 12Gy of γ -irradiation and sacrificed 4 hours later. Tail wholemounts were prepared, as described in **Figure 1**, and stained for γ -H2AX and activated caspase 3 (AC3). Results show absent or minimal levels of staining in control tails with graduated levels of increased staining with increasing doses of γ -irradiation. Scale bar represents 20 μ m.

compared to vehicle treated control. However from D2 onwards to D21 a statistically significant increase was observed compared to vehicle treated control. Maximum numbers were seen at D3 where the average number of BrdU positive cells versus control was 109.7 vs 8.7. This confirms active proliferation occurring in skin where *chk1* was ablated in keeping with previously observed multiplication of LRCs.

In a paper published by Tumber et al (Tumber et al, 2004) label retaining cells were identified by transient conditional expression of H2B-GFP regulated by a Tet-“on” system. In murine hair follicles, bulge label retaining cells (LRCs) which are H2B-GFP positive, only modestly contributes to hair follicle regrowth in early anagen and not in telogen nor late anagen (see Figure 21A). Bulge cells do not generally cross the transition zone between bulge and newly generated follicle downgrowth (denoted by arrowheads). In contrast, following *chk1* ablation, LRC multiplication is associated with the presence of BrdU positive cells in the entire bulge region (B) and secondary germ regions (SecG) in telogen (Figure 21B - demonstrated by a confocal image taken 3 days after 4OHT treatment). This suggests the original LRC which were confined to the bulge or stem cell niche have now expanded to populate and constitute the rest of the hair follicle and this implies LRC differentiation in order to fulfill this function (Cotsarelis et al, 1990; Ito et al, 2002; Jaks et al, 2008; Morris & Potten, 1999). The label which is detected now identifies keratinocytes in various stages of differentiation but which have originated from the stem cell population.

5.1.3. *Chk1* Ablation Results in an Accumulation of DNA Damage in the Skin

In response to double strand DNA breaks (DSB), for example due to γ -irradiation, H2AX becomes phosphorylated at serine 139 (which is then known as γ -H2AX) which acts to recruit DSB break recognition and repair proteins to these nascent sites. It is crucial that DSBs are repaired, thereby preventing mutations, genomic instability and cell death. Accumulation of unrepaired DSB often leads to cellular death which can be observed by detecting the cleaved or the activated form of caspase 3 (AC3). In a control experiment animals were irradiated with either 4Gy

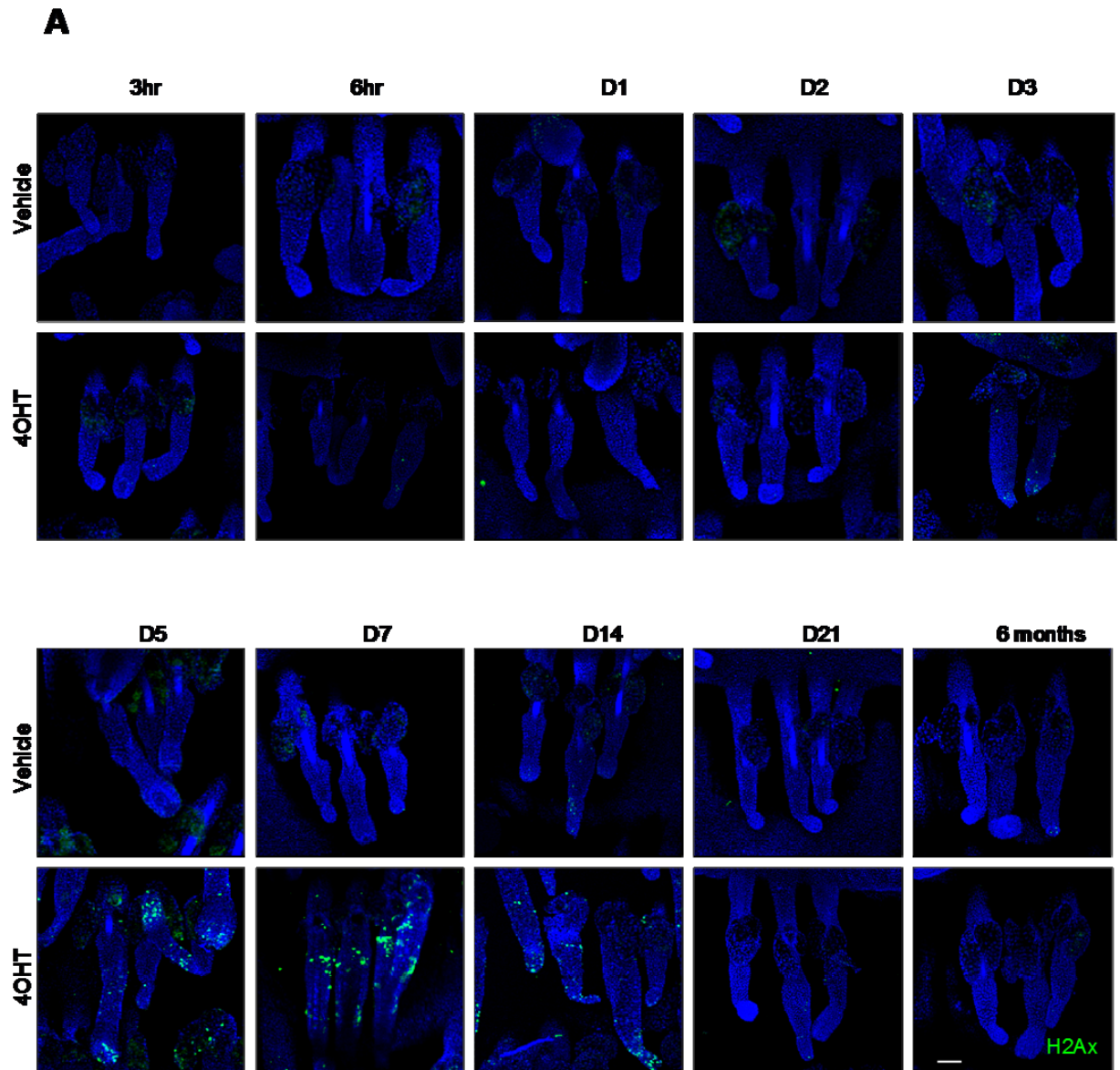
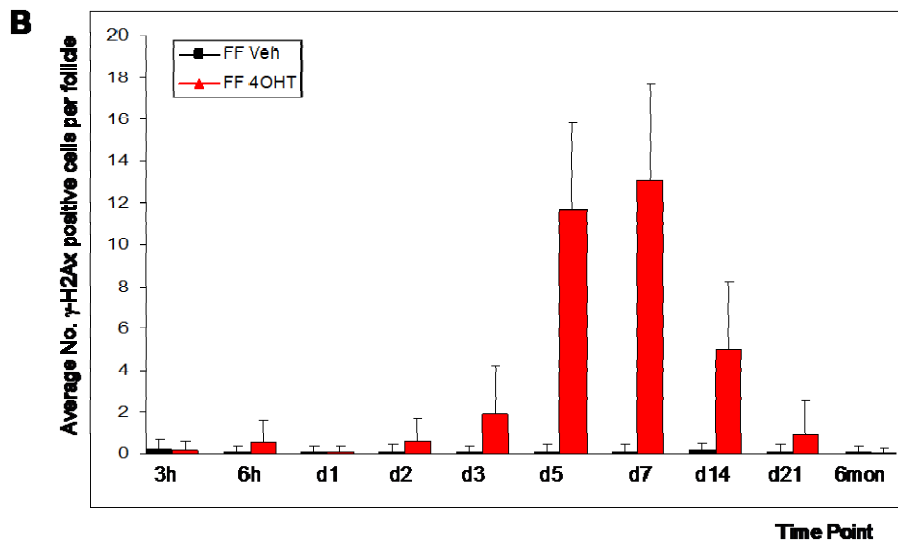


Figure 23 - γ -H2AX Expression in Skin Following *Chk1* Ablation

Chk1^{flox/flox} // *K14CreER*^{T2} // *LacZ* mice were treated with vehicle or topical 4OHT and animals sacrificed at various time points. **A** Wholemount tail preparations were made from tail skin, stained for γ -H2AX and imaged using confocal microscopy. **B** γ -H2AX positive cells were quantified per follicle, for 3 triplet follicles (9 follicles) per animal in 3 separate animals for each data set at each time point. This is shown as the mean \pm SD. **C** The difference in median number of γ -H2AX positive cells between control and experimental group was compared using Mann Whitney Test. A marked increase in γ -H2AX staining was seen at D5 and D7. Scale bar represents 40 μ m.



C

Time Point	Difference between median no. of γ -H2AX cells per follicle Mann-Whitney Test (p-value)
3hr	P=0.822
6hr	P=0.307
D1	P=1.000
D2	P=0.139
D3	P=0.0001
D5	P<0.0001
D7	P<0.0001
D14	P<0.0001
D21	P=0.069
6 mon	P=0.815

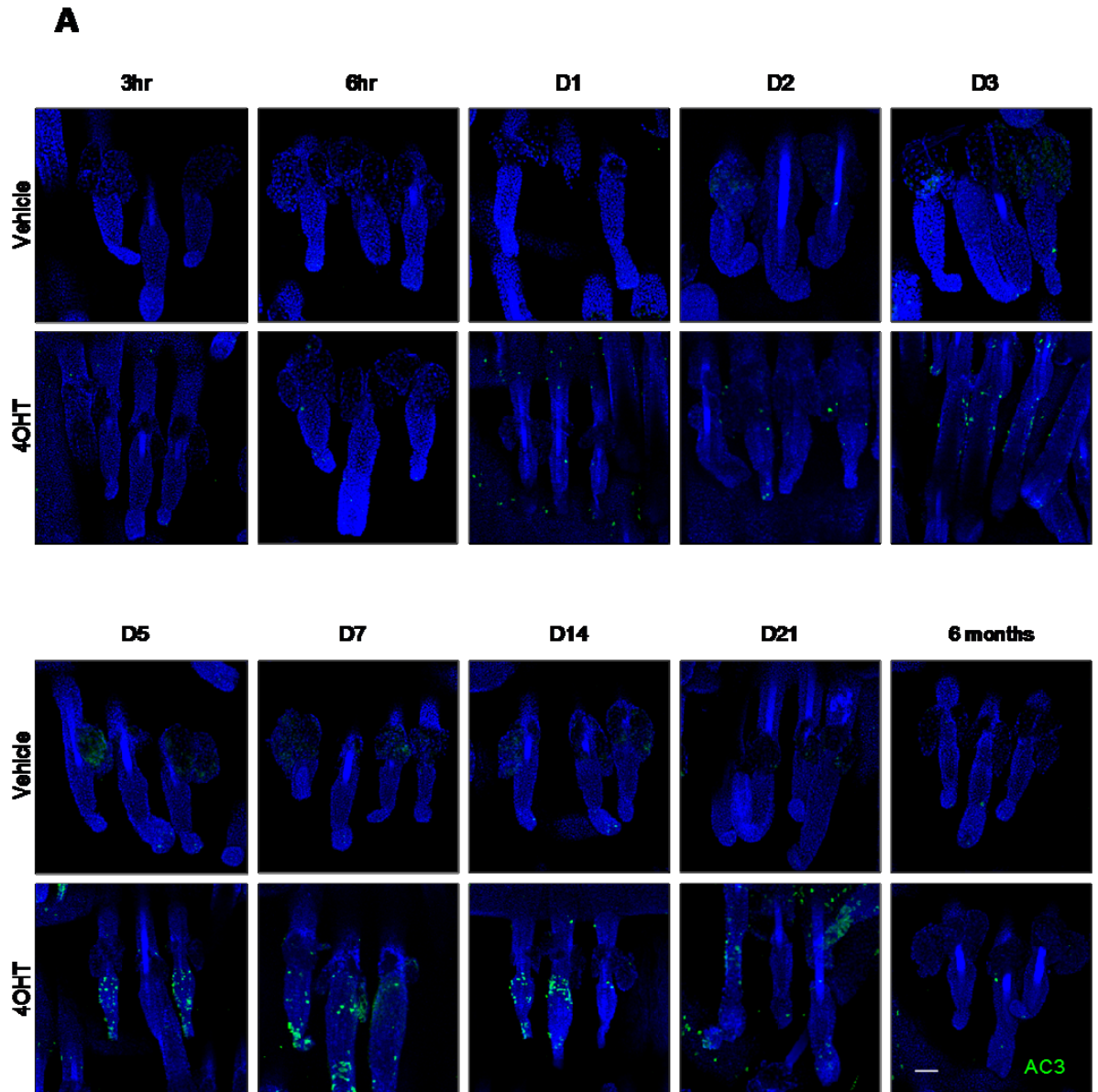
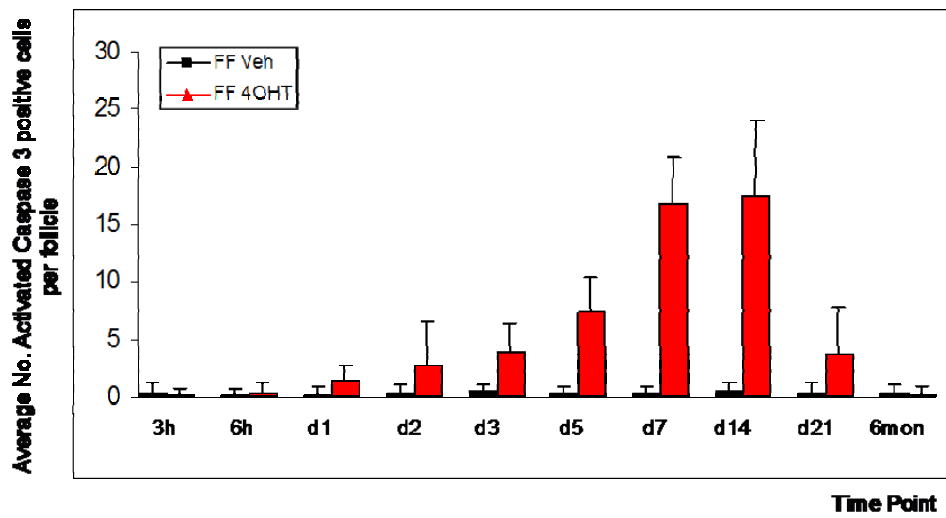


Figure 24 - Activated Caspase 3 Expression in Skin Following *Chk1* Ablation

Chk1^{flox/flox} // *K14CreER*^{T2} // *LacZ* mice were treated with vehicle or topical 4OHT and animals sacrificed at various time points. **A** Wholemount tail preparations were made from tail skin, stained for activated caspase 3 (AC3) and imaged using confocal microscopy. **B** AC3 positive cells were quantified per follicle, for 3 triplet follicles (9 follicles) per animal in 3 separate animals for each data set at each time point. This is shown as the mean +/- SD. **C** The difference in median number of AC3 positive cells between control and experimental group was compared using Mann Whitney Test. A marked increase in AC3 staining was seen at D7 and D14. Scale bar represents 40µm.

B**C**

Time Point	Difference between median no. of AC3 cells per follicle Mann-Whitney Test (p-value)
3hr	P=0.586
6hr	P=0.723
D1	P=0.0001
D2	P=0.0011
D3	P<0.0001
D5	P<0.0001
D7	P<0.0001
D14	P<0.0001
D21	P=0.0001
6 mon	P=0.876

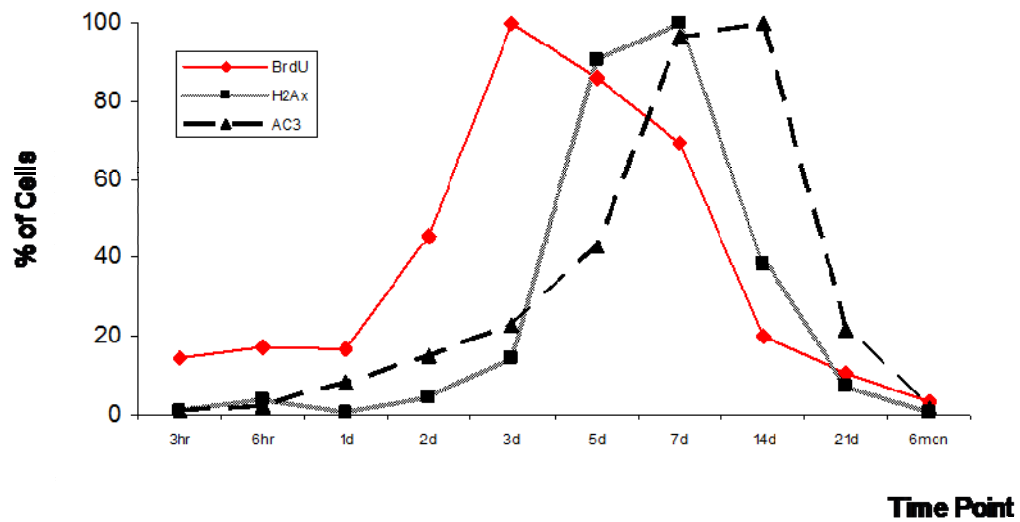


Figure 25 - Timelines for Tissue Changes Following *Chk1* Ablation

It has been shown that following *chk1* loss, hair follicle LRCs were stimulated to proliferate and undergo cell division. This was accompanied by an accumulation of γ -H2AX and AC3 staining. To attempt to chronologically order these events, graphs were plotted for each event, normalized to 100% of the maximum average score. Results demonstrated peak LRC counts occurred before peak H2AX counts, which was followed by peak AC3 counts.

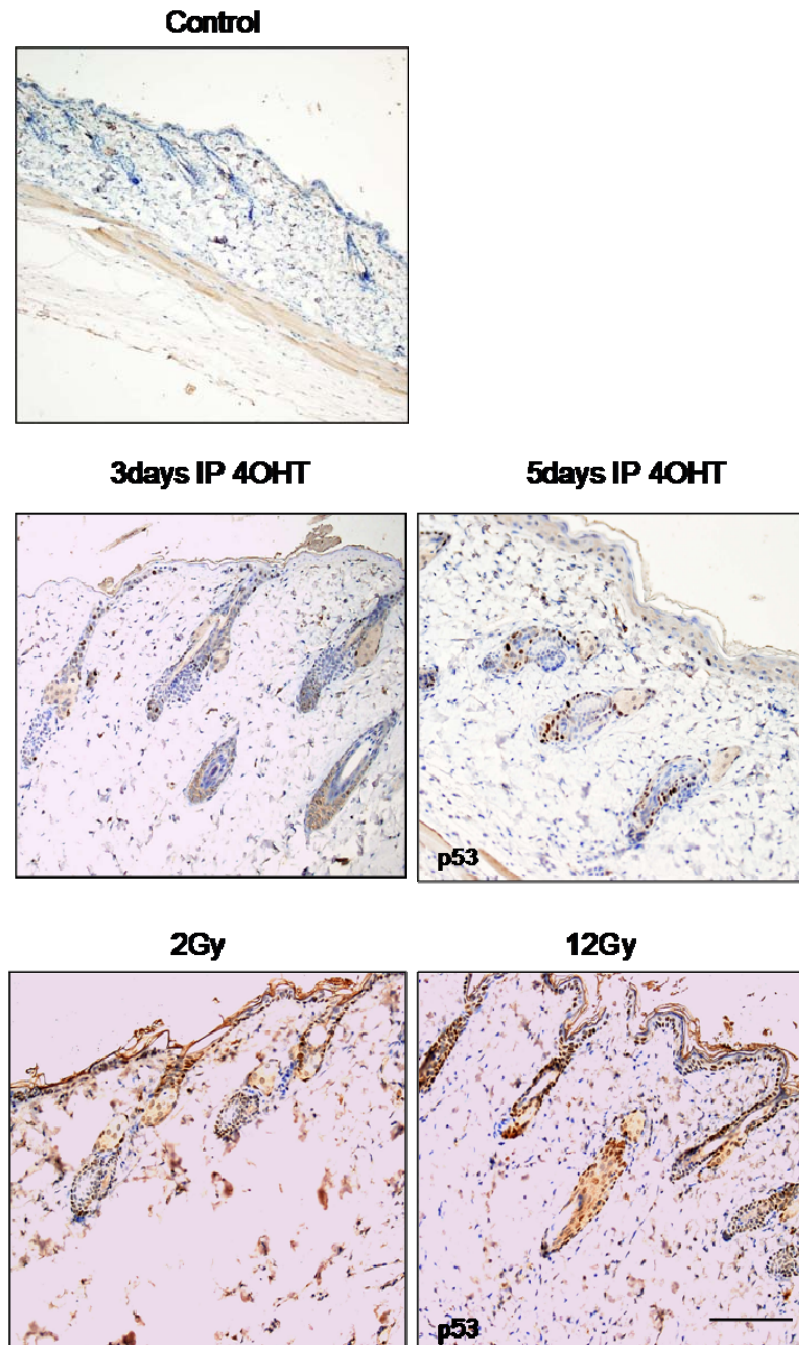


Figure 26 - p53 Expression in Skin Following *Chk1* Abaltion

To determine if apoptosis seen subsequent to *chk1* loss is associated with the accumulation of p53, immunohistochemical staining was performed on paraffin fixed skin following 5 days of IP 4OHT treatment in *chk1* flox/flox // *K14CreER*^{T2} // *LacZ* mice (middle panels). Increased p53 staining was observed. Mice irradiated with 2Gy and 12Gy γ -irradiation served as positive controls (lower panels). Scale bar represents 50 μ m.

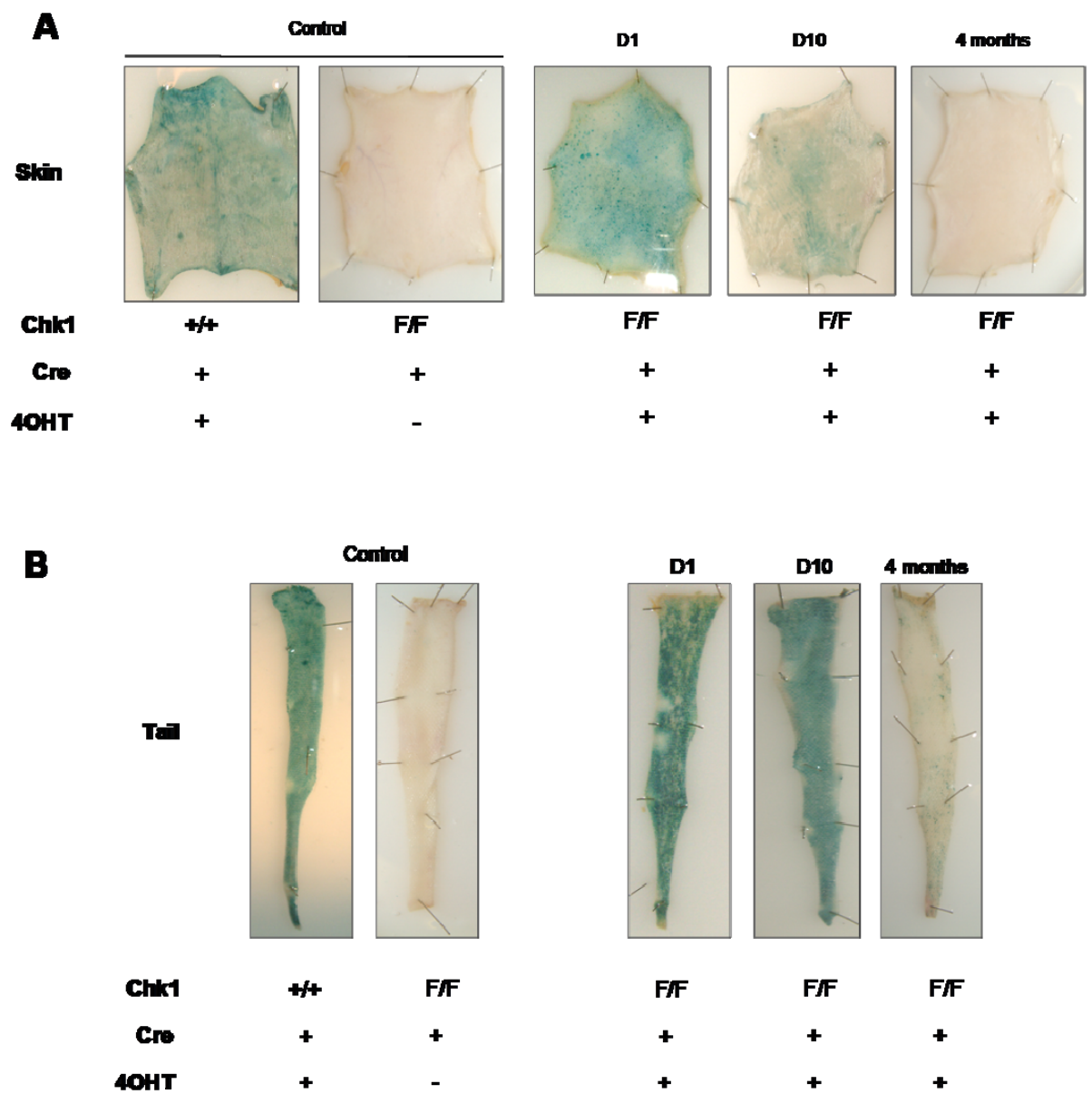
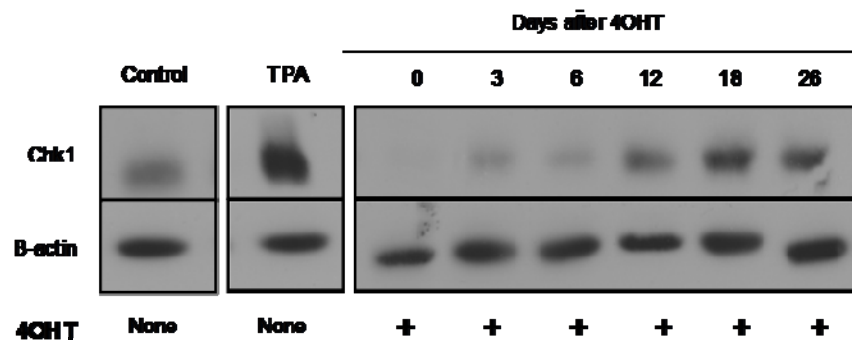


Figure 27 - Repopulation of Skin by Unrecombined Cells Following *Chk1* Ablation

A time course study was conducted using β -Gal staining to allow lineage tracing and determine the long-term fate of *chk1* recombined cells (*chk1* Δ/Δ) in skin. *Chk1*^{flox/flox} // *K14CreER*^{T2} // *LacZ* mice were treated with 4OHT or vehicle and *chk1*^{+/+} // *K14CreER*^{T2} // *LacZ* mice were treated with 4OHT. At various time points (shown here at D1, D10 and 4 months) **A** dorsal skin and **B** tail skin was harvested, wholemounts prepared and β -Gal staining performed. **C** Protein extracts were made from the dorsal skin of these animals. After undergoing initial recombination, β -Gal staining showed *chk1* Δ/Δ cells were gradually lost and tissue was repopulated by unrecombined cells. Western blotting showed substantial decrease in Chk1 expression initially but Chk1 expression returned at later times following recombination.



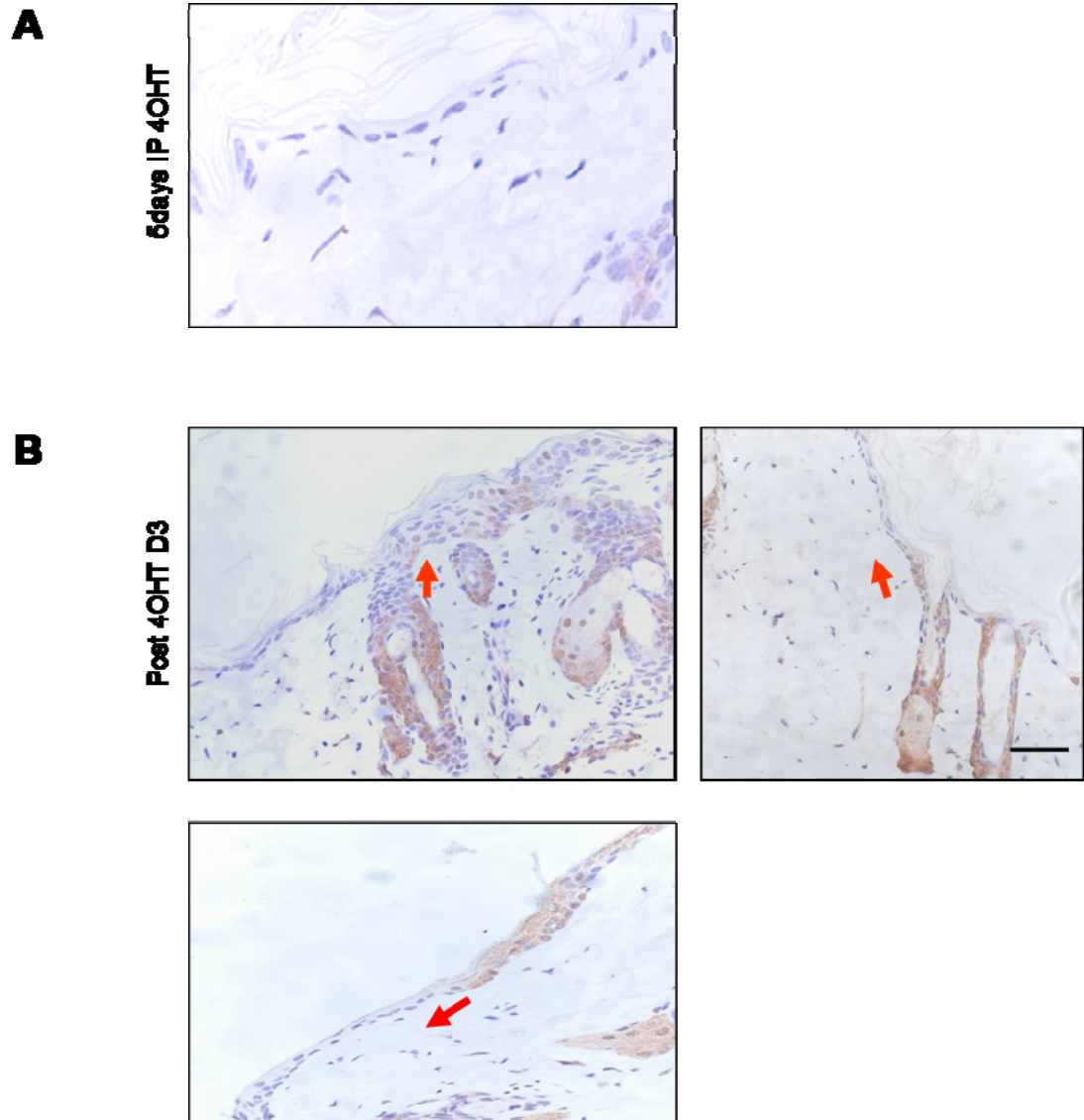


Figure 28 - The Interfollicular Epidermis Maybe Repopulated by Cells from the Follicle Following *Chk1* Ablation

To study the pattern of repopulation by unrecombined cells in the epithelium, *chk1* flox/flox // *K14CreER^{T2}* // *LacZ* mice were treated with 5 days of IP 4OHT (D-5 to D-1). Skin was harvested at various time points **A** D0 and **B** D3, prepared in paraffin blocks and sections stained for Chk1. As repopulation by unrecombined cells occurred, the first areas where Chk1 expression reappeared was in the hair follicles, and only later in the interfollicular epidermis. This observation suggests that the interfollicular epithelium is being repopulated by cells originating from the hair follicles. Scale bar represents 50 μ m.

or 12Gy of γ -irradiation and sacrificed 4 hours later (see Figure 22). Tail wholemounts were prepared and stained for γ -H2AX and AC3. Results show absent or minimal levels of staining in control tails with graduated levels of increased staining with increasing doses of γ -irradiation. In order to determine whether deletion of *chk1* induces DNA damage, *chk1* flox/flox // *K14CreER^{T2}* // *LacZ* mice were treated with vehicle or topical 4OHT and animals sacrificed at various time points (Figure 23A, B, C). Wholemount epidermal preparations were made, γ -H2AX staining performed and imaging performed using confocal microscopy. The number of γ -H2AX positive cells per follicle was counted for 3 triplet follicles (9 follicles) per animal in 3 separate animal for each data set at each time point. Control γ -H2AX staining was minimal, <1 positive cell on average per follicle. However, following *chk1* loss, there was substantial increase in γ -H2AX staining in tissue. A significant increase in the median number of γ -H2AX positive cells between vehicle and 4OHT treated groups was observed from D3 to D14. The peak difference was observed at D7 of 120 fold over control. Thereafter staining decreased and by D21 there was no statistical difference compared to normal. These findings indicate that following *chk1* ablation from D3 to D14, there is an accumulation of DNA damage as demonstrated by γ -H2AX staining.

5.1.4. *Chk1* Ablation Results in Increased Apoptosis in the Skin

In the same tissue samples as used in the experiment above staining for active caspase 3 (AC3) was also performed to assay for apoptosis (see Figure 24A, B, C). The number of AC3 positive cells per follicle was counted for 3 triplet follicles (9 follicles) per animal in 3 separate animals for each data set at each time point. Control AC3 staining was minimal, <1 positive cells on average per follicle. A significant increase in the median number of AC3 positive cells was observed in the 4OHT treated group compared to vehicle alone from D1 to D21. Peak difference was seen around D14 of 36 fold over control. These findings indicate that following *chk1* ablation from D3 to D14, there is greatly increased level of

apoptosis. It is likely that apoptosis is being initiated in cells which accumulate unrepaired DNA, as assayed by γ -H2AX staining (see 5.1.3).

5.1.5. The Frequency of Staining Events Suggest LRC Proliferation Precedes DNA Damage and Apoptosis

Following *chk1* loss in tissue several events have been recorded (see Figures 19-24). Hair follicle LRCs were stimulated to proliferate and undergo cell division. This was accompanied by an accumulation of γ -H2AX and AC3 staining. To visualise the order of these events a combined graph was plotted with each event normalized to 100% (of the maximum score) (see Figure 25). Results demonstrate that LRC proliferation peaked at around 3 days. This was followed by a peak of γ -H2AX positive cells at around 7 days which was followed by a peak of AC3 positive cells at 14 days. As Chk1 signalling is an essential pathway in maintaining genomic integrity during cell division (particularly by signalling S-M and G2-M delay in response to replication errors), the loss of *chk1* is a convincing explanation for the accumulation DNA damage. The burden of unrepaired DNA is the likely trigger for subsequent apoptosis. The order of events however, suggests *chk1* loss caused LRC multiplication as an early event and it is not clear whether γ -H2AX and AC3 activation are required for LRC multiplication or if this process is reliant on alternative signals.

5.1.6. *Chk1* Loss Results in p53 Induction

To determine if apoptosis seen subsequent to *chk1* loss is associated with the accumulation of p53, immunohistochemical staining was performed on paraffin fixed skin following 5 days of IP 4OHT treatment in *chk1*^{flox/flox} // *K14CreER*^{T2} // *LacZ* mice (see Figure 26). Increased p53 staining was observed after 3 and 5 days of IP 4OHT particularly in the bulge region, outer root sheath and basal epidermis. This indicates an upregulation and stabilization of p53 following *chk1*

loss which is most likely due to activation of DNA damage response pathways. Mice irradiated with 2Gy and 12Gy γ -irradiation served as positive controls.

5.1.7. *Chk1* Ablated Skin is Repopulated by Unrecombined Cells (Unflox “Wild Type”)

Chk1 loss caused apoptosis in mouse skin tissue, however no overt long-term pathology was noted. Using β -Gal staining to trace the fate of *chk1* recombined cells (*chk1* Δ/Δ) in skin, a time course was performed. *Chk1* flox/flox // *K14CreER^{T2}* // *LacZ* mice were treated with a 5 day protocol of intraperitoneal 4OHT (D-5 to D-1) and at various time points (D1, D10 and 4 months) dorsal skin (see Figure 27A) and tail (see Figure 27B) was harvested, wholemounts prepared and β -Gal staining performed. In the dorsal skin, at D1 there is widespread β -Gal staining suggesting a large proportion of *chk1* Δ/Δ cells in the epithelium. However, at D10 the pattern of β -Gal staining appeared variegated, with β -Gal positive areas being interspersed with white areas indicative of unrecombined cells. With time, the proportion of white areas increased till at 4 months there was minimal representation of *chk1* Δ/Δ cells. In the tail, a similar pattern of replacement of *chk1* Δ/Δ areas by unrecombined cells occurred except that the loss of β -Gal positive cells occurred at a somewhat slower rate. For example, at D10 recombined cells were still numerous but over time the skin was ultimately repopulated by unrecombined cells. This data indicates that *chk1* Δ/Δ cells do not persist in tissue. As previously shown there is evidence for an accumulation of γ -H2AX and apoptosis which suggests cells lacking *chk1* go on to accumulate genomic instability and die. In turn, unrecombined cells repopulate the skin thus maintaining overall tissue homeostasis.

Protein extracts were also made from the dorsal skin of these animals (Figure 27C). Western blotting showed a substantial decrease in Chk1 expression that peaked at around D0 to D3. However, Chk1 expression returned between D12 and D18. This confirms that unrecombined cells progressively repopulate the skin presumably to replace *chk1* Δ/Δ cells then die. Interestingly the level of Chk1 expression was higher compared to unperturbed skin following recombination at

D18 and D21. This could be explained by increased proliferative activity of the unrecombined cells, required to compensate for cellular death compared to the normal telogen or resting state hair follicles.

5.1.8. Hair Follicle Stem Cells May be Responsible for Repopulation of the Interfollicular Epidermis

To study the pattern of repopulation by unrecombined cells in the epithelium, *chk1* flox/flox // *K14CreER^{T2}* // *LacZ* mice were treated with 5 days of IP 4OHT (D-5 to D-1). Skin was harvested at various time points, prepared in paraffin blocks and sections stained for Chk1 (see Figure 28). Immediately after 4OHT treatment, there was significantly reduced expression Chk1 throughout the epithelium (Figure 28A). D3 after 4OHT treatment, consistent with tissue repopulation by unrecombined cells, Chk1 expressing cells were now detected (Figure 28B). Chk1 positive cells seemed to appear first in the hair follicles and only later in the interfollicular epidermis. This observation is suggestive that the epithelium is being repopulated by cells originating from the hair follicles. The red arrow shows the potential “direction” of reconstitution taken by these cells.

5.2. Discussion

Hair follicle bulge stem cells have been shown to exhibit pluripotency, increased clonogenic potential and are able to reconstitute various tissue types within the skin, such as epithelium, hair follicles and sebaceous glands in transplantation experiments (Braun et al, 2003; Cotsarelis et al, 1990; Tumber et al, 2004). The accepted view is that these long lived cells remain relatively quiescent over their lifetime. LRCs can be recruited into active proliferation during hair growth, but this involves only a very small number of cells (Morris & Potten, 1999) or in response to epithelial wounding (Ito et al, 2005).

Recently this understanding has been challenged by the discovery of an actively cycling LGR5 positive population (Jaks et al, 2008) which is also pluripotent and exhibits increased clonogenicity and longevity. It is unclear if these represent different populations within a spectrum of stem cell types required for normal homeostasis (Lin & Andersen, 2008; Matyskiela et al, 2009), how they may interact with one another or indeed if they are interchangeable. Given data suggesting that bulge stem cell represent the cells of origin of DMBA/TPA derived tumours (Bailleul et al, 1990; Brown et al, 1998; Owens & Watt, 2003; Perez-Losada & Balmain, 2003), I decided to focus my studies on this cell population.

Using a BrdU labelling technique (Bickenbach, 1981; Bickenbach & Chism, 1998; Braun et al, 2003; Cotsarelis et al, 1990) (see Figure 17), long-term label retention within DNA was used to assay for bulge stem cells. The mice were injected with BrdU early in neonatal life, when they were relatively hairless and undergoing a period of rapid tissue expansion and hair morphogenesis (Braun et al, 2003). Given the active role for hair follicle stem cells in constituting various skin lineages during this period, this is understood to be the reason why BrdU incorporates into DNA of cells which otherwise remain relatively quiescent in adulthood (Castilho et al, 2009). After these mice were aged, staining for BrdU identifies these quiescent long-term label retaining cells or LRCs. The dose of BrdU used in this protocol was titrated to provide optimum staining efficacy on confocal microscopy (see Figure 17) in mice aged 8-11 weeks (see Methods,

2.10). The optimal dose was found to be lower than in published studies (Braun et al, 2003). Indeed, published doses were sometimes, associated with a high variability of LRCs counts in control animals after short aging intervals from 4-10 weeks (Morris & Potten, 1994; Morris & Potten, 1999) although it appeared reliable for long term aging experiments (Morris & Potten, 1999). Using doses employed in this study, I found highly reproducible and consistent LRC counts for short term aging (see Figure 19) which provided a more stringent platform for inter-mouse comparisons.

Tail harvesting and assays for LRC numbers commenced when the mice were 8 weeks of age. This corresponds to mice undergoing the second prolonged phase of telogen which is thought to last several weeks (Muller-Rover et al, 2001). This allowed standardisation of the hair cycle phase between mice during which experimentation was performed. When choosing follicles for cell quantification, only those conforming morphologically to telogen were selected and follicles that appeared to be in catagen or anagen were excluded. This is crucial as follicles undergoing catagen for example, would under normal hair cycling conditions be expected to demonstrate a degree of activated caspase 3 (AC3) staining but not follicles in anagen or telogen, which naturally should not be mistaken for AC3 activity occurring as a result of experimental manipulation.

The key finding from this chapter is that *chk1* ablation in skin resulted in substantial LRC proliferation. This is a novel finding. Two hypotheses are proposed to explain this phenomenon.

The first is that a novel mechanism involving *chk1* mediated checkpoint activation exists within stem cells in order to maintain LRC quiescence. In somatic cells stable ectopic expression of a few select genes can in fact induce a pluripotent growth active state, for example *Oct4*, *Sox2*, *Nanog* and *Lin28* (Yu et al, 2007) which shows that a small but select number of factors can influence stem cell phenotype and fate. In skin stem cells, WNT has been shown to be a major regulator of hair follicle morphogenesis, renewal and anagen promotion (Castilho et al, 2009; DasGupta & Fuchs, 1999; Gat et al, 1998; Greco et al, 2009; Nguyen et al, 2006). WNT has already been implicated in a variety of processes required for embryonic development and primitive germ stem cells (Liu et al, 2008). Continuous and unrestrained tissue growth is neither

physiological nor desirable. In a study by Gutkind and colleagues, they show that constitutive overexpression of *Wnt1* in mouse skin led to unrestrained hair follicle growth resulting in alopecia and exhaustion of the bulge stem cell population, ie. depletion of the LRC compartment (Castilho et al, 2009). To counteract continual activation of WNT would therefore suggest an important role for negative regulation. In key study by Fuchs and colleagues (Tumbar et al, 2004), microarray analysis of skin LRCs (marked by transient expression of “Tet-on” regulated H2B-Green Fluorescent Protein, see Figure 21A) showed upregulated mRNA expression of factors involved in inhibition of the WNT signalling cascade, such as Secreted frizzled-related protein 1 (*Sfrp1*) and Disabled homolog 2 (*Dab2*) (Hocevar et al, 2003). In a subsequent study by Vogel and colleagues (Ohyama et al, 2006) they isolated skin bulge stem cells and performed microarray expression analysis. Again they found an upregulation of negative WNT signalling factors such as WNT inhibitory factor 1 (*WIF1*) and Bone morphogenetic protein 1 (*BMP1*). Unsurprisingly a variety of cell cycle associated factors were shown to be upregulated (Tumbar et al, 2004) as part of this inhibitory network including Growth Arrest Specific 1, Latent TGF β binding protein 1/2/3 and Transforming Growth Factor β 2 .

Taken together these studies suggest LRCs require active negative regulation in order to counteract and restrain ongoing proliferation signals [reviewed by (Li & Clevers, 2010)]. Proliferation and participation in morphogenesis is suggested to be the default state of these stem cell (Fuchs, 2007) which highlights the importance of this negative regulatory network. Interestingly, this is in complete contrast to the situation with LGR5+ve cells where the dermal papillae region has been shown to have high levels of WNT signalling (Kishimoto et al, 2000; Shimizu & Morgan, 2004) and secrete noggin, a BMP antagonist (Botchkarev et al, 2001). This is also discussed in Chapter 8 (see 8.2).

Chk1 has not been identified in either of these experiments performed on skin stem cells but in a microarray analysis of mammary stem cells, *chk1* was found to be transcriptionally upregulated (Behbod et al, 2006). To date follow up experiments to test the function of *chk1* in mammary stem cells have yet to be performed. Although this evidence only points to a possible association in stem cells, evidence to suggest a possible role of checkpoints in regulating or influencing cell quiescence or senescence has been published in separate

context. For example, a study by Rimkus et al (Rimkus et al, 2008) demonstrates dramatic evidence for negative checkpoint in quiescent neuronal cells. RNAi knockdown of *ATM* in *Drosophila*, which signals downstream via *chk2* and *chk1*, resulted in reentry of post mitotic neurons into cell cycle. Cell cycle reentry was followed by DNA damage and apoptosis and these events resemble the fate of *chk1* ablated LRCs. The animals displayed pathological changes similar to that found in the human disease equivalent Ataxia Telangiectasia (Savitsky et al, 1995). Furthermore, key evidence exists to show checkpoint proteins have a significant role in maintaining oncogene induced senescence - both in transformed cells *in vitro* and from *in vivo* studies that demonstrate that this pathway is crucial in restraining tumorigenesis (Bartkova et al, 2005; Di Micco et al, 2006). This evidence suggests that the possible role of *chk1* in maintaining stem cell quiescence cannot be excluded, although if confirmed would represent a novel function of this protein. Also, given *chk1* is understood to be active only in cells undergoing cell division or that have incurred DNA damage during the cell cycle [reviewed by (Smith et al, 2010)], its role in a quiescent population of cells would certainly challenge our understanding of the role of checkpoint pathways. Therefore I would argue that the role for *chk1* in LRC warrants further investigation.

The second explanation for *chk1* ablation induced LRC proliferation could lie in the fact that LRCs become active and cycle in response to tissue wounding. LRCs are thought to contribute only modestly to hair follicle homeostasis. As shown in Figure 21 in telogen and catagen LRC are confined to the upper bulge region (Figure 21A). In early anagen there is some evidence to show modest LRC proliferation in the lower bulge contributing to the formation of the nascent hair follicle (Tumbar et al, 2004). However the number of LRCs involved is small and they seldom venture across the bulge/dermal papillae boundary. In late anagen they again localize to the upper bulge only (Figure 21B). In contrast, my data demonstrates marked LRC proliferation with positive cells found in the entire bulge region (B) and secondary germ regions (SecG) (Figure 21B). This is therefore consistent with a non-physiological event. It has been shown that LRCs can be induced to proliferate in vast numbers by epithelial perturbation for example in response to epithelial wounding (Ito et al, 2005). Given *chk1* ablation induces a significant degree of DNA damage and apoptosis (Figure 23 and 24) in

the hair follicles as well as the interfollicular epithelium, this may in fact represent sufficient perturbation to normal homeostasis with which to trigger LRCs proliferation and reconstitution of the damaged hair follicles. Using immunohistochemical staining, following *chk1* ablation, Chk1 expressing cells seemed to appear first in the hair follicles only later followed by the epidermis (see Figure 28). This observation is suggestive that the epithelium is being repopulated by cells originating from the hair follicles. The red arrow shows the potential “direction” of reconstitution taken by these cells. Ordinarily hair follicle bulge cells do not contribute to interfollicular epidermal homeostasis, which is maintained by their own population of interfollicular stem cells (Clayton et al, 2007; Ito et al, 2005). However, under certain circumstances, such as epithelial wounding (Ito et al, 2005), bulge stem cells play a crucial role in re-epithelialization and thus they are postulated to serve as a “reserve” progenitor population for the interfollicular epithelium. The pattern of Chk1 expressing cell repopulation observed suggests the possibility of a similar “wounding phenomena” occurring as a result of *chk1* ablation. In response to this, the bulge cells are induced to repopulate the entire epidermal layer. The exact mechanism of this “wounding phenomenon” induced by *chk1* ablation is unclear. To summarise, LRC proliferation might in fact be in response to *chk1* mediated disruption of epithelial function leading to recruitment of LRCs in order to maintain homeostasis.

However, peak proliferation preceded DNA damage and apoptosis (see Figure 25). Therefore, the kinetics favour the explanation that *chk1* loss lead to a removal of negative regulation which triggered proliferation which resulted in dysregulated DNA synthesis and segregation leading to acquisition of DNA damage followed by apoptosis. Nevertheless neither possibility can be dismissed at this stage, nor that both events are occurring concurrently. Proposed investigations to test these hypotheses further and establish the mechanisms involved in *chk1* mediated LRC proliferation are discussed in Future Perspectives. (see 8.2)

I showed an upregulation and stabilization of p53 linked to *chk1* loss (see Figure 26), however at this stage the role of p53 in mediating apoptosis is unclear. It has been shown in that in an *AhCre* murine model, conditional *chk1* knockout induces apoptosis and p53 but the phenotype was not rescued by crossing onto a

p53 knockout background (Greenow et al, 2009). Hence it appears that *p53* is not obligatory for apoptosis secondary to *chk1* loss.

Following *chk1* ablation in the skin, I showed that the tissue is eventually repopulated over 1-3 weeks by unrecombined cells (see Figure 27). Greenow et al noted a similar phenotype in the intestine (Greenow et al, 2009). Using *AhCre* conditional *chk1* knockout murine model, *chk1* loss resulted in death of crypt cells associated with loss of Chk1 mRNA and protein expression. But Chk1 was re-expressed by day 5 in the tissue as a result of repopulation by cells bearing the unrecombined allele. As with my skin data, it was interesting to note that despite a seemingly major tissue regeneration process occurring there was no evidence of pathological changes. Reconstitution of the tissue by unrecombined cells was therefore evidently able to adequately maintain homeostasis in both the skin and intestine.

**Chapter 6. Mechanisms for Explaining *Chk1*
Ablation and Resultant Tumour
Suppression**

6.1. Results

6.1.1. *Chk1* Ablation Caused a Depletion of Label Retaining Cells and Reduced Tumour Formation but Homeostasis is Maintained

In Chapter 5 (see 5.1.3 and 5.1.4), I have shown that *chk1* ablation leads to LRC proliferation and an accumulation of DNA damage and apoptosis. In *chk1* ablated skin, the tissue is eventually repopulated by cells which had escaped recombination. During this process, skin homeostasis appears intact with no gross pathology observed. Working models for LRC or bulge stem cell fate following *chk1* ablation are represented schematically in Figure 29. This will be explored in greater detail in Chapter 6, Discussion 6.2. One possible view is that bulge stem cells in *chk1**flox/flox* // *K14CreER^{T2}* // *LacZ* mice (in blue) when undergoing 4OHT mediated recombination into *chk1* Δ/Δ cells (in red) undergo aberrant replication, accumulate DNA damage and eventually undergo apoptosis Figure 29A. Recombination however, is not achieved in all cells and unrecombined stem cells go on to proliferate and repopulate the bulge stem cell niche.

In order to test this hypothesis, two experiments were performed. In the first, Keratin 15 staining was used as a cell cytokeratin or cytoskeletal protein to identify cells possessing progenitor like properties within mouse epithelia (Liu et al, 2003; Lyle et al, 1998; Serrels et al, 2009). It should be noted however, that Keratin15 marks not only stem cells but also the transit amplifying cell populations. The latter is an intermediary cell type which is thought to arise from stem cell division, capable of multiple rounds of divisions before becoming terminally differentiated [reviewed by (Jones et al, 2007)]. In *chk1**flox/flox* // *K14CreER^{T2}* // *LacZ* mice following 5 days of intraperitoneal 4OHT treatment (D-5 to D-1), as described previously, LRC numbers are reduced at day 10 (see Figure 30). However, levels of keratin 15 positive cells remains relatively constant compared to control. This could suggest that unrecombined progenitor cells are able proliferate to maintain this population.

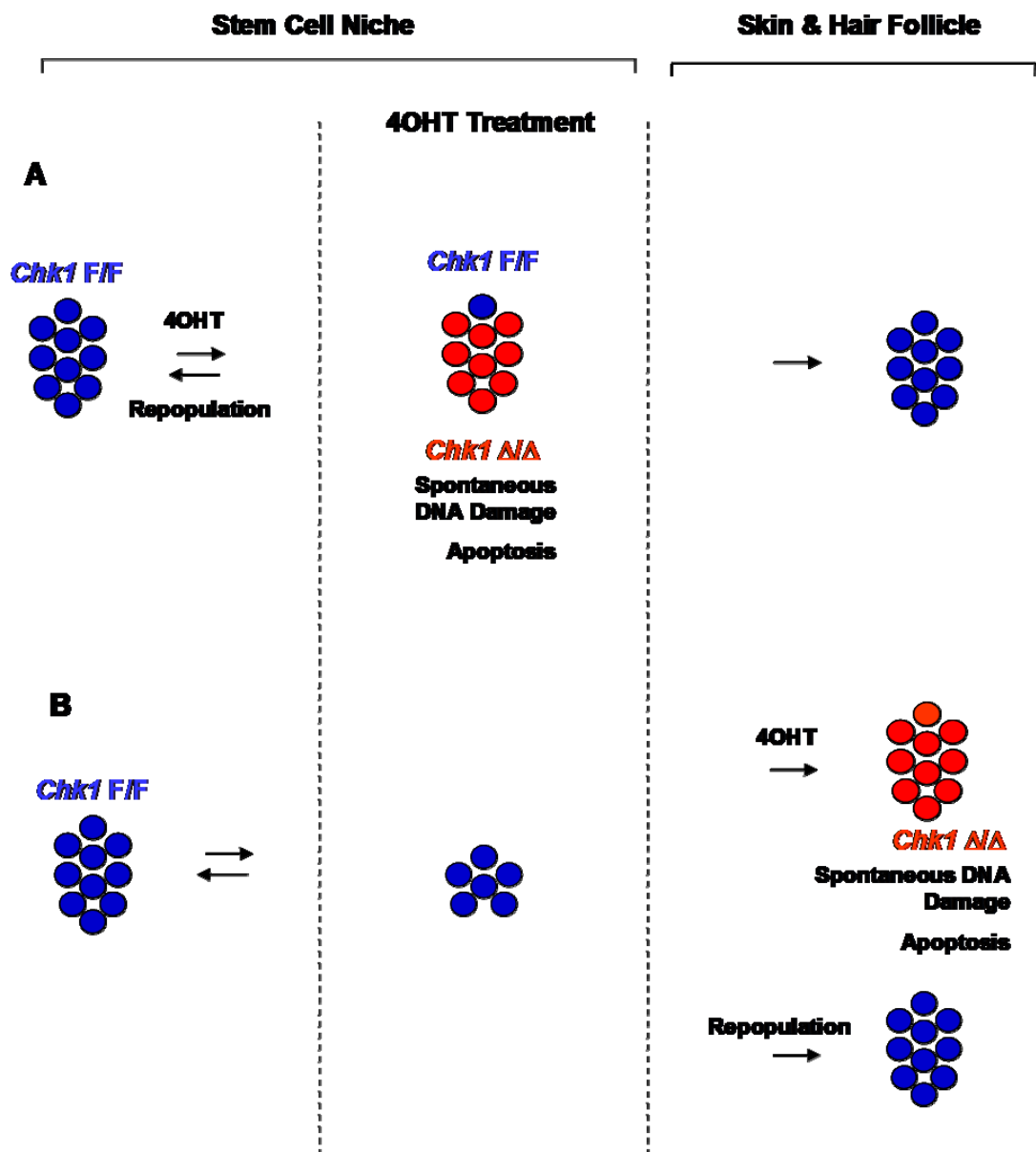


Figure 29 - Models of Stem Cell Fate Following *Chk1* Ablation

A schematic diagram showing potential consequences of *chk1* ablation on both the bulge stem cell compartment (left column) and somatic cell compartment (right column).

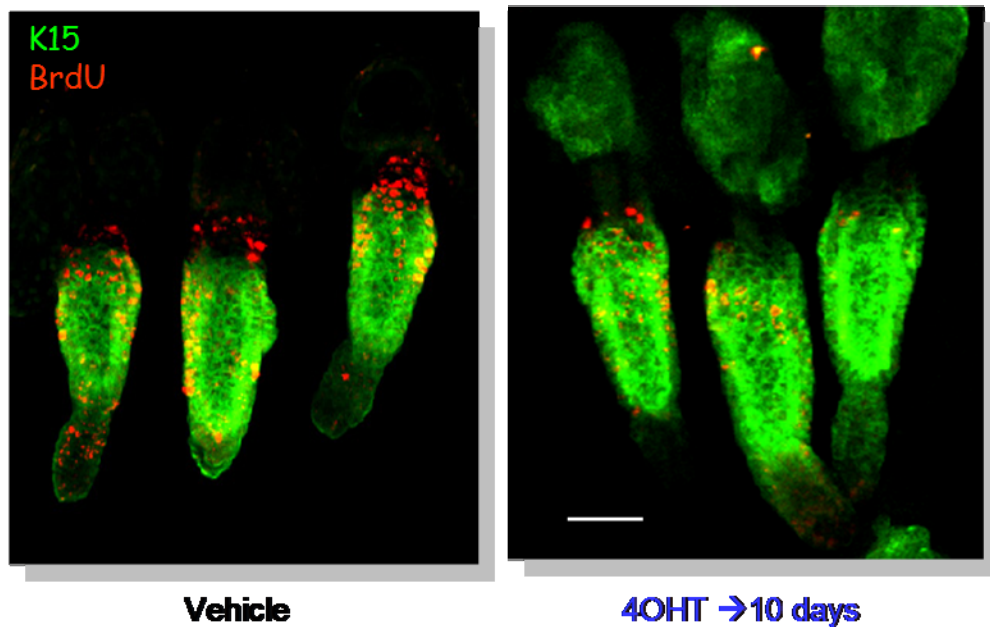


Figure 30 - Keratin 15 Expression Following *Chk1* Ablation

Neonatal *chk1* flox/flox // *K14CreER^{T2}* // *LacZ* mice were labelled with brdU to assay for label retaining cells (LRCs). The mice were allowed to age to around 8 weeks, then treated with IP 4OHT (D-5 to D-1) or vehicle. Wholmount epidermis was prepared, stained for keratin 15 (K15) and imaged using confocal microscopy. Numbers of K15 positive cells remains relatively constant although LRC cells were reduced following 4OHT. Scale bar represents 40 μ m.

Analyses of the pattern of co-staining (yellow) between BrdU positive (red) and K15 positive (green), allowance being given for the fact that BrdU is a nuclear stain and K15 a cell cytokeratin, allows a degree of insight into the hierarchy of differentiation or “stemness” in these two populations. The true bulge region contains BrdU cells which do not co-stain. Co-staining is seen in the region below the bulge which has been understood to be the region containing bulge stem cells which have exited the niche and are undergoing differentiation and proliferation (Braun et al, 2003; Ito et al, 2002; Ito et al, 2005; Jaks et al, 2008). Therefore, this implies K15 fails to mark a subset (arguably, the majority) of cells traditionally associated with a high degree of “stemness” ie. LRCs.

To further test the idea that bulge stem cell repopulation affects tumour formation, *chk1*flox/flox // *K14CreER^{T2}* // *LacZ* mice were treated with 5 days (days -5 to -1) of intraperitoneal 4OHT but DMBA treatment was delayed till D10 instead of the usual application at D3 (see Figure 31A). This was compared to two cohorts from previous experiments described in Chapter 4 (see 4.1.1) which were *chk1* flox/flox // *K14CreER^{T2}* // *LacZ* mice + vehicle and *chk1* flox/flox // *K14CreER^{T2}* // *LacZ* mice treated with 4OHT and then 3 days later with DMBA. All received the standard TPA protocol. As shown previously, D3 DMBA resulted in significantly fewer papillomas. Given that the disappearance of β -Gal staining and re-expression of Chk1 takes place over 1-3 weeks, a 10 day delay in DMBA application (D10 DMBA) was expected to allow the bulge time to undergo substantial repopulation by unrecombined stem cells before being subjected to carcinogens. Papillomas were quantified weekly for 30 weeks beginning at TPA application. The D10 DMBA group developed a similar number of papillomas to the control group with no statistically significant difference observed for tumour numbers at 30 weeks (Mann Whitney $p=0.50$). There was however a statistically significant difference between DMBA D10 versus DMBA D3 tumour numbers at 30 weeks (Mann Whitney, $p<0.0001$). Hence the delay in DMBA application was able to rescue the papilloma suppression phenotype. This suggests that *chk1* ablation reduced the number of available stem cell targets for chemical carcinogenesis in the short term but unrecombined stem cells were able to repopulate the bulge niche reconstituting the number of targets available for transformation. This is graphically represented in Figure 31B. Following 4OHT treatment at DMBA

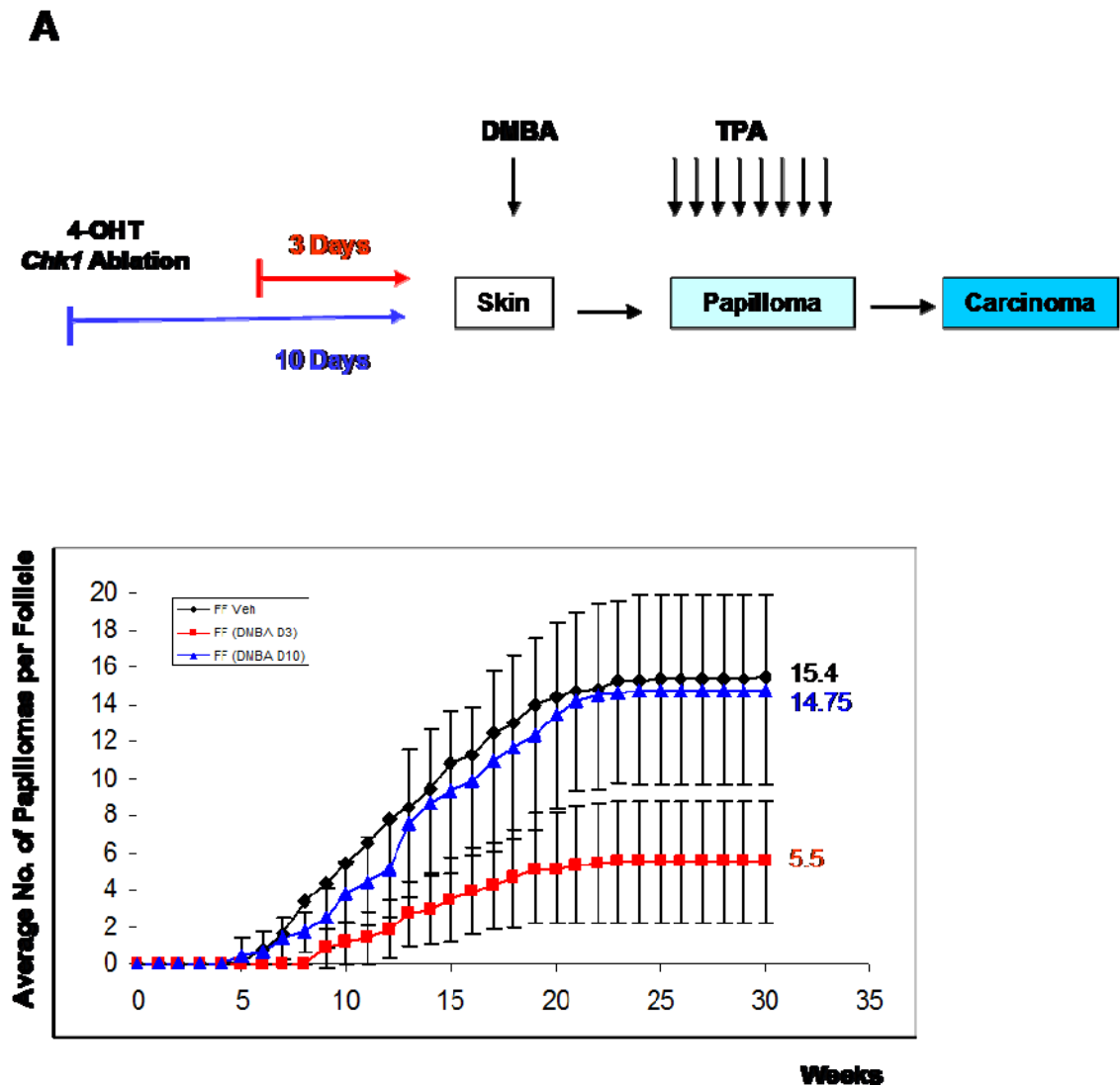
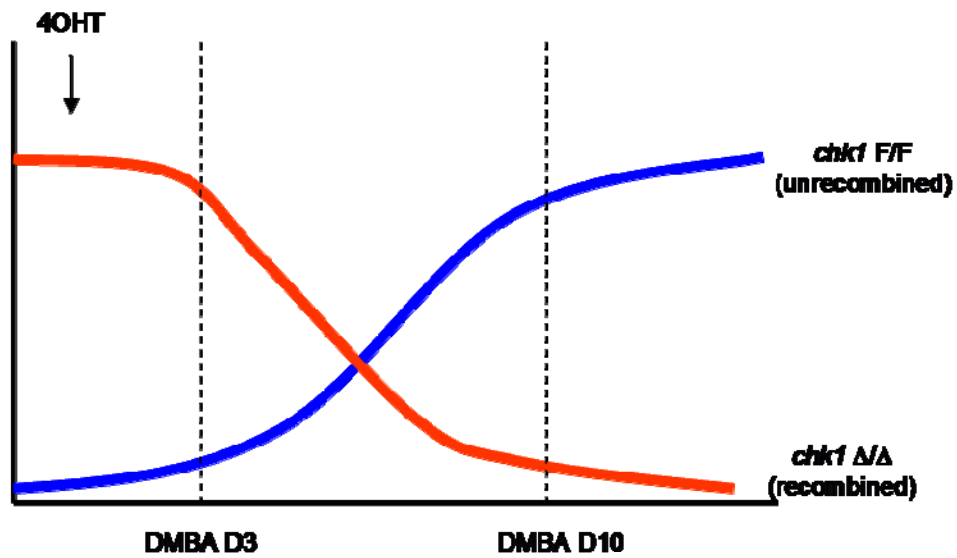


Figure 31 - Delaying DMBA Application Following *Chk1* Ablation

A *Chk1* flox/flox // *K14CreER^{T2}* // *LacZ* mice were treated with IP 4OHT (D-5 to D-1) but DMBA treatment was delayed till D10 instead of the usual application at D3. This was compared to two cohorts from previous experiments described in Figure 3, Chapter 2 which were *chk1* flox/flox // *K14CreER^{T2}* // *LacZ* mice + vehicle and *chk1* flox/flox // *K14CreER^{T2}* // *LacZ* mice treated with 4OHT and then 3 days later with DMBA. All received the standard TPA protocol. The D10 DMBA application group displayed papilloma development similar to the vehicle treated group (Mann Whitney $p=0.50$). A statistically significant difference between D10 DMBA versus D3 DMBA papilloma numbers was observed (Mann Whitney, $p<0.0001$).

B

B Graphical representation showing that the reduction in papilloma formation when DMBA is applied at D3 following 4OHT treatment versus at D10 may be due to the prevalence of *chk1* recombined stem cells (Δ/Δ) versus unrecombined (F/F) in skin tissue. At D10 following 4OHT treatment, F/F cells are repopulating the skin following attrition of Δ/Δ cells.

application at D3, carcinogen treatment occurs when a large proportion of the target stem cells are *chk1* recombined (Δ/Δ). When DMBA application is delayed, unrecombined (flox/flox) cells to repopulate the tissue (see Figure 27), thereby increasing the number of stem cells.

6.1.2. *Chk1* Ablation Reduces Hyperplasia Normally Caused by TPA

Tissue hyperplasia is an important step in selecting the outgrowth of *H-ras* mutant cells to form papillomas (Boutwell et al, 1982; Kemp, 2005). If *chk1* ablation led to transient stem cell depletion, it follows the ability of skin to respond to tissue promotion might be impaired. To test this, *chk1* flox/flox // *K14CreER^{T2}* // *LacZ* mice were treated with either 5 days of intraperitoneal 4OHT or vehicle and then 4 weeks of TPA (twice a week) (Figure 32A). Animals were sacrificed after 4 weeks, skin sections prepared from paraffin blocks and stained with H&E. Epidermal thickness and length of telogen and anagen hair follicles were recorded (Figure 32B). Mice treated with 4OHT had significantly reduced epidermal thickness (Mann Whitney test, $p=0.017$), telogen follicle length (Mann Whitney test, $p=0.004$) and anagen follicle length (Mann Whitney test, $p=0<0.001$). This indicates that *chk1* ablation attenuated TPA induced hyperplasia. This may also be a contributory factor for the reduction in numbers of papillomas observed following *chk1* ablation (Figure 32C).

6.1.3. *Chk1* Ablation May be Selectively Targeting *H-Ras* Mutant Stem Cells for Apoptosis

To test if *chk1* ablation selectively induces a greater degree of DNA damage and apoptosis in oncogene-transformed stem cells compared to non-transformed stem cells, DMBA application was performed 3 days prior to 4OHT treatment in *chk1*flox/flox // *K14CreER^{T2}* // *LacZ* mice (DMBA \rightarrow 4OHT). Skin was then exposed to TPA as per standard protocol over 20 weeks. In Figure 33A data from these mice are compared to two cohorts from previous DMBA/TPA

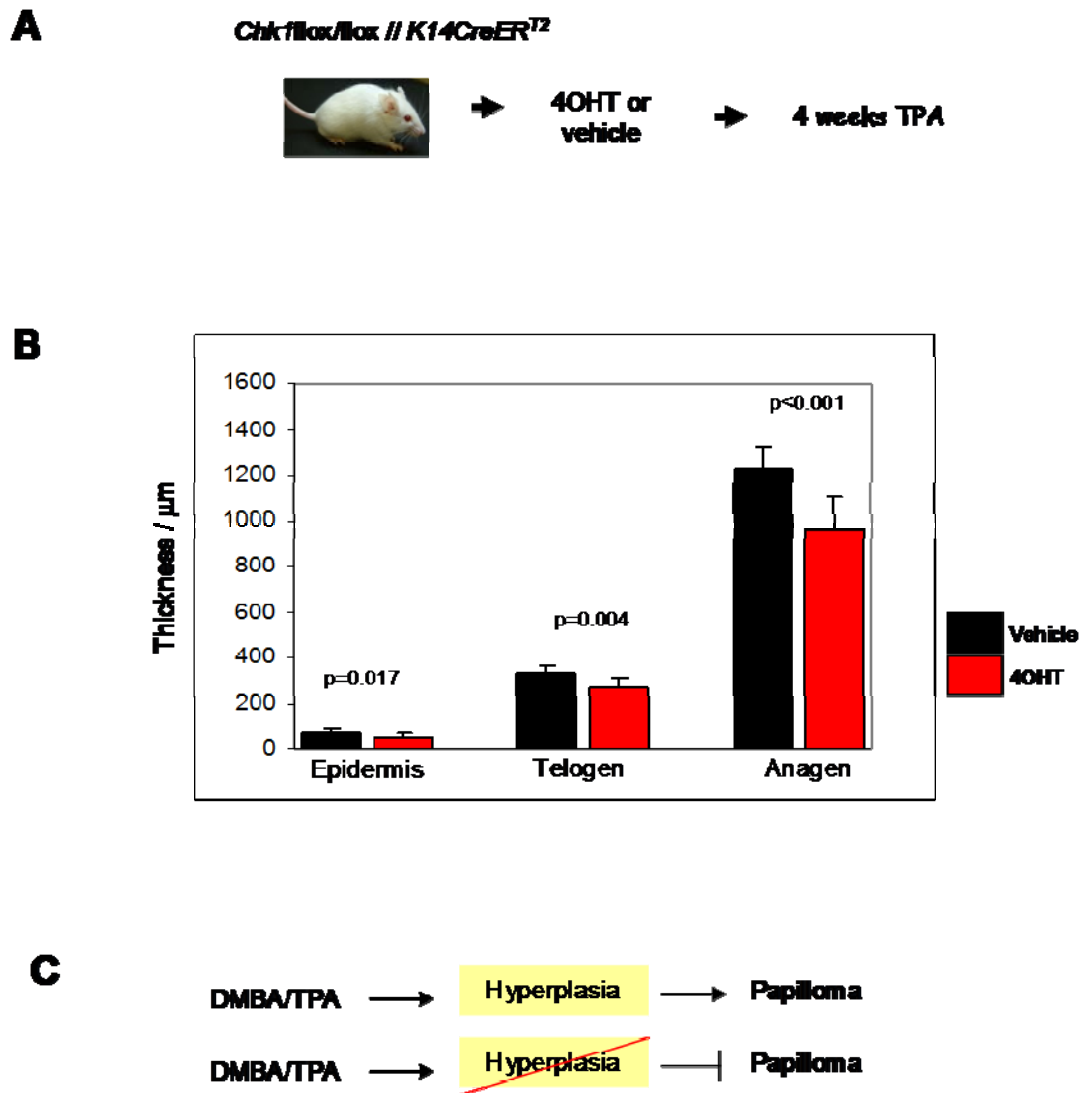


Figure 32 - TPA Induced Skin Hyperplasia and *Chk1* Ablation

A *Chk1*^{flox/flox} // *K14CreER*^{T2} // *LacZ* mice were treated with IP 4OHT or vehicle and then with 4 weeks of TPA (twice a week). **B** Epidermal thickness and length of telogen and anagen hair follicles were recorded at the end of the experiment. Mice treated with 4OHT had significantly reduced epidermal thickness (Mann Whitney test, $p=0.017$), telogen follicle length (Mann Whitney test, $p=0.004$) and anagen follicle length (Mann Whitney test, $p=0.001$). **C** Papilloma outgrowth from skin pre-treated with DMBA is thought to depend on intermediary hyperplasia. If this reaction is attenuated, it may well be a contributory factor for the reduction in papillomas following *chk1* ablation.

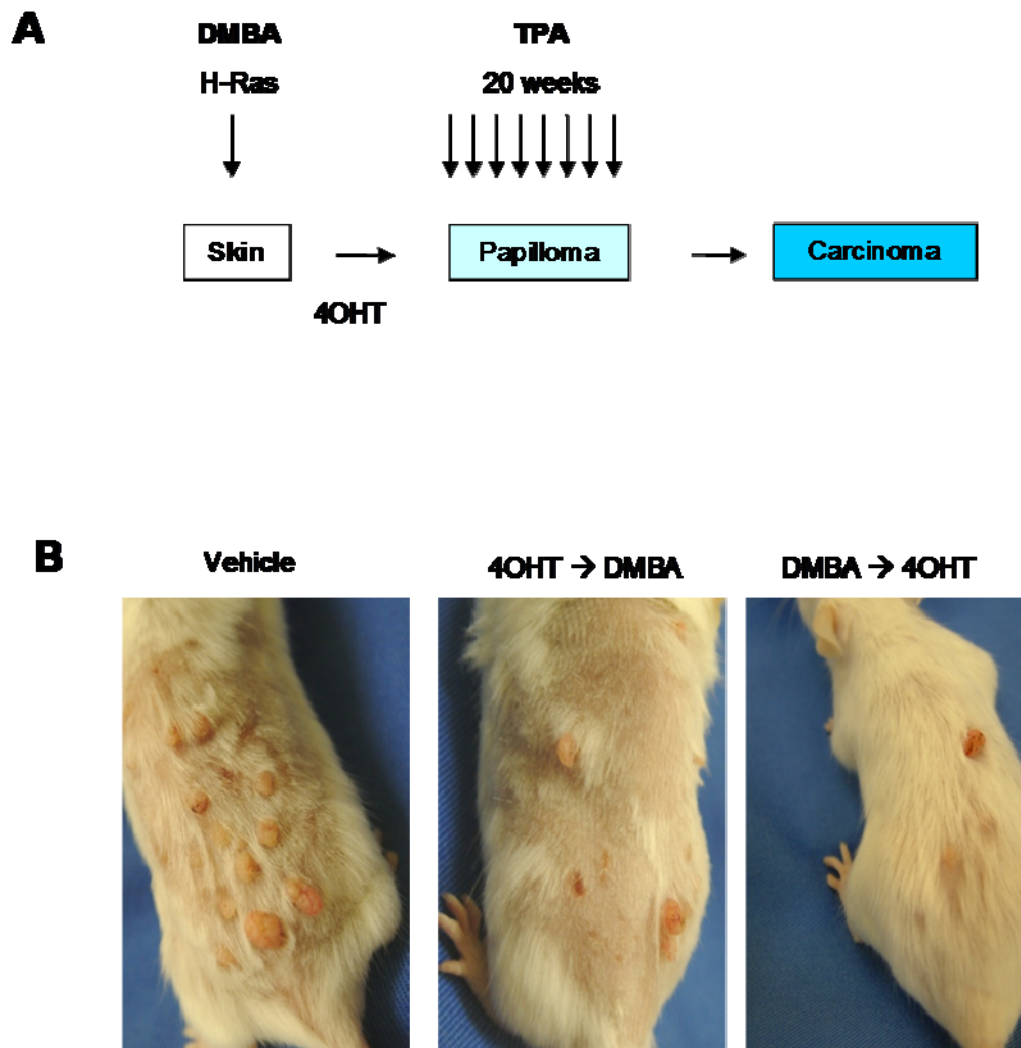
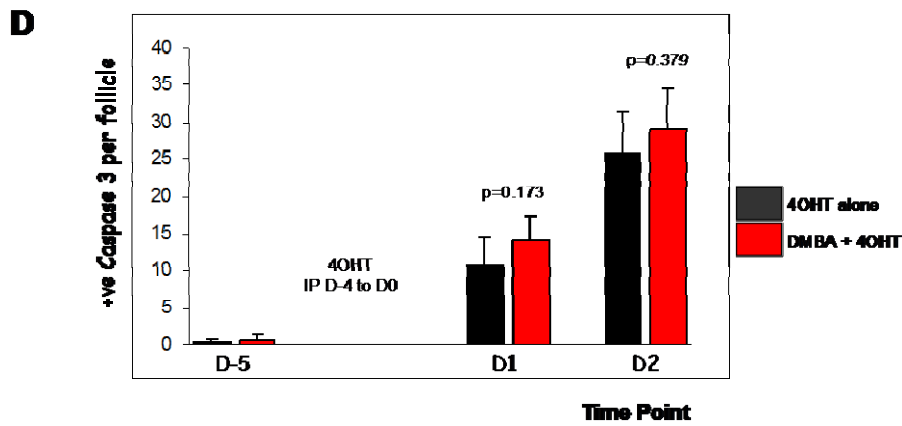
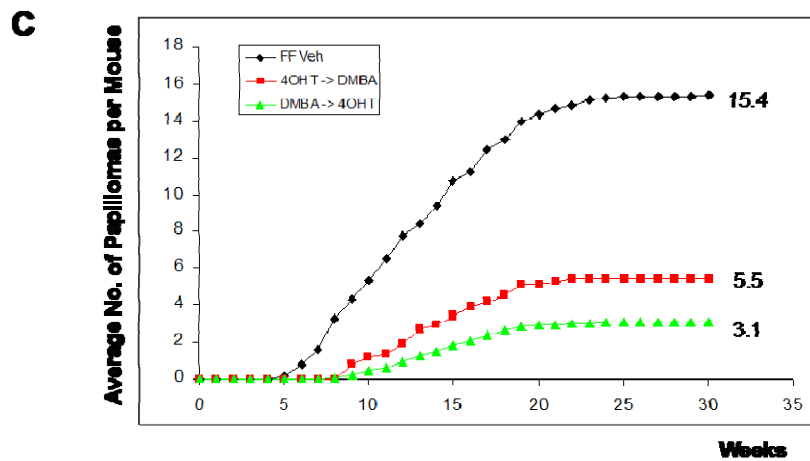


Figure 33 - TPA Induced Skin Hyperplasia and *Chk1* Ablation

A *Chk1* flox/flox // *K14CreER*^{T2} // *LacZ* mice were treated with IP 4OHT or vehicle and then with 4 weeks of TPA (twice a week). **B** Epidermal thickness and length of telogen and anagen hair follicles were recorded at the end of the experiment. Mice treated with 4OHT had significantly reduced epidermal thickness (Mann Whitney test, $p=0.017$), telogen follicle length (Mann Whitney test, $p=0.004$) and anagen follicle length (Mann Whitney test, $p=0<0.001$).



C Papilloma outgrowth from skin pre-treated with DMBA is thought to depend on intermediary hyperplasia. If this reaction is attenuated, it may well be a contributory factor for the reduction in papillomas following *chk1* ablation. **D** Comparing apoptosis in mouse skin following *chk1* ablation with or without prior DMBA treatment.

experiments as detailed in Figure 13. In brief, *chk1*flox/flox // *K14CreER^{T2}* // *LacZ* mice were treated with vehicle, 3 days later with DMBA, then TPA (control) and *chk1*flox/flox // *K14CreER^{T2}* // *LacZ* mice were treated with 4OHT, 3 days later with DMBA, then TPA (4OHT → DMBA). DMBA → 4OHT mice showed substantially reduced papilloma formation over 30 weeks (Figure 33B,C) compared to control, as was the case with 4OHT → DMBA mice. The average number of papillomas per mouse DMBA → 4OHT versus control was 3.1 vs. 15.4 (Mann Whitney, $p < 0.0001$). Interestingly, the average number of papillomas per mouse in the DMBA → 4OHT versus 4OHT → DMBA cohorts was statistically different, 3.1 vs. 5.5 (Mann Whitney, $p = 0.032$).

To attempt to quantitate the degree of apoptosis in hair follicles, *chk1*flox/flox // *K14CreER^{T2}* // *LacZ* mice were treated with IP 4OHT alone or DMBA 2 weeks prior to IP 4OHT application. Wholmount epidermis samples were prepared, stained for activated caspase 3 (AC3) and visualised using confocal microscopy (Figure 33D). The number of AC3 positive cells were quantified per follicle, for 2 sets of triplet follicles in one animal, for each cohort at each time point. No significant difference in average number of AC3 positive cells per follicle was seen between the two groups at D1 and D2 following 4OHT (D-5 to D-1), Mann Whitney, $p = 0.173$ and $p = 0.379$ respectively. Nevertheless, at both time points there was a trend towards a greater number of AC3 cells observed in the DMBA pre-treated skin. Perhaps statistical significance was not observed due to the small difference in magnitude and small sample size (2 animals per time point). Given a significant reduction in average number of papilloma formation in DMBA pre-treated skin, it is possible that a *chk1* ablation induces apoptosis to a greater degree in *H-ras* transformed stem cells as opposed to non-transformed stem cells.

6.1.4. *Chk1* Ablation Delays Hair Regrowth

Although no gross pathology was noted in the skin following *chk1* ablation, we investigated the effect on hair regrowth after shaving, which is an indicator of the rate of epithelial renewal following *chk1* ablation. *Chk1*flox/flox // *K14CreER^{T2}* // *LacZ* and *chk1*^{+/+} // *K14CreER^{T2}* // *LacZ* mice were treated with

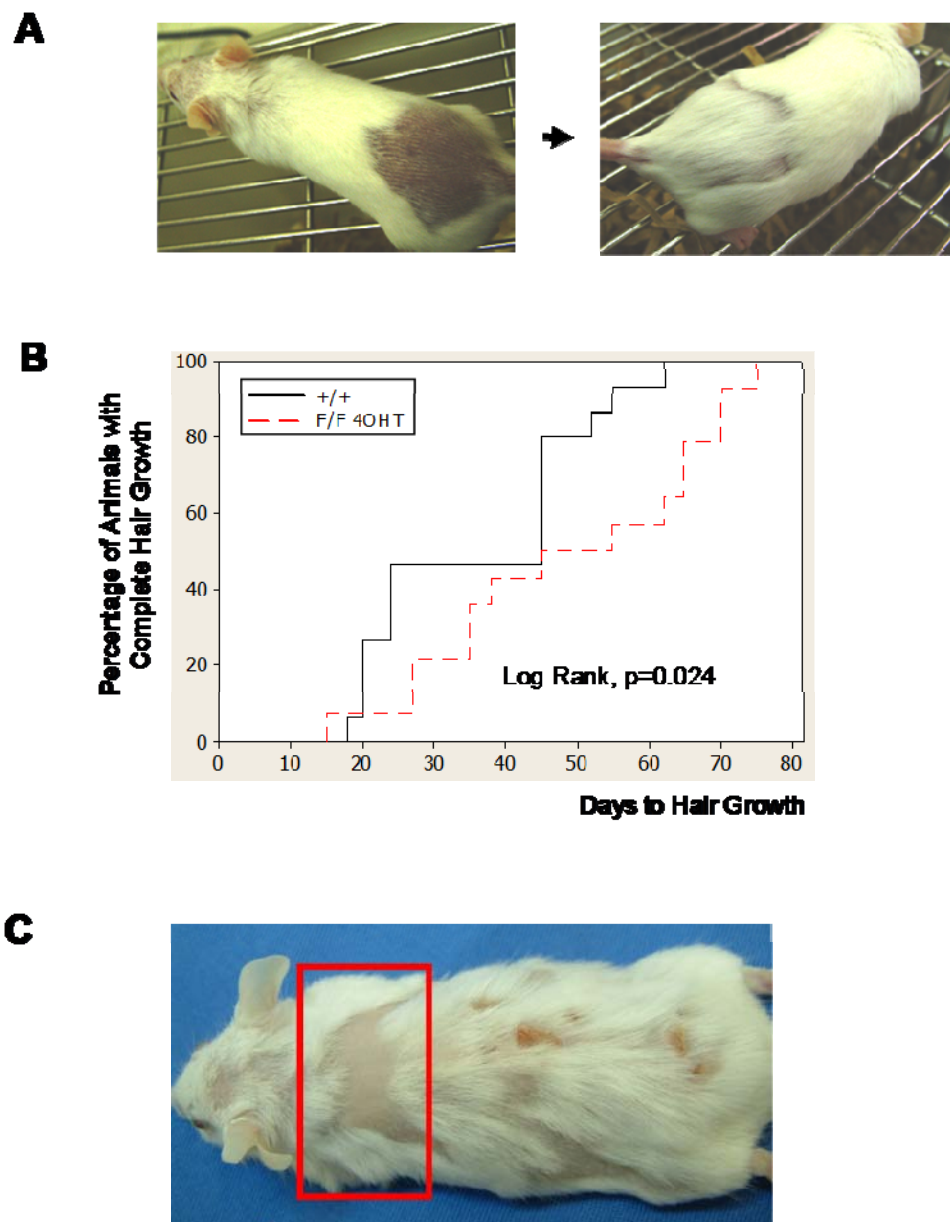


Figure 34 - Effect of *Chk1* Ablation on Hair Growth

A *Chk1* flox/flox // *K14CreER^{T2}* // *LacZ* and *chk1* +/+ // *K14CreER^{T2}* // *LacZ* mice were treated with IP 4OHT and underwent shaving of the lower $\frac{1}{3}$ to $\frac{1}{2}$ of the dorsal skin. The time taken for hair regrowth was recorded. **B** Time taken for hair regrowth was significantly longer in *chk1* flox/flox animals compared to control (log rank $p=0.024$). **C** Also noted in a small number of *chk1* flox/flox // *K14CreER^{T2}* // *LacZ* treated with 4OHT and the DMB/TPA protocol, after 20+ weeks, bald patches began to emerge in the dorsal skin.

IP 4OHT and underwent shaving of the lower $\frac{1}{3}$ to $\frac{1}{2}$ of the dorsal skin (see Figure 34A). The time taken for hair regrowth was recorded. This was found to be significantly longer in *chk1*^{flox/flox} animals compared to *chk1*^{+/+} control (log rank $p=0.024$) (Figure 34B).

In a subset of *chk1*^{flox/flox} // *K14CreER*^{T2} // *LacZ* mice treated with 4OHT and then commenced on DMBA/TPA (Figure 13), after around 20 weeks bald patches were noted to occur in the dorsal skin (Figure 34C). These regions of alopecia persisted till the animals were eventually sacrificed.

Taken together, these two observations suggest that the loss of *chk1* reduces the rate of epithelial renewal in adult skin. The explanation of this phenomenon possibly lies in my previous observations that *chk1* loss causes stem cell (LRC) proliferation (see Figure 19). Ruzankina et al (Ruzankina et al, 2007) using *ATR* knockout mice (*ATR* being the direct upstream activator of *chk1*), observed that genetic deletion in the presence of proliferative stimulus resulted in an ageing phenomenon with hair greying, delayed hair regeneration and baldness. In these mice, conditional *ATR* ablation resulted in attrition of recombined cells followed by repopulation by unrecombined cells over time - which is similar to our observations in *chk1* conditional knockout mice. After three rounds of *ATR* ablation with intervals to allow for repopulation by unrecombined cells, accompanied by hair plucking / depilation, this resulted in progressively more severe delay hair regeneration, hair greying and alopecia after each cycle. The authors note that loss of tissue homeostasis through stem and progenitor cell attrition has previously been proposed as a model to explain the general organismal decline associated with ageing (Chen, 2004; Pelicci, 2004; Rando, 2006; Sharpless & DePinho, 2004). Because *ATR* deletion led to the depletion of stem and progenitor cells, their interpretation of their results indicate that stem and progenitor cell attrition may be the primary cause of reduced regenerative capacity. They propose that *ATR* deletion may render a majority of stem cells replication incompetent, leading to an overreliance on the remaining *ATR*-expressing *ATR*^{flox/-} stem cells that escaped lox recombination. These surviving *ATR*-expressing stem and progenitor cells may subsequently be lost either by natural causes or by additional replicative stress acquired during pool regeneration; thus, these residual cells may be insufficient to maintain tissue homeostasis over the long term. In support of this model, they also observed a

dramatic loss of CD34⁺ follicle bulge stem cells soon after depilation-induced anagen (Ruzankina et al, 2007). While these bulge stem cells regenerated to a sufficient degree to drive a delayed anagen phase, they recovered poorly in subsequent regenerative cycles, and their depletion was ultimately associated with follicle degeneration and hair loss.

The explanations proposed by Ruzankina et al (Ruzankina et al, 2007) may also explain my observations with regards delayed hair regrowth and alopecia seen in *chk1* ablated animals (see Figure 34). Loss of *chk1* may be inducing stem cell proliferation leading to additional “replicative stress” on the remaining pool of unrecombined cells reducing their regenerative capacity in the long term.

6.2. Discussion

6.2.1. Models for Label Retaining Cell / Stem Cell Fate Following *Chk1* Ablation

Two working models to explain label retaining cell / stem cell fate following *chk1* ablation are represented schematically in Figure 29.

One possible view is that bulge stem cells in *chk1*^{flox/flox} // *K14CreER*^{T2} // *LacZ* mice (in blue) undergo 4OHT mediated recombination into *chk1* Δ/Δ cells (in red), and as a result undergo aberrant replication without the usual licensing mechanisms to halt cell division in the face of replication damage or errors occurs. This leads to an accumulation of DNA damage, the burden of which will eventually result in apoptosis Figure 29A. From published data (Greenow et al, 2009; Ruzankina et al, 2007) and from work in this thesis, we know recombination is not achieved in all cells. In this model, the hypothesis states that unrecombined stem cells proliferate to repopulate and reconstitute the bulge stem cell niche thereby maintaining normal tissue homeostasis. In Chapter 4 (see Figure 13), it is shown that chemical carcinogenesis initiation 3 days after *chk1* ablation, caused a marked reduction in papilloma formation. If stem cell numbers are indeed reduced, then this piece of experimental data supports the hypothesis. Furthermore, when the tissue is allowed to recover by delaying DMBA till day 10 (see Figure 31), the number of papillomas that developed were similar to controls which suggests a restoration of the number of stem cell targets available for carcinogenesis. Figure 31B is a further graphical representation illustrating the importance of the DMBA timing after 4OHT application in influencing the number of papillomas that develop. In these *chk1* ablated mice which are aged no gross pathology is noted which implies homeostasis is being maintained. In this model it is presumed the stem cells and somatic cells which escape initial recombination contribute significantly to maintaining homeostasis.

As demonstrated in Figure 19 (see 5.1.2), *chk1* ablation causes proliferation of LRC cells. The alternative hypothesis (see Figure 29B) states the main trigger for

LRC proliferation are signals derived from somatic tissue. I have observed an accumulation of DNA damage (see Figure 23) and apoptosis (see Figure 24) occurring in mouse skin following recombination. It is possible that these processes (and associated events) result in changes in tissue homeostasis which trigger response mechanisms that cause the normally quiescent LRCs to proliferate in order to replenish cell death within the somatic compartment. It is also entirely possible that both hypotheses are true, and that both processes occur simultaneously following *chk1* ablation.

In order to clarify the situation above, experiments would need to be conducted to allow separate assessment of events occurring in two separate cell populations within the skin stem cells and somatic cells - focussing on *chk1* expression, proliferation, DNA damage and apoptosis. This would require an ability to assay stem cells over a period of time and even after stem cell division has occurred. Unfortunately the BrdU LRC assay presents limitations in this regard because subsequent rounds of cell division lead to dilution of the label. Additionally, it is not possible to re-label a mouse with BrdU subsequent to the neonatal period. Therefore it has not been possible to define, if following *chk1* ablation in adult skin for example, the bulge is truly reconstituted by stem cells which have escaped recombination even though K15 staining did not diminish (see Figure 30). Nor has it been possible to determine if proliferating LRCs consisted of cells which successfully underwent recombination or had escaped recombination or both. As alluded to, expression of surface markers, for example K15 or CD34, as surrogates for label retention presents limitations as there is limited agreement on co-expression as is their validity for identifying stem cells as defined by pluripotency, clonogenicity and longevity (Fuchs, 2009; Myung et al, 2009a; Myung et al, 2009b; Tumbar et al, 2004).

Further experimental limitations I encountered emerged due to the acid denaturation step used to reveal the BrdU epitope for antibody staining. Acid denaturation has been reported to destroy antibody binding epitopes (Cappella et al, 2008; Eisch & Mandyam, 2007), ie. affecting the accuracy of assaying for Chk1 expression, DNA damage and apoptosis. Methods to overcome this have been described including using EdU (5-ethynyl-2'deoxyuridine) (Cappella et al, 2008; Lin et al, 2009) as an alternative thymidine analogue to BrdU. The detection of EdU, using the Invitrogen Click-iT® kit, does not require an acid

denaturation step but instead relies on an azide- ethynyl copper catalysed reaction. Although no protocols have been published for the use of EdU in *in vivo* skin or tail staining, I attempted to trial EdU as an alternative to brdU staining to assay for proliferation by *in vivo* injections. Unfortunately I was not able to successfully optimize the protocol and hence was not able to utilize this reagent in this thesis. This work is currently being followed on by other members of my laboratory. Another approach would be to endogenously label cells with a fluorescent marker to obviate the need for epitope recovery and antibody binding. I have obtained a mice expressing the conditionally activated ROSA26 *loxP-stop-loxP RFP* reporter (Luche et al, 2007) which are currently being crossed with the *chk1flox/flox* strain in order to produce a *chk1flox/flox // K14CreER^{T2} // loxP-stop-loxP RFP* mouse. This will eventually allow *chk1* genetic ablation to be assayed by RFP expression which is amenable to detection using confocal imaging, cell sorting and other techniques without the need for epitope recovery. Both of these approaches are discussed in greater detail in Future Perspectives 8.2.

In the DMBA/TPA carcinogenesis protocol, skin hyperplasia is an important step for the outgrowth of papillomas (Boutwell et al, 1982; Kemp, 2005). *H-ras* transformed cells require ongoing promotion for clonal expansion and growth into visible papillomas. If TPA promotion is withheld or terminated prematurely, the result is a reduction in number of papillomas observed (Balmain et al, 1984; Kemp, 2005). In skin that was *chk1* ablated, there was an overall reduction in epidermal thickness and hair follicle length compared to control, indicating a reduced hyperplastic response to TPA induction (see Figure 32). This could also be a factor contributing towards the reduction in numbers of papillomas observed following *chk1* ablation. Prior reports have suggested “stem cell exhaustion” as a means to explain a reduced hair regrowth following depilation (Ruzankina et al, 2007). Stem cell depletion was brought about by the conditional ablation of *ATR* which is the direct upstream activator of *chk1*. In my mice, presumably the skin has an attenuated ability to develop tissue hyperplasia in response to TPA due to reduction in number of stem cells available following *chk1* ablation - at least within 10-14 days following first application of tamoxifen (see Figure 31). Therefore, in addition to a reduction in number of available stem cell targets for carcinogenesis, the reduction in

papilloma number following *chk1* ablation may be due to an attenuated hyperplastic response.

It is also possible that *chk1* loss might be selectively targeting *H-ras* mutant cells for apoptosis (see Figure 33). By reversing the order of DMBA and 4OHT application, (DMBA → 4OHT) in *chk1* flox/flox // *K14CreER^{T2}* // *LacZ* mice the average number of papillomas per mouse was significantly reduced compared to 4OHT → DMBA and vehicle treated mice. This suggests that fewer targets were available for carcinogenesis in the DMBA and 4OHT treated skin compared to DMBA treated skin alone. Nevertheless quantification of the number of apoptotic cells using confocal microscopy in DMBA → 4OHT versus 4OHT alone mice did not show any significant difference (Figure 33D). In this experiment however statistical significance may have been compromised by lack of numbers and I believe verification would require a bigger cohort. Previous studies have shown oncogene transformation induces a marked DNA damage response in cultured cells. Consequent checkpoint activation is essential for the cell to undergo oncogene-induced senescence (Bartkova et al, 2005; Bartkova et al, 2006; Di Micco et al, 2006). If these checkpoint mechanisms were abrogated there could be a significant accumulation of potentially lethal genetic lesions. Work carried out on human *in vivo* specimens show a marked upregulation of senescent markers and checkpoint activation in pre-malignant lesion compared to normal tissue (Bartkova et al, 2005; Bartkova et al, 2006; Di Micco et al, 2006). This argues that once oncogene-activation occurs, cells may actually engage checkpoint mechanisms preferentially compared to the non-transformed state. In mice which undergo *chk1* ablation followed by DMBA treatment, my results suggest that *H-ras* transformed cells maybe particularly sensitive to *chk1* deletion. This would be consistent with the hypothesis that oncogene transformed cells are preferentially reliant on checkpoint mechanisms to engage senescence and escape abortive DNA replication and apoptosis.

6.2.2. *Chk1* Ablation May be Causing Bulge Niche Exhaustion

When the skin was shaved and hair growth rate recorded, *chk1* ablation delayed hair re-growth. Additionally sporadic bald patches appeared after long term TPA which induces a state of forced anagen (see Figure 34). A similar phenomenon has been observed in *ATR* knockout mice (Ruzankina et al, 2007). Repeated rounds of hair depilation accompanied by *ATR* conditional ablation resulted in delayed hair regeneration as well as hair greying. This was attributed to depletion of the bulge stem cell compartment. In my mice *chk1* ablation is followed by repopulation by unrecombined cells. This will likely have the effect of recruiting normally quiescent stem cells into active cycling. Premature or repeated rounds of stem cell division have the consequence of terminal ageing, due to the finite number of divisions permissible within the cells' lifespan (He et al, 2009; Muller-Sieburg & Sieburg, 2008; Voog & Jones, 2010). In this case, *chk1* ablation seems to have reduced the regenerative capability of the skin leading to alopecia in the presence of continual proliferative stimulus (TPA) and delayed hair regrowth.

6.2.3. *H-Ras* and Non-*H-Ras* Transformed Stem Cells do not Repopulate the Bulge Niche Symmetrically

DMBA treatment will result in only a tiny proportion of stem cells actually acquiring an *H-ras* mutation, estimated to be in the order of one in 10^6 . As discussed I hypothesize that *chk1* ablation temporarily reduces the number of bulge cells available for carcinogenesis. In the following 1-3 weeks, there are 2 possible patterns in which the surviving *H-ras* transformed and non-*H-ras* transformed stem cells might repopulate the bulge niche 1) symmetrical repopulation would result in proportionately increased numbers of both *H-ras* transformed and non-*H-ras* transformed cells 2) non-symmetrical repopulation resulting in proportionately fewer of either *H-ras* transformed or non-*H-ras* transformed cells (see Figure 35A). If scenario 1 was true then I would expect a 1-3 week delay in papilloma development but that eventual papilloma numbers

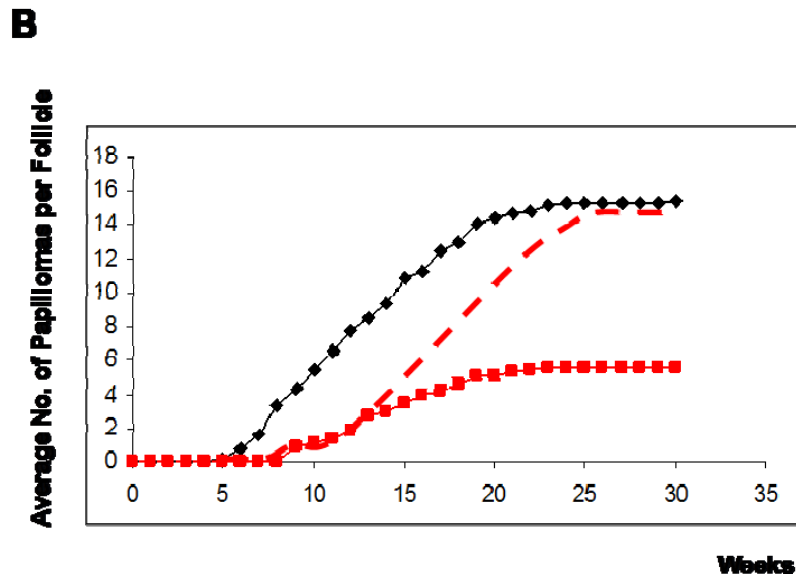
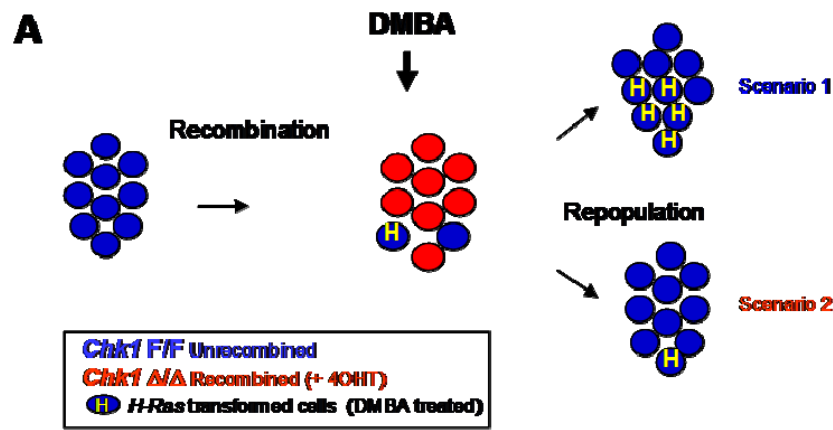


Figure 35 - The Effect of *Chk1* Ablation on the Stem Cell Niche and Tumour Formation

When *chk1* flox/flox // *K14CreER^{T2}* // *LacZ* mice are treated with 4OHT, bulge stem cells undergo recombination (*chk1* Δ/Δ) thereby presenting fewer cells available for chemical carcinogenesis. From lineage tracing experiments, Chk1 protein expression assays (Chapter 3) and chemical carcinogenesis experiments where the papilloma reduction phenotype is rescued, it can be concluded that repopulation of the bulge niche is relatively complete within 1-3 weeks. Given this time scale the question remains as to why permanent suppression of papilloma numbers occurs (**Figure 35B**, solid red line). **A** It is likely that DMBA treatment will result in only a tiny proportion of stem cells acquiring the *H-ras* mutation, in the order of one in 10⁶. *Chk1* ablation reduces the number of bulge cells available for carcinogenesis and presumably, proportionately the number of transformed stem cells. In the following 1-3 weeks, there are 2 possible patterns in which the remaining *H-ras* and non-*H-ras* transformed stem cells might undergo repopulation to reconstitute the bulge niche 1) Symmetrical repopulation resulting in equivalent numbers of *H-ras* and non-*H-ras* transformed cells 2) Non-symmetrical repopulation resulting in fewer of more of either *H-ras* or non-*H-ras* transformed cells. **B** If scenario 1 was true, then we would expect a 1-3 week delay in papilloma development but eventual papilloma numbers similar to control (dotted red line). However, papilloma numbers were permanently suppressed to around 1/3 that of control (solid red line).

would reach a similar plateau to control (Figure 35B, dotted red line). However, experimentally it was observed that papilloma numbers were suppressed to around $\frac{1}{3}$ that of control (Figure 35B, solid red line). This observation would therefore be more consistent with scenario 2, where asymmetrical repopulation of the niche resulted in fewer *H-ras* transformed cells compared to non-*H-ras* transformed cells. It is unclear why this is the case. Studies have shown *ras* oncogene transformation induces cellular senescence, and in pre-malignant tumours this has been implicated as a barrier against tumour progression (Braig et al, 2005; Collado et al, 2005; Di Micco et al, 2006; Ferbeyre, 2007; Sun et al, 2007). In one study, lung adenomas from *K-rasV12* activated mice were examined (Collado et al, 2005). They were found to strongly express senescence associated immunohistochemical markers, stained strongly for senescence-associated β -gal and senescence-associated heterochromatin foci. In contrast malignant lung adenocarcinomas were negative or stained very weakly. The authors also compared protein extracts from DMBA/TPA induced skin papillomas versus normal skin by immunoblotting for senescent markers p19^{ARF}, p16^{INK4a}, DcR2, Dec1 and p15^{INK4b}. Levels were upregulated in papillomas but not normal skin. Therefore, in my experiments, perhaps *H-ras* transformed stem cells became senescent and thereby repopulated the bulge at a reduced frequency.

If *H-ras* transformed cells repopulated the bulge at a slower rate (compared to non transformed cells) this will result in bulge niches containing proportionately fewer transformed cells. This being the case, a lower burden of transformed cells in each niche might be responsible for the observation of fewer papillomas. An observation by Williams et al (Williams et al, 1992) alludes to this hypothesis, whereby in murine intestine, crypts in which only a minority of cells undergo oncogene transformation are not able to form tumours. Only in crypts where the majority of cells undergo initial transformation are able to form tumours. It is known that the bulge niche is a tightly regulated environment, paracrine signaling being a major player, with significant control constantly being exerted over the fate of stem cell differentiation and proliferation (Scadden, 2006). High Ras expression for example, has been shown to decrease gap junction intercellular communication (GJIC) (Ito et al, 2006; Lee et al, 2004) which is thought to be important for tumourigenesis. Therefore, it is possible that only

when a critical number of *ras* transformed cells are present in the bulge, that papilloma outgrowth is permissible.

Chapter 7. Additional Results

7.1. Results

7.1.1. Hemizygous *Chk1* Ablation did not Affect Papilloma Incidence but Increased the Rate of Conversion to Carcinomas

To assess the consequences of hemizygous *chk1* deletion on skin tumour formation *in vivo*, DMBA/TPA chemical carcinogenesis was performed in *chk1* flox/+ // *K14CreER^{T2}* // *LacZ* mice which were treated with IP 4OHT prior to DMBA (n=19). As results from previous experiments (see Figure 13) had shown no statistical significance between papilloma numbers between control group *chk1* flox/flox // *K14CreER^{T2}* // *LacZ*, n=19 (+ vehicle) and *chk1* +/+ // *K14CreER^{T2}* // *LacZ*, n=20 (+ 4OHT), [Mann Whitney p=0.065] these two groups were combined and used for the purpose of comparison with this experimental group. After 30 weeks, there was no significant difference in average papilloma numbers between *chk1* flox/+ // *K14CreER^{T2}* // *LacZ* mice & IP 4OHT versus control groups, 16.6 versus 14.6 respectively, Mann Whitney p=0.183 (see Figure 36A). In contrast, the rate of conversion from papilloma to carcinoma was significantly higher in the *chk1* flox/+ // *K14CreER^{T2}* // *LacZ* mice + IP 4OHT group compared to control group, 9.7% versus 5.6%, chi squared test p<0.025.

In previous experiments (see Figure 14) the rate of carcinoma conversion of *chk1* flox/flox // *K14CreER^{T2}* // *LacZ* treated with IP 4OHT 3 days prior to DMBA was documented. In comparison, the rate of conversion of papillomas to carcinomas in *chk1* flox/+ // *K14CreER^{T2}* // *LacZ* mice & IP 4OHT was significantly higher compared to *chk1* flox/flox // *K14CreER^{T2}* // *LacZ* & 4OHT, 9.7% versus 2%, chi squared test p<0.020 (Figure 36B). There was no statistically significant difference between control and *chk1* flox/flox // *K14CreER^{T2}* // *LacZ* & 4OHT, 5.6% versus 2%, chi squared test p>0.10. β -Gal assay performed on (Figure 36C, i) papillomas and carcinomas obtained from *chk1* flox/+ // *K14CreER^{T2}* // *LacZ* mice & IP 4OHT produced a positive reaction. These tumours were obtained from mice that were sacrificed either due to unsustainable tumour burden according to Home Office regulations or when they had reached 60 weeks post

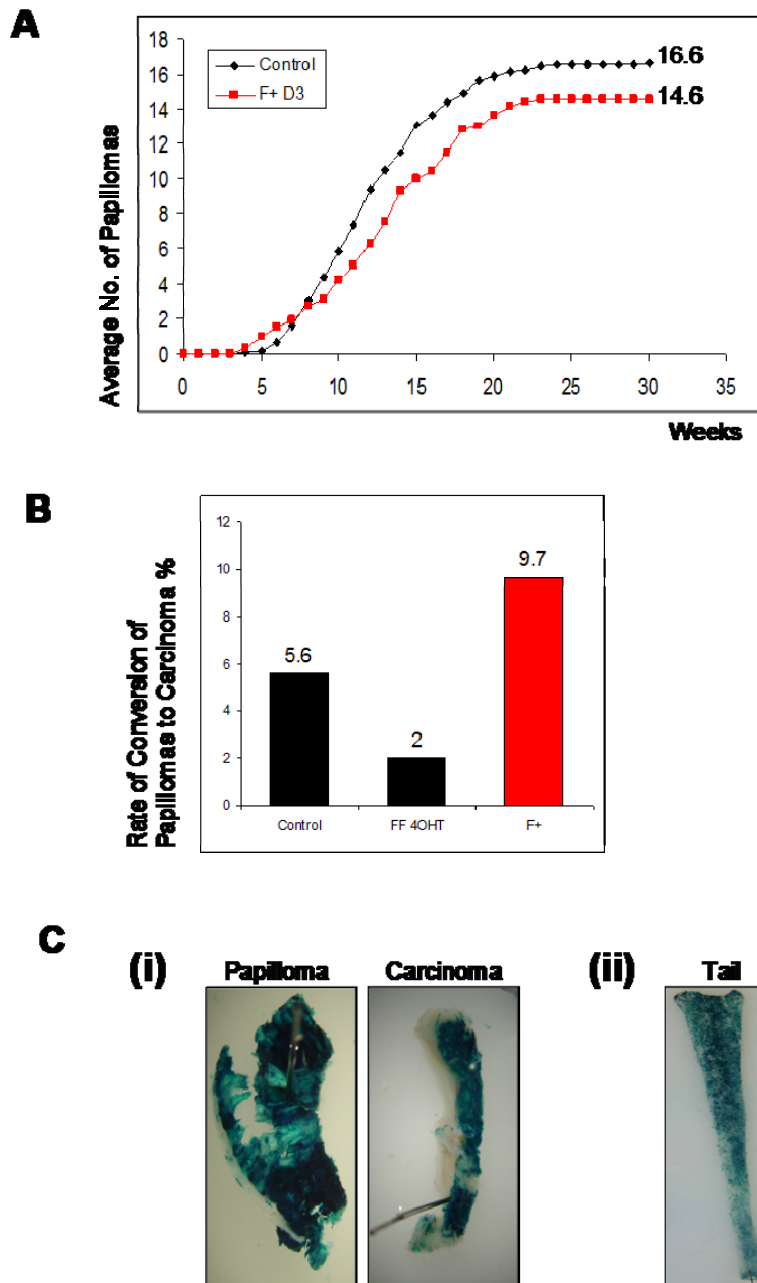


Figure 36 - The Effect of *Chk1* Hemizyosity on Tumour Formation

A DMBA/TPA chemical carcinogenesis was performed in *chk1 flox/+ // K14CreER^{T2} // LacZ* mice following IP 4OHT (D-5 to D-1) treatment, n=19. The control group consisted of *chk1 flox/flox // K14CreER^{T2} // LacZ*, n=19 (no 4OHT) and *chk1 +/+ // K14CreER^{T2} // LacZ*, n=20 (+ vehicle). After 30 weeks, there was no significant difference in average papilloma numbers between control and F/+ groups, 16.6 versus 14.6 respectively, Mann Whitney p=0.183. **B** The rate of conversion from papilloma to carcinoma was significantly higher in the *chk1 flox/+ // K14CreER^{T2} // LacZ* mice & IP 4OHT (D-5 to D-1) group compared to the control group, 9.7% versus 5.6% chi squared test p<0.025. Rate of conversion of *chk1 flox/+ // K14CreER^{T2} // LacZ* mice & IP 4OHT (D-5 to D-1) was significantly higher compared to *chk1 flox/flox // K14CreER^{T2} // LacZ*, (4OHT and DMBA at D3), 9.7% versus 2% chi squared test p<0.020. There was no statistically significant difference between control and *chk1 flox/flox // K14CreER^{T2} // LacZ*, (4OHT and DMBA at D3), 5.6% versus 2% chi squared test p>0.10. **C** β -galactosidase assay performed on (i) papillomas and carcinomas obtained from *chk1 flox/+ // K14CreER^{T2} // LacZ* mice & IP 4OHT (D-5 to D-1) produced a positive reaction. Similarly the (ii) tails taken at sacrifice from these animals also produced a positive β -galactosidase reaction.

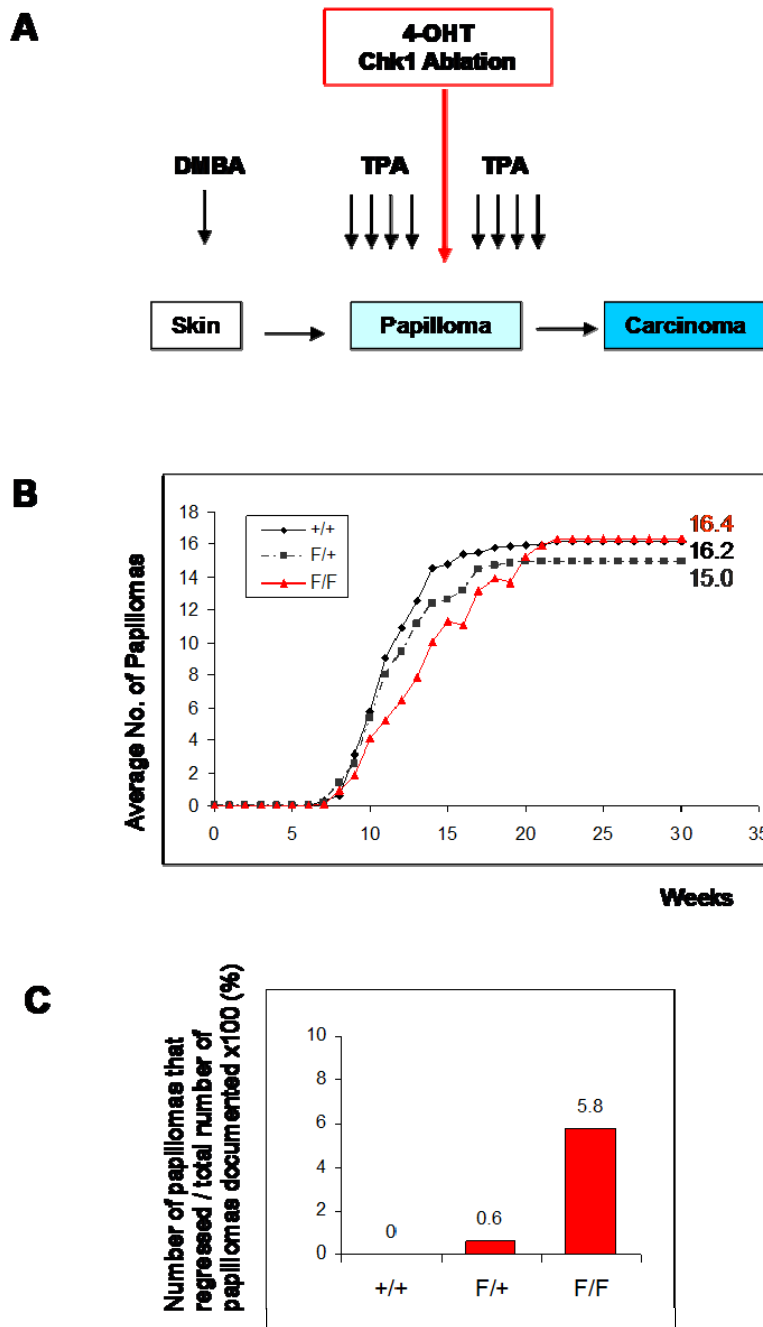


Figure 37 - The Effect of *Chk1* Ablation on Pre-Formed Papillomas

A To determine the effect of complete or hemizygous *chk1* ablation in tumours that have already formed, *chk1* flox/flox // *K14CreER^{T2}* // *LacZ* (n=21) and *chk1* flox/+ // *K14CreER^{T2}* // *LacZ* (n=22) mice were commenced on the DMBA/TPA carcinogenesis protocol. When the mice had achieved near maximal papillomas burden – usually between weeks 12 to 15, the mice were treated with IP 4OHT (D-5 to D-1) to induce genetic recombination. Control group was *chk1* +/+ // *K14CreER^{T2}* // *LacZ* (n=20) treated with 4OHT. **B** At 30 weeks, there was no significant difference between average number of papillomas between control and FF (+ 4OHT) group, 16.2 versus 16.4, Mann Whitney p=0.968. No significant difference between average number of papillomas between control and flox/+ (F+) + 4OHT group, 16.2 versus 15.0, Mann Whitney p=0.339. No significant difference between average number of papillomas between flox/flox (FF) + 4OHT and flox/+ (F+) + 4OHT group, 16.4 versus 15.0, Mann Whitney p=0.501. **C** In some animals *chk1* ablation resulted in the regression of smaller papillomas, diameter <2mm. In flox/flox (FF) + 4OHT, the rate of papilloma regression (no. papillomas that regressed / no. of papillomas that formed x100 %) was 5.8%, in flox/+ (F+) + 4OHT the rate was 0.6% and in control animals the rate was 0%. Regression was never observed in tumours greater than 2mm in diameter.

TPA. Similarly (Figure 1C, ii) tails taken at sacrifice from these animals also produced a positive β -Gal reaction. This indicates that hemizygous *chk1* ablation does not result in cell death and repopulation by unrecombined cells as was the case with *chk1* Δ/Δ .

7.1.2. *Chk1* Ablation in Formed Papillomas Resulted in Regression in Smaller Papillomas but did not Lead to an Overall Reduction in Tumour Burden

To test the effect of complete and hemizygous *chk1* ablation on papillomas that have already formed, *chk1*flox/flox // *K14CreER*^{T2} // *LacZ* (n=21) and *chk1* flox/+ // *K14CreER*^{T2} // *LacZ* (n=22) mice were commenced on the DMBA/TPA carcinogenesis protocol (see Figure 37A). Control group was *chk1*+/+ // *K14CreER*^{T2} // *LacZ* (n=20). When the mice had achieved near maximal papillomas burden - between weeks 12 to 15, the mice were treated with IP 4OHT (D-5 to D-1) to induce genetic recombination. At 30 weeks, there was no significant difference between average number of papillomas in control versus *chk1*flox/flox groups, 16.2 versus 16.4, Mann Whitney p=0.968 (Figure 37B). No significant difference was observed between average number of papillomas in control versus *chk* flox/+ groups, 16.2 versus 15.0, Mann Whitney p=0.339. No significant difference was observed between average number of papillomas in *chk1*flox/flox versus *chk1*flox/+ groups, 16.4 versus 15.0, Mann Whitney p=0.501.

It was noted however, that in some animals *chk1* ablation resulted in the regression of smaller papillomas with diameters <2mm (Figure 37C). In the *chk1*flox/flox group, the rate of papilloma regression [number of papillomas that regressed / number of papillomas that formed x100 (%)] was 5.8%, in the *chk1*flox/+ group the rate was 0.6% and in control animals the rate was 0%. Regression was never observed in tumours greater than 2mm in diameter in any group. These results suggest that *chk1* ablation may lead to regression of smaller tumours.

7.1.3. Generation of Murine Carcinoma Cell Lines from DMBA/TPA Induced Carcinomas

In order to establish a system to analyse the effects of *chk1* deletion in carcinoma cells, cell lines were generated (see Figure 38). DMBA/TPA induced carcinomas that developed in *chk1flox/flox // K14CreER^{T2} // LacZ* mice (where no 4OHT treatment was given) were cut into pieces and placed in culture flasks with medium. Outgrowth cells were isolated and passaged. PCR confirmed a *chk1flox/flox // K14CreER^{T2} // LacZ* genotype. *In vitro* when these cells were cultured in the presence of 4OHT over 5 days, subsequent western blotting for Chk1 showed substantial protein depletion (Joanne Smith, *personal communication*).

Cells were then implanted as allografts in nude mice to confirm tumourigenic capability *in vivo*. One cell line consisting of predominantly squamous carcinoma cell type was chosen (Identification number - 57468), and cells injected subcutaneously in nude mice at 1×10^6 and 2×10^6 cells / animal in 100uL medium. Successful tumour formation rates were 30% (6 out of 20) and 60% (12 out of 20) respectively. Carcinomas that formed were fixed and embedded in paraffin and analysis confirmed histological features consistent with an epithelial carcinoma.

Six mice which were injected with 2×10^6 cells / animal in 100uL medium and which had formed allograft tumours were treated with 5 days of IP 4OHT. Two mice were sacrificed the day after the final injection and β -Gal assay performed which showed positivity, confirming the ability to genetically inactivate *chk1* in transplanted carcinomas. The tumours in the other four mice were allowed to progress over 2 weeks and the mice were then sacrificed and tumour size measured. This was compared to four mice injected with 2×10^6 cells / animal in 100uL medium which formed allograft tumours but did not receive 4OHT treatment, also sacrificed after 2 weeks. The average longest tumour diameter in the 4OHT treated animals was 73mm (SD 33mm) and in the control group 95mm (SD 27mm), the difference not being statistically significant (Mann Whitney Test $p=0.16$).

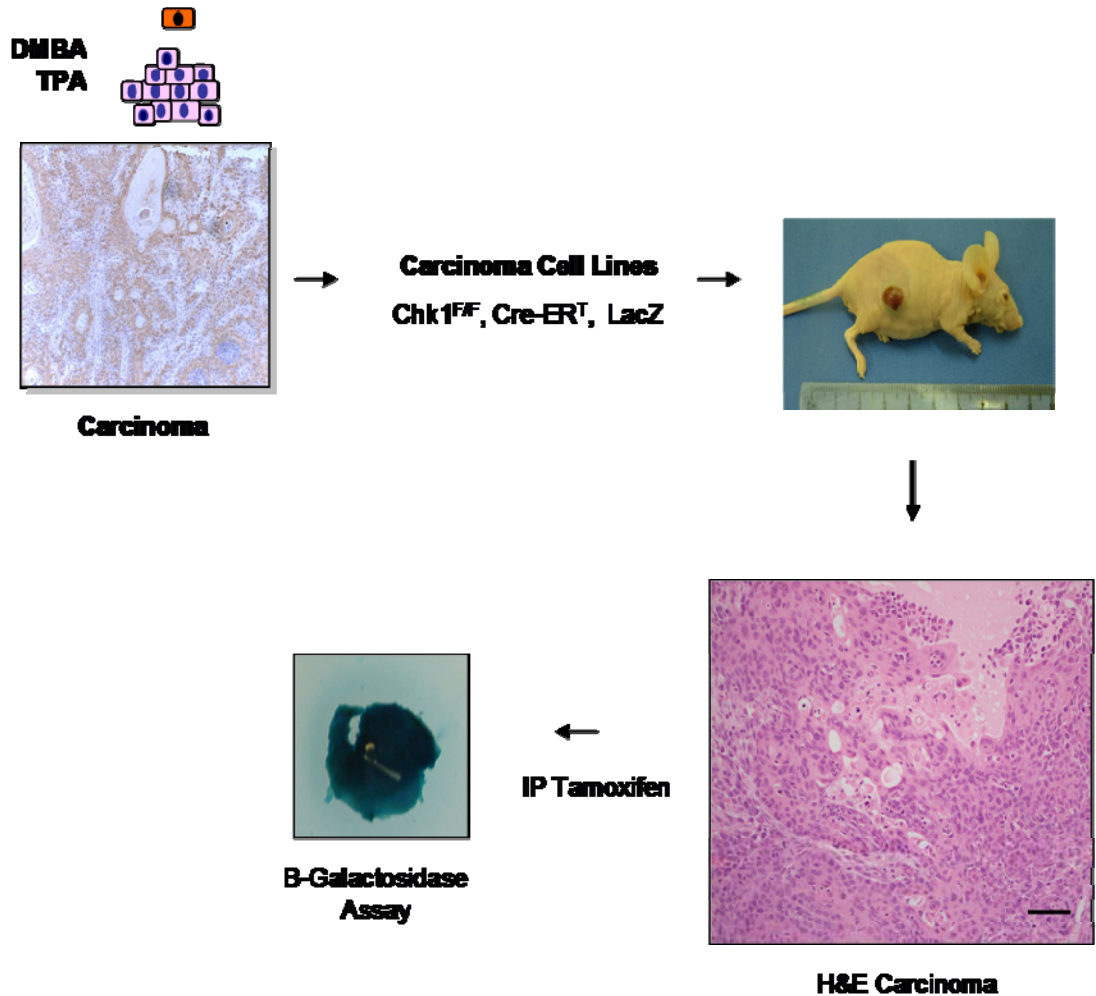


Figure 38 - Generation of Murine Cancer Cell Lines from DMBA/TPA Induced Carcinomas

Cell lines were generated from carcinomas that developed in *chk1 flox/flox // K14CreER^{T2} // LacZ* mice secondary to DMBA/TPA. When the mice were culled, carcinomas were cut into pieces and plated in culture flasks with medium. Outgrowth cells were isolated and passaged. PCR confirmed *chk1 flox/flox // K14CreER^{T2} // LacZ* genotype. *In vitro* when these cells were cultured in the presence of 4OHT over 5 days, subsequent western blotting for *chk1* showed significant protein knockdown (Joanne Smith, *personal communication*). To confirm that these carcinoma cells possessed tumourigenic capability *in vivo*, the cells were implanted as allografts in nude mice. Implanted carcinomas that formed were fixed and embedded in paraffin and analysis confirmed histological features consistent with an epithelial carcinoma. Mice bearing allograft carcinomas were also treated with 5 days of IP 4OHT and β -galactosidase assay performed which showed positivity, confirming the ability to genetically inactivate *chk1* in transplanted carcinomas. Scale bar represents 20 μ m.

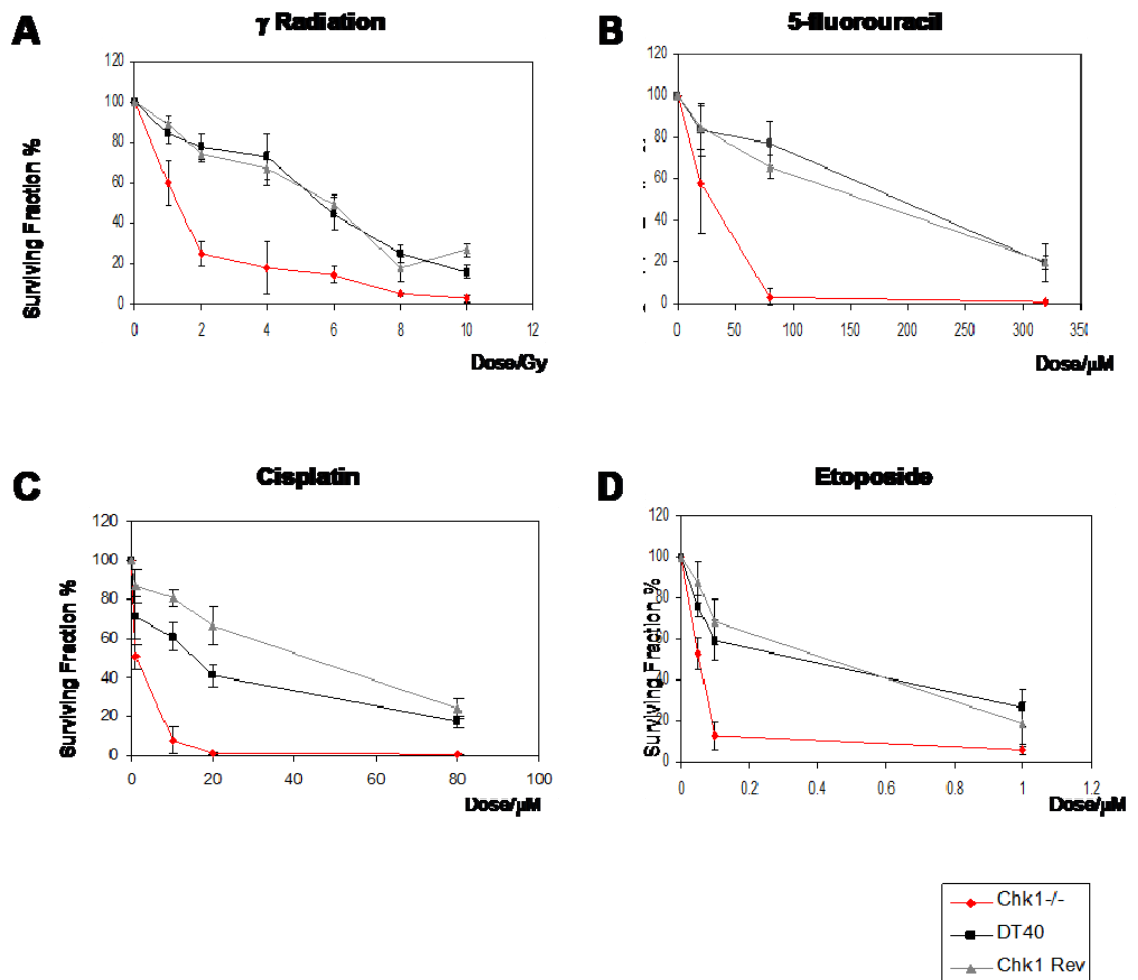


Figure 39 - Genotoxic Treatment and *Chk1* Knockout DT40 Lymphoma Cells

Four common agents used in oncology care were used to treat *chk1*^{-/-}, WT and *chk1* revertant DT40 avian lymphoma cells to determine if these could synergistically enhance tumour cell kill. These were γ -irradiation, cisplatin, 5-fluorouracil, and etoposide. Cells were cultured with cells for 12 hours, then washed free and clonogenic survival assays performed. Cells were exposed to γ -irradiation and then cultured. All agents reduced clonogenic survival in *chk1*^{-/-} cells to a much greater extent than in controls.

7.1.4. *Chk1* Loss Sensitizes Tumour Cells to the Cytotoxic Effects of Anti-Cancer Therapy in DT40 Lymphoma Cells

Four common agents used agents in oncology care were used to treat *chk1* *-/-*, *WT* and *chk1* revertant DT40 avian lymphoma cells. These cell lines were generated within our own laboratory (Zachos et al, 2003b). These were γ -irradiation, cisplatin, 5-fluorouracil, and etoposide (see Figure 39). Drugs were cultured with cells for 12 hours and washed away, and clonogenic survival assays performed. For the experiment involving irradiation, cultured cells were exposed to γ -irradiation and subjected to clonogenic survival assays. All agents reduced clonogenic survival in *chk1* *-/-* cells more severely than controls, thus confirming synergistic tumour kill (Robinson et al, 2006; Zachos et al, 2003b).

7.2. Discussion

In mice, constitutive *chk1* knockout is embryonic lethal (Liu et al, 2000b; Takai et al, 2000). Mice with hemizygous loss are able to age normally and no gross pathology is noted. However, when *chk1*^{+/-} mice were crossed onto a *WNT-1* transgenic background, mammary tumours appear to occur marginally earlier although at a similar incidence (Liu et al, 2000b). In one report, analysis of mammary tissue from *chk1*^{+/-} mice revealed evidence of cell cycle miscoordination with inappropriate cell cycle entry despite incompletely repaired or replicated DNA (Lam et al, 2004). Therefore, partial *chk1* loss was proposed to exert a haploinsufficient tumour suppressor effect putatively through disruption of normal cell cycle co-ordination. Nevertheless their findings were based on *in vitro* data and it has not been clarified whether *chk1* loss complete or hemizygous, promotes carcinogenesis (Liu et al, 2000a) or alternatively causes death of incipient cancer cells and acts as a barrier for cancer formation *in vivo* (Bartkova et al, 2005; Bartkova et al, 2006; Gorgoulis et al, 2005).

To assess the effect of *chk1* hemizyosity on skin tumour formation *in vivo*, DMBA/TPA chemical carcinogenesis and *chk1* recombination was performed in *chk1* flox/+ // *K14CreER*^{T2} // *LacZ* mice (see Figure 36). No significant difference in papilloma formation was observed but compared to controls, hemizyosity significantly increased the rate of conversion to carcinomas. β -Gal assays indicate that skin, papillomas and carcinomas retained the recombined allele in sacrificed animals, confirming the presence of long term hemizyosity during the stages of tumour initiation and progression. This is in contrast to previously described *chk1*flox/flox // *K14CreER*^{T2} // *LacZ* animals treated with tamoxifen where repopulation of the ablated tissue by unrecombined (wild type) cells occurred within 1-3 weeks. These findings appear to confirm *chk1* hemizyosity exerts a haploinsufficient tumour suppressor effect (Lam et al, 2004) however, only in carcinoma conversion but not in papilloma development. It is unclear however if the wild type allele is retained during DMBA/TPA carcinogenesis. Limited preliminary work using Chk1 protein antibody staining on paraffin embedded papillomas and carcinomas specimens suggest Chk1

expression is retained (data not shown), which suggests a functioning wild type allele, but further work is required to fully confirm this.

To test the effect of complete and hemizygous *chk1* ablation on papillomas that have already formed, *chk1flox/flox // K14CreER^{T2} // LacZ* and *chk1flox/+ // K14CreER^{T2} // LacZ* mice were commenced on the DMBA/TPA carcinogenesis protocol (see Figure 37). The control group was *chk1+/+ // K14CreER^{T2} // LacZ*. When the mice had achieved either maximal or near to maximal papilloma burden - between weeks 12 to 15, the mice were treated with IP 4OHT (D-5 to D-1) to induce *chk1* genetic recombination. *Chk1* ablation in pre-formed papillomas did not lead to a statistically significant overall reduction in papilloma numbers. It was noted however, that in some animals *chk1* ablation resulted in the regression of smaller papillomas with diameters <2mm (Figure 37C). In the *chk1flox/flox* group, the rate of papilloma regression was 5.8%, in the *chk1flox/+* group the rate was 0.6% and in control animals the rate was 0%. Regression was never observed in tumours greater than 2mm in diameter in any group. This is a very interesting result as it suggests *chk1* ablation may lead to tumour regression in small papillomas. Perhaps this is explained by the fact that smaller papillomas have less connective tissue component and do not have necrotic areas compared to larger tumours. This might allow the epithelial components to be better perfused by the vasculature. This would result in better delivery of 4OHT and an increased degree of recombination. Given previous results showing *chk1* ablation leads to apoptosis in somatic stem cells, tumour cell death could potentially explain the regression observed.

In the experiment described, 4OHT was administered when the majority of the papillomas were relatively advanced ie. at least >2mm diameter. However to study the effect of tumour regression in small or incipient papillomas, it would be necessary to repeat the experiment with 4OHT administered at an earlier stage of tumourigenesis for example at 6-8 weeks after TPA commencement, when the majority of papillomas would be <2mm in diameter. Another useful experimental approach would be to use topical 4OHT (Lo Celso et al, 2004; Murayama et al, 2007). This could potentially allow long term ablation beyond the 5 days of IP 4OHT, without encumbering significant systemic toxicity (for example aerodigestive epithelial toxicity as described in Chapter 3, Figure 11.

My results in Chapter 5 (see 5.1.3, 5.1.4 and 5.1.6) show an accumulation of DNA damage and apoptosis following *chk1* ablation within the hair follicle. Therefore, it is reasonable to hypothesize that papilloma regression might be caused by apoptosis following *chk1* ablation. In order to confirm this, I would propose a lineage tracing experiment to track the fate of *chk1* deleted cells. We have obtained mice expressing *RFP* where promoter is under *loxP-stop-loxP* control (see Figure 40) (Luche et al, 2007) and we are currently crossing these mice to our floxed *chk1* mice. The goal would be to produce mice in which genetic ablation of *chk1* can be assayed by RFP expression which is amenable to detection using confocal imaging, cell sorting and other techniques. This will allow analysis on a cell by cell basis of the tumour which may show heterogenous response depending on *chk1* status or other molecular determinants. This will be discussed further in Concluding Remarks (see 8.1) and Future Perspectives (see 8.2).

Chk1 inhibition has been proposed as a novel strategy for anti-cancer treatment (Zhou & Bartek, 2004) and Chk1 inhibitors are currently in development and are entering early phase clinical trials (Garber, 2005). Using our model it would have been a relevant experimental question to ablate *chk1* after carcinoma formation to determine the effect on carcinomas progression. However, in our mice, the window period between the first appearance of a carcinoma and when the animal needs to be culled for animal welfare reasons as stipulated in our Home Office Project License, is only between 1-2 weeks at most. This did not allow enough duration for a full course of IP 4OHT to be applied followed by a reasonable period of observation to record any objective responses, so these experiments were not conducted. In order to take advantage of a conditional knockout murine system to assess the effect of *chk1* ablation in murine carcinomas, I derived carcinoma cell lines from the DMBA/TPA carcinomas.

I established *in vitro* cell lines derived from DMBA/TPA induced carcinomas that had developed in *chk1*flox/flox // *K14CreER*^{T2} // *LacZ* mice (where no 4OHT treatment was given). When these cells were cultured in the presence of 4OHT over 5 days, subsequent western blotting for Chk1 showed substantial protein knockdown (Joanne Smith, Beatson Institute, *personal communication*). Cells were then implanted as allografts in nude mice to confirm tumourigenic capability *in vivo* and tumours demonstrated histological features consistent

with a malignant epithelial carcinoma. Mice bearing allograft carcinomas were also treated with 5 days of IP 4OHT and β -Gal assay performed which showed positivity, confirming the ability to genetically inactivate *chk1* in transplanted carcinomas. I observed that the size of tumours formed after 4OHT treatment after 2 weeks compared to non treated control were not statistically significantly different however, there was a trend towards larger tumours in the treated group. This is in keeping with the data demonstrated in Figure 36 where loss of Chk1 in the late stages of tumour growth appears to accelerate carcinogenesis. This has already been discussed in more detail earlier in this section. These mammalian cell lines generated could potentially be utilised for a variety of experimental purposes.

The Cre/LoxP system provides the option for temporal control over genetic ablation. In our laboratory we have previously generated a DT40 *chk1*^{-/-} vertebrate, avian lymphoma cell line which was engineered to possess a constitutive *chk1* knock out. Using this system it has been shown that *chk1* loss synergises tumour cells to cytotoxic kill using common anti-cancer agents including γ -irradiation (Zachos et al, 2003b) and 5-fluorouracil (Robinson et al, 2006). The potential for Chk1 inhibition as a novel cancer as well as the concept of synthetic lethality has been discussed in Chapter 1 (see 01.4.2.11.4.2.1). In the series of experiments using clonogenic survival assays I show synergistic elimination of tumour cells in cells deficient in Chk1 with γ -irradiation, 5-fluorouracil, cisplatin and etoposide (see Figure 4). The mammalian murine cell lines would be useful to confirm these findings and to determine the relative efficacy of different anticancer therapies in combination with *chk1* knockdown. As stated previously Chk1 inhibition is currently being explored as a potential anti-cancer strategy Currently it is uncertain as to which agents would synergise most effectively with *chk1* inhibitors.

Chapter 8. Summary Conclusion and Future Perspectives

8.1. Summary Conclusion

Chk1 knockout mice are embryonically lethal and this necessitated a conditional knockout approach in this project (Liu et al, 2000b). I utilised a Cre/LoxP regulated system whereby exon 2 of mouse *chk1*, which bears the translational initiation sequence as well as a region of the kinase domain, was flanked by *loxP* regions. Recombination was effected by activation of Cre-ER^{T2} (Indra et al, 1999) from tamoxifen administration. In this system to limit *chk1* deletion to specific tissues only, Cre-ER^{T2} was expressed under the control of a keratin-14 promoter (McLean et al, 2004) in primarily the epidermal skin as well as other squamous epithelia. Verification of genetic recombination was assisted by β -galactosidase assay performed for the conditional expression of a ROSA26 *LacZ* reporter gene

8.1.1. Summary of Chapter 3

In Chapter 3, I outline the breeding, maintenance and genotyping of these mice on an albino FVB background. As expected, no *chk1* homozygous knockout mice were born. Hemizygous knockout mice were phenotypically similar to *chk1* competent mice, without any demonstrable pathology. When *chk1*^{flox/flox} // *K14CreER*^{T2} // *LacZ* were induced with 4OHT, immunohistochemistry of the interfollicular epidermis and hair follicles and western blotting of skin extracts confirmed a significant reduction in Chk1 protein expression. PCR genotyping revealed the presence of the recombined allele and by β -galactosidase assay of fresh prepared tissue confirmed genetic recombination. When aged these mice did not display any gross pathology. A survey of Chk1 protein levels in different organs in wild type mice revealed variable Chk1 expression from very low expression in brain to higher expression in the skin and gut.

8.1.2. Summary of Chapter 4

In Chapter 4, I describe how I induced papillomas and carcinomas in the dorsal skin of mice using a chemical carcinogenesis protocol of DMBA (tumour initiator) followed by TPA (tumour promoter) application. In the *chk1*flox/flox // *K14CreER^{T2}* // *LacZ* + 4OHT group, rate of papilloma formation was significantly delayed compared to control. The average number of papillomas was significantly reduced as were their average sizes. There was a trend toward a reduction in the rate of conversion from papillomas to carcinomas but this was not statistically significant. Papillomas from ablated animals, as was the case with controls, all expressed Chk1 strongly. This means papillomas that arose in genetically ablated animals did so out of cells which escaped recombination. These results suggest that papilloma formation requires *chk1*.

8.1.3. Summary of Chapter 5

In Chapter 5, I describe studies looking at the effects of *chk1* ablation on adult skin, including especially consequences on the bulge label retaining cell (LRC) population (the putative stem cell population in the skin). Following *chk1* ablation, I observed initial proliferation of LRCs with a significant increase in numbers. Proliferation was confirmed using short term BrdU labelling. Additionally I observed an accumulation of DNA damage and apoptosis with p53 induction in the skin. Over the longer term, depletion of the LRC bulge population was observed. It became evident that the recombined or *chk1* floxed cells were being removed by apoptosis and being replaced by unrecombined cells over a period of 2-3 weeks in the skin. During this process no gross pathology is demonstrable in the normal skin and homeostasis is apparently maintained. It is unclear how LRC proliferation is triggered, and two possibilities have been proposed. The first is that the loss of *chk1* is occurring within LRCs which directly stimulates proliferation. It has been noted from array studies of skin stem cells that *WNT* pathway is repressed by expression of negative regulators (Tumbar et al, 2004) and that *WNT* signalling is intricately linked to hair follicle growth and morphogenesis (Castilho et al, 2009; Greco et al, 2009). *Chk1* has been upregulated in mammary stem cells (Behbod et al, 2006). Therefore Chk1 could be regulating proliferation of LRCs through a yet unknown mechanism. The

time line of proliferation followed by DNA damage and apoptosis observed would support the former. The second possibility is that cellular DNA damage and apoptosis in the skin may be signalling the LRC to proliferate. It is well known that in LRC respond to tissue damage by proliferating in order to renew the tissue and maintain homeostasis (Ito et al, 2005). In fact it has been proposed that the LRC bulge population represent a “reserve” of stem cells that is activated by tissue perturbation [reviewed by (Li & Clevers, 2010)]. In my opinion neither hypothesis can be ruled out at this stage, neither can the possibility that the two are occurring concurrently. Certainly modulation of LRC proliferation following *chk1* ablation would be a novel phenomenon and I go on to discuss possible experiments that might help elucidate this in Future Perspectives (see 8.2)

8.1.4. Summary of Chapter 6

In Chapter 6, I show that despite loss of LRC stained cells in the bulge following *chk1* ablation, the niche is repopulated by keratin-15 expressing cells. This suggests that despite a transient decrease in the number of bulge stem cells (which is supported by the fact that there is a reduction in tumour formation induced by DMBA/TPA), the niche is repopulated within 2-3 weeks. In further experiments, induction of tumours with DMBA/TPA was delayed following *chk1* ablation to allow the skin and stem cell niche to recover and be repopulated by unrecombined cells. This reversed the phenotype of papilloma suppression and the average number of tumours formed were similar to control. Again this provides further evidence that the mechanism for papilloma reduction could be attributed to stem cell depletion. However, I also show that the “number of targets” model may be insufficient to explain tumour suppression. I observed that *chk1* ablation also reduced the ability of skin to mount a hyperplastic response to tumour promotion by TPA. Hyperplasia is a key intermediary step required to allow the outgrowth of *h-Ras* transformed cells into papillomas. Additionally, when *chk1* ablation was performed after DMBA application on the skin, this reduced papilloma formation even further compared to *chk1* ablation before DMBA application. Thus it is possible that *chk1* ablation induces apoptosis to a greater degree in *h-ras* transformed stem cells as opposed to non-

transformed stem cells. Finally, although *chk1* ablation did not result in gross pathology in the skin, it delayed hair re-growth when the dorsal skin was shaved.

8.1.5. Summary of Chapter 7

In Chapter 7, I show that hemizygous *chk1* ablation did not reduce papilloma formation but increased the rate of conversion to carcinomas. This is in keeping with a previously suggested role for *chk1* in exerting a haploinsufficient tumour suppressor effect. However my data suggests that this role is only relevant in the latter stages of carcinoma development. In *chk1*flox/flox // *K14CreER*^{T2} // *LacZ* mice which had already formed papillomas, 4OHT administration resulted in regression of the smaller subset of papillomas but not those >2mm. The average number of papillomas was not significantly different compared to controls. This effect remains unexplained and further experiments to investigate this are discussed in Future Perspectives (see 8.2). I also describe the generation of murine carcinoma cell lines from *chk1*flox/flox // *K14CreER*^{T2} // *LacZ* mice and their ability to form tumours in allogenic nude mice assays. I also describe data showing synergistic tumour cell killing using a *chk1*^{-/-} DT40 avian lymphoma cell line with a variety of cytotoxic agents.

In summary in this thesis, I present my experimental findings using a novel conditional *chk1* knockout mouse model in the skin. Abrogation of *chk1*, a serine-threonine kinase that is activated after DNA damage, strongly reduced the formation of chemically induced skin tumours. Further investigation of the role of *chk1* on a tissue level suggests that this effect could be mediated via hair follicle stem cells, the sub-population from which tumours are thought to arise. I have observed that deletion of *chk1* causes cell proliferation, DNA damage, and apoptosis within the hair follicle, however the populations affected and the order of events in individual cells have yet to be clearly defined.

It has been proposed that the combination of existing conventional DNA damaging agents ie. chemotherapy and radiotherapy with G2 checkpoint inhibitors may provide a novel way to treat human cancers (see 1.4.2). This strategy is based on the observation that G1 checkpoint defects occur commonly

in the majority of all cancer types, and that these cancers become more reliant (compared to normal tissues) on G2 checkpoints particularly in responding to DNA damage - radiotherapy and chemotherapy. Therefore, combining a G2 checkpoint inhibitor with a DNA damaging agent could selectively kill tumor cells, but spare the normal cells, thus offering a clinically relevant therapeutic option with a wide therapeutic window. Chk1 kinase has a dominant role in regulating the G2 checkpoint. Therefore, not surprisingly, pharmaceutical Chk1 inhibitors are currently in development.

8.2. Future Perspectives

I have demonstrated that *chk1* ablation in mouse skin leads to proliferation of label retaining cells (LRCs) accompanied by an accumulation of DNA damage and apoptosis. However the populations affected and the order of events in individual cells have not been clearly defined. For example, it is not clear if *chk1* depletion is occurring within LRCs which triggers a limited number of rounds of cell division, leading to DNA misreplication, damage and subsequent apoptosis. Alternatively, LRCs are known to be a repository cells responsible for maintaining tissue homeostasis in the face of physiological perturbation (Ito et al, 2005). In that case, LRC proliferation may be a homeostatic response to tissue death occurring in non-stem cells following *chk1* ablation. The limitations of labeling cells with BrdU include the necessity of using an acid denaturation step to recover the nuclear epitopes (Braun et al, 2003). This reduces the accuracy of further antibody staining which is necessary to allow co-localization with proliferation, DNA damage and apoptotic markers to trace events on a cell to cell basis. Therefore we are trialing the use of EdU (5-ethynyl-2'deoxyuridine) (Cappella et al, 2008) as an alternative thymidine analogue to BrdU which does not require acid denaturation but whose identification relies on an azide-ethynyl copper catalysed reaction. Although the use of EdU has been reported in the *in vivo* setting (Zeng et al, 2010), its use for long term labeling is not reported and it is not known if “housekeeping” DNA repair mechanisms will remove EdU over time which would limit its usefulness. If successful however, this technique should allow us to co-localize LRCs and correlate their location with cellular proliferation, DNA damage and apoptosis on a cell by cell basis following *chk1* ablation.

In order to assay gene recombination, 2 methods have been employed in this project, direct antibody staining and *LacZ* reporter gene detection using B-galactosidase reaction. Protein quantification may have its limitations. *Chk1* is not expressed uniformly in all cell types (see Chapter 3). Even within the same tissue, there can be wide variability. In the skin, a higher expression is expected in actively proliferating cells (for example during anagen) but low expression in slowly or non-proliferating cells (for example in telogen). This may lead to a failure to identify recombined cells which are not expressing a detectable level

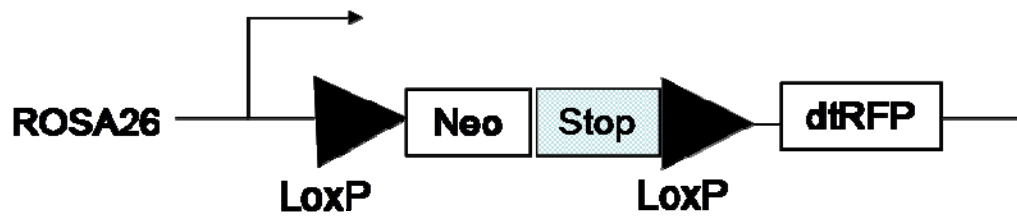


Figure 40 - *In vivo* RFP Reporter System

A conditionally activated ROSA26 *loxP-stop-loxP RFP* reporter mouse has been obtained and is being crossed with the conditional *chk1* knockout strain in order to produce a *chk1* flox/flox // *K14CreER^{T2}* // *loxP-stop-loxP RFP* mouse. This will allow traceability of *chk1* recombined cells using confocal microscopy and *in vivo* imaging in future experiments

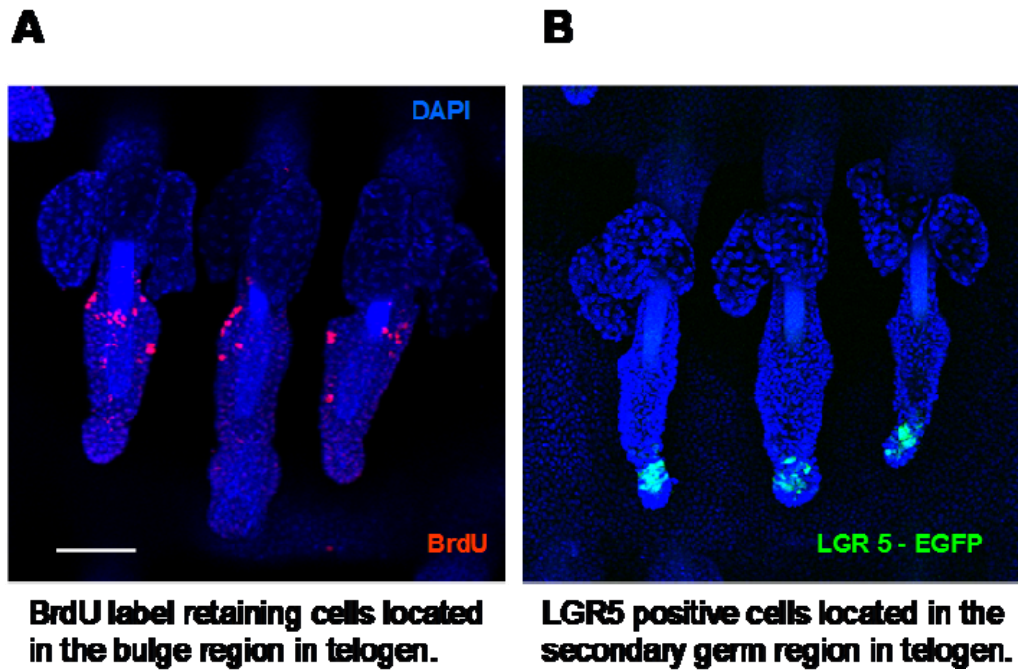


Figure 41 - LGR5 Stem Cells

Confocal microscopy of tail wholemounts showing (i) label retaining cells (LRC) marked by long term BrdU retention. These are typically found in the bulge region during hair telogen. (ii) LGR5 positive stem cells, which express enhanced green fluorescent protein (EGFP) under the control of the *Lgr5* promoter, identify cells in the secondary germ region in hair telogen. Scale bar represents 40 μ m.

of protein due to the hair cycle phase they are in. A β -galactosidase reaction allows for a more direct method to identify genetic recombination but requires the tissue fixed in a different way compared to that for immunohistochemistry (see Methods 2.5) which hampers the subsequent use of this material for additional antibody staining. Therefore to overcome these limitations I have obtained a conditionally activated ROSA26 *loxP-stop-loxP RFP* reporter mouse which I am in the process of crossing with our own *chk1*flox/flox strain to produce a *chk1*flox/flox // *K14CreER^{T2}* // *loxP-stop-loxP RFP* mouse. The RFP construct consists of a tandem-dimer (Luche et al, 2007) where 2 modified DsRed subunits are covalently fused (see Figure 40). The construct also contains a floxed transcriptional “stop” element and targeted into the ROSA26 locus via homologous recombination. This reporter strain has been shown not to undergo spontaneous recombination after monitoring in a variety of tissues. When ubiquitously activated in embryogenesis, no developmental effects were observed. There was reliable detection in fixed tissue and wholemount tissue and compatibility with co-GFP expressing cells. My results in Chapter 5 (see 5.1.3 and 5.1.4) show an accumulation of DNA damage and apoptosis following *chk1* ablation within the hair follicle. Therefore, it is reasonable to hypothesize that following 4OHT application and *chk1* ablation, tumour regression in a subset of papillomas could be caused by apoptosis (see Chapter 7). In order to confirm this, I propose a lineage tracing experiment to track the fate of *chk1* deleted cells using the *loxP-stop-loxP RFP* mice (Luche et al, 2007). The aim would be to allow genetic ablation of *chk1* to be assayed by RFP expression which is amenable to detection using confocal imaging, cell sorting and other techniques. These animals can also be subjected to DMBA/TPA tumourigenesis. In the papillomas that form, 4OHT administration will cause concurrent *chk1* ablation and RFP expression in the same cells. This could potentially allow analysis on a cell by cell basis of the live (*in vivo*) tumour which is not possible using *LacZ* staining - as described by Morton et al (Morton et al, 2010). This could also provide information as to the role of wild type cell recombination in tumours following *chk1* ablation as is seen in normal skin.

Stem cells are conventionally thought to represent only a small minority of skin cells and have been shown to reside in the bulge region of the hair follicle. They have been identified using BrdU label retention (LRCs) and have been shown to

possess multipotency, longevity and quiescence under normal homeostatic conditions (see Figure 41A). More recently, a separate and distinct cell population marked by leucine-rich G protein-coupled Receptor 5 expression (LGR5+ve) has been identified and has been shown to also possess stem cells like properties - in the gut (Barker et al, 2007) and the skin (Jaks et al, 2008) (Figure 41B). In the skin, LGR5+ve stem cells have been found primarily in the region between the lower bulge and dermal papilla. LGR5+ve cells displayed enhanced clonogenicity in *in vitro* and *in vivo* assays. In nude mice transplantation assays, LGR5+ve cells were able to reconstitute all major hair follicle components. Strikingly, rather than being quiescent, they seem to be actively dividing and participate in reconstituting hair follicles in lineage tracing experiments. This is a completely novel finding and challenges our conventional understanding of stem cells.

In skin stem cells, WNT has been shown to be a major regulator of hair follicle morphogenesis, renewal and anagen promotion (Castilho et al, 2009; DasGupta & Fuchs, 1999; Gat et al, 1998; Greco et al, 2009; Nguyen et al, 2006). Studies however, show that there is active WNT signalling inhibition in the bulge region. Microarray analysis of skin LRCs demonstrate upregulated mRNA expression of factors involved in inhibition of the WNT signalling cascade (Ohyama et al, 2006; Tumber et al, 2004) In contrast to the bulge, the dermal papillae region which regulates development of the epidermal follicle, has been shown to have high levels of WNT signalling (Kishimoto et al, 2000; Shimizu & Morgan, 2004). In addition, there is active secretion of noggin, a Bone Morphogenic Protein antagonist (Botchkarev et al, 2001) - BMP a negative regulator of WNT signalling. The dermal papillae happens to be the tissue region where LGR5+ve cells reside (Jaks et al, 2008). Therefore the two populations clearly occupy a different tissue niche which is regulated quite differently.

It has now been proposed that there exists two distinct stem cell populations within the skin, a quiescent LRC population and an actively dividing LGR5+ve population [reviewed by (Li & Clevers, 2010)]. Each appears to have a defined niche and interestingly apparently different roles in homeostasis. The LGR5+ve expressing population actively divides to renew constant cell turnover whereas the quiescent population appears to function as a “reserve” in case of tissue perturbation (Ito et al, 2005). It is less clear however how these two cell

population interact, whether the cell populations are interchangeable and how they ultimately affect carcinogenesis. Furthermore, it is not known what the role of *chk1* and checkpoint mechanisms play in this newly discovered but important LGR5+ve population, in particular in the interplay with carcinogenesis. To investigate this, we have obtained *Lgr5-EGFP-Ires-CreER^{T2}* (Jaks et al, 2008) where the endogenous *Lgr5* promoter controls expression of enhanced green fluorescent protein (EGFP) and the CreER^{T2} fusion protein. By crossing these mice to our *chk1*flox/flox mice we will be able to selective knockout *chk1* in LGR5+ve cells in the skin and trace their fate *in vivo* and *in vitro* following cell isolation procedures. Furthermore, the role of *Lgr5* in carcinogenesis is unknown for example, it is not known if these stem cells can give rise to tumours (Rosen & Jordan, 2009). It will be possible to chemically induce DMBA/TPA tumours in these mice and trace the fate of LGR5+ve cells to address this question.

List of References

- Abbas T, Dutta A (2009) p21 in cancer: intricate networks and multiple activities. *Nat Rev Cancer* 9(6): 400-414
- Agliano A, Martin-Padura I, Mancuso P, Marighetti P, Rabascio C, Pruneri G, Shultz LD, Bertolini F (2008) Human acute leukemia cells injected in NOD/LtSz-scid/IL-2Rgamma null mice generate a faster and more efficient disease compared to other NOD/scid-related strains. *Int J Cancer* 123(9): 2222-2227
- Ahn J, Prives C (2002) Checkpoint kinase 2 (Chk2) monomers or dimers phosphorylate Cdc25C after DNA damage regardless of threonine 68 phosphorylation. *J Biol Chem* 277(50): 48418-48426
- Ahn JY, Schwarz JK, Piwnica-Worms H, Canman CE (2000) Threonine 68 phosphorylation by ataxia telangiectasia mutated is required for efficient activation of Chk2 in response to ionizing radiation. *Cancer Res* 60(21): 5934-5936
- Al-Hajj M, Wicha MS, Benito-Hernandez A, Morrison SJ, Clarke MF (2003) Prospective identification of tumorigenic breast cancer cells. *Proc Natl Acad Sci U S A* 100(7): 3983-3988
- Alison MR, Lim SM, Nicholson LJ (2010) Cancer stem cells: problems for therapy? *J Pathol*
- Archambault V, Glover DM (2009) Polo-like kinases: conservation and divergence in their functions and regulation. *Nat Rev Mol Cell Biol* 10(4): 265-275
- Aressy B, Ducommun B (2008) Cell cycle control by the CDC25 phosphatases. *Anticancer Agents Med Chem* 8(8): 818-824
- Argyris TS, Slaga TJ (1981) Promotion of carcinomas by repeated abrasion in initiated skin of mice. *Cancer Res* 41(12 Pt 1): 5193-5195
- Arin MJ, Longley MA, Wang XJ, Roop DR (2001) Focal activation of a mutant allele defines the role of stem cells in mosaic skin disorders. *J Cell Biol* 152(3): 645-649
- Audeh MW, Carmichael J, Penson RT, Friedlander M, Powell B, Bell-McGuinn KM, Scott C, Weitzel JN, Oaknin A, Loman N, Lu K, Schmutzler RK, Matulonis U, Wickens M, Tutt A (2010) Oral poly(ADP-ribose) polymerase inhibitor olaparib in patients with BRCA1 or BRCA2 mutations and recurrent ovarian cancer: a proof-of-concept trial. *Lancet* 376(9737): 245-251
- Bahassi EM, Ovesen JL, Riesenberger AL, Bernstein WZ, Hasty PE, Stambrook PJ (2008) The checkpoint kinases Chk1 and Chk2 regulate the functional

associations between hBRCA2 and Rad51 in response to DNA damage. *Oncogene* 27(28): 3977-3985

Bailleul B, Surani MA, White S, Barton SC, Brown K, Blessing M, Jorcano J, Balmain A (1990) Skin hyperkeratosis and papilloma formation in transgenic mice expressing a ras oncogene from a suprabasal keratin promoter. *Cell* 62(4): 697-708

Bakkenist CJ, Kastan MB (2003) DNA damage activates ATM through intermolecular autophosphorylation and dimer dissociation. *Nature* 421(6922): 499-506

Balmain A, Ramsden M, Bowden GT, Smith J (1984) Activation of the mouse cellular Harvey-ras gene in chemically induced benign skin papillomas. *Nature* 307(5952): 658-660

Bao S, Wu Q, McLendon RE, Hao Y, Shi Q, Hjelmeland AB, Dewhirst MW, Bigner DD, Rich JN (2006) Glioma stem cells promote radioresistance by preferential activation of the DNA damage response. *Nature* 444(7120): 756-760

Barker N, van Es JH, Kuipers J, Kujala P, van den Born M, Cozijnsen M, Haegebarth A, Korving J, Begthel H, Peters PJ, Clevers H (2007) Identification of stem cells in small intestine and colon by marker gene Lgr5. *Nature* 449(7165): 1003-1007

Bartek J, Lukas C, Lukas J (2004) Checking on DNA damage in S phase. *Nat Rev Mol Cell Biol* 5(10): 792-804

Bartkova J, Horejsi Z, Koed K, Kramer A, Tort F, Zieger K, Guldborg P, Sehested M, Nesland JM, Lukas C, Orntoft T, Lukas J, Bartek J (2005) DNA damage response as a candidate anti-cancer barrier in early human tumorigenesis. *Nature* 434(7035): 864-870

Bartkova J, Rezaei N, Liontos M, Karakaidos P, Kletsas D, Issaeva N, Vassiliou LV, Kolettas E, Niforou K, Zoumpourlis VC, Takaoka M, Nakagawa H, Tort F, Fugger K, Johansson F, Sehested M, Andersen CL, Dyrskjot L, Orntoft T, Lukas J, Kittas C, Helleday T, Halazonetis TD, Bartek J, Gorgoulis VG (2006) Oncogene-induced senescence is part of the tumorigenesis barrier imposed by DNA damage checkpoints. *Nature* 444(7119): 633-637

Baumann M, Krause M, Hill R (2008) Exploring the role of cancer stem cells in radioresistance. *Nat Rev Cancer* 8(7): 545-554

Behbod F, Xian W, Shaw CA, Hilsenbeck SG, Tsimelzon A, Rosen JM (2006) Transcriptional profiling of mammary gland side population cells. *Stem Cells* 24(4): 1065-1074

Beranek DT (1990) Distribution of methyl and ethyl adducts following alkylation with monofunctional alkylating agents. *Mutat Res* 231(1): 11-30

Berenblum I, Shubik P (1949) The persistence of latent tumour cells induced in the mouse's skin by a single application of 9:10-dimethyl-1:2-benzanthracene. *Br J Cancer* 3(3): 384-386

- Bertoni F, Codegani AM, Furlan D, Tibiletti MG, Capella C, Broggin M (1999) CHK1 frameshift mutations in genetically unstable colorectal and endometrial cancers. *Genes Chromosomes Cancer* 26(2): 176-180
- Bianchi AB, Aldaz CM, Conti CJ (1990) Nonrandom duplication of the chromosome bearing a mutated Ha-ras-1 allele in mouse skin tumors. *Proc Natl Acad Sci U S A* 87(17): 6902-6906
- Bickenbach JR (1981) Identification and behavior of label-retaining cells in oral mucosa and skin. *J Dent Res* 60 Spec No C: 1611-1620
- Bickenbach JR, Chism E (1998) Selection and extended growth of murine epidermal stem cells in culture. *Exp Cell Res* 244(1): 184-195
- Blanpain C, Lowry WE, Geoghegan A, Polak L, Fuchs E (2004) Self-renewal, multipotency, and the existence of two cell populations within an epithelial stem cell niche. *Cell* 118(5): 635-648
- Blasina A, de Weyer IV, Laus MC, Luyten WH, Parker AE, McGowan CH (1999) A human homologue of the checkpoint kinase Cds1 directly inhibits Cdc25 phosphatase. *Curr Biol* 9(1): 1-10
- Bomken S, Fiser K, Heidenreich O, Vormoor J (2010) Understanding the cancer stem cell. *Br J Cancer* 103(4): 439-445
- Botchkarev VA, Botchkareva NV, Nakamura M, Huber O, Funa K, Lauster R, Paus R, Gilchrist BA (2001) Noggin is required for induction of the hair follicle growth phase in postnatal skin. *FASEB J* 15(12): 2205-2214
- Boutros R, Lobjois V, Ducommun B (2007) CDC25 phosphatases in cancer cells: key players? Good targets? *Nat Rev Cancer* 7(7): 495-507
- Boutwell RK, Verma AK, Ashendel CL, Astrup E (1982) Mouse skin: a useful model system for studying the mechanism of chemical carcinogenesis. *Carcinog Compr Surv* 7: 1-12
- Braig M, Lee S, Loddenkemper C, Rudolph C, Peters AH, Schlegelberger B, Stein H, Dorken B, Jenuwein T, Schmitt CA (2005) Oncogene-induced senescence as an initial barrier in lymphoma development. *Nature* 436(7051): 660-665
- Braun KM, Niemann C, Jensen UB, Sundberg JP, Silva-Vargas V, Watt FM (2003) Manipulation of stem cell proliferation and lineage commitment: visualisation of label-retaining cells in whole mounts of mouse epidermis. *Development* 130(21): 5241-5255
- Braun KM, Watt FM (2004) Epidermal label-retaining cells: background and recent applications. *J Invest Dermatol Symp Proc* 9(3): 196-201
- Brown EJ, Baltimore D (2000) ATR disruption leads to chromosomal fragmentation and early embryonic lethality. *Genes Dev* 14(4): 397-402

- Brown K, Strathdee D, Bryson S, Lambie W, Balmain A (1998) The malignant capacity of skin tumours induced by expression of a mutant H-ras transgene depends on the cell type targeted. *Curr Biol* 8(9): 516-524
- Bunting SF, Callen E, Wong N, Chen HT, Polato F, Gunn A, Bothmer A, Feldhahn N, Fernandez-Capetillo O, Cao L, Xu X, Deng CX, Finkel T, Nussenzweig M, Stark JM, Nussenzweig A (2010) 53BP1 inhibits homologous recombination in Brca1-deficient cells by blocking resection of DNA breaks. *Cell* 141(2): 243-254
- Burma S, Chen BP, Murphy M, Kurimasa A, Chen DJ (2001) ATM phosphorylates histone H2AX in response to DNA double-strand breaks. *J Biol Chem* 276(45): 42462-42467
- Burns PA, Kemp CJ, Gannon JV, Lane DP, Bremner R, Balmain A (1991) Loss of heterozygosity and mutational alterations of the p53 gene in skin tumours of interspecific hybrid mice. *Oncogene* 6(12): 2363-2369
- Byun TS, Pacek M, Yee MC, Walter JC, Cimprich KA (2005) Functional uncoupling of MCM helicase and DNA polymerase activities activates the ATR-dependent checkpoint. *Genes Dev* 19(9): 1040-1052
- Cai Z, Chehab NH, Pavletich NP (2009) Structure and activation mechanism of the CHK2 DNA damage checkpoint kinase. *Mol Cell* 35(6): 818-829
- Caldecott KW, Aoufouchi S, Johnson P, Shall S (1996) XRCC1 polypeptide interacts with DNA polymerase beta and possibly poly (ADP-ribose) polymerase, and DNA ligase III is a novel molecular 'nick-sensor' in vitro. *Nucleic Acids Res* 24(22): 4387-4394
- Cangi MG, Cukor B, Soung P, Signoretti S, Moreira G, Jr., Ranashinge M, Cady B, Pagano M, Loda M (2000) Role of the Cdc25A phosphatase in human breast cancer. *J Clin Invest* 106(6): 753-761
- Cappella P, Gasparri F, Pulici M, Moll J (2008) A novel method based on click chemistry, which overcomes limitations of cell cycle analysis by classical determination of BrdU incorporation, allowing multiplex antibody staining. *Cytometry A* 73(7): 626-636
- Cappelli E, Taylor R, Cevasco M, Abbondandolo A, Caldecott K, Frosina G (1997) Involvement of XRCC1 and DNA ligase III gene products in DNA base excision repair. *J Biol Chem* 272(38): 23970-23975
- Carr AM (2002) Checking that replication breakdown is not terminal. *Science* 297(5581): 557-558
- Castilho RM, Squarize CH, Chodosh LA, Williams BO, Gutkind JS (2009) mTOR mediates Wnt-induced epidermal stem cell exhaustion and aging. *Cell Stem Cell* 5(3): 279-289
- Chakravarti D, Ibeanu GC, Tano K, Mitra S (1991) Cloning and expression in Escherichia coli of a human cDNA encoding the DNA repair protein N-methylpurine-DNA glycosylase. *J Biol Chem* 266(24): 15710-15715

- Chalmers AJ, Lakshman M, Chan N, Bristow RG (2010) Poly(ADP-ribose) polymerase inhibition as a model for synthetic lethality in developing radiation oncology targets. *Semin Radiat Oncol* 20(4): 274-281
- Chehab NH, Malikzay A, Appel M, Halazonetis TD (2000) Chk2/hCds1 functions as a DNA damage checkpoint in G(1) by stabilizing p53. *Genes Dev* 14(3): 278-288
- Chen J (2004) Senescence and functional failure in hematopoietic stem cells. *Exp Hematol* 32(11): 1025-1032
- Chong JP, Mahbubani HM, Khoo CY, Blow JJ (1995) Purification of an MCM-containing complex as a component of the DNA replication licensing system. *Nature* 375(6530): 418-421
- Ciccia A, Elledge SJ (2010) The DNA damage response: making it safe to play with knives. *Mol Cell* 40(2): 179-204
- Cimprich KA, Cortez D (2008) ATR: an essential regulator of genome integrity. *Nat Rev Mol Cell Biol* 9(8): 616-627
- Clarke MF, Dick JE, Dirks PB, Eaves CJ, Jamieson CH, Jones DL, Visvader J, Weissman IL, Wahl GM (2006) Cancer stem cells--perspectives on current status and future directions: AACR Workshop on cancer stem cells. *Cancer Res* 66(19): 9339-9344
- Clayton E, Doupe DP, Klein AM, Winton DJ, Simons BD, Jones PH (2007) A single type of progenitor cell maintains normal epidermis. *Nature* 446(7132): 185-189
- Coin F, Oksenysh V, Egly JM (2007) Distinct roles for the XPB/p52 and XPD/p44 subcomplexes of TFIIH in damaged DNA opening during nucleotide excision repair. *Mol Cell* 26(2): 245-256
- Collado M, Gil J, Efeyan A, Guerra C, Schuhmacher AJ, Barradas M, Benguria A, Zaballos A, Flores JM, Barbacid M, Beach D, Serrano M (2005) Tumour biology: senescence in premalignant tumours. *Nature* 436(7051): 642
- Cortez D, Wang Y, Qin J, Elledge SJ (1999) Requirement of ATM-dependent phosphorylation of brca1 in the DNA damage response to double-strand breaks. *Science* 286(5442): 1162-1166
- Cotsarelis G, Sun TT, Lavker RM (1990) Label-retaining cells reside in the bulge area of pilosebaceous unit: implications for follicular stem cells, hair cycle, and skin carcinogenesis. *Cell* 61(7): 1329-1337
- Coulombe PA, Kopan R, Fuchs E (1989) Expression of keratin K14 in the epidermis and hair follicle: insights into complex programs of differentiation. *J Cell Biol* 109(5): 2295-2312
- Cox MM, Goodman MF, Kreuzer KN, Sherratt DJ, Sandler SJ, Marians KJ (2000) The importance of repairing stalled replication forks. *Nature* 404(6773): 37-41
- Critchlow SE, Bowater RP, Jackson SP (1997) Mammalian DNA double-strand break repair protein XRCC4 interacts with DNA ligase IV. *Curr Biol* 7(8): 588-598

- Crittenden SL, Leonhard KA, Byrd DT, Kimble J (2006) Cellular analyses of the mitotic region in the *Caenorhabditis elegans* adult germ line. *Mol Biol Cell* 17(7): 3051-3061
- Dai Y, Grant S (2010) New insights into checkpoint kinase 1 in the DNA damage response signaling network. *Clin Cancer Res* 16(2): 376-383
- Daley JM, Laan RL, Suresh A, Wilson TE (2005) DNA joint dependence of pol X family polymerase action in nonhomologous end joining. *J Biol Chem* 280(32): 29030-29037
- Dantzer F, de La Rubia G, Menissier-De Murcia J, Hostomsky Z, de Murcia G, Schreiber V (2000) Base excision repair is impaired in mammalian cells lacking Poly(ADP-ribose) polymerase-1. *Biochemistry* 39(25): 7559-7569
- DasGupta R, Fuchs E (1999) Multiple roles for activated LEF/TCF transcription complexes during hair follicle development and differentiation. *Development* 126(20): 4557-4568
- Delacroix S, Wagner JM, Kobayashi M, Yamamoto K, Karnitz LM (2007) The Rad9-Hus1-Rad1 (9-1-1) clamp activates checkpoint signaling via TopBP1. *Genes Dev* 21(12): 1472-1477
- Di Micco R, Fumagalli M, Cicalese A, Piccinin S, Gasparini P, Luise C, Schurra C, Garre M, Nuciforo PG, Bensimon A, Maestro R, Pelicci PG, d'Adda di Fagagna F (2006) Oncogene-induced senescence is a DNA damage response triggered by DNA hyper-replication. *Nature* 444(7119): 638-642
- Dimitrova DS, Gilbert DM (1999) The spatial position and replication timing of chromosomal domains are both established in early G1 phase. *Mol Cell* 4(6): 983-993
- DiTullio RA, Jr., Mochan TA, Venere M, Bartkova J, Sehested M, Bartek J, Halazonetis TD (2002) 53BP1 functions in an ATM-dependent checkpoint pathway that is constitutively activated in human cancer. *Nat Cell Biol* 4(12): 998-1002
- Dobzhansky T (1946) Genetics of Natural Populations. Xiii. Recombination and Variability in Populations of *Drosophila Pseudoobscura*. *Genetics* 31(3): 269-290
- Doyle LA, Ross DD (2003) Multidrug resistance mediated by the breast cancer resistance protein BCRP (ABCG2). *Oncogene* 22(47): 7340-7358
- Dyson N (1998) The regulation of E2F by pRB-family proteins. *Genes Dev* 12(15): 2245-2262
- Edelman MJ, Bauer KS, Jr., Wu S, Smith R, Bisacia S, Dancey J (2007) Phase I and pharmacokinetic study of 7-hydroxystaurosporine and carboplatin in advanced solid tumors. *Clin Cancer Res* 13(9): 2667-2674
- Eisch AJ, Mandyam CD (2007) Adult neurogenesis: can analysis of cell cycle proteins move us "Beyond BrdU"? *Curr Pharm Biotechnol* 8(3): 147-165

Eramo A, Lotti F, Sette G, Pillozzi E, Biffoni M, Di Virgilio A, Conticello C, Ruco L, Peschle C, De Maria R (2008) Identification and expansion of the tumorigenic lung cancer stem cell population. *Cell Death Differ* 15(3): 504-514

Espada J, Calvo MB, Diaz-Prado S, Medina V (2009) Wnt signalling and cancer stem cells. *Clin Transl Oncol* 11(7): 411-427

Falck J, Mailand N, Syljuasen RG, Bartek J, Lukas J (2001) The ATM-Chk2-Cdc25A checkpoint pathway guards against radioresistant DNA synthesis. *Nature* 410(6830): 842-847

Farmer H, McCabe N, Lord CJ, Tutt AN, Johnson DA, Richardson TB, Santarosa M, Dillon KJ, Hickson I, Knights C, Martin NM, Jackson SP, Smith GC, Ashworth A (2005) Targeting the DNA repair defect in BRCA mutant cells as a therapeutic strategy. *Nature* 434(7035): 917-921

Ferbeyre G (2007) Barriers to Ras transformation. *Nat Cell Biol* 9(5): 483-485

Feuring-Buske M, Gerhard B, Cashman J, Humphries RK, Eaves CJ, Hogge DE (2003) Improved engraftment of human acute myeloid leukemia progenitor cells in beta 2-microglobulin-deficient NOD/SCID mice and in NOD/SCID mice transgenic for human growth factors. *Leukemia* 17(4): 760-763

Fong PC, Boss DS, Yap TA, Tutt A, Wu P, Mergui-Roelvink M, Mortimer P, Swaisland H, Lau A, O'Connor MJ, Ashworth A, Carmichael J, Kaye SB, Schellens JH, de Bono JS (2009) Inhibition of poly(ADP-ribose) polymerase in tumors from BRCA mutation carriers. *N Engl J Med* 361(2): 123-134

Forsburg SL (2008) The MCM helicase: linking checkpoints to the replication fork. *Biochem Soc Trans* 36(Pt 1): 114-119

Frade JM (2002) Interkinetic nuclear movement in the vertebrate neuroepithelium: encounters with an old acquaintance. *Prog Brain Res* 136: 67-71

Frame S, Balmain A (1999) Target genes and target cells in carcinogenesis. *Br J Cancer* 80 Suppl 1: 28-33

Fuchs E (2007) Scratching the surface of skin development. *Nature* 445(7130): 834-842

Fuchs E (2009) Finding one's niche in the skin. *Cell Stem Cell* 4(6): 499-502

Fuchs E, Tumber T, Guasch G (2004) Socializing with the neighbors: stem cells and their niche. *Cell* 116(6): 769-778

Furth J, Kahn M (1937) The transmission of leukaemia of mice with a single cell. *American Journal of Cancer* 31: 276-282

Gao MQ, Choi YP, Kang S, Youn JH, Cho NH (2010) CD24+ cells from hierarchically organized ovarian cancer are enriched in cancer stem cells. *Oncogene* 29(18): 2672-2680

- Garber K (2005) New checkpoint blockers begin human trials. *J Natl Cancer Inst* 97(14): 1026-1028
- Gat U, DasGupta R, Degenstein L, Fuchs E (1998) De Novo hair follicle morphogenesis and hair tumors in mice expressing a truncated beta-catenin in skin. *Cell* 95(5): 605-614
- Gatei M, Sloper K, Sorensen C, Syljuasen R, Falck J, Hobson K, Savage K, Lukas J, Zhou BB, Bartek J, Khanna KK (2003) Ataxia-telangiectasia-mutated (ATM) and NBS1-dependent phosphorylation of Chk1 on Ser-317 in response to ionizing radiation. *J Biol Chem* 278(17): 14806-14811
- Gerdes B, Ramaswamy A, Kersting M, Ernst M, Lang S, Schuermann M, Wild A, Bartsch DK (2001) p16(INK4a) alterations in chronic pancreatitis-indicator for high-risk lesions for pancreatic cancer. *Surgery* 129(4): 490-497
- Gil J, Peters G (2006) Regulation of the INK4b-ARF-INK4a tumour suppressor locus: all for one or one for all. *Nat Rev Mol Cell Biol* 7(9): 667-677
- Ginestier C, Hur MH, Charafe-Jauffret E, Monville F, Dutcher J, Brown M, Jacquemier J, Viens P, Kleer CG, Liu S, Schott A, Hayes D, Birnbaum D, Wicha MS, Dontu G (2007) ALDH1 is a marker of normal and malignant human mammary stem cells and a predictor of poor clinical outcome. *Cell Stem Cell* 1(5): 555-567
- Goodell MA, Brose K, Paradis G, Conner AS, Mulligan RC (1996) Isolation and functional properties of murine hematopoietic stem cells that are replicating in vivo. *J Exp Med* 183(4): 1797-1806
- Gorgoulis VG, Vassiliou LV, Karakaidos P, Zacharatos P, Kotsinas A, Liloglou T, Venere M, Ditullio RA, Jr., Kastrinakis NG, Levy B, Kletsas D, Yoneta A, Herlyn M, Kittas C, Halazonetis TD (2005) Activation of the DNA damage checkpoint and genomic instability in human precancerous lesions. *Nature* 434(7035): 907-913
- Gottlieb TM, Jackson SP (1993) The DNA-dependent protein kinase: requirement for DNA ends and association with Ku antigen. *Cell* 72(1): 131-142
- Gould KL, Nurse P (1989) Tyrosine phosphorylation of the fission yeast cdc2+ protein kinase regulates entry into mitosis. *Nature* 342(6245): 39-45
- Gratzner HG (1982) Monoclonal antibody to 5-bromo- and 5-iododeoxyuridine: A new reagent for detection of DNA replication. *Science* 218(4571): 474-475
- Grawunder U, Wilm M, Wu X, Kulesza P, Wilson TE, Mann M, Lieber MR (1997) Activity of DNA ligase IV stimulated by complex formation with XRCC4 protein in mammalian cells. *Nature* 388(6641): 492-495
- Greco V, Chen T, Rendl M, Schober M, Pasolli HA, Stokes N, Dela Cruz-Racelis J, Fuchs E (2009) A two-step mechanism for stem cell activation during hair regeneration. *Cell Stem Cell* 4(2): 155-169
- Greenow KR, Clarke AR, Jones RH (2009) Chk1 deficiency in the mouse small intestine results in p53-independent crypt death and subsequent intestinal compensation. *Oncogene* 28(11): 1443-1453

Grigoryan T, Wend P, Klaus A, Birchmeier W (2008) Deciphering the function of canonical Wnt signals in development and disease: conditional loss- and gain-of-function mutations of beta-catenin in mice. *Genes Dev* 22(17): 2308-2341

Gupta PB, Chaffer CL, Weinberg RA (2009) Cancer stem cells: mirage or reality? *Nat Med* 15(9): 1010-1012

Harbour JW, Dean DC (2000) The Rb/E2F pathway: expanding roles and emerging paradigms. *Genes Dev* 14(19): 2393-2409

He S, Nakada D, Morrison SJ (2009) Mechanisms of stem cell self-renewal. *Annu Rev Cell Dev Biol* 25: 377-406

Hegi ME, Diserens AC, Gorlia T, Hamou MF, de Tribolet N, Weller M, Kros JM, Hainfellner JA, Mason W, Mariani L, Bromberg JE, Hau P, Mirimanoff RO, Cairncross JG, Janzer RC, Stupp R (2005) MGMT gene silencing and benefit from temozolomide in glioblastoma. *N Engl J Med* 352(10): 997-1003

Helin K, Harlow E, Fattaey A (1993) Inhibition of E2F-1 transactivation by direct binding of the retinoblastoma protein. *Mol Cell Biol* 13(10): 6501-6508

Hewitt HB (1953) Studies of the quantitative transplantation of mouse sarcoma. *Br J Cancer* 7(3): 367-383

Hirao A, Kong YY, Matsuoka S, Wakeham A, Ruland J, Yoshida H, Liu D, Elledge SJ, Mak TW (2000) DNA damage-induced activation of p53 by the checkpoint kinase Chk2. *Science* 287(5459): 1824-1827

Hocevar BA, Mou F, Rennolds JL, Morris SM, Cooper JA, Howe PH (2003) Regulation of the Wnt signaling pathway by disabled-2 (Dab2). *EMBO J* 22(12): 3084-3094

Hochegger H, Takeda S, Hunt T (2008) Cyclin-dependent kinases and cell-cycle transitions: does one fit all? *Nat Rev Mol Cell Biol* 9(11): 910-916

Hoeller D, Dikic I (2009) Targeting the ubiquitin system in cancer therapy. *Nature* 458(7237): 438-444

Hosoya A, Lee JM, Cho SW, Kim JY, Shinozaki N, Shibahara T, Shimono M, Jung HS (2008) Morphological evidence of basal keratinocyte migration during the re-epithelialization process. *Histochem Cell Biol* 130(6): 1165-1175

Huelsken J, Vogel R, Erdmann B, Cotsarelis G, Birchmeier W (2001) beta-Catenin controls hair follicle morphogenesis and stem cell differentiation in the skin. *Cell* 105(4): 533-545

Indra AK, Warot X, Brocard J, Bornert JM, Xiao JH, Chambon P, Metzger D (1999) Temporally-controlled site-specific mutagenesis in the basal layer of the epidermis: comparison of the recombinase activity of the tamoxifen-inducible Cre-ER(T) and Cre-ER(T2) recombinases. *Nucleic Acids Res* 27(22): 4324-4327

Ishibashi K (1950) Studies on the number of cells necessary for the transplantation of Yoshida sarcoma; transmission of the tumor with a single cell. *Gann* 41(1): 1-14

Ito M, Kizawa K, Toyoda M, Morohashi M (2002) Label-retaining cells in the bulge region are directed to cell death after plucking, followed by healing from the surviving hair germ. *J Invest Dermatol* 119(6): 1310-1316

Ito M, Liu Y, Yang Z, Nguyen J, Liang F, Morris RJ, Cotsarelis G (2005) Stem cells in the hair follicle bulge contribute to wound repair but not to homeostasis of the epidermis. *Nat Med* 11(12): 1351-1354

Ito S, Ito Y, Senga T, Hattori S, Matsuo S, Hamaguchi M (2006) v-Src requires Ras signaling for the suppression of gap junctional intercellular communication. *Oncogene* 25(16): 2420-2424

Ito S, Kuraoka I, Chymkowitch P, Compe E, Takedachi A, Ishigami C, Coin F, Egly JM, Tanaka K (2007) XPG stabilizes TFIIH, allowing transactivation of nuclear receptors: implications for Cockayne syndrome in XP-G/CS patients. *Mol Cell* 26(2): 231-243

Izumi T, Brown DB, Naidu CV, Bhakat KK, Macinnes MA, Saito H, Chen DJ, Mitra S (2005) Two essential but distinct functions of the mammalian abasic endonuclease. *Proc Natl Acad Sci U S A* 102(16): 5739-5743

Jackson SP, Bartek J (2009) The DNA-damage response in human biology and disease. *Nature* 461(7267): 1071-1078

Jaks V, Barker N, Kasper M, van Es JH, Snippert HJ, Clevers H, Toftgard R (2008) Lgr5 marks cycling, yet long-lived, hair follicle stem cells. *Nat Genet* 40(11): 1291-1299

Jimeno A, Rudek MA, Purcell T, Laheru DA, Messersmith WA, Dancey J, Carducci MA, Baker SD, Hidalgo M, Donehower RC (2008) Phase I and pharmacokinetic study of UCN-01 in combination with irinotecan in patients with solid tumors. *Cancer Chemother Pharmacol* 61(3): 423-433

Jirmanova L, Bulavin DV, Fornace AJ, Jr. (2005) Inhibition of the ATR/Chk1 pathway induces a p38-dependent S-phase delay in mouse embryonic stem cells. *Cell Cycle* 4(10): 1428-1434

Jones PH, Simons BD, Watt FM (2007) Sic transit gloria: farewell to the epidermal transit amplifying cell? *Cell Stem Cell* 1(4): 371-381

Jonker JW, Freeman J, Bolscher E, Musters S, Alvi AJ, Titley I, Schinkel AH, Dale TC (2005) Contribution of the ABC transporters Bcrp1 and Mdr1a/1b to the side population phenotype in mammary gland and bone marrow of mice. *Stem Cells* 23(8): 1059-1065

Kaelin WG, Jr. (2005) The concept of synthetic lethality in the context of anticancer therapy. *Nat Rev Cancer* 5(9): 689-698

- Kaina B, Christmann M, Naumann S, Roos WP (2007) MGMT: key node in the battle against genotoxicity, carcinogenicity and apoptosis induced by alkylating agents. *DNA Repair (Amst)* 6(8): 1079-1099
- Kaldis P, Sutton A, Solomon MJ (1996) The Cdk-activating kinase (CAK) from budding yeast. *Cell* 86(4): 553-564
- Kao HI, Bambara RA (2003) The protein components and mechanism of eukaryotic Okazaki fragment maturation. *Crit Rev Biochem Mol Biol* 38(5): 433-452
- Kastan MB, Bartek J (2004) Cell-cycle checkpoints and cancer. *Nature* 432(7015): 316-323
- Kemp CJ (2005) Multistep skin cancer in mice as a model to study the evolution of cancer cells. *Semin Cancer Biol* 15(6): 460-473
- Keyomarsi K, Tucker SL, Buchholz TA, Callister M, Ding Y, Hortobagyi GN, Bedrosian I, Knickerbocker C, Toyofuku W, Lowe M, Herliczek TW, Bacus SS (2002) Cyclin E and survival in patients with breast cancer. *N Engl J Med* 347(20): 1566-1575
- Khleif SN, DeGregori J, Yee CL, Otterson GA, Kaye FJ, Nevins JR, Howley PM (1996) Inhibition of cyclin D-CDK4/CDK6 activity is associated with an E2F-mediated induction of cyclin kinase inhibitor activity. *Proc Natl Acad Sci U S A* 93(9): 4350-4354
- Kim CJ, Lee JH, Song JW, Cho YG, Kim SY, Nam SW, Yoo NJ, Park WS, Lee JY (2007) Chk1 frameshift mutation in sporadic and hereditary non-polyposis colorectal cancers with microsatellite instability. *Eur J Surg Oncol*
- Kim JK, Diehl JA (2009) Nuclear cyclin D1: an oncogenic driver in human cancer. *J Cell Physiol* 220(2): 292-296
- Kim YC, Gerlitz G, Furusawa T, Catez F, Nussenzweig A, Oh KS, Kraemer KH, Shiloh Y, Bustin M (2009) Activation of ATM depends on chromatin interactions occurring before induction of DNA damage. *Nat Cell Biol* 11(1): 92-96
- Kimble JE, White JG (1981) On the control of germ cell development in *Caenorhabditis elegans*. *Dev Biol* 81(2): 208-219
- Kinzler KW, Nilbert MC, Vogelstein B, Bryan TM, Levy DB, Smith KJ, Preisinger AC, Hamilton SR, Hedge P, Markham A, et al. (1991) Identification of a gene located at chromosome 5q21 that is mutated in colorectal cancers. *Science* 251(4999): 1366-1370
- Kishimoto J, Burgeson RE, Morgan BA (2000) Wnt signaling maintains the hair-inducing activity of the dermal papilla. *Genes Dev* 14(10): 1181-1185
- Klein AM, Doupe DP, Jones PH, Simons BD (2007) Kinetics of cell division in epidermal maintenance. *Phys Rev E Stat Nonlin Soft Matter Phys* 76(2 Pt 1): 021910

Kotnis A, Du L, Liu C, Popov SW, Pan-Hammarstrom Q (2009) Non-homologous end joining in class switch recombination: the beginning of the end. *Philos Trans R Soc Lond B Biol Sci* 364(1517): 653-665

Kovary K, Bravo R (1991) The jun and fos protein families are both required for cell cycle progression in fibroblasts. *Mol Cell Biol* 11(9): 4466-4472

Kozlov SV, Graham ME, Peng C, Chen P, Robinson PJ, Lavin MF (2006) Involvement of novel autophosphorylation sites in ATM activation. *EMBO J* 25(15): 3504-3514

Kumagai A, Dunphy WG (2000) Claspin, a novel protein required for the activation of Chk1 during a DNA replication checkpoint response in *Xenopus* egg extracts. *Mol Cell* 6(4): 839-849

Kumagai A, Dunphy WG (2003) Repeated phosphopeptide motifs in Claspin mediate the regulated binding of Chk1. *Nat Cell Biol* 5(2): 161-165

Kumagai A, Lee J, Yoo HY, Dunphy WG (2006) TopBP1 activates the ATR-ATRIP complex. *Cell* 124(5): 943-955

Kusuhara H, Sugiyama Y (2007) ATP-binding cassette, subfamily G (ABCG family). *Pflugers Arch* 453(5): 735-744

Lajtha LG (1979) Stem cell concepts. *Differentiation* 14(1-2): 23-34

Lam MH, Liu Q, Elledge SJ, Rosen JM (2004) Chk1 is haploinsufficient for multiple functions critical to tumor suppression. *Cancer Cell* 6(1): 45-59

Lapidot T, Sirard C, Vormoor J, Murdoch B, Hoang T, Caceres-Cortes J, Minden M, Paterson B, Caligiuri MA, Dick JE (1994) A cell initiating human acute myeloid leukaemia after transplantation into SCID mice. *Nature* 367(6464): 645-648

Lathia JD, Venere M, Rao MS, Rich JN (2010) Seeing is Believing: Are Cancer Stem Cells the Loch Ness Monster of Tumor Biology? *Stem Cell Rev*

Lee JH, Paull TT (2005) ATM activation by DNA double-strand breaks through the Mre11-Rad50-Nbs1 complex. *Science* 308(5721): 551-554

Lee JS, Collins KM, Brown AL, Lee CH, Chung JH (2000) hCds1-mediated phosphorylation of BRCA1 regulates the DNA damage response. *Nature* 404(6774): 201-204

Lee KW, Jung JW, Kang KS, Lee HJ (2004) p38 is a key signaling molecule for H-ras-induced inhibition of gap junction intercellular communication in rat liver epithelial cells. *Ann N Y Acad Sci* 1030: 258-263

Lees JA, Saito M, Vidal M, Valentine M, Look T, Harlow E, Dyson N, Helin K (1993) The retinoblastoma protein binds to a family of E2F transcription factors. *Mol Cell Biol* 13(12): 7813-7825

Li J, Williams BL, Haire LF, Goldberg M, Wilker E, Durocher D, Yaffe MB, Jackson SP, Smerdon SJ (2002) Structural and functional versatility of the FHA domain in

- DNA-damage signaling by the tumor suppressor kinase Chk2. *Mol Cell* 9(5): 1045-1054
- Li L, Clevers H (2010) Coexistence of quiescent and active adult stem cells in mammals. *Science* 327(5965): 542-545
- Li M, Indra AK, Warot X, Brocard J, Messaddeq N, Kato S, Metzger D, Chambon P (2000) Skin abnormalities generated by temporally controlled RXRalpha mutations in mouse epidermis. *Nature* 407(6804): 633-636
- Liang C, Weinreich M, Stillman B (1995) ORC and Cdc6p interact and determine the frequency of initiation of DNA replication in the genome. *Cell* 81(5): 667-676
- Liang F, Romanienko PJ, Weaver DT, Jeggo PA, Jasin M (1996) Chromosomal double-strand break repair in Ku80-deficient cells. *Proc Natl Acad Sci U S A* 93(17): 8929-8933
- Lin G, Huang YC, Shindel AW, Banie L, Wang G, Lue TF, Lin CS (2009) Labeling and tracking of mesenchymal stromal cells with EdU. *Cytotherapy* 11(7): 864-873
- Lin KK, Andersen B (2008) Have hair follicle stem cells shed their tranquil image? *Cell Stem Cell* 3(6): 581-582
- Lindahl T, Barnes DE (2000) Repair of endogenous DNA damage. *Cold Spring Harb Symp Quant Biol* 65: 127-133
- Liu E, Li X, Yan F, Zhao Q, Wu X (2004) Cyclin-dependent kinases phosphorylate human Cdt1 and induce its degradation. *J Biol Chem* 279(17): 17283-17288
- Liu F, Kohlmeier S, Wang CY (2008) Wnt signaling and skeletal development. *Cell Signal* 20(6): 999-1009
- Liu J, Smith CL, DeRyckere D, DeAngelis K, Martin GS, Berger JM (2000a) Structure and function of Cdc6/Cdc18: implications for origin recognition and checkpoint control. *Mol Cell* 6(3): 637-648
- Liu Q, Guntuku S, Cui XS, Matsuoka S, Cortez D, Tamai K, Luo G, Carattini-Rivera S, DeMayo F, Bradley A, Donehower LA, Elledge SJ (2000b) Chk1 is an essential kinase that is regulated by Atr and required for the G(2)/M DNA damage checkpoint. *Genes Dev* 14(12): 1448-1459
- Liu Y, Lyle S, Yang Z, Cotsarelis G (2003) Keratin 15 promoter targets putative epithelial stem cells in the hair follicle bulge. *J Invest Dermatol* 121(5): 963-968
- Ljungman M (2005) Activation of DNA damage signaling. *Mutat Res* 577(1-2): 203-216
- Lo Celso C, Prowse DM, Watt FM (2004) Transient activation of beta-catenin signalling in adult mouse epidermis is sufficient to induce new hair follicles but continuous activation is required to maintain hair follicle tumours. *Development* 131(8): 1787-1799

- Lopez-Girona A, Tanaka K, Chen XB, Baber BA, McGowan CH, Russell P (2001) Serine-345 is required for Rad3-dependent phosphorylation and function of checkpoint kinase Chk1 in fission yeast. *Proc Natl Acad Sci U S A* 98(20): 11289-11294
- Loser DA, Shibata A, Shibata AK, Woodbine LJ, Jeggo PA, Chalmers AJ (2010) Sensitization to radiation and alkylating agents by inhibitors of poly(ADP-ribose) polymerase is enhanced in cells deficient in DNA double-strand break repair. *Mol Cancer Ther* 9(6): 1775-1787
- Luche H, Weber O, Nageswara Rao T, Blum C, Fehling HJ (2007) Faithful activation of an extra-bright red fluorescent protein in "knock-in" Cre-reporter mice ideally suited for lineage tracing studies. *Eur J Immunol* 37(1): 43-53
- Lundgren K, Walworth N, Booher R, Dembski M, Kirschner M, Beach D (1991) mik1 and wee1 cooperate in the inhibitory tyrosine phosphorylation of cdc2. *Cell* 64(6): 1111-1122
- Lyle S, Christofidou-Solomidou M, Liu Y, Elder DE, Albelda S, Cotsarelis G (1998) The C8/144B monoclonal antibody recognizes cytokeratin 15 and defines the location of human hair follicle stem cells. *J Cell Sci* 111 (Pt 21): 3179-3188
- Lyle S, Christofidou-Solomidou M, Liu Y, Elder DE, Albelda S, Cotsarelis G (1999) Human hair follicle bulge cells are biochemically distinct and possess an epithelial stem cell phenotype. *J Invest Dermatol Symp Proc* 4(3): 296-301
- Lynch HT, Lynch JF, Lynch PM, Attard T (2008a) Hereditary colorectal cancer syndromes: molecular genetics, genetic counseling, diagnosis and management. *Fam Cancer* 7(1): 27-39
- Lynch HT, Silva E, Snyder C, Lynch JF (2008b) Hereditary breast cancer: part I. Diagnosing hereditary breast cancer syndromes. *Breast J* 14(1): 3-13
- Ma Y, Lu H, Tippin B, Goodman MF, Shimazaki N, Koiwai O, Hsieh CL, Schwarz K, Lieber MR (2004) A biochemically defined system for mammalian nonhomologous DNA end joining. *Mol Cell* 16(5): 701-713
- Ma Y, Pannicke U, Schwarz K, Lieber MR (2002) Hairpin opening and overhang processing by an Artemis/DNA-dependent protein kinase complex in nonhomologous end joining and V(D)J recombination. *Cell* 108(6): 781-794
- Mackay HJ, Twelves CJ (2003) Protein kinase C: a target for anticancer drugs? *Endocr Relat Cancer* 10(3): 389-396
- Maiorano D, Moreau J, Mechali M (2000) XCDT1 is required for the assembly of pre-replicative complexes in *Xenopus laevis*. *Nature* 404(6778): 622-625
- Makino S (1956) Further evidence favoring the concept of the stem cell in ascites tumors of rats. *Ann N Y Acad Sci* 63(5): 818-830
- Malanchi I, Peinado H, Kassen D, Hussenet T, Metzger D, Chambon P, Huber M, Hohl D, Cano A, Birchmeier W, Huelsken J (2008) Cutaneous cancer stem cell

- maintenance is dependent on beta-catenin signalling. *Nature* 452(7187): 650-653
- Malumbres M, Barbacid M (2009) Cell cycle, CDKs and cancer: a changing paradigm. *Nat Rev Cancer* 9(3): 153-166
- Masumoto H, Muramatsu S, Kamimura Y, Araki H (2002) S-Cdk-dependent phosphorylation of Sld2 essential for chromosomal DNA replication in budding yeast. *Nature* 415(6872): 651-655
- Matsuoka S, Edwards MC, Bai C, Parker S, Zhang P, Baldini A, Harper JW, Elledge SJ (1995) p57KIP2, a structurally distinct member of the p21CIP1 Cdk inhibitor family, is a candidate tumor suppressor gene. *Genes Dev* 9(6): 650-662
- Matsuoka S, Huang M, Elledge SJ (1998) Linkage of ATM to cell cycle regulation by the Chk2 protein kinase. *Science* 282(5395): 1893-1897
- Matyskiela ME, Rodrigo-Brenni MC, Morgan DO (2009) Mechanisms of ubiquitin transfer by the anaphase-promoting complex. *J Biol* 8(10): 92
- McGarry TJ, Kirschner MW (1998) Geminin, an inhibitor of DNA replication, is degraded during mitosis. *Cell* 93(6): 1043-1053
- McLean GW, Komiyama NH, Serrels B, Asano H, Reynolds L, Conti F, Hodivala-Dilke K, Metzger D, Chambon P, Grant SG, Frame MC (2004) Specific deletion of focal adhesion kinase suppresses tumor formation and blocks malignant progression. *Genes Dev* 18(24): 2998-3003
- Mechali M (2010) Eukaryotic DNA replication origins: many choices for appropriate answers. *Nat Rev Mol Cell Biol* 11(10): 728-738
- Megosh L, Halpern M, Farkash E, O'Brien TG (1998) Analysis of ras gene mutational spectra in epidermal papillomas from K6/ODC transgenic mice. *Mol Carcinog* 22(3): 145-149
- Mejia-Guerrero S, Quejada M, Gokgoz N, Gill M, Parkes RK, Wunder JS, Andrulis IL (2010) Characterization of the 12q15 MDM2 and 12q13-14 CDK4 amplicons and clinical correlations in osteosarcoma. *Genes Chromosomes Cancer* 49(6): 518-525
- Moore N, Lyle S (2010) Quiescent, slow-cycling stem cell populations in cancer: a review of the evidence and discussion of significance. *J Oncol* 2011
- Morris RJ (2004) A perspective on keratinocyte stem cells as targets for skin carcinogenesis. *Differentiation* 72(8): 381-386
- Morris RJ, Coulter K, Tryson K, Steinberg SR (1997) Evidence that cutaneous carcinogen-initiated epithelial cells from mice are quiescent rather than actively cycling. *Cancer Res* 57(16): 3436-3443
- Morris RJ, Potten CS (1994) Slowly cycling (label-retaining) epidermal cells behave like clonogenic stem cells in vitro. *Cell Prolif* 27(5): 279-289

- Morris RJ, Potten CS (1999) Highly persistent label-retaining cells in the hair follicles of mice and their fate following induction of anagen. *J Invest Dermatol* 112(4): 470-475
- Morton JP, Timpson P, Karim SA, Ridgway RA, Athineos D, Doyle B, Jamieson NB, Oien KA, Lowy AM, Brunton VG, Frame MC, Evans TR, Sansom OJ (2010) Mutant p53 drives metastasis and overcomes growth arrest/senescence in pancreatic cancer. *Proc Natl Acad Sci U S A* 107(1): 246-251
- Mu D, Hsu DS, Sancar A (1996) Reaction mechanism of human DNA repair excision nuclease. *J Biol Chem* 271(14): 8285-8294
- Mueller PR, Coleman TR, Kumagai A, Dunphy WG (1995) Myt1: a membrane-associated inhibitory kinase that phosphorylates Cdc2 on both threonine-14 and tyrosine-15. *Science* 270(5233): 86-90
- Mulherkar R, Kirtane BM, Ramchandani A, Mansukhani NP, Kannan S, Naresh KN (2003) Expression of enhancing factor/phospholipase A2 in skin results in abnormal epidermis and increased sensitivity to chemical carcinogenesis. *Oncogene* 22(13): 1936-1944
- Muller-Rover S, Handjiski B, van der Veen C, Eichmuller S, Foitzik K, McKay IA, Stenn KS, Paus R (2001) A comprehensive guide for the accurate classification of murine hair follicles in distinct hair cycle stages. *J Invest Dermatol* 117(1): 3-15
- Muller-Sieburg C, Sieburg HB (2008) Stem cell aging: survival of the laziest? *Cell Cycle* 7(24): 3798-3804
- Muller H, Helin K (2000) The E2F transcription factors: key regulators of cell proliferation. *Biochim Biophys Acta* 1470(1): M1-12
- Murayama K, Kimura T, Tarutani M, Tomooka M, Hayashi R, Okabe M, Nishida K, Itami S, Katayama I, Nakano T (2007) Akt activation induces epidermal hyperplasia and proliferation of epidermal progenitors. *Oncogene* 26(33): 4882-4888
- Myung P, Andl T, Ito M (2009a) Defining the hair follicle stem cell (Part I). *J Cutan Pathol* 36(9): 1031-1034
- Myung P, Andl T, Ito M (2009b) Defining the hair follicle stem cell (Part II). *J Cutan Pathol* 36(10): 1134-1137
- Naim V, Rosselli F (2009) The FANCD1 pathway and mitosis: a replication legacy. *Cell Cycle* 8(18): 2907-2911
- Naito M, DiGiovanni J (1989) Genetic background and development of skin tumors. *Carcinog Compr Surv* 11: 187-212
- Narbonne P, Roy R (2006) Inhibition of germline proliferation during *C. elegans* dauer development requires PTEN, LKB1 and AMPK signalling. *Development* 133(4): 611-619

- Neuman E, Sellers WR, McNeil JA, Lawrence JB, Kaelin WG, Jr. (1996) Structure and partial genomic sequence of the human E2F1 gene. *Gene* 173(2): 163-169
- Nguyen H, Rendl M, Fuchs E (2006) Tcf3 governs stem cell features and represses cell fate determination in skin. *Cell* 127(1): 171-183
- Niida H, Katsuno Y, Banerjee B, Hande MP, Nakanishi M (2007) Specific role of Chk1 phosphorylations in cell survival and checkpoint activation. *Mol Cell Biol* 27(7): 2572-2581
- Nospikel T (2009) DNA repair in mammalian cells : Nucleotide excision repair: variations on versatility. *Cell Mol Life Sci* 66(6): 994-1009
- O'Brien CA, Pollett A, Gallinger S, Dick JE (2007) A human colon cancer cell capable of initiating tumour growth in immunodeficient mice. *Nature* 445(7123): 106-110
- O'Donovan A, Davies AA, Moggs JG, West SC, Wood RD (1994) XPG endonuclease makes the 3' incision in human DNA nucleotide excision repair. *Nature* 371(6496): 432-435
- Ohyama M, Terunuma A, Tock CL, Radonovich MF, Pise-Masison CA, Hopping SB, Brady JN, Udey MC, Vogel JC (2006) Characterization and isolation of stem cell-enriched human hair follicle bulge cells. *J Clin Invest* 116(1): 249-260
- Olaussen KA, Dunant A, Fouret P, Brambilla E, Andre F, Haddad V, Taranchon E, Filipits M, Pirker R, Popper HH, Stahel R, Sabatier L, Pignon JP, Tursz T, Le Chevalier T, Soria JC (2006) DNA repair by ERCC1 in non-small-cell lung cancer and cisplatin-based adjuvant chemotherapy. *N Engl J Med* 355(10): 983-991
- Owens DM, Watt FM (2003) Contribution of stem cells and differentiated cells to epidermal tumours. *Nat Rev Cancer* 3(6): 444-451
- Owens DM, Wei S, Smart RC (1999) A multihit, multistage model of chemical carcinogenesis. *Carcinogenesis* 20(9): 1837-1844
- Pagano M, Pepperkok R, Verde F, Ansorge W, Draetta G (1992) Cyclin A is required at two points in the human cell cycle. *EMBO J* 11(3): 961-971
- Pallis AG, Karamouzis MV (2010) DNA repair pathways and their implication in cancer treatment. *Cancer Metastasis Rev* 29(4): 677-685
- Pardee AB (1974) A restriction point for control of normal animal cell proliferation. *Proc Natl Acad Sci U S A* 71(4): 1286-1290
- Pearce DJ, Taussig D, Simpson C, Allen K, Rohatiner AZ, Lister TA, Bonnet D (2005) Characterization of cells with a high aldehyde dehydrogenase activity from cord blood and acute myeloid leukemia samples. *Stem Cells* 23(6): 752-760
- Pegg AE (2000) Repair of O(6)-alkylguanine by alkyltransferases. *Mutat Res* 462(2-3): 83-100

- Pellicci PG (2004) Do tumor-suppressive mechanisms contribute to organism aging by inducing stem cell senescence? *J Clin Invest* 113(1): 4-7
- Pellegrini M, Celeste A, Difilippantonio S, Guo R, Wang W, Feigenbaum L, Nussenzweig A (2006) Autophosphorylation at serine 1987 is dispensable for murine Atm activation in vivo. *Nature* 443(7108): 222-225
- Peng CY, Graves PR, Thoma RS, Wu Z, Shaw AS, Piwnica-Worms H (1997) Mitotic and G2 checkpoint control: regulation of 14-3-3 protein binding by phosphorylation of Cdc25C on serine-216. *Science* 277(5331): 1501-1505
- Perez-Losada J, Balmain A (2003) Stem-cell hierarchy in skin cancer. *Nat Rev Cancer* 3(6): 434-443
- Peters JM (2002) The anaphase-promoting complex: proteolysis in mitosis and beyond. *Mol Cell* 9(5): 931-943
- Petersen BO, Lukas J, Sorensen CS, Bartek J, Helin K (1999) Phosphorylation of mammalian CDC6 by cyclin A/CDK2 regulates its subcellular localization. *EMBO J* 18(2): 396-410
- Pines J (1995) Cyclins, CDKs and cancer. *Semin Cancer Biol* 6(2): 63-72
- Pines J, Hunter T (1989) Isolation of a human cyclin cDNA: evidence for cyclin mRNA and protein regulation in the cell cycle and for interaction with p34cdc2. *Cell* 58(5): 833-846
- Podust VN, Tiwari N, Stephan S, Fanning E (1998) Replication factor C disengages from proliferating cell nuclear antigen (PCNA) upon sliding clamp formation, and PCNA itself tethers DNA polymerase delta to DNA. *J Biol Chem* 273(48): 31992-31999
- Polager S, Ginsberg D (2009) p53 and E2f: partners in life and death. *Nat Rev Cancer* 9(10): 738-748
- Pollard TD EW (2004) *Cell Biology*, Pennsylvania: Saunders.
- Polyak K, Kato JY, Solomon MJ, Sherr CJ, Massague J, Roberts JM, Koff A (1994) p27Kip1, a cyclin-Cdk inhibitor, links transforming growth factor-beta and contact inhibition to cell cycle arrest. *Genes Dev* 8(1): 9-22
- Potten CS (1981) Cell replacement in epidermis (keratopoiesis) via discrete units of proliferation. *Int Rev Cytol* 69: 271-318
- Potten CS, Owen G, Booth D (2002) Intestinal stem cells protect their genome by selective segregation of template DNA strands. *J Cell Sci* 115(Pt 11): 2381-2388
- Prince ME, Sivanandan R, Kaczorowski A, Wolf GT, Kaplan MJ, Dalerba P, Weissman IL, Clarke MF, Ailles LE (2007) Identification of a subpopulation of cells with cancer stem cell properties in head and neck squamous cell carcinoma. *Proc Natl Acad Sci U S A* 104(3): 973-978

- Quintana E, Shackleton M, Sabel MS, Fullen DR, Johnson TM, Morrison SJ (2008) Efficient tumour formation by single human melanoma cells. *Nature* 456(7222): 593-598
- Quintanilla M, Brown K, Ramsden M, Balmain A (1986) Carcinogen-specific mutation and amplification of Ha-ras during mouse skin carcinogenesis. *Nature* 322(6074): 78-80
- Rando TA (2006) Stem cells, ageing and the quest for immortality. *Nature* 441(7097): 1080-1086
- Ray D, Kiyokawa H (2008) CDC25A phosphatase: a rate-limiting oncogene that determines genomic stability. *Cancer Res* 68(5): 1251-1253
- Reynisdottir I, Polyak K, Iavarone A, Massague J (1995) Kip/Cip and Ink4 Cdk inhibitors cooperate to induce cell cycle arrest in response to TGF-beta. *Genes Dev* 9(15): 1831-1845
- Ricci-Vitiani L, Lombardi DG, Pilozzi E, Biffoni M, Todaro M, Peschle C, De Maria R (2007) Identification and expansion of human colon-cancer-initiating cells. *Nature* 445(7123): 111-115
- Richardson C, Jasin M (2000) Frequent chromosomal translocations induced by DNA double-strand breaks. *Nature* 405(6787): 697-700
- Richardson C, Moynahan ME, Jasin M (1998) Double-strand break repair by interchromosomal recombination: suppression of chromosomal translocations. *Genes Dev* 12(24): 3831-3842
- Rijnkels M, Rosen JM (2001) Adenovirus-Cre-mediated recombination in mammary epithelial early progenitor cells. *J Cell Sci* 114(Pt 17): 3147-3153
- Riley T, Sontag E, Chen P, Levine A (2008) Transcriptional control of human p53-regulated genes. *Nat Rev Mol Cell Biol* 9(5): 402-412
- Rimkus SA, Katzenberger RJ, Trinh AT, Dodson GE, Tibbetts RS, Wassarman DA (2008) Mutations in String/CDC25 inhibit cell cycle re-entry and neurodegeneration in a Drosophila model of Ataxia telangiectasia. *Genes Dev* 22(9): 1205-1220
- Robinson HM, Jones R, Walker M, Zachos G, Brown R, Cassidy J, Gillespie DA (2006) Chk1-dependent slowing of S-phase progression protects DT40 B-lymphoma cells against killing by the nucleoside analogue 5-fluorouracil. *Oncogene* 25(39): 5359-5369
- Roe FJ, Carter RL, Mitchley BC, Peto R, Hecker E (1972) On the persistence of tumour initiation and the acceleration of tumour progression in mouse skin tumorigenesis. *Int J Cancer* 9(2): 264-273
- Rosen JM, Jordan CT (2009) The increasing complexity of the cancer stem cell paradigm. *Science* 324(5935): 1670-1673

- Roth DB, Wilson JH (1986) Nonhomologous recombination in mammalian cells: role for short sequence homologies in the joining reaction. *Mol Cell Biol* 6(12): 4295-4304
- Rothkamm K, Kruger I, Thompson LH, Lobrich M (2003) Pathways of DNA double-strand break repair during the mammalian cell cycle. *Mol Cell Biol* 23(16): 5706-5715
- Rottenberg S, Jaspers JE, Kersbergen A, van der Burg E, Nygren AO, Zander SA, Derksen PW, de Bruin M, Zevenhoven J, Lau A, Boulter R, Cranston A, O'Connor MJ, Martin NM, Borst P, Jonkers J (2008) High sensitivity of BRCA1-deficient mammary tumors to the PARP inhibitor AZD2281 alone and in combination with platinum drugs. *Proc Natl Acad Sci U S A* 105(44): 17079-17084
- Rowley R, Hudson J, Young PG (1992) The wee1 protein kinase is required for radiation-induced mitotic delay. *Nature* 356(6367): 353-355
- Rozen P, Macrae F (2006) Familial adenomatous polyposis: The practical applications of clinical and molecular screening. *Fam Cancer* 5(3): 227-235
- Ruzankina Y, Pinzon-Guzman C, Asare A, Ong T, Pontano L, Cotsarelis G, Zediak VP, Velez M, Bhandoola A, Brown EJ (2007) Deletion of the developmentally essential gene ATR in adult mice leads to age-related phenotypes and stem cell loss. *Cell Stem Cell* 1(1): 113-126
- Saleh-Gohari N, Helleday T (2004) Conservative homologous recombination preferentially repairs DNA double-strand breaks in the S phase of the cell cycle in human cells. *Nucleic Acids Res* 32(12): 3683-3688
- Santamaria D, Barriere C, Cerqueira A, Hunt S, Tardy C, Newton K, Caceres JF, Dubus P, Malumbres M, Barbacid M (2007) Cdk1 is sufficient to drive the mammalian cell cycle. *Nature* 448(7155): 811-815
- Sartori AA, Lukas C, Coates J, Mistrik M, Fu S, Bartek J, Baer R, Lukas J, Jackson SP (2007) Human CtIP promotes DNA end resection. *Nature* 450(7169): 509-514
- Sausville EA, Arbuick SG, Messmann R, Headlee D, Bauer KS, Lush RM, Murgu A, Figg WD, Lahusen T, Jaken S, Jing X, Roberge M, Fuse E, Kuwabara T, Senderowicz AM (2001) Phase I trial of 72-hour continuous infusion UCN-01 in patients with refractory neoplasms. *J Clin Oncol* 19(8): 2319-2333
- Savitsky K, Bar-Shira A, Gilad S, Rotman G, Ziv Y, Vanagaite L, Tagle DA, Smith S, Uziel T, Sfez S, Ashkenazi M, Pecker I, Frydman M, Harnik R, Patanjali SR, Simmons A, Clines GA, Sartiel A, Gatti RA, Chessa L, Sanal O, Lavin MF, Jaspers NG, Taylor AM, Arlett CF, Miki T, Weissman SM, Lovett M, Collins FS, Shiloh Y (1995) A single ataxia telangiectasia gene with a product similar to PI-3 kinase. *Science* 268(5218): 1749-1753
- Scadden DT (2006) The stem-cell niche as an entity of action. *Nature* 441(7097): 1075-1079

Scharenberg CW, Harkey MA, Torok-Storb B (2002) The ABCG2 transporter is an efficient Hoechst 33342 efflux pump and is preferentially expressed by immature human hematopoietic progenitors. *Blood* 99(2): 507-512

Schatton T, Murphy GF, Frank NY, Yamaura K, Waaga-Gasser AM, Gasser M, Zhan Q, Jordan S, Duncan LM, Weishaupt C, Fuhlbrigge RC, Kupper TS, Sayegh MH, Frank MH (2008) Identification of cells initiating human melanomas. *Nature* 451(7176): 345-349

Schmidt-Ullrich R, Paus R (2005) Molecular principles of hair follicle induction and morphogenesis. *Bioessays* 27(3): 247-261

Schwarz JK, Lovly CM, Piwnica-Worms H (2003) Regulation of the Chk2 protein kinase by oligomerization-mediated cis- and trans-phosphorylation. *Mol Cancer Res* 1(8): 598-609

Scoville DH, Sato T, He XC, Li L (2008) Current view: intestinal stem cells and signaling. *Gastroenterology* 134(3): 849-864

Serrels B, Serrels A, Mason SM, Baldeschi C, Ashton GH, Canel M, Mackintosh LJ, Doyle B, Green TP, Frame MC, Sansom OJ, Brunton VG (2009) A novel Src kinase inhibitor reduces tumour formation in a skin carcinogenesis model. *Carcinogenesis* 30(2): 249-257

Shackleton M, Vaillant F, Simpson KJ, Stingl J, Smyth GK, Asselin-Labat ML, Wu L, Lindeman GJ, Visvader JE (2006) Generation of a functional mammary gland from a single stem cell. *Nature* 439(7072): 84-88

Sharpless E, Chin L (2003) The INK4a/ARF locus and melanoma. *Oncogene* 22(20): 3092-3098

Sharpless NE, DePinho RA (2004) Telomeres, stem cells, senescence, and cancer. *J Clin Invest* 113(2): 160-168

Sherr CJ (1996) Cancer cell cycles. *Science* 274(5293): 1672-1677

Sheu YJ, Stillman B (2006) Cdc7-Dbf4 phosphorylates MCM proteins via a docking site-mediated mechanism to promote S phase progression. *Mol Cell* 24(1): 101-113

Shiloh Y, Kastan MB (2001) ATM: genome stability, neuronal development, and cancer cross paths. *Adv Cancer Res* 83: 209-254

Shimada M, Niida H, Zineldeen DH, Tagami H, Tanaka M, Saito H, Nakanishi M (2008) Chk1 is a histone H3 threonine 11 kinase that regulates DNA damage-induced transcriptional repression. *Cell* 132(2): 221-232

Shimizu H, Morgan BA (2004) Wnt signaling through the beta-catenin pathway is sufficient to maintain, but not restore, anagen-phase characteristics of dermal papilla cells. *J Invest Dermatol* 122(2): 239-245

Shultz LD, Lyons BL, Burzenski LM, Gott B, Chen X, Chaleff S, Kotb M, Gillies SD, King M, Mangada J, Greiner DL, Handgretinger R (2005) Human lymphoid and

- myeloid cell development in NOD/LtSz-scid IL2R gamma null mice engrafted with mobilized human hemopoietic stem cells. *J Immunol* 174(10): 6477-6489
- Singh SK, Hawkins C, Clarke ID, Squire JA, Bayani J, Hide T, Henkelman RM, Cusimano MD, Dirks PB (2004) Identification of human brain tumour initiating cells. *Nature* 432(7015): 396-401
- Smith J, Tho LM, Xu N, Gillespie DA (2010) The ATM-Chk2 and ATR-Chk1 pathways in DNA damage signaling and cancer. *Adv Cancer Res* 108: 73-112
- Smits VA, Reaper PM, Jackson SP (2006) Rapid PIKK-dependent release of Chk1 from chromatin promotes the DNA-damage checkpoint response. *Curr Biol* 16(2): 150-159
- Sobol RW, Prasad R, Evenski A, Baker A, Yang XP, Horton JK, Wilson SH (2000) The lyase activity of the DNA repair protein beta-polymerase protects from DNA-damage-induced cytotoxicity. *Nature* 405(6788): 807-810
- Solomon MJ, Glotzer M, Lee TH, Philippe M, Kirschner MW (1990) Cyclin activation of p34cdc2. *Cell* 63(5): 1013-1024
- Sorensen CS, Hansen LT, Dziegielewski J, Syljuasen RG, Lundin C, Bartek J, Helleday T (2005) The cell-cycle checkpoint kinase Chk1 is required for mammalian homologous recombination repair. *Nat Cell Biol* 7(2): 195-201
- Sorensen CS, Syljuasen RG, Falck J, Schroeder T, Ronnstrand L, Khanna KK, Zhou BB, Bartek J, Lukas J (2003) Chk1 regulates the S phase checkpoint by coupling the physiological turnover and ionizing radiation-induced accelerated proteolysis of Cdc25A. *Cancer Cell* 3(3): 247-258
- Soriano P (1999) Generalized lacZ expression with the ROSA26 Cre reporter strain. *Nat Genet* 21(1): 70-71
- Spradling A, Drummond-Barbosa D, Kai T (2001) Stem cells find their niche. *Nature* 414(6859): 98-104
- Sriuranpong V, Mutirangura A, Gillespie JW, Patel V, Amornphimoltham P, Molinolo AA, Kerekhanjanarong V, Supanakorn S, Supiyaphun P, Rangdaeng S, Voravud N, Gutkind JS (2004) Global gene expression profile of nasopharyngeal carcinoma by laser capture microdissection and complementary DNA microarrays. *Clin Cancer Res* 10(15): 4944-4958
- Srivenugopal KS, Yuan XH, Friedman HS, Ali-Osman F (1996) Ubiquitination-dependent proteolysis of O6-methylguanine-DNA methyltransferase in human and murine tumor cells following inactivation with O6-benzylguanine or 1,3-bis(2-chloroethyl)-1-nitrosourea. *Biochemistry* 35(4): 1328-1334
- Stawinska M, Cygankiewicz A, Trzcinski R, Mik M, Dziki A, Krajewska WM (2008) Alterations of Chk1 and Chk2 expression in colon cancer. *Int J Colorectal Dis* 23(12): 1243-1249

Stewart ZA, Leach SD, Pietsenpol JA (1999) p21(Waf1/Cip1) inhibition of cyclin E/Cdk2 activity prevents endoreduplication after mitotic spindle disruption. *Mol Cell Biol* 19(1): 205-215

Stoimenov I, Helleday T (2009) PCNA on the crossroad of cancer. *Biochem Soc Trans* 37(Pt 3): 605-613

Stucki M, Pascucci B, Parlanti E, Fortini P, Wilson SH, Hubscher U, Dogliotti E (1998) Mammalian base excision repair by DNA polymerases delta and epsilon. *Oncogene* 17(7): 835-843

Stupp R, Mason WP, van den Bent MJ, Weller M, Fisher B, Taphoorn MJ, Belanger K, Brandes AA, Marosi C, Bogdahn U, Curschmann J, Janzer RC, Ludwin SK, Gorlia T, Allgeier A, Lacombe D, Cairncross JG, Eisenhauer E, Mirimanoff RO (2005) Radiotherapy plus concomitant and adjuvant temozolomide for glioblastoma. *N Engl J Med* 352(10): 987-996

Sugasawa K, Ng JM, Masutani C, Iwai S, van der Spek PJ, Eker AP, Hanaoka F, Bootsma D, Hoeijmakers JH (1998) Xeroderma pigmentosum group C protein complex is the initiator of global genome nucleotide excision repair. *Mol Cell* 2(2): 223-232

Sugasawa K, Ng JM, Masutani C, Maekawa T, Uchida A, van der Spek PJ, Eker AP, Rademakers S, Visser C, Aboussekhra A, Wood RD, Hanaoka F, Bootsma D, Hoeijmakers JH (1997) Two human homologs of Rad23 are functionally interchangeable in complex formation and stimulation of XPC repair activity. *Mol Cell Biol* 17(12): 6924-6931

Sun P, Yoshizuka N, New L, Moser BA, Li Y, Liao R, Xie C, Chen J, Deng Q, Yamout M, Dong MQ, Frangou CG, Yates JR, 3rd, Wright PE, Han J (2007) PRAK is essential for ras-induced senescence and tumor suppression. *Cell* 128(2): 295-308

Syljuasen RG, Sorensen CS, Hansen LT, Fugger K, Lundin C, Johansson F, Helleday T, Sehested M, Lukas J, Bartek J (2005) Inhibition of human Chk1 causes increased initiation of DNA replication, phosphorylation of ATR targets, and DNA breakage. *Mol Cell Biol* 25(9): 3553-3562

Takahashi T, Nowakowski RS, Caviness VS, Jr. (1995) The cell cycle of the pseudostratified ventricular epithelium of the embryonic murine cerebral wall. *J Neurosci* 15(9): 6046-6057

Takai H, Naka K, Okada Y, Watanabe M, Harada N, Saito S, Anderson CW, Appella E, Nakanishi M, Suzuki H, Nagashima K, Sawa H, Ikeda K, Motoyama N (2002) Chk2-deficient mice exhibit radioresistance and defective p53-mediated transcription. *EMBO J* 21(19): 5195-5205

Takai H, Tominaga K, Motoyama N, Minamishima YA, Nagahama H, Tsukiyama T, Ikeda K, Nakayama K, Nakanishi M, Nakayama K (2000) Aberrant cell cycle checkpoint function and early embryonic death in Chk1(-/-) mice. *Genes Dev* 14(12): 1439-1447

- Takisawa H, Mimura S, Kubota Y (2000) Eukaryotic DNA replication: from pre-replication complex to initiation complex. *Curr Opin Cell Biol* 12(6): 690-696
- Tanaka T, Nasmyth K (1998) Association of RPA with chromosomal replication origins requires an Mcm protein, and is regulated by Rad53, and cyclin- and Dbf4-dependent kinases. *EMBO J* 17(17): 5182-5191
- Taniguchi T, Tischkowitz M, Ameziane N, Hodgson SV, Mathew CG, Joenje H, Mok SC, D'Andrea AD (2003) Disruption of the Fanconi anemia-BRCA pathway in cisplatin-sensitive ovarian tumors. *Nat Med* 9(5): 568-574
- Tao ZF, Lin NH (2006) Chk1 inhibitors for novel cancer treatment. *Anticancer Agents Med Chem* 6(4): 377-388
- Taussig DC, Miraki-Moud F, Anjos-Afonso F, Pearce DJ, Allen K, Ridler C, Lillington D, Oakervee H, Cavenagh J, Agrawal SG, Lister TA, Gribben JG, Bonnet D (2008) Anti-CD38 antibody-mediated clearance of human repopulating cells masks the heterogeneity of leukemia-initiating cells. *Blood* 112(3): 568-575
- Tomkinson AE, Chen L, Dong Z, Leppard JB, Levin DS, Mackey ZB, Motycka TA (2001) Completion of base excision repair by mammalian DNA ligases. *Prog Nucleic Acid Res Mol Biol* 68: 151-164
- Tort F, Hernandez S, Bea S, Camacho E, Fernandez V, Esteller M, Fraga MF, Burek C, Rosenwald A, Hernandez L, Campo E (2005) Checkpoint kinase 1 (CHK1) protein and mRNA expression is downregulated in aggressive variants of human lymphoid neoplasms. *Leukemia* 19(1): 112-117
- Tsai LH, Lees E, Faha B, Harlow E, Riabowol K (1993) The cdk2 kinase is required for the G1-to-S transition in mammalian cells. *Oncogene* 8(6): 1593-1602
- Tsien JZ, Chen DF, Gerber D, Tom C, Mercer EH, Anderson DJ, Mayford M, Kandel ER, Tonegawa S (1996) Subregion- and cell type-restricted gene knockout in mouse brain. *Cell* 87(7): 1317-1326
- Tsvetkov LM, Yeh KH, Lee SJ, Sun H, Zhang H (1999) p27(Kip1) ubiquitination and degradation is regulated by the SCF(Skp2) complex through phosphorylated Thr187 in p27. *Curr Biol* 9(12): 661-664
- Tumbar T, Guasch G, Greco V, Blanpain C, Lowry WE, Rendl M, Fuchs E (2004) Defining the epithelial stem cell niche in skin. *Science* 303(5656): 359-363
- Usui T, Ohta T, Oshiumi H, Tomizawa J, Ogawa H, Ogawa T (1998) Complex formation and functional versatility of Mre11 of budding yeast in recombination. *Cell* 95(5): 705-716
- Van Duuren BL, Sivak A, Katz C, Seidman I, Melchionne S (1975) The effect of aging and interval between primary and secondary treatment in two-stage carcinogenesis on mouse skin. *Cancer Res* 35(3): 502-505
- Vassar R, Rosenberg M, Ross S, Tyner A, Fuchs E (1989) Tissue-specific and differentiation-specific expression of a human K14 keratin gene in transgenic mice. *Proc Natl Acad Sci U S A* 86(5): 1563-1567

Verlinden L, Vanden Bempt I, Eelen G, Drijkoningen M, Verlinden I, Marchal K, De Wolf-Peeters C, Christiaens MR, Michiels L, Bouillon R, Verstuyf A (2007) The E2F-regulated gene Chk1 is highly expressed in triple-negative estrogen receptor /progesterone receptor /HER-2 breast carcinomas. *Cancer Res* 67(14): 6574-6581

Vermeulen L, De Sousa EMF, van der Heijden M, Cameron K, de Jong JH, Borovski T, Tuynman JB, Todaro M, Merz C, Rodermond H, Sprick MR, Kemper K, Richel DJ, Stassi G, Medema JP (2010) Wnt activity defines colon cancer stem cells and is regulated by the microenvironment. *Nat Cell Biol* 12(5): 468-476

Vigo E, Muller H, Prosperini E, Hateboer G, Cartwright P, Moroni MC, Helin K (1999) CDC25A phosphatase is a target of E2F and is required for efficient E2F-induced S phase. *Mol Cell Biol* 19(9): 6379-6395

Visvader JE, Lindeman GJ (2008) Cancer stem cells in solid tumours: accumulating evidence and unresolved questions. *Nat Rev Cancer* 8(10): 755-768

Voog J, Jones DL (2010) Stem cells and the niche: a dynamic duo. *Cell Stem Cell* 6(2): 103-115

Wakabayashi M, Ishii C, Inoue H, Tanaka S (2008) Genetic analysis of CHK1 and CHK2 homologues revealed a unique cross talk between ATM and ATR pathways in *Neurospora crassa*. *DNA Repair (Amst)* 7(12): 1951-1961

Walker M, Black EJ, Oehler V, Gillespie DA, Scott MT (2009) Chk1 C-terminal regulatory phosphorylation mediates checkpoint activation by de-repression of Chk1 catalytic activity. *Oncogene* 28(24): 2314-2323

Walter J, Newport J (2000) Initiation of eukaryotic DNA replication: origin unwinding and sequential chromatin association of Cdc45, RPA, and DNA polymerase alpha. *Mol Cell* 5(4): 617-627

Wei J, Wunderlich M, Fox C, Alvarez S, Cigudosa JC, Wilhelm JS, Zheng Y, Cancelas JA, Gu Y, Jansen M, Dimartino JF, Mulloy JC (2008) Microenvironment determines lineage fate in a human model of MLL-AF9 leukemia. *Cancer Cell* 13(6): 483-495

Welch S, Hirte HW, Carey MS, Hotte SJ, Tsao MS, Brown S, Pond GR, Dancey JE, Oza AM (2007) UCN-01 in combination with topotecan in patients with advanced recurrent ovarian cancer: a study of the Princess Margaret Hospital Phase II consortium. *Gynecol Oncol* 106(2): 305-310

Wend P, Holland JD, Ziebold U, Birchmeier W (2010) Wnt signaling in stem and cancer stem cells. *Semin Cell Dev Biol* 21(8): 855-863

West RB, Yaneva M, Lieber MR (1998) Productive and nonproductive complexes of Ku and DNA-dependent protein kinase at DNA termini. *Mol Cell Biol* 18(10): 5908-5920

Williams ED, Lowes AP, Williams D, Williams GT (1992) A stem cell niche theory of intestinal crypt maintenance based on a study of somatic mutation in colonic mucosa. *Am J Pathol* 141(4): 773-776

- Winkler GS, Araujo SJ, Fiedler U, Vermeulen W, Coin F, Egly JM, Hoeijmakers JH, Wood RD, Timmers HT, Weeda G (2000) TFIIH with inactive XPD helicase functions in transcription initiation but is defective in DNA repair. *J Biol Chem* 275(6): 4258-4266
- Wu C, Alman BA (2008) Side population cells in human cancers. *Cancer Lett* 268(1): 1-9
- Xu-Welliver M, Pegg AE (2002) Degradation of the alkylated form of the DNA repair protein, O(6)-alkylguanine-DNA alkyltransferase. *Carcinogenesis* 23(5): 823-830
- Xu X, Tsvetkov LM, Stern DF (2002) Chk2 activation and phosphorylation-dependent oligomerization. *Mol Cell Biol* 22(12): 4419-4432
- Yilmaz OH, Valdez R, Theisen BK, Guo W, Ferguson DO, Wu H, Morrison SJ (2006) Pten dependence distinguishes haematopoietic stem cells from leukaemia-initiating cells. *Nature* 441(7092): 475-482
- Yu J, Vodyanik MA, Smuga-Otto K, Antosiewicz-Bourget J, Frane JL, Tian S, Nie J, Jonsdottir GA, Ruotti V, Stewart R, Slukvin II, Thomson JA (2007) Induced pluripotent stem cell lines derived from human somatic cells. *Science* 318(5858): 1917-1920
- Yu Q, Sicinska E, Geng Y, Ahnstrom M, Zagozdzon A, Kong Y, Gardner H, Kiyokawa H, Harris LN, Stal O, Sicinski P (2006) Requirement for CDK4 kinase function in breast cancer. *Cancer Cell* 9(1): 23-32
- Yun MH, Hiom K (2009) CtIP-BRCA1 modulates the choice of DNA double-strand-break repair pathway throughout the cell cycle. *Nature* 459(7245): 460-463
- Zachos G, Black EJ, Walker M, Scott MT, Vagnarelli P, Earnshaw WC, Gillespie DA (2007) Chk1 is required for spindle checkpoint function. *Dev Cell* 12(2): 247-260
- Zachos G, Rainey M, Gillespie DA (2003a) Lethal errors in checkpoint control--life without Chk1. *Cell Cycle* 2(1): 14-16
- Zachos G, Rainey MD, Gillespie DA (2003b) Chk1-deficient tumour cells are viable but exhibit multiple checkpoint and survival defects. *Embo J* 22(3): 713-723
- Zachos G, Rainey MD, Gillespie DA (2005) Chk1-dependent S-M checkpoint delay in vertebrate cells is linked to maintenance of viable replication structures. *Mol Cell Biol* 25(2): 563-574
- Zaugg K, Su YW, Reilly PT, Moolani Y, Cheung CC, Hakem R, Hirao A, Liu Q, Elledge SJ, Mak TW (2007) Cross-talk between Chk1 and Chk2 in double-mutant thymocytes. *Proc Natl Acad Sci U S A* 104(10): 3805-3810
- Zeng C, Pan F, Jones LA, Lim MM, Griffin EA, Sheline YI, Mintun MA, Holtzman DM, Mach RH (2010) Evaluation of 5-ethynyl-2'-deoxyuridine staining as a sensitive and reliable method for studying cell proliferation in the adult nervous system. *Brain Res* 1319: 21-32

Zetterberg A, Larsson O (1985) Kinetic analysis of regulatory events in G1 leading to proliferation or quiescence of Swiss 3T3 cells. *Proc Natl Acad Sci U S A* 82(16): 5365-5369

Zhou BB, Bartek J (2004) Targeting the checkpoint kinases: chemosensitization versus chemoprotection. *Nat Rev Cancer* 4(3): 216-225

Zou L, Elledge SJ (2003) Sensing DNA damage through ATRIP recognition of RPA-ssDNA complexes. *Science* 300(5625): 1542-1548